Comparison of techniques for measuring the water content of soil and other porous media

Brendan Hugh George

BScAgr (Hons)

Department of Agricultural Chemistry & Soil Science

University of Sydney

New South Wales

Australia

A thesis submitted in the fulfillment of the requirements for the degree of Master of Science in Agriculture

MCMXCIX

Chapter one

A review of the literature concerning the measurement of water in porous material

1.1. MEASURING MOISTURE STATUS OF POROUS MATERIALS

There are three common ways of measuring the moisture in porous materials viz gravimetric, potential and volumetric measurements. The preferred determination depends on how the information required will be employed. For example, a plant biologist may prefer to discuss moisture with respect to potential, as this is how a plant responds to moisture in the soil-plant-air continuum. Gravimetric determination, more correctly termed wetness, is the most widely utilised technique (across disciplines) for moisture content determination, as it is simple and well understood. Conversely, volumetric moisture content is most commonly used in irrigated agriculture as the reported figures can readily be converted to volumes of water required for optimum growth. With the development of electronic instrumentation for soil moisture determination, the volumetric basis of soil moisture measurement is now the most utilised of the methodologies. However, the relationship between the methodologies, the soil moisture characteristic (Section 1.1.4.2), requires explanation to allow a comparison between available *in situ* technologies.

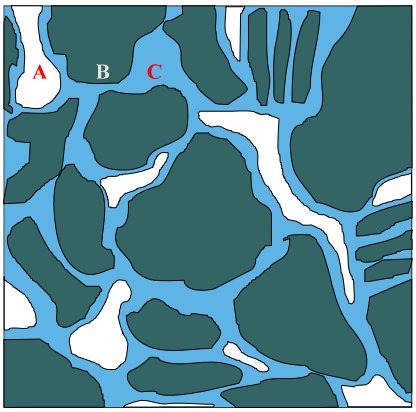

Figure 1-1 Schematic representation of soil matrix indicating relationship between air (A), soil particles (B) and water (C).

Soil, as a porous medium, can be considered with respect to moisture status, a combination of three components: air, solid, and water. The relationship between the three components as shown in Figure 1-1 determines how water in soil moves, its ability to act as a solvent and its availability to plants.

1.1.1 Wetness

The most common method for determination of moisture in soil is by removing a physical sample from the site in question. The sample is weighed, dried in an oven at 100 °C to 110 °C for 24 to 48 hours, and then re-weighed (Reynolds, 1970a; 1970b; Gardner, 1986). The gravimetric moisture content, termed wetness (w), is then determined:

$$w = \frac{\left(\text{soil mass}_{\text{wet}} - \text{soil mass}_{\text{dry}}\right)}{\text{soil mass}_{\text{dry}}} \tag{1-1}$$

The advantage of this system is that samples are easily acquired and the moisture content readily determined. However, this is offset by the method being destructive in nature, thus disallowing repeated sampling at the same location in the field. Secondly, the w (Mg Mg^{-1}), though a good indication of the moisture status, is not as useful to the plant scientist as volumetric moisture and potential.

Variation in drying ovens (± 15 °C) set at 100 to 110 °C is common (Gardner, 1986). The temperature variation influences the eventual dry state of the material. Water in the matrix is considered (by Gardner) to be either structural (derived by components of the mineral lattice) or adsorbed (attached to the lattice). Nutting (1943) indicated with representative thermal drying curves the effect drying temperature exerts on the recorded wet mass to dry mass ratio. A more appropriate temperature for drying could be between 165 °C and 175 °C (Gardner, 1986). However, this temperature range would affect the rate of organic matter oxidation. The time of drying is insignificant after two days. Gardner (1986) reports a loss of 0.3 % moisture in a silt loam sample weighed after drying at two days and then ten days. A sample of 50 to 100 g is sufficient for moisture determination, especially with respect to drying time and finer textured soil (Reynolds, 1970a; Starr *et al.*, 1995).

In the field a sound procedure for collection and storage of samples is important in reducing error and increasing accuracy of actual determination. Reynolds (1970a) found that samples could be appropriately stored for up to 168 hours with a one-percent loss in determined soil moisture content before oven drying. The standard deviations of multiple moisture determination (in the 0 – 80 mm layer of soil) can be reduced by accounting for percentage of

stones present in the profile and excluding the soil surface vegetation thereby reducing the effect of organic matter decomposition (Reynolds, 1970b). The number of samples required to achieve a nominated estimate of the true mean with accepted standard error (from ± 10 to ± 2 %) at 95 % confidence varied from 1 - 7 to 125 samples respectively for two locations (Reynolds, 1970b; 1970c). Reynolds (1970c) further suggested (his Table 3) that the vegetation class is considered in determining the number of samples required. Reynolds (1970a) does however note that the difference in wetness (w) in a sampling area is not only due to the methodology of determination, but greatly influenced by the soil composition and geography. That is, there is an effect of the inherent spatial variability.

Gravimetric sampling is utilised in many field studies where *in situ* volumetric moisture content is calibrated against samples collected from close proximity to permanent or temporarily placed sensors. For example see Burrows & Kirkham (1958); Greacen & Hignett (1979); Hodgson & Chan (1979); Topp *et al.* (1982b); and Evett & Steiner (1995). Moisture content determined by the gravimetric method is consistently referred to as *the standard technique* for moisture measurement.

1.1.2 Energy - potential

The energy status of the water present in soil may be referred to in different terms. A measure of the water content in soil (and other porous media), does not necessarily indicate how much water is available to the plant (for transpiration), or the energy status of the water. Water will move from areas of high energy to low energy with the energy status referred to as the *water potential* (Kabat & Beekma, 1994). Hanks (1992) defines soil water potential as:

> *"the amount of work that a unit quantity of water in an equilibrium soil-water (or plant-water) system is capable of doing when it moves to a pool of water in the reference state at the same temperature".*

The potential is considered negative in unsaturated soil. Potential may be reported as energy per unit mass (J kg^{-1}), volume (kPa or MPa) or weight (m - water). The (soil) water potential may be determined thus:

$$\Psi_w = \Psi_m + \Psi_s + \Psi_p \quad (1\text{-}2)$$

where:

Ψ_m is the *matric potential*, the potential that attracts (adhesion) and binds (cohesion) water to the soil, (Yeh & Guzman-Guzman, 1995). Hanks (1992) expresses the Ψ_m as the vertical distance between a point in the soil and the water level of a manometer connected to that point;

Ψ_s is the *solute (osmotic) potential* and is related to the presence of dissolved substances in the soil. The solute potential is normally neglected in water potential calculations except in saline (Rawlins & Campbell, 1986) and semi-arid situations (Carrow *et al.*, 1990), and;

Ψ_p is the *pressure potential*, defined by Hanks (1992) as the vertical distance from a point in question to the free water surface. The pressure (submergence) potential is a measure of the pressure exerted on a point by the overburden pressure. Pressure potential can be measured by a piezometer and in unsaturated soil is zero and therefore neglected (Yeh & Guzmann-Guzmann, 1995).

To obtain the overall potential the effect of gravity needs to be considered and the total potential is determined as:

$$\Psi_t = \Psi_w + \Psi_g \quad (1\text{-}3)$$

Noting Ψ_t is the *total potential*, and Ψ_g is the *gravitational potential*, the vertical distance from an arbitrary reference elevation to the measurement point.

Though potential is generally the primary factor influencing movement of water through soil, other components such as thermal and electrical gradients, discussed in detail by Rose (1968) and Campbell (1988), can affect water movement. Corey & Klute (1985) review the development of the "total soil water potential" concept and question the process of water movement. The need to separate the mechanical effect (diffusion) and the chemical effect (convection) assuring both independently have zero fluxes for measurement is highlighted. Corey & Klute (1985) validate this position by relating the ability of the total potential concept to drive the process of water movement to inherent membrane permeability to solute transport. If this process is accepted then their conclusion that no single potential (as a function of the

soil solution) will indicate the direction of net transport of the water component is reasonable. A detailed discussion of this theory and the distillation of fundamental components of total potential are beyond the scope of this discussion.

The soil water potential has a unique relationship with the volumetric soil water content. This relationship, termed the soil moisture characteristic, is determined primarily by soil type and soil aggregation and is discussed further in Section 1.1.4.2. The complexity of the relationship between soil moisture and potential in soil complicates the ability to convert from one unit to another especially with respect to continued *in situ* measurements. This complexity detracts from the use of potential-based instrumentation for irrigation management.

1.1.3 Volumetric moisture content

Water status of soil can be determined on a volume basis, θ ($m^3\ m^{-3}$), where θ is the volume of the liquid phase per unit bulk volume of soil. This is the most popular method of reporting the moisture status of soil with respect to repeated *in situ* measurement, especially regarding irrigation scheduling. θ is calculated from wetness if the bulk density of the soil is known (or estimated) as shown in Equation 1-4:

$$\theta = w \times \frac{\rho_b}{\rho_w} \tag{1-4}$$

Where ρ_b is the bulk density of the soil, (Mg m^{-3}); ρ_w is the density of water (assume unity for units of Mg m^{-3}), and; *w* is wetness (Mg Mg^{-1}) as defined in Equation 1-1.

Most *in situ* techniques are field calibrated to account for bulk density effects and report moisture on a volume basis. The accuracy of the bulk density and wetness determination dictates the accuracy of the calculated volumetric moisture content as discussed by Gardner (1986). The determination of soil bulk density is discussed in further detail in Section 1.1.4.1.

1.1.4 Relationship of methodologies

1.1.4.1 Bulk density

To allow for a comparison between techniques, parameters such as bulk density and relationships such as the soil moisture characteristic require consideration. The bulk density (ρ_b) of the soil is an important consideration in converting w to θ as shown in Equation 1-4. In this situation ρ_b is the ratio of the mass of solids to the bulk volume of the soil and is expressed in units of mass per volume (Mg m^{-3}). Most calculation of ρ_b occurs with the dry weight of soil (Blake & Hartge, 1986). In some soil types, especially reactive clays such as those dominated by montmorillonite and illite, a significant change between wet and dry bulk density due to swelling and shrinkage of the sample can occur (Ross, 1985). Cullen & Everett (1995) suggest that reporting soil moisture content is an important consideration in all ρ_b sampling.

As with most soil physical parameters there are several methods to estimate the *in situ* ρ_b including: coring, clod immersion, excavation and sand replacement, and radiation methods. The radiation methods outlined by Vomocil (1954) and Blake & Hartge (1986) will not be discussed in detail here. The core method is based on insertion of a cylindrical metal sampler into the soil. There are many and varied samplers with Starr *et al.* (1995) suggesting a minimum diameter of 30 mm to reduce variability in measurement technique. The core is weighed and dried (at 105 ^{o}C for 24 hours) then re-weighed. The loss of water yields w (Equation 1-1), the ρ_b (Mg m^3) is determined:

$$\rho_b = \frac{\text{dry soil weight}}{\text{volume of sampler}} \qquad (1\text{-}5)$$

A recent comparison of several core methods for determination of ρ_b indicated all methods satisfactory "when used by a trained operator" (Dickey *et al.,* 1993). The time taken to collect samples with the different methods ranged from 5 minutes to 48 minutes per sample, an important consideration for sampling budgets. Care is required in sample collection to minimise compaction of the soil in the sampler. This is particularly relevant in extreme conditions where wet soil may introduce error into the sampling due to viscous flow when hammering the cylinder into the soil. Also, when the soil is very dry it may shatter, again increasing the error associated with sampling. Careful observation during sample collection will minimise errors arising from viscous flow and shattering (Blake & Hartge, 1986).

The sand excavation method outlined by Blake & Hartge (1986) is an ASTM (1991) method used in surface determination of ρ_b, especially in loose material. Soil is excavated and

weighed. Sand (of known mass to volume ratio) replaces the soil and ρ_b is determined from this quantity.

In situ conditions occasionally inhibit the satisfactory employment of the core or sand replacement methods. For example, if there is a significant proportion of stones in the horizon of interest, obtaining a close fitting and undisturbed sample inside the ring can become difficult. The wax block (or clod) method, which employs the Archimedes principle, is a viable alternative. This method (again described in detail by Blake & Hartge, 1986) requires an intact soil clod. The aggregate is weighed, covered in wax (paraffin) and then the displacement is measured. Tisdall (1955) found with different soil that the wax block method tended to overestimate ρ_b compared to the core method. She attributed this to the exclusion of inter-pore spaces.

The preferred technique for determination of ρ_b is determined by the antecedent conditions at sampling. The core method is the most popular and if used with consideration to potential sampling errors is robust.

1.1.4.2 Soil moisture characteristic

Childs (1940) developed the relationship between soil water potential and soil moisture content. This relationship is primarily determined by soil type (particularly particle size) and influenced by physical conditions such as porosity and connectivity of pores. A schematic example of this relationship is shown in Figure 1-2.

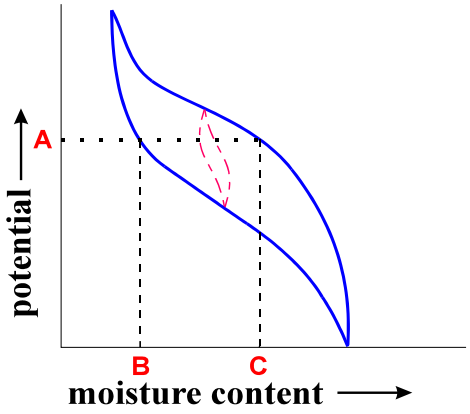

Figure 1-2 Soil moisture characteristic indicating effect of hysteresis. At potential *A* moisture content will be between point *B* and *C* (after Payne, 1988). Changing wetting and drying cycles will determine the resultant hysteretic curve.

The soil moisture characteristic will determine the amount of water available to the plant for transpiration (termed *available water*). The available water is described variously as either the difference between field capacity (full point) and wilting point (Hanks, 1992), or the difference between field capacity and the refill point (Cull, 1992). The determination of field capacity is vague because differing terminology is accepted. Generally speaking, field capacity relates to the amount of water retained in the soil after complete saturation and drainage due to gravitation forces. Cullen & Everett (1995) and Ahuja & Nielsen (1990) discuss the terminology in greater detail. Wilting point relates to moisture retained in the soil with a corresponding potential too great for plants to extract water. Thus the plants wilt and even after the addition of water will not recover. In production agriculture the refill point is determined by a marked decrease in the daily water use of the plant (assuming similar meteorological conditions) and corresponds to loss of production due to moisture stress (Briscoe, 1984). Care needs to be exercised when utilising the moisture characteristic as the relationship is influenced by hysteresis as shown in Figure 1-2.

The relationship between the matric potential and water content, shown in Equation 1-6 (Klute 1986), relies on the determination of the two constants that not only relate to a particular soil texture and structure, but also to the wetting history of the sample (Campbell, 1988).

$$\Psi_m = -a\theta^{-b} \tag{1-6}$$

Where a and b are constants for the identified soil sample. Equation 1-6 is limited in use especially in dry soil due to (potentially) large error.

1.2. MEASURING IN SITU MOISTURE CONTENT WITH NEUTRON MODERATION

1.2.1 Introduction

The use of NMM in measurement of soil water content is widespread. The technique is extensively used in scientific studies (e.g. Burrows & Kirkham, 1958; Greacen & Hignett, 1979; McKenzie *et al.*, 1990; Kamgar *et al.*, 1993) and in industry (Cull, 1992; Johnson & Borough, 1992; Hanson & Dickey, 1993).

1.2.2 Basis of the NMM technique

The neutron moderation technique is based on the measurement of fast moving neutrons that are slowed (thermalised) by an elastic collision with existing hydrogen particles in the soil. Gardner & Kirkham (1952) developed the NMM technique with others such as van Bavel *et al.*, (1956); Holmes (1956); and Williams *et al.* (1981).

The high energy, fast moving neutrons are a product of radioactive decay. Originally the source utilised was Radium/Beryllium, however more commonly used today is Americium/Beryllium. For example, Campbell Scientific Nuclear utilise a sealed Am^{241}/Be source of strength 100 mCi ($=3.7\times10^{-8}$ Bq). Fast neutrons (> 5 MeV) are expelled from the decaying source following interaction between an alpha emitter (Am^{241}) and Be. The high-energy neutrons travel into the soil matrix where continued collisions with soil constituent nuclei thermalise the neutrons, that is the neutron energy dissipates to a level of less than 0.25 eV. The returning thermalised neutrons collide in the detector tube (BF_3) with the Boron nuclei emitting an alpha particle that in turn creates a charge that is counted by a scalar. This is related to the ratio of emitted fast neutrons.

The transfer of energy from the emitted fast neutron (where mass is 1.67×10^{-21}kg) is greatest when it collides with particles of a similar size. In the soil matrix H^+ is a similar mass yielding elastic collisions with emitted high-energy neutrons. Hydrogen (H^+) is present in the soil as a constituent of soil organic matter, soil clay minerals, and water. Water is the only form of H^+ that will change from measurement to measurement. Therefore any change in the counts recorded by the NMM is due to a change in the moisture with an increase in counts relating to an increase in moisture content.

Gardner & Kirkham (1952) indicated (their Table 1) that hydrogen, due to its large nuclear cross Section (probability that the fast neutron will interact with the atom), and increasing scattering cross section (relative to other atoms present) as the neutrons lost energy, was very efficient in slowing neutrons. Fast neutrons may be "lost" (captured) to the soil matrix when elements such as fluorine, chlorine, potassium, iron (Lal, 1974; Carneiro & de Jong, 1985), boron (Wilson, 1988b) and manganese are present. Other factors also influence the relationship between emission of fast neutrons and soil water content affecting calibration and are discussed in Section 1.2.3.

Considerable refinement of neutron meter design and production has occurred in the last forty years with units now more portable and electronics more stable. Factors including the effect of

source and detector separation (Olgaard & Haahr, 1967; Wilson & Ritchie, 1986) and temperature stabilisation of electronics have been incorporated in modern neutron meter design.

1.2.3 NMM calibration

The need for calibration of the NMM in different porous materials invokes interesting discussion. Neutron meters are commonly provided with (factory) standard calibrations for use in common soil types. In Australia, Cull (1979) established a series of standard calibrations and currently these calibrations are extensively used in the irrigation industry (pers. comm., P. Cull; Irricrop Technologies International Pty Ltd, Australia). Other research indicates support for a "universal calibration" encompassing the difference in neutron scattering due to bulk density and texture (Chanasyk & McKenzie, 1986). In irrigated agriculture, in many soil types, farmers who measure changes in moisture content commonly utilise "universal calibrations" with reasonable success. Success of the "universal calibration" in scientific studies is limited with field studies indicating that soil moisture determination by the neutron moderation method is affected by other specific soil conditions. Greacen *et al.* (1981) detailed, in field and laboratory conditions, a calibration procedure for the neutron moisture method in Australian soil.

Consideration of bulk density (ρ_b, Mg m^{-3}) is the major concern in calibrating the NMM in field studies. Holmes (1966) discussed the influence of ρ_b on calibration with the change in ρ_b affecting the macroscopic absorption cross section (for thermal neutrons). Olgaard & Haahr (1968) disagreed with Holmes (1966) indicating the effect of ρ_b actually influenced the transport cross sections of fast and slow neutrons. A multi-group neutron diffusion theory was used by Wilson & Ritchie (1986) to show a linear response of the neutron moisture meter to a change in matrix density and neutron scattering cross section. Comparing *in situ* determination to re-packed soil, Carneiro & De Jong (1985) found a linear relationship yielded a suitable calibration for their soil, a red-yellow Podzolic. However, Wilson & Ritchie (1986) differed in their findings indicating that a non-linear response of the neutron moisture meter was evident with respect to the thermal neutron absorption cross section and soil-water density. The error associated with deriving the water content indicating the minimum error likely to be achieved (dependent on chemical limitations of soil description) is ± 1.6 % to ± 3.5 % θ (Wilson, 1988b). Little consideration of these parameters occurs in many field studies regarding calibration of NMM response to soil water content. Most calibrations undertaken encompass

the errors associated with neutron capture, thermal neutron cross-section and neutron scattering cross section as is evident by exclusion of these parameters in discussion. An example of this is the discussion of Carneiro & de Jong (1985) where the authors contend that the difference in slope estimation between two soils is probably due to differences in clay content, Fe and Ti content or ρ_b of re-packed columns.

Field calibration of neutron meters is most commonly carried out with a linear equation (from regression analysis) derived for a particular soil type and/or horizon in the form:

$$\theta = a + b \times n \tag{1-7}$$

Where θ is the volumetric moisture content ($m^3\ m^{-3}$); *a* is a constant (intercept); *b* is a constant (slope); *n* is the neutron count or neutron count ratio. Greacen *et al.* (1981) indicated that correct regression of count (ratio) on water content (water content as the independent variable) reduced the possibility of introducing a bias to the calibration.

The neutron moisture calibration generally involves taking neutron readings in the extremes of wet (field capacity) and dry soil and relating this to wetness (*w*). ρ_b is either calculated or estimated to yield a neutron moisture content to known moisture content relationship. A second method of calibration relates the determination of the neutron thermal adsorption and diffusion constants as shown by Vachaud *et al.* (1977). This method is not widely used for calibration of the NMM.

1.2.4 Field operation

A particular advantage of the NMM technique is the ability to obtain repeated measurements down the soil profile as shown in Figure 1-3. In the field, aluminium (Carneiro & de Jong, 1985) or PVC (Chanasyk & McKenzie, 1986) tubes, are inserted into the soil and stoppered to minimise water entry. Readings are taken at depths down the profile with a nominated count time (e.g. sixteen seconds). Commonly in irrigated systems three aluminium tubes are then averaged and moisture reported as a single reading. This aims to counter the effect of spatial variability reducing the value of the measured moisture content data (Cull, 1979). Readings may be taken with the neutron meter as a raw count or a count relative to a reading in a drum of water or in the instrument shield (Greacen *et al*, 1981). The count ratio was utilised to minimise potential drift in instrument readings. Improved stability of electronics and reduced drift in counting mechanisms in the past fifteen years has diminished the importance of this process. However, regular (as opposed to daily) calibration on a monthly or seasonal basis should be carried out.

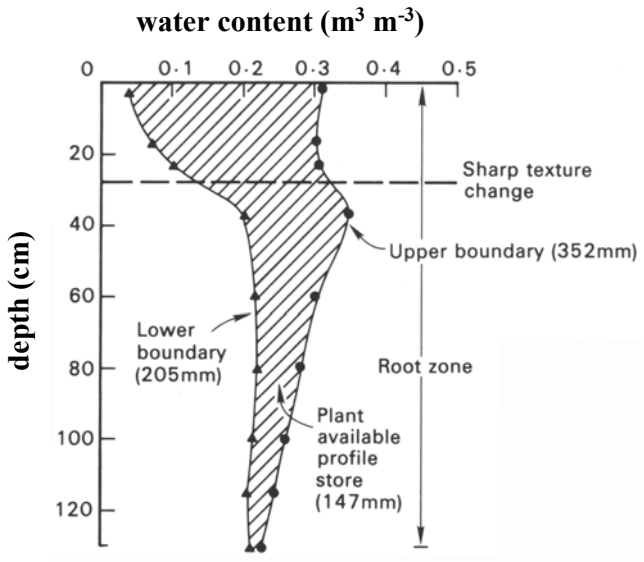

Figure 1-3 Soil moisture profile determined by NMM technique (after Williams *et al.* 1981)

1.2.5 Radiation hazard

A disadvantage of the NMM technique is the radioactive source. In NSW and other Australian states a licence is required to operate, own and store neutron meters. Gee *et al.* (1976) reported the radiation hazards associated with neutron fluxes in two neutron meters with an activity of 100 mCu concluding that safe operation incorporated an awareness with respect to time spent in close proximity to the source (i.e. carrying the meter) and neutron escape through the soil surface. Neutron meters are commercially available with differing activities commonly between 10 and 100 mCu. The activity needs to be considered with respect to the radiation hazard, however as shown by van Bavel *et al.* (1961) and Haverkamp *et al.* (1984) larger source activities will yield lower variation in recorded neutron counts. An alternative action is to increase the count time of the meter. However, economically this is often difficult to justify.

1.3. DIELECTRIC PROPERTIES OF SOIL

1.3.1 Introduction

The three physical components present in soil, from (Figure 1-1) are air, water and soil solid. The electromagnetic properties of these three components at 20 °C differs from air (K_{air} = 1, by definition), to solid (K_{solid} ≈ 2-5), and water (K_{water} = 80.18) (Weast, 1975) dominating the total dielectric. It is this different property of the K_{water} that enables the use of the dielectric technique for moisture determination in many porous media and especially soil.

The electromagnetic properties of soil and other porous materials have been studied at length in the past seventy years. Early work of Drake *et al.* (1930) and Wyman (1930) investigated the measurement of dielectric constants in aqueous solutions. During the 1970's advances in electronics allowed Hipp (1974) to determine the effect of bulk density, soil moisture and excitation frequency (30 MHz to 4 GHz) on the measured dielectric of two prepared soil samples in an air filled coaxial line.

Soil is considered a lossy medium with dispersive properties with respect to electromagnetic studies. The dielectric constant (*K*, unitless) refers to a particles' ability to align itself with an induced electromagnetic field and is determined by the ratio of the potential between electrically charged plates in a non-conducting material (ε) relative to identical plates in a vacuum (ε_o). The relationship (Equation 1-8) can be considered as the result of the material's ability to reduce the effective charge on the bodies in the medium:

$$K = \frac{\varepsilon}{\varepsilon_o} = \varepsilon' \qquad (1\text{-}8)$$

Noting that *K* is synonymous with ε' (permittivity); ε_o equals 8.85 pF m^{-1} (von Hippel, 1967). *K* is dependant on the electrically induced polarizability of the dielectric material and the angular frequency (ω) of the imposed field (White & Zegelin, 1995).

Soil is a conductive media with electrical losses occurring. To account for these losses determination of the dielectric (permittivity) becomes:

$$K^* = K' - jK'' \tag{1-9}$$

Where K^* is the complex dielectric (ε* permittivity); K' is the real dielectric (ε' permittivity) component; K'' the imaginary component (ε"); and j is an imaginary constant (√-1). The ratio of the imaginary component (K" or ε") to the real component (K' or ε') can be considered as the phase lag between the induced electric field and the response of the dielectric:

$$\tan\delta = \frac{\left(K'' + \frac{\sigma_o}{\omega_f \varepsilon_o}\right)}{K'} \tag{1-10}$$

Where σ_o is the dc or zero frequency conductivity; and ω_f the angular frequency. Often tan δ (Equation 1-10) is assumed to be much less than one. In lossy situations, such as heavy textured soil (bound water and surface conduction) or saline conditions; especially in relation to larger moisture contents, this is not correct (White & Zegelin, 1995). Thus the determination of the complex dielectric may be expressed as:

$$K^* = K' + j\left(K'' + \frac{\sigma_o}{\omega_f \varepsilon_o}\right) \tag{1-11}$$

Assuming K' >> K" then Equation 1-11 may be simplified with the measured dielectric, termed the apparent dielectric (K_a), approximating the complex dielectric:

$$K_a \approx K^* \tag{1-12}$$

For this relationship to hold requires tan δ << 1 (Equation 1-10).

1.3.2 The effect of frequency

The selection of the operating frequency can impact on the measured dielectric. The relaxation time (period in which a particle can no longer orientate itself with the induced field due to large frequency, τ) is determined by Stokes' Law as:

$$\tau = \frac{4\pi\eta r_m^3}{kT} \tag{1-13}$$

where η is the viscosity in relation to a liquid; T is the temperature (°K); k Boltzmann's constant (≈ 1.38062×10^{-23}); and r_m is the molecular radius (White & Zegelin, 1995). For

water it can be shown that the relaxation frequency ($1/\tau$) is around 10 GHz. At frequencies below 10 GHz, *K* is independent of ω and for water K' >> K" as shown in Figure 1-4.

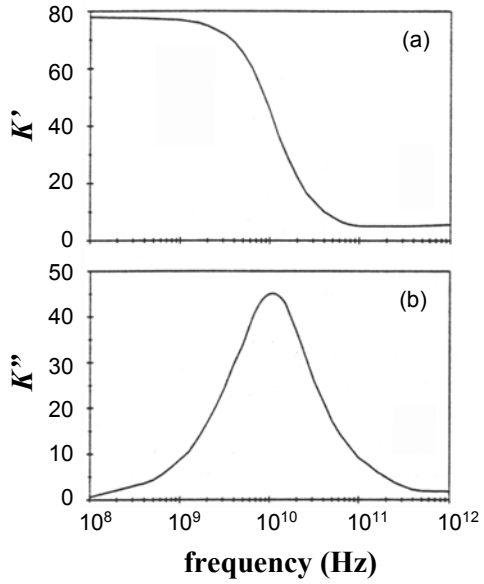

Figure 1-4 The effect of frequency on the real (K') and imaginary (K") dielectric (after White & Zegelin, 1995).

The initial study of Wyman (1930) and Childs (1940) was limited by the capability of the equipment operating at lower frequencies. From Figure 1-4 *K'* is at a maximum (= 80) between 100 MHz and 1 GHz. Corresponding to this maximum dielectric losses are small (*K"* < 5). Much study with dielectric based techniques is therefore undertaken at frequencies greater than 100 MHz (Topp *et al.*, 1980; Dean *et al.*, 1987; Tomer & Anderson, 1995; Gaskin & Miller, 1996). Operation at larger frequencies can reduce the effect of the imaginary component as well as the influence of σ. However, some researchers are suggesting that lower frequencies (around 20 MHz) can be utilised (Hilhorst & Dirksen, 1994) though experimental data demonstrating this is rare. Campbell (1990) shows (his Figure 10) that at 30 % θ in a Manchester silt, at 20 MHz, *K"* is considerably larger than when measured at 50 MHz.

1.3.3 Temperature effect on dielectric measurement

The dielectric constant of free water (K_w) is dependent on temperature and this can be estimated in the relationship:

$$K_w = 78.54\left[1 - 4.579\times10^{-3}(T-25) + 1.19\times10^{-5}(T-25)^2 - 2.8\times10^{-8}(T-25)^3\right] \quad (1\text{-}14)$$

Where T is the temperature in °K (Zegelin *et al.*, 1992). In establishing their universal equation, Topp *et al.* (1980) found temperature was not significant between 5 °C (278 °K) and 40 °C (313 °K). However in Australian conditions where near surface soil temperatures may exceed 50 °C, correction to K_w at 25 °C (298 °K) is recommended by Zegelin *et al.* (1992) by measuring temperature concurrently with K_a determination. The effect of temperature on a silt soil at 34.2% θ for various frequencies is shown in Figure 1-5. (after Campbell, 1990). Correction for temperature varies with different soil and in sandy soil a correction factor between -0.00269θ °K^{-1} (Perrson & Berndtsson, 1998) and –0.00286θ °K^{-1} (Halbertsma *et al.*, 1995) if extreme soil temperatures are experienced. In a medium-heavy textured soil Peppin *et al.* (1995) suggested a simple temperature correction of 0.00175θ °K^{-1} arguing the absolute water content errors increased linearly and the temperature dependence of the K_a determination of water in the soil matrix is lower than that of free water. Pepin *et al.* (1995) found the error associated over a 15 °K change in temperature in a 0.4m soil profile with an average θ of 0.15 $m^3\ m^{-3}$ is 0.004 $m^3\ m^{-3}$.

Correction for temperature needs to be considered with the change in bulk soil electrical conductivity (σ) (Perrson & Berndtsson, 1998) and TDR users then need to decide if this error is significant to their reported work. If extreme soil temperatures (say > 40 °C) are not encountered it is unlikely the correction for temperature will significantly improve the determination of θ in most studies.

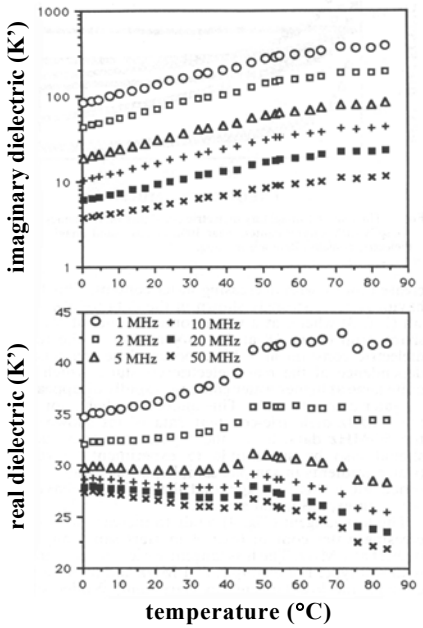

Figure 1-5 The effect of temperature on measured dielectric (Campbell, 1990).

1.4. TIME-DOMAIN REFLECTOMETRY (TDR)

1.4.1 Introduction

The time-domain reflectometry (TDR) technique is based on the generation of a fast rise-time voltage pulse in either a step-wave or impulse formation. This generation and travel of the EM wave is shown schematically in Figure 1-6 and the relationship between systems is discussed in further detail in Section 1.4.12. Essentially, the travel time of the EM wave along probes buried in the porous media is measured and the K_a calculated. The K_a is then related to θ either empirically (after Topp *et al.*, 1980) or via various physically based mixing models (e.g. Whalley, 1993; Ferre *et al.,* 1996). Topp *et al.* (1982) and Topp & Davis (1985) pioneered field use of the technique with much development occurring in the following seventeen years concerning hardware and software design and applications of the TDR technique. Instruments may be adapted cable testers (e.g. Zegelin, 1992) or dedicated instruments (e.g. Skaling, 1992) operating in a portable or stationary capacity (Baker & Allmaras, 1990; Heimovaara & Bouten, 1990; Herkelrath *et al.*, 1991).

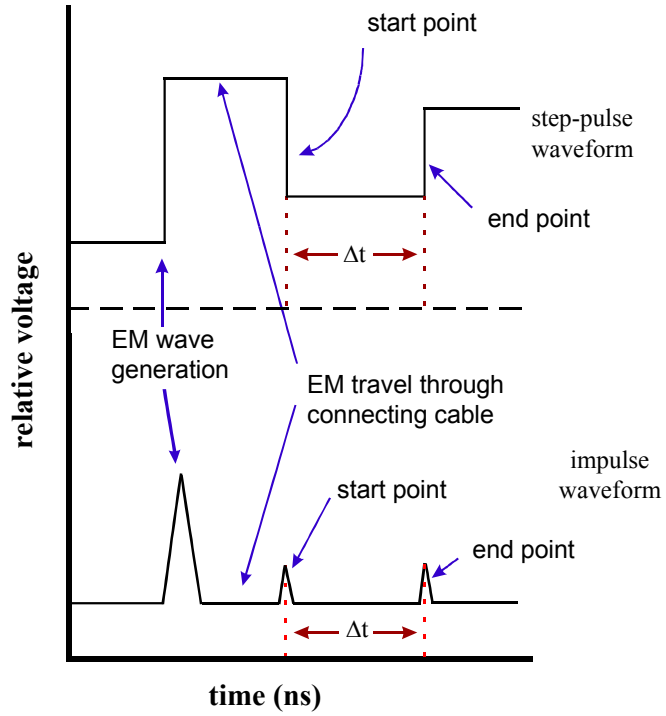

Figure 1-6 Idealised waveform generation for step pulse and impulse TDR systems

1.4.2 Measurement principle of time-domain reflectometry

A waveform in the transverse electromagnetic mode (TEM) is generated and propagated via a shielded extension cable to an unshielded guide (called a waveguide or probe) of known length embedded in the soil. At the end of the probe the wave is reflected due to the large impedance and returns to the TDR instrument. This is shown schematically (after Topp *et al.*, 1994) in Figure 1-7. The phase velocity (v_p) of a TEM in a medium is related to the apparent dielectric and magnetic permeability (μ, H m^{-1}) by the equation:

$$v_p = \frac{1}{\sqrt{(K\mu)}} c_o \tag{1-15}$$

Where c_o is the velocity of the EM wave in a vacuum (free space). The μ ($4\pi \times 10^{-7}$ H m^{-1} in a vacuum; Wyseure *et al.*, 1997) of the soil usually equals unity (Roth *et al.*, 1992) and the loss factor is thus neglected. The travel time of the TEM wave along the probes (of length L) is simplified:

$$t = \frac{2L}{v} \tag{1-16}$$

von Hippel (1967) shows the relationship between the phase velocity (v) and the dielectric constant as:

$$v_p = \frac{c}{\sqrt{\left(K' \frac{1 + \sqrt{\left(1 + \tan^2 \delta\right)}}{2} \right)}} \tag{1-17}$$

Noting that tan δ (from Equation 1-10) is the loss factor. If tan δ << 1 then combining Equation 1-16 with Equation 1-17 and rearranging simplifies to:

$$K_a = \left(\frac{c\Delta t}{2L} \right)^2 \tag{1-18}$$

This equation is fundamental to the TDR technique and dielectric determination in porous media. Note that either L or $2L$ are used in this equation depending on the software of the TDR system. Some systems, such as TRASE® TDR (SEC) automatically considers the travel length 'down and back' along the probes (Soilmoisture Equipment Corporation, 1993). If soil is saturated, the travel time of the EM wave along the probes is prolonged and the calculated

K_a is large. If the soil is dry the travel time along the probes is short and the K_a is therefore low.

1.4.3 Electromagnetic wave reflection - determination of impedance

As the generated EM wave travels along the extension cable and into the soil guided by the probes proportions of the wave are reflected when a change in impedance occurs. The partial reflections reduce the energy in the EM wave and can interfere with the end-point determination of the waveform (White & Zegelin, 1995). Initial optimism of Topp *et al.* (1982a; 1982b) and Topp & Davis (1985) for multiple reflection interpretation in light textured soil has been complicated by the effect of accounting for soil layering (Yanuka *et al.*, 1988) and especially attenuative media (Topp *et al.*, 1988). The basis of multiple reflection interpretation involves an understanding of the changing impedance on the propagating velocity and strength of the TEM wave. The intrinsic impedance (Z) of the generated TEM is given by the coupling of the electric and magnetic field vectors expressed as (von Hippel, 1967):

$$Z = \frac{E}{H} = \sqrt{\frac{\mu^*}{\varepsilon^*}} \tag{1-19}$$

For a non-conducting medium the ratio of the permeability to permittivity can be considered as shown on the left-hand side of Equation 1-19. Lossy situations complicate the relationship somewhat with the consideration of bulk soil electrical conductivity (σ) required (Kraus, 1984):

$$Z = \sqrt{\frac{j\omega\mu}{\sigma + j\omega\varepsilon}} \tag{1-20}$$

If we persist in attempting to simplify the relationship the portion of the propagated EM wave reflected (at the discontinuity) can be determined:

$$Z_s = \frac{Z_0}{\sqrt{K_a}} \tag{1-21}$$

Remembering the assumption in Equation 1-12, reducing μ^* (= 1) in non-ferromagnetic media and noting Z_s is the impedance of a probe buried in the porous media at the end of a extension cable with characteristic impedance, Z_0 (Yanuka *et al.*, 1988). The impedance of an extension cable can then be calculated by:

$$Z_0 = Z_{TDR}\sqrt{K_{ref}}\left(\frac{1+\rho_r}{1-\rho_r}\right) \tag{1-22}$$

Where Z_{TDR} is the output impedance of the TDR instrument; K_{ref} is the dielectric value of a known material; and ρ_r is the reflection coefficient (White & Zegelin, 1995). The change of impedance between Z_0 and Z_s causes the partial reflection of the EM wave and the voltage reflection coefficient (ρ_r) is defined by Kraus (1984) and White & Zegelin (1995) as:

$$\rho_r = \left(\frac{Z_s - Z_0}{Z_s + Z_0}\right) = \left(\frac{V_1}{V_0}\right) - 1 \qquad (1\text{-}23)$$

Where V_0 and V_1 can be determined from generated TDR trace as shown schematically in Figure 1-7. Topp *et al.'s* (1982a, 1992b) early work with discontinuities has been adapted by Hook *et al.* (1992) and is discussed further in Section 1.4.12.2. The determination of ρ_r is useful in probe geometry design and determination of σ_b as discussed in further detail in Sections 1.4.4 and 1.4.7.

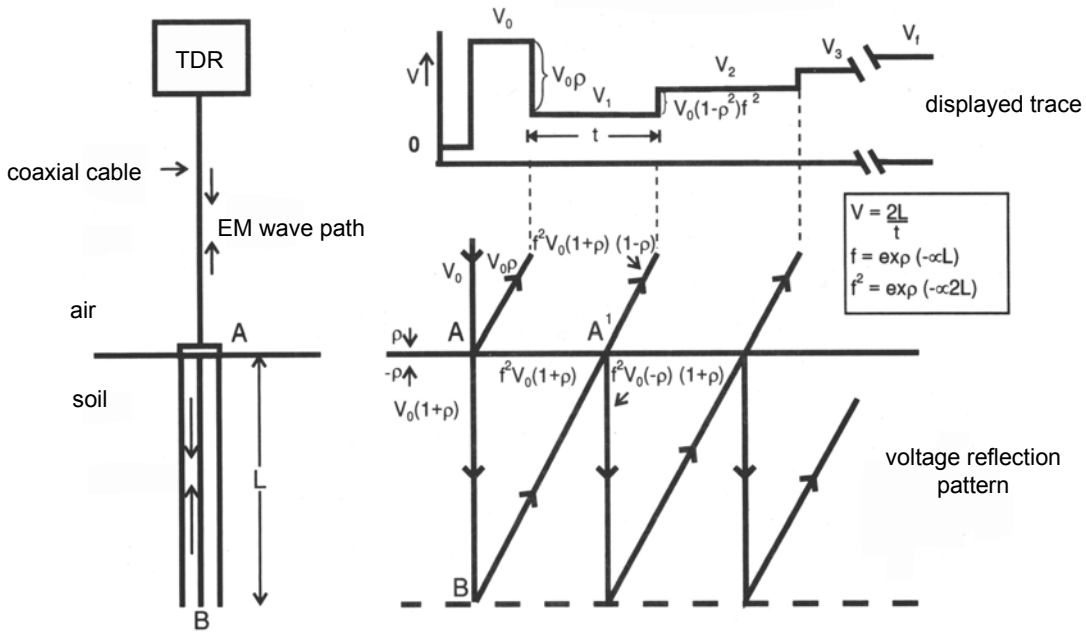

Figure 1-7 Schematic diagram of a TDR trace from a three-wire probe of length L in porous media. The travel time (t) is shown. The voltage levels V_0 and V_1 relate to voltage measured along the extension cable and at the end of the probes (waveguides) before the wave is fully reflected respectively. V_f is the voltage after multiple reflections (after Topp *et al.*, 1994).

1.4.4 TDR probe geometry, design and sensitivity

An advantage of TDR and other dielectric based techniques is the ability to develop sensors to measure moisture content in different situations. Early work was carried out in coaxial cylinders (Topp *et al.*, 1980) where a known volume of soil is sampled. *In situ* applications

require ready insertion of probes maintaining intimate contact with the surrounding media. This limits the use of coaxial cells and other probes (Figure 1-8) have been developed. Recent adaptations of probes include a hollow probe capable of simultaneous ψ measurement with θ (Baumgartner *et al.*, 1994); a coil probe for "point based" measurement (Nissan *et al.*, 1998); and a surface probe (White & Zegelin, 1995) though no detail of its performance is reported. Zegelin *et al.* (1989; 1992) and Heimovaara (1993) offer a detailed discussion on probe design.

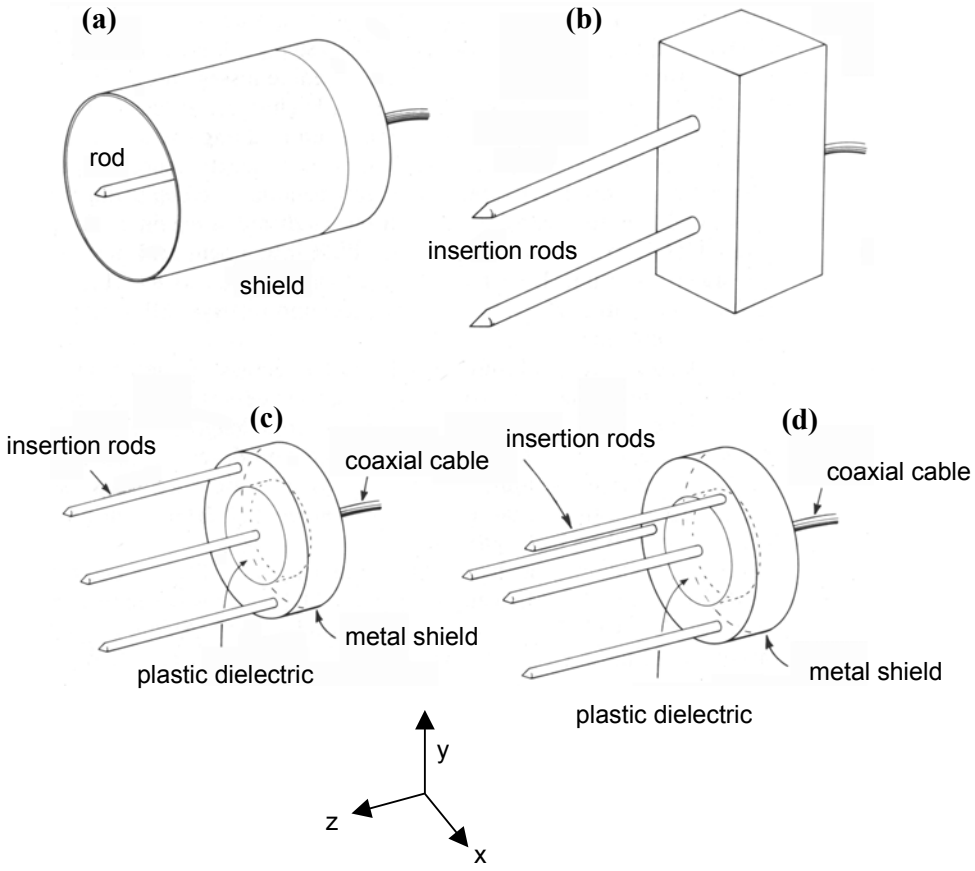

Figure 1-8 Commonly used probes for measurement of θ with the TDR technique. (a) is the coaxial cell used in early work, (b) a parallel two-wire probe that normally operates with a balun to transform the unbalanced EM wave from the TDR instrument to a balanced form propagated along the wires, (c) widely used three-wire probe (especially in permanent logging situations) and, (d) four-wire probe (after Zegelin *et al.*, 1992).

An important aspect of probe design relates to the sensitivity of the generated EM wave to soil moisture. The electric field distribution for a uniform media is shown in Figure 1-9 (Zegelin *et al.*, 1989). Baker & Lascano (1989) empirically assessed the sensitivity of TDR probes to moisture content. Knight (1991) corrected this approach accounting for the sensitivity of the EM wave in the *x* and *y*-plane (Figure 1 of Baker & Lascano, 1989). For two-wire and three-wire probes Knight (1992) indicated the importance of probe diameter (*b*) with respect to the

wire spacing (*d*). Knight (1992), suggests that the diameter to probe spacing should be a minimum of 0.1 with 90 % of the energy contained within a cylinder of radius 1.845*d* (from his Equation 49). If the *b/d* < 0.1 a "skin effect" is likely and air-gaps present can affect the measured travel time and K_a determination.

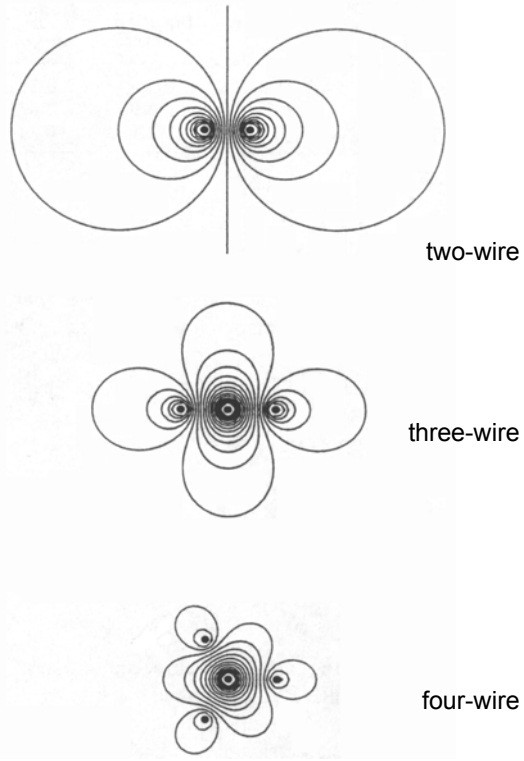

Figure 1-9 Dimensionless electric field distribution for two-, three- and four-wire TDR probes (after Zegelin *et al.*, 1989).

A consistent problem with TDR probes in field situations relates to effective measurement length of the probes in saline soil. As the EM wave loses power the reflected voltage (V_r) decreases and if no reflection occurs the transit time of the EM wave cannot be determined. Dalton (1992) indicated the effect of σ and θ on maximum probe length for three different soil types. The "worst case scenario" is a combination of high σ and high θ (his Figure 8-14), not uncommon in Australian soil, especially active shrink-swell clays. One method of improving wave reflection (and measurement of V_r) is coating the probes with a low loss dielectric coating such as PVC to reflect a portion of the EM wave. Successful application of the coating has been achieved by Baran (1994), Look *et al.* (1994), and Stacheder *et al.*, (1994). In particular the work of Baran (1994) is promising in that the probes were placed in a gravel clay mix and were successfully re-inserted for further trials. The design of the probe (waveguide) tip is important to assist in the longevity of applied coating (pers. comm., R. Fundinger; IMKO Gmbh, Germany)

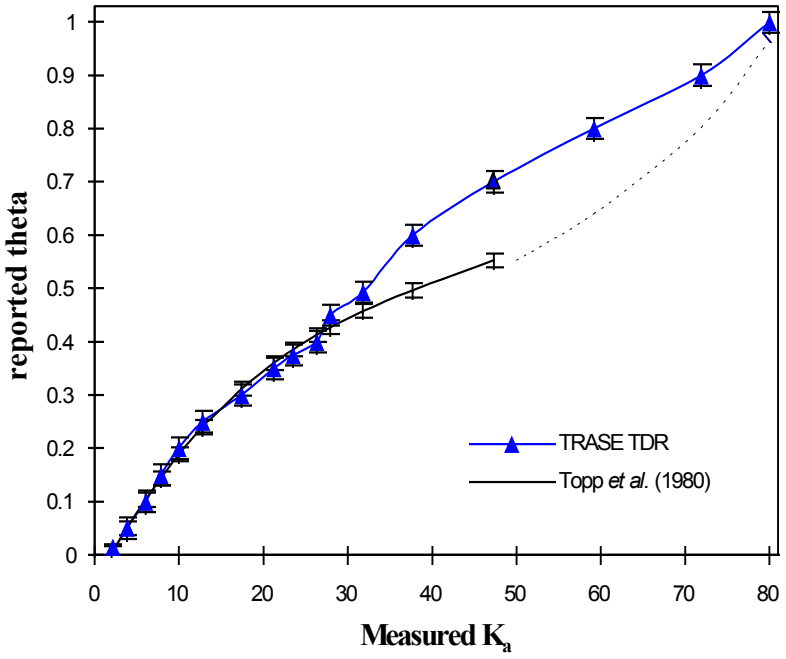

Figure 1-10 Calibration of θ from measured K_a for the TRASE® TDR instrument (Skaling, 1992) plotted with Topp et al's (1980) "universal equation". Reported error is the nominated ± 0.02 θ for the TRASE® TDR and ± 0.013 θ for Topp *et al.'s* (1980) calibration in mineral soil.

Re-calibration of the EM wave travel time versus K_a is necessary to account for the lowered sensitivity of the probe. If employed a different calibration is required to the standard calibration offered by Soilmoisture Equipment Corporation shown in Figure 1-10 (compared to Topp et al.'s 1980 "universal" calibration). Analysis of the effect of the coating on the EM wave is still not fully understood with a numerical solution offered by Knight *et al.* (1997) for two- and three-wire probes. Rothe *et al* (1997) agree with Ferre *et al.* (1996) in accounting for the effect of PVC coating on the probes. Rothe *et al.* in their paper investigating the installation of TDR probes, suggest that pre-drilling of probe holes in preparation for permanent placement is necessary where probes have a diameter > 6 mm. This is to reduce the compression of soil and will influence the measured θ irrespective of the PVC coating or lack thereof.

1.4.5 TDR calibration

In order to utilise dielectric techniques the association between K_a and θ requires quantification. θ is related to K_a either empirically or by a physical model. Topp *et al.* (1980) empirically derived a third-order polynomial relationship:

$$\theta = -5.3\times10^{-2} + 2.92\times10^{-2} K_a - 5.5\times10^{-4} K_a^2 + 4.3\times10^{-6} K_a^3 \quad (1\text{-}24)$$

The universal calibration predicted the θ (± 0.025 $m^3\ m^{-3}$) from measured K_a for mineral soil between 10 °C < T < 36 °C for the range of moisture contents 0 < θ < 0.55 $m^3\ m^{-3}$ with a variation in ρ_b from 1.14 to 1.44 Mg m^{-3}. This equation still forms the basis of most reported θ by the TDR technique (Topp & Davis, 1985; Zegelin *et al.*, 1989; Zegelin *et al.*, 1992; and Topp *et al.*, 1994). To account for organic soil Roth *et al.* (1992) developed Equation 1-25 and Equation 1-26 for ferric soil. The ferric soil (Rhodic ferralsols, FAO) magnetic permeability (μ) at 30 MHz was measured at 1.01 and 1.04 with 18.4 % and 18.5 % iron respectively (Roth *et al.*, 1992). They concluded that if errors of ± 0.015 $m^3\ m^{-3}$ for mineral soil and ± 0.035 $m^3\ m^{-3}$ for organic soil are acceptable then site specific calibration was unnecessary.

$$K(\theta) = 0.994 + 10.51\theta + 88.54\theta^2 + 28.92\theta^3 \quad \text{(organic soil, } r^2 = 0.996\text{, SD} = 2.52) \quad (1\text{-}25)$$

$$K(\theta) = 3.92 - 46.07\theta + 374\theta^2 - 320\theta^3 \quad \text{(ferric soil, } r^2 = 0.987\text{, SD} = 1.59) \quad (1\text{-}26)$$

The empirical relationship K(θ) is limited by conditions such as dry soil (θ < 0.05) where the K_{soil} dominates (Zegelin *et al.*, 1992) and in other porous media such as grain and ore (Zegelin & White, 1994). Further questions relating heavy soil types and the effect of bound water (Dirksen & Dasberg, 1993), especially in Australian conditions (Bridge *et al.*, 1996), have focussed research towards determining a physically based relationship between measured K_a and reported θ. Other research has identified site or soil specific problems, e.g. influence of minerals such as iron (Robinson *et al.*, 1994).

1.4.6 The refractive index and mixing models

More recently, a linear relationship between θ and $\sqrt{K_a}$ (termed the refractive index) has been introduced in TDR calibration studies. This term, used extensively in dielectric studies (e.g. Fellner-Feldegg, 1969), was initially reported in soil TDR research by Herkelrath *et al.* (1991) in their equation 6. The derivation of $\sqrt{K_a}$ should be considered. Remembering Equation 1-15 and considering soil as a lossy medium, the ratio of the propagating velocity (c_o) in a vacuum to that of the dielectric is termed the index of refraction:

$$\eta = \frac{c_o}{v_p} = \sqrt{\frac{\varepsilon^* \mu^*}{\varepsilon_o \mu_o}} \tag{1-28}$$

Where v_p is the velocity of propagation. Remembering the complex dielectric ($K^* = \frac{\varepsilon_o}{\varepsilon^*}$) and accounting for the magnetic equivalent:

$$K_m^* = \frac{\mu^*}{\mu_o} \tag{1-29}$$

The v_p can be determined by:

$$v_p = \frac{c_o}{\sqrt{K^* K_m^*}} \tag{1-30}$$

This equation is Equation 1-15 as K^*_m (also termed μ) equals unity in non-ferromagnetic media. The term, $\sqrt{K^*}$ is reported as $\sqrt{K_a}$ (from Equation 1-12) and is termed the *refractive index*.

Whalley (1993), using a mixing model, derived a linear relationship between the $\sqrt{K_a}$ and θ incorporating ρ_b:

$$\sqrt{K_a} = \theta(\sqrt{K_w} - 1) + \frac{\rho_b}{2.65}(\sqrt{K_s} - 1) + 1 \tag{1-31}$$

Whalley (1993) plotted previously published data (Zegelin *et al.*, 1989 - Bungendore sand) with a Redhill sand yielding similar slopes and intercepts. An important consideration however is the effect of bound water in the soil matrix due to the change in dielectric properties. Equation 1-31 does not account for this change in dielectric properties. White *et al.* (1994) questioned Whalley's (1993) finding regarding the slope of Equation 1-31 ($\sqrt{K'_w}$ -1 = 8.56). They calculated the slope of Equation 1-31 in bulk water to be 7.933 < $\sqrt{K_{a,w}}$ -1 < 7.966 and significantly different to that of Whalley (1993). Whalley (1994) argues that though scientifically the linear calibration is empirically derived (and therefore similar to the approach of Topp *et al.* (1980) and others), pragmatically the actual differences calculated by White *et al.* (1994) are not important as θ determination varies by little more than 1 %. However, White *et al.'s* point remains that many models offered are in fact a semi-empirical calibration. Further, the *a priori* knowledge required often renders the relationship unusable in field conditions.

Returning to the discussion on the use of models, Ferre *et al*. (1996) report the K(θ) relationship as:

$$\theta = a\sqrt{K_a} + b \tag{1-32}$$

Where *a* and *b* are constants. To use the $\sqrt{K_a}$ a measurement of the parameters *a* and *b* is then required. The relationship of travel time along the probe in soil to that of the probe in air (T/T_{air}) is plotted (Hook & Livingston, 1996) yielding a slope ($1/\sqrt{K_w}$-1= 0.1256 at 20 ^oC) for non clay soil, similar to that found by Herkelrath *et al.* (1991). The intercept is determined by comparing the travel time along probes in air to the travel time along the same probes in oven dry soil (T_s/T_{air}) where common values range from 1.4 to 1.7. The applicability of this research to a wide range of soil types is yet to be considered, especially with respect to clay soil and the effect of bound water.

Whalley (1993) used a simplified mixing model to derive the $\sqrt{K_a}$ to θ relationship. Tinga *et al.* (1973) developed a two-phase model to estimate K_a:

$$K_a = \left(\phi_a K_a^{\alpha} + \phi_b K_b^{\alpha}\right)^{\frac{1}{\alpha}} \tag{1-33}$$

Where ϕ is the volume fraction for components *a* and *b* respectively and α is a geometrical parameter (adapted from Zegelin *et al.*, 1992). When the field is parallel to the measurement, α = 1, and when the field is perpendicular, α = -1. Application of a mixing model approach (van Loon *et al.*, 1991) in frozen and unfrozen soil yielded results similar to Topp *et al.*'s (1980) empirical relationship. Dirksen & Dasberg (1993) also utilised the theoretical mixing Maxwell-De Loor model (rewritten by Dobson *et al.*, 1985) to quantify the relationship of K_a and θ. This model, Whalley (1993) presented in a simplified format as:

$$K^{\alpha} = K_s^{\alpha}\phi_s + K_w^{\alpha}\phi_w + K_a^{\alpha}\phi_a \tag{1-34}$$

Again α is a mixing parameter constant; and subscripts *s*, *w*, and *a* relate to solid, water and air respectively. Roth *et al.* (1990), using a "composite dielectric approach", developed a calibration for the TDR technique with an associated error of ± 0.013 $m^3\,m^{-3}$. Roth and his co-workers concluded that to achieve this calibration, further parameters such as porosity (η) and the dielectric determination of the soil matrix need to be assessed, especially in dry soil. Dirksen & Dasberg (1993) separated the water component of the model to account for tightly held "bound" water in the soil matrix. They preferred the Maxwell-De Loor model (their Equation 2) to the α mixing model. As opposed to Roth *et al.* (1990) who used an approximation of the geometric parameter (α = 0.46), Dirksen & Dasberg (1993) found α

varied between $-0.10 < \alpha < 0.81$ (for seven mineral soils). Zegelin *et al.* (1992), in controlled conditions with the electric field perpendicular to the layering ($\alpha = -1$), found the assumption of the dielectric medium being immersed in a uniform electric field (e.g. between parallel plates of a capacitor) to be invalid with the TDR technique utilising probes. The expectation of the mixing model that isotropic conditions exist is not valid along the unshielded probes in soil. This is related to the sensitivity of measurement along the probes in the soil matrix as discussed in detail in Section 1.4.4.

A physically based calibration is preferred in determining the $K(\theta)$ relationship in soil (Whalley, 1993). However, until now the extra parameters required (Roth *et al.*, 1990; Bohl & Roth, 1994; Malicki *et al.*, 1996) have deterred most users from employing physically derived mixing models and the use of the refractive index. White *et al.* (1994) though acknowledging the benefit of such an approach, suggest that most physically derived models are in fact "semi-empirical". The majority of reported θ measurements by the TDR technique is determined by the Topp *et al.* (1980) "universal" empirical Equation 1-24 or derivatives thereof (e.g. Skaling, 1992).

1.4.7 Bulk density effect on TDR calibration

Particular attention has focussed on the effect of soil bulk density or porosity on the measurement of K_a by TDR. Incorporating ρ_b into their calibration of θ against time (ns) Ledieu *et al.* (1986) showed a change of 0.1 Mg m^{-3} caused a variation of 0.0034 m^3 m^{-3} in reported θ. Jacobsen & Schjonning (1993a; 1993b), Dirksen & Dasberg (1993), and Malicki *et al.* (1996) have also investigated the effect of ρ_b (and or porosity) in detail. Jacobsen & Schjonning (1993a) included ρ_b, clay content and organic matter content in a third order polynomial equation (Equation 1-35) from their study of five topsoil and subsoil samples (their table 1). The incorporation of ρ_b, clay content and organic matter (OM) though significant, improved the model fit (adjusted r^2) only marginally from an already very good 0.980 to 0.989.

$$\theta = -3.41\times10^{-2} + 3.45\times10^{-2}K_a - 1.14\times10^{-3}K_a^2 + 1.71\times10^{-5}K_a^3 - 3.70\times10^{-2}\rho_b + 7.36\times10^{-4}\%clay + 4.77\times10^{-3}\%OM \quad (1\text{-}35)$$

Investigating the impact of ρ_b utilising theoretical calculations Dirksen & Dasberg (1993) indicate (their Figure 3) that with decreasing ρ_b Topp *et al.'s* (1980) calibration underestimates θ.

To increase sensitivity in the θ(K) relationship to the change in ρ_b we can normalise with respect to ρ_b, giving (Malicki *et al.*, 1996):

$$\theta(K_a,\rho_b) = \frac{\sqrt{K_a} - 0.819 - 0.168\rho_b - 0.159\rho_b^2}{7.17 + 1.18\rho_b} \quad (1\text{-}36)$$

In a field study conducted by Jacobsen & Schjonning (1993b) the authors found that the inclusion of ρ_b did not improve their laboratory calibration equation (Equation 1-35) concluding this was due to the small improvement offered versus the uncertainty of measurement.

Jacobsen & Schjonning (1993a) considered that an increase in ρ_b yields a corresponding increase in specific surface area leading to higher K_a. This finding concurs with those of Dirksen & Dasberg (1993) where their theoretical calculations (their Figure 2) with the Maxwell-De Loor model indicate that with increasing specific surface the actual θ will increase for the same measured K_a.

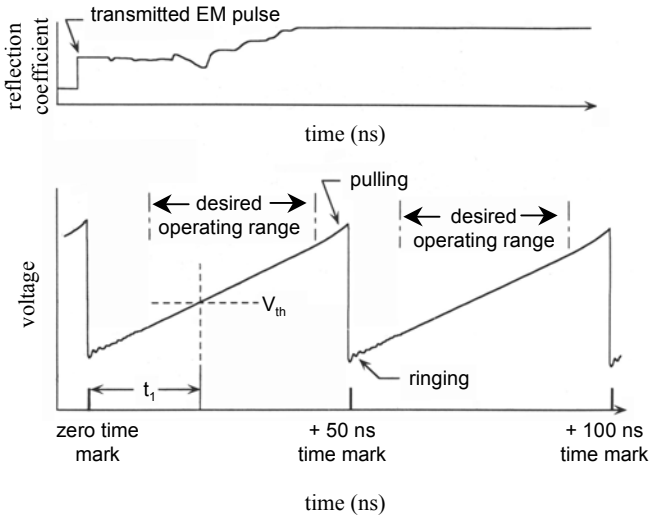

Figure 1-11 Relationship for a Tektronix 1502B/C TDR instrument of the generated waveform used for K_a determination and the associated time base waveform used to determine the actual travel time of the propagated TEM pulse (after Hook & Livingstone, 1995).

1.4.8 Bulk soil electrical conductivity (σ) effect on θ measurement

The bulk soil electrical conductivity (σ, S m^{-1}) can affect the determination of θ by increasing the K" component of the K* (Equation 1-11) from:

$$K'' = K''_p + \frac{\sigma}{\omega} \tag{1-37}$$

where K''_p (ε''_p) is the imaginary component due to polarisation losses (described in further detail by White & Zegelin, 1995), and recalling ω is the angular frequency (rads s^{-1}).

Thus the loss tangent (tan δ), Equation 1-10, is not much less than one as is required for Equation 1-12 and Equation 1-18. The TDR technique is then susceptible to over estimation of the θ as is detailed by Topp *et al.* (1988), Dalton (1992), White & Zegelin (1995) and Wyseure *et al.* (1997). Dalton (1992) concluded when *pore-water* σ reaches 0.8 S m^{-1} over-estimation of θ occurs. Vanclooster *et al.* (1993) suggest this figure could be 1.0 S m^{-1}. Wyseure *et al.* (1997) agree with the results of Vanclooster *et al.* (1993) suggesting that at large σ calibration will be required. They further suggest that to avoid this situation short extension cables and reduced length of probes will assist in end-point determination. To date there is no comprehensive study of this limitation in Australian soil.

The real and imaginary components of *K* are affected by frequency as shown in Figure 1-4. The generated EM wave may be transformed (Heimovaara, 1994a; 1994b) to yield the operational frequencies. As discussed in detail earlier in Section 1.3.2 early studies of dielectric properties were hampered by an inability to operate at frequencies insensitive to the effect of soil salinity. Campbell (1990) detailed the effect of frequency on component K between 1 to 50 MHz especially due to the ionic conductivity of the soil solution. Possible causes of dielectric loss include charged double layers; the Maxwell-Wagner effect; bound water; surface conductivity; and ionic conductivity, but Campbell (1990) could not (apart from ionic conductivity) explain the change of K" with respect to frequency. Clearly the interaction of the σ and K" in relation to dielectric losses is complex and requires further detailed understanding. However, remember that EM loss can be minimised by generating frequencies between 50 MHz and 10 GHz (White & Zegelin, 1995).

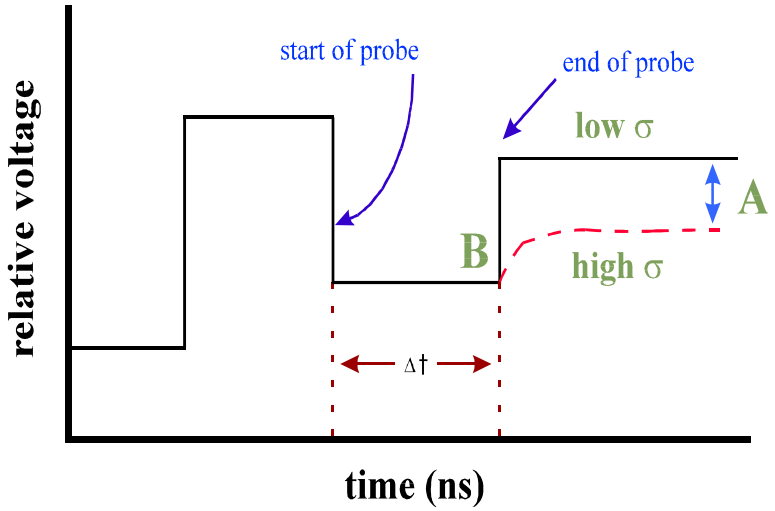

Figure 1-12 Schematic diagram of effect of increasing s on waveform as determined by step-pulse TDR system. Noting at point *A* the returning relative voltage (and thus reflection coefficient) decreases as the σ increases. For θ determination the measured travel time (Δt) is important.

An advantage of the influence of σ on the TDR waveform (schematically shown in Figure 1-12) is the ability to observe solute movement, especially through saturated soil. Much study is being undertaken to develop a better understanding and application of this phenomenon. For example see Topp *et al.* (1988); Zegelin *et al.* (1989); Kachanoski *et al.* (1992); Vanclooster *et al.* (1993; 1995); Ward *et al.* (1994) and Kim *et al.* (1998). Discussion here, however, is limited to the determination of θ by the TDR technique, and not application of the technique to solute studies.

1.4.9 Time measurement errors

The timing mechanism employed inside the (Tektronix 1502B/C cable tester) TDR instrument is more accurate at nominated times (12 - 42 ns, 62 - 92 ns and 112 - 142 ns) with individual errors (47 ps) well below nominated specifications of 411 ps (Hook & Livingston, 1995). Their experimental technique was based on the use of remotely switched diodes and a differentiated waveform detection and is discussed further in Section 1.4.12. The effect of "ramping" and "ringing" on the time base marker in shown in Figure 1-10 and Figure 1-13. This instability can lead to possible problems with waveform interpretation, especially with long extension cable and dry sandy soil (pers. comm., J. Norris; SEC, USA). Ramping and ringing lead to a change in generated waveform frequency with an idealised step-pulse TDR waveform in relation to achieved waveform with current instruments shown in Figure 1-13.

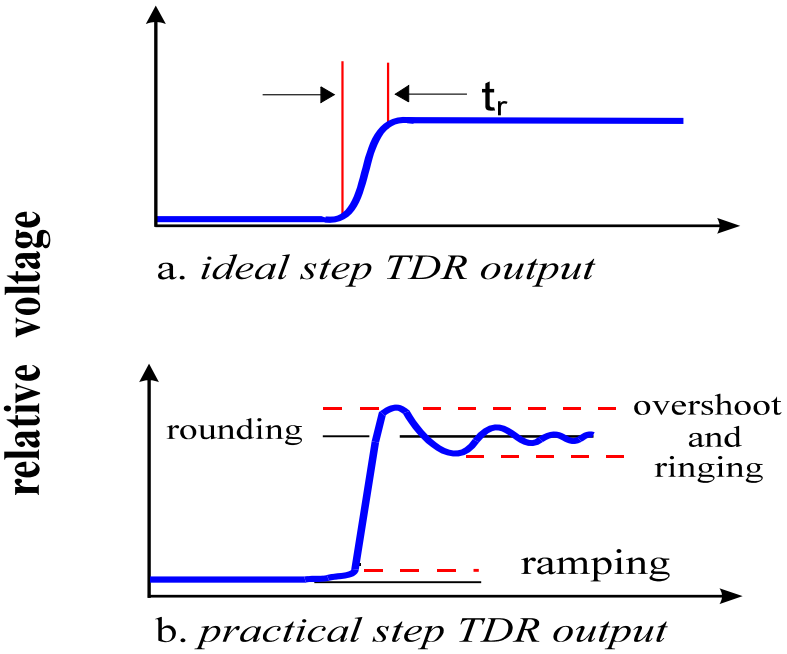

Figure 1-13 Diagram of ideal and practical step pulse (adapted from Hewlett Packard AN918, Figure 4) where t_r is the TDR system rise time.

1.4.10 Extension cables

An important component in the TDR system is the extension cable (transmission cable) transferring the EM signal from the TDR unit to the embedded probe. The observed waveform actually travels out to the probe and back. The favoured extension cable between the TDR instrument and the probe is the coaxial cable (Topp & Davis, 1985; Heimovaara, 1993). Television cable was used in some earlier installations due to improved transmission characteristics (Herkelrath *et al.*, 1991). This system requires the use of baluns to transform the unbalanced wave to a balanced form. The development and adaptation of unbalanced probes (Zegelin *et al.*, 1989) lead to an increase in the use of coaxial cable in transferring the EM signal to the buried probes. Commonly, RG-58 type cable is used in multiplexed arrays to a distance of < 30 m. Some systems prefer RG-8 (or similar) lower loss cable in signal transfer. However the cost of low-loss cable often limits use, especially in large arrays.

Though known to affect the travel of the generated EM wave, it is assumed in TDR calculations that the cable does not influence the reported moisture content. Others have concentrated on the effect of increasing cable length on the electromagnetic waves, especially the high-frequency component (Heimovaara, 1993). Of particular interest has been the effect of the cable length on bulk electrical conductivity measurements, the frequency domain

interpretation of the TEM wave (Heimovaara, 1993; 1994; Reece, 1998). Heimovaara (1993) found a change in the start-point determination with increasing cable length. This increased the error of the reported q and Heimovaara suggested that minimum probe lengths (0.05 m to 0.2 m) be used with associated maximum cable lengths (≈ 3.2 m to ≈ 24.1 m respectively). Herkelrath *et al.* (1991) investigated the potential impact of extension cable, in their case television cable, on reported moisture content. They concluded that the different lengths of cable did not impact on moisture content determination. Results of the EM wave through the television cable for different lengths is shown in Figure 1-14. Fortuitously, to simplify the automated capture of waveforms, Herkelrath and his co-workers used cable of 15 m length for all multiplexed measurements.

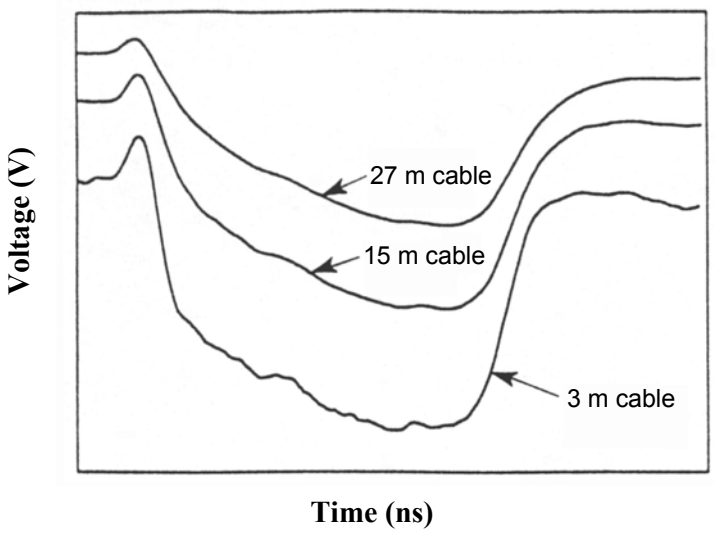

Figure 1-14 The effect of television cable length on the TDR waveform reported by Herkelrath *et al.* (1991).

1.4.11 Field operation

In the field, probes (predominantly stainless steel) are generally of two forms, being either balanced (two-wire) or unbalanced (three-wire) as shown in Figure 1-15. Generally, two wire probes are used for portable measurement and the three wire probes for permanently placed probes. For detailed discussion on this see Zegelin *et al.* (1989).

Effective length of probes (and therefore the depth of measurement) will be determined by the power of the step pulse generated by the TDR, the soil type (heavy clay attenuates the EM wave more than sandier soil types) and the moisture content of the soil (Dalton, 1992). Probes of 2 m length have been successfully used to measure moisture content in a gravelly Australian

soil (Zegelin *et al*., 1992). However, in wet heavy clay soil, probe (waveguide) length has sometimes been reduced to as little as 200 mm. This current problem is being rectified by increasing the power and stability of the EM wave and by coating probes with a thin cover of a low dielectric material (pers. comm., J. Norris; SEC, USA). The aim is to ensure that a percentage of the wave will travel the length of the probes and be reflected allowing determination of Δt.

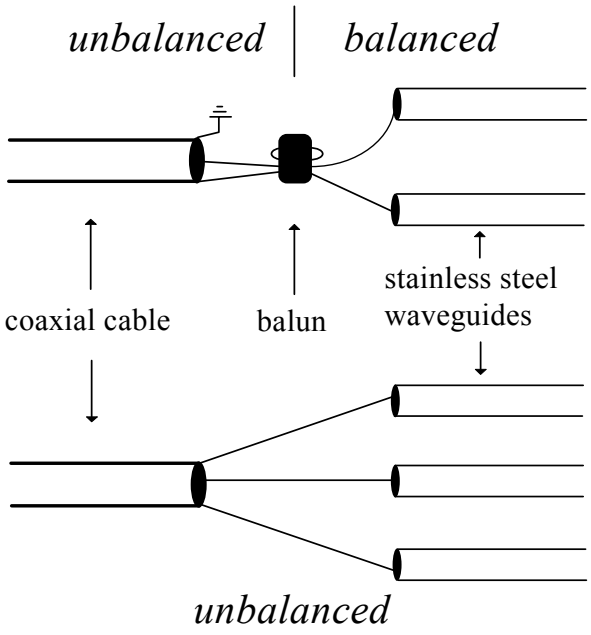

Figure 1-15 Schematic diagram illustrating the connection of the coaxial cable (unbalanced signal) to the stainless steel probes through a balun for the two-wire system (balanced), and direct to the probes in the three-wire system (unbalanced).

1.4.12 Current situation with TDR instrument development

There are several different TDR systems measuring moisture and solute transport in porous media. The development of TDR instruments can be generalised into the two categories:

(*i*) step-pulse TDR systems being either, (*a*) Tektronix (1502 B/C) cable tester based TDR configurations, or (*b*) dedicated TDR systems.

(*ii*) impulse TDR systems

1.4.12.1 Step-pulse TDR systems based on Tektronix cable testers

In the past twenty years the majority of TDR systems have been developed for use with the Tektronix 1502 (Beaverton, Oregon, USA) series cable testers. These cable testers are not

developed specifically for soil moisture determination and usually custom software programs are written to assist in end-point determination, especially in automated situations. A tunnel diode circuit generates a fast rising step voltage and this is then propagated via extension cable to the probe. In its most primitive form a ruler is used to measure the 'apparent length' of the wave from the Tektronix screen and then calculations are undertaken to derive the moisture content.

Campbell Scientific TDR system

This TDR system consists of a Tektronix 1502B/C cable tester linked to a logger and multiplexed through a series of switches and extension cables to probe in the field as shown schematically in Figure 1-16. The cable tester is interfaced to a datalogger with the EM wave propagated via RG58 or RG8 coaxial cable through three switching levels to 300 mm long twin wire probes (Anonymous, 1991). Moisture content is calculated from Topp *et al.*'s (1980) or Ledieu *et al.*'s (1986) equations. The Campbell Scientific systems are also widely used in the engineering field (e.g. Janoo *et al.,* 1994).

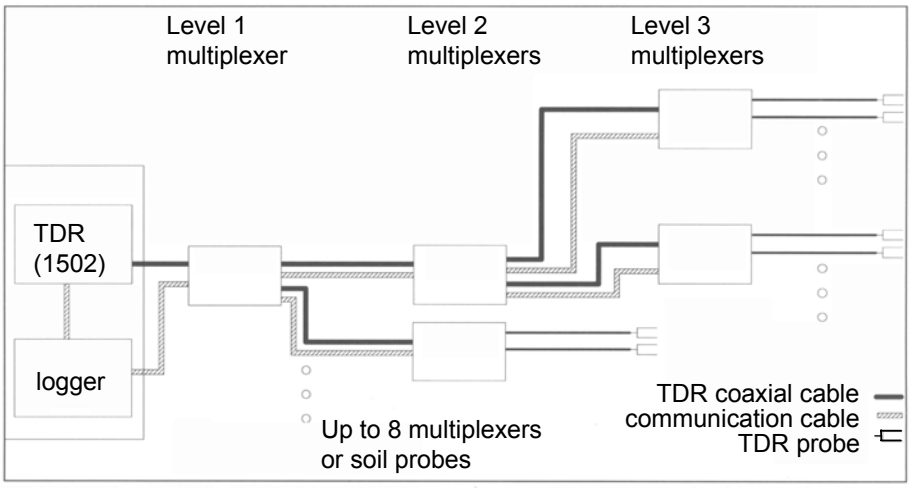

Figure 1-16 Schematic diagram of the Campbell Scientific TDR system designed for field or laboratory studies with multiple probes (PB30) (after Campbell Scientific, 1995).

Vadose Zone Equipment

As opposed to Campbell Scientific this system operates with a laptop computer for control and storage of information from the cable tester. The system configuration is similar to Campbell Scientific. The system was developed from work undertaken by Evett (1994).

Other available systems

Many scientists throughout the world have adapted TDR systems to achieve specific functions such as irrigation scheduling or automated readings. There have been TDR systems developed by CSIRO Environmental Mechanics (Canberra, Australia) and others (e.g. Heimovaara & de Water, 1993). Availability of the systems is often limited to the country of origin or specific research applications. The TDR system developed by CSIRO, Pyelab (Zegelin, 1992), is now commercially offered through Campbell Scientific.

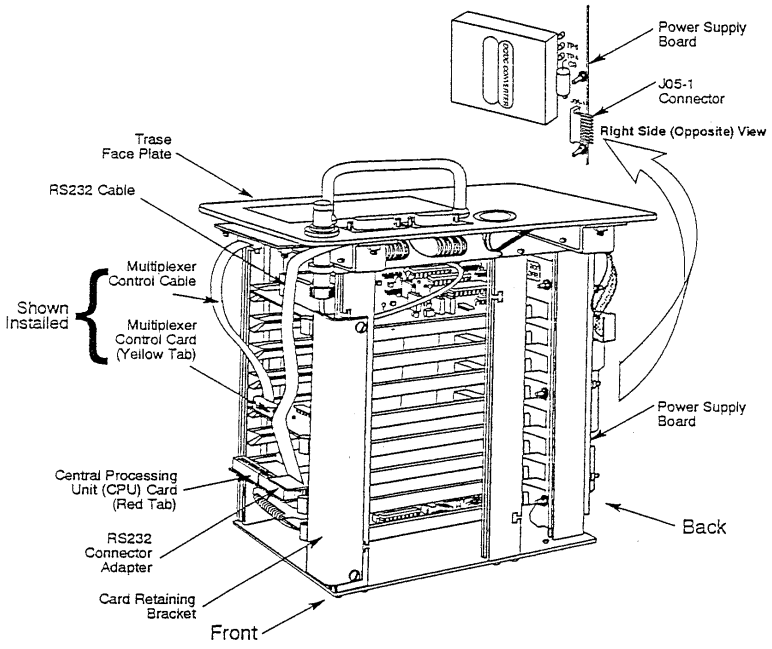

Figure 1-17 Schematic diagram of the TRASE® TDR system developed by Soilmoisture Equipment Corporation (SEC technical drawing).

1.4.12.2 Dedicated step pulse TDR instruments

TRASE® TDR

Skaling (1992) details the development of the Soilmoisture Equipment Corporation TDR, the TRASE® (Time Reflectometry Analysis of Signal Energy). This dedicated TDR instrument differs from Tektronix based systems in architecture design (modular construction) and EM wave generation. The TRASE® TDR system, shown schematically in Figure 1-17, uses a step recovery diode system to generate the step pulse EM wave. Skaling (1992) reports that this system allows greater energy in the EM wave and this increases potential extension cable length and assists in measurement determination in attenuative materials. Data is unavailable to support this claim. Another feature of the TRASE® TDR system is the digitising capability with respect to the "measurement window". The TRASE® TDR system, operating with a

nominated measurement window, will record 1000 (or 1200 in later machines) voltage points with time. This varies from Tektronix units that operate with 256 points. The greater number of measurement points assists with the on-board automatic tangent fitting regimes (pers. comm. H. Fancher; SEC, USA). The TRASE® TDR system is capable of multiplexing up to 256 probes through a double level-switching array.

TRIME TDR system

The TRIME (Time-domain Reflectometry with Intelligent Microdule Elements) reported by Stacheder *et al.* (1994) system differs from other step-pulse TDR systems as shown in Figure 1-18 and Figure 1-19. By scanning the voltage axis (y-axis) the TRIME TDR system measures the time of arrival of a predefined voltage level ($t_{(x-1)}$ in Figure 1-19). End-point determination is obtained in similar fashion to other step-pulse TDR techniques; that is, tangents are drawn from the curve of the output and the intersection point determines the travel time of the wave along the probe. The K_a is determined by Equation 1-18 and converted to moisture content via a probe specific fifth-order polynomial (Fundinger *et al.*, 1995).

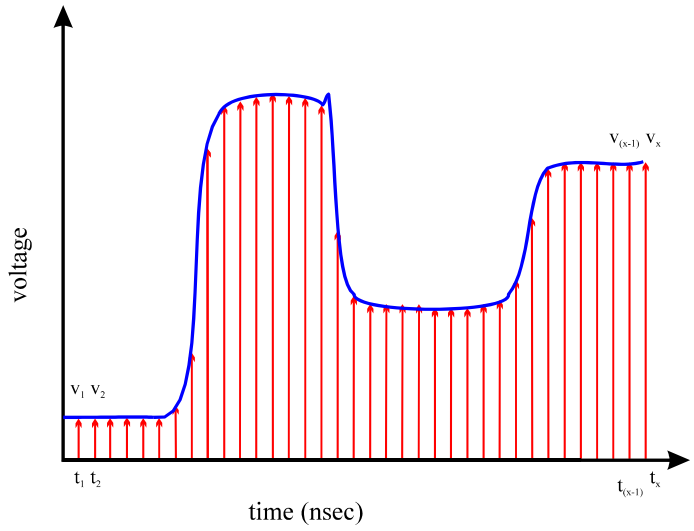

Figure 1-18 Standard procedure for measurement of generated EM pulse. EM wave voltage determined is measured at discrete time intervals.

The TRIME TDR system (Figure 1-19) is dependent on the returning EM wave of greater amplitude than the incident EM wave. The system is configured to reduce impedance mismatches and operates with short extension cables (Stacheder *et al.*, 1994). The TRIME system is limited to soil with a $\sigma < 0.1$ S m^{-1}. Larger σ leads to a depression of the returning EM wave with the critical voltage not obtained. To partly overcome this problem probes are coated with PVC concentrating a proportion of the energy of the reflected EM wave. The PVC coating reduces the measurement volume of the probes in soil (Ferre *et al.*, 1996) as discussed

in Section 1.4.4. The ability of the TRIME system for simultaneous measurement of σ as well as θ will be complicated by the PVC coating of the probes. The coating reduces the proportion of propagation of low frequencies (< 300 MHz) and dc voltage of the EM wave. This will reduce the susceptibility of the wave to attenuation that is necessary in determining the σ. However, as shown by Stacheder *et al.* (1994), a relationship does exist between σ and the amplitude (specific to the TRIME TDR) of the reflected wave (dimensionless).

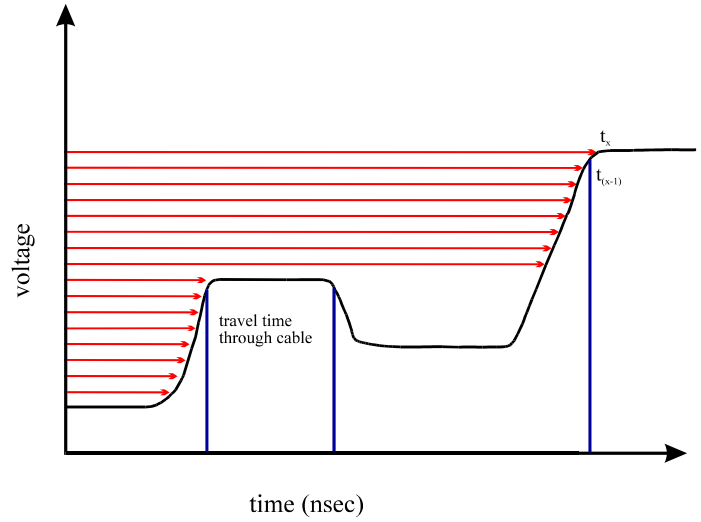

Figure 1-19 TRIME method of measuring the EM wave as it travels from the TDR along the coaxial cable and into the soil via probes (after Stacheder *et al.*, 1994).

Moisture Point TDR

Based on the work of Hook *et al.* (1992, 1995), this system operates with a fast rise step pulse EM wave. The distinguishing feature of the Moisture Point (MP) TDR system is the use of diodes along segmented probes. This improves the signal to noise ratio. Several positive aspects of this approach include:

- use of longer extension cable (to at least 100 m);
- improved end-point reflection in saline and heavy (clay) soil types;
- simplification of component TDR electronics;
- discrete measurement down the soil profile in one location.

The instrument can read a profile (standard configuration of five segments) in less than 90 seconds with an "absolute" accuracy of ± 2.5 %, and has a universal calibration curve with a resolution of 1.0 % (Anonymous, 1994). Dasberg *et al.* (1995) calibrated the MP TDR system successfully in the laboratory with a (Bungendore) sand. Calibration in the field indicated greater variability and this was attributed to a small measurement volume (diameter < 10 mm)

and inherent soil moisture variability. Another conclusion included the possibility of preferential flow of water along the inserted probe leading to preferential water flow during irrigation and elevated θ determination compared to other techniques such as NMM (Dasberg *et al.*, 1995). More recently Frueh & Hopmans (1997) successfully calibrated the segmented probe in field and laboratory conditions for a gravelly soil. They noted that re-installation was required for successful *in situ* calibration. The probes were inserted into an oversized hole and back filled. This indicates potential problems as again the small sphere of influence can lead to siting difficulty *in situ* for representative θ measurements. A detailed study of the use of MP TDR systems in heavy soil is yet to be undertaken.

Impulse TDR systems

Malicki & Skierucha (1989), Malicki (1990) and Malicki *et al.* (1992) pioneered work with impulse based TDR systems in measuring θ in porous media. Figure 1-6 schematically indicates the relationship between an EM wave generated with an impulse-based TDR instrument as opposed to a step-pulse generated EM wave. The EM waveform resembles the function $\sin^2 t$ where $0 < t < 300$ ns (Malicki, 1990). K_a is determined from measurement of the travel time of the EM wave along the probes embedded in the porous media, as occurs with step-pulse based TDR systems. From Figure 1-6 the impulse TDR system operates by the introduction of a fast (< 200 psec) spike (needle) which then travels along the extension cable and down the probes in the soil. When the EM wave reaches the end of the probes the high impedance causes a second characteristic (though of smaller magnitude) peak. The travel time is measured as the distance between the peaks and moisture content is then determined in a similar fashion to step-pulse TDR calculations (Malicki & Skierucha, 1989; Malicki *et al.*, 1992). Malicki (1990) using an empirical approach related the measured EM wave velocity to θ:

$$\theta = \exp\left(2.29 - 9.25\times10^{-2}v + 8\times10^{-4}v^2 - 2.63\times10^{-6}v^3\right) \qquad (1\text{-}38)$$

where v is the velocity of the propagated EM wave in soil. Determination of the σ is similar to that of step-pulse TDR systems (Malicki *et al.*, 1994; pers. comm., M. Malicki; Polish Academy of Sciences, Poland). Several practical questions remain about the use of impulse TDR for moisture measurement. The problem, as with step pulse TDR systems, lies with the tolerance of attenuation before the signal is not detectable. The impulse TDR system has not been widely used in Australian conditions to date.

1.4.13 TDR Summary

A summary of the various TDR systems and configurations is given in Table 1. The TDR technique in general is developing rapidly research is increasing in developing further applications of TDR such as surface measurements (Selker *et al.*, 1993; White & Zegelin, 1995), profile measurements (Hook *et al.*, 1992), long range multiplexing of probes, combined soil water content and potential (Baumgartner *et al.*, 1994) and solute transport determination (e.g. Kachanoski *et al.*, 1994).

1.5. FREQUENCY-DOMAIN (CAPACITANCE) TECHNIQUE

1.5.3 Introduction

The frequency-domain technique is similar to that of TDR in that the apparent dielectric (K_a) relationship to moisture content (θ) is exploited. Wyman (1930) identified the relationship between capacitance and soil moisture in the late 1920's. However, the use of capacitance based techniques was not possible due to the inability to select oscillating frequencies not influenced by the bulk soil electrical conductivity (σ). Malicki (1983), following the work of Thomas (1966), developed a working *in situ* capacitance based sensor. Widespread use of frequency-domain (FD) sensors followed development of a down-hole portable instrument (Dean *et al.*, 1987). In a second paper evaluating the instrument, Bell *et al.* (1987) produced an *in situ* "universal" calibration. Other FD sensors utilise short probes in a similar design to the TDR technique (Robinson & Dean, 1993; Hilhorst & Dirksen, 1994).

Capacitance (C), measured in Farads (F), is defined as the amount of charge (Q) required to increase the voltage (V) by one volt between two plates separated by a known distance containing an insulating material:

$$C = \frac{Q}{V} \tag{1-39}$$

A high frequency transistor oscillator (generally ≈ 150 MHz) operates with the soil (dielectric) forming part of an ideal capacitor as shown in Equation 1-40:

$$C = \frac{K\varepsilon_o A}{S} \tag{1-40}$$

Where K is related to C via the interaction of the total electrode area (A) and spacing of the electrodes (S), remembering that (ε_o), the permittivity of free space is constant (White & Zegelin, 1995).

TDR instrument	EM generation	Source	Use	Multiplexing	Probe configuration	Reference information
Campbell Scientific	Tektronix based, step pulse	Campbell Scientific Inc., Logan UT, USA	stationary	30m extension cable limit, 2nd and 3rd level switches	balanced systems	Baker & Allmaras (1990)
Easy Test	Impulse TDR	Easy Test Ltd, Lublin, Poland	stationary or portable	2nd level switches, 36 channels	balanced, 50 mm probes	Malicki (1990)
Heimovaara	Tektronix based, step pulse	University of Amsterdam, Amsterdam, The Netherlands	stationary	2nd level switches, 144 channels	balanced	Heimovaara & de Water (1993)
Moisture point TDR	dedicated step pulse, diodes utilised	Environmental Sensors Inc, Victoria B.C., Canada	segmented probe, portable and stationary	limited (profile sensors, say four probes), 100m coax	balanced, segmented profile probe	Hook *et al.* (1992)
Pyelab	Tektronix based, step pulse	Environmental Mechanics Laboratory, Canberra ACT, Australia	stationary	30m coax limit	mainly unbalanced	Zegelin (1992)
TRASE	dedicated step pulse, time digitisation	Soilmoisture Equipment Corporation, Santa Barbara CA, USA	portable and stationary	30m coax limitation, 256 channels	balanced and unbalanced	Skaling (1992)
TRIME	dedicated step pulse, voltage threshold	IMKO Micromodultechnik, Ettlingen, Germany	portable or stationary	*1)* dumb sensor 3.6m limit (six sensors per module); *2)* 2^{+} km smart sensor	no balun un-balanced, coated probes only	Stacheder *et al.* (1994)
Vadose Zone Equipment	Tektronix based, step pulse	Vadose Zone Equipment Company, Amarillo TX, USA	stationary and portable	30m coax limit, 2nd and 3rd level switches	balanced and unbalanced	Evett (1994)

Ideally, the soil is situated between two plates (electrodes) forming a capacitor, however in a field situation the design of the capacitance probe is not ideal with either two annular rings (electrodes) placed within a plastic access tube in the soil, or a single electrode inserted into the soil. The measured area is now removed from between the electrodes to outside the access tube as shown in Figure 1-20. However, sensitivity to change in soil moisture is reduced (Nadler & Lapid, 1996). The measurement area is considered a "fringe field" (Thomas, 1966) as the main influence on the oscillating wave is the uniform interior of the access tube. As the soil dielectric inside the access tube should not change, the soil water will influence the measured capacitance. Thus in a field situation the measured C is determined as:

$$C = gK \tag{1-41}$$

Where C is related to K via a geometrical constant (g) measured in Farads (F), (Whalley *et al.*, 1992). g depends upon electrode spacing, area and orientation of the electrodes in the soil and ε_o (White & Zegelin, 1995). The relationship between C and frequency (F, measured in Hz) is dependent on the operating design of the capacitance probe. For a down-hole sensor, Whalley *et al.* (1992), give the relationship as:

$$F = \frac{1}{2\pi\sqrt{L}}\sqrt{\left(\frac{1}{C}+\frac{1}{C_b}+\frac{1}{C_c}\right)} \tag{1-42}$$

Where L is the inductance of the oscillator; C is the measured capacitance of the sensor elements; C_b is the base capacitance; and C_c the collector capacitance of the oscillator circuit. Equation 1-42 may be simplified by combining the soil component capacitance and other constants to form:

$$F = \frac{1}{2\pi\sqrt{LC}} \tag{1-43}$$

This assumption is valid for FD measurement in soil if constituent parameters do not change with time. To account for the sensor design a normalised frequency is determined (Didcot, 1992; Paltineanu & Starr, 1997):

$$F_u = \frac{\left(F_a - F_s\right)}{\left(F_a - F_w\right)} \tag{1-44}$$

Where F_u is the normalised universal frequency; F_a is the frequency measured in air (inside a PVC tube); and F_s is the measured frequency in soil (again inside a PVC tube). This process is

used with portable (Dean *et al.*, 1987) and stationary (Starr & Paltineanu, 1998) down-hole FD sensors.

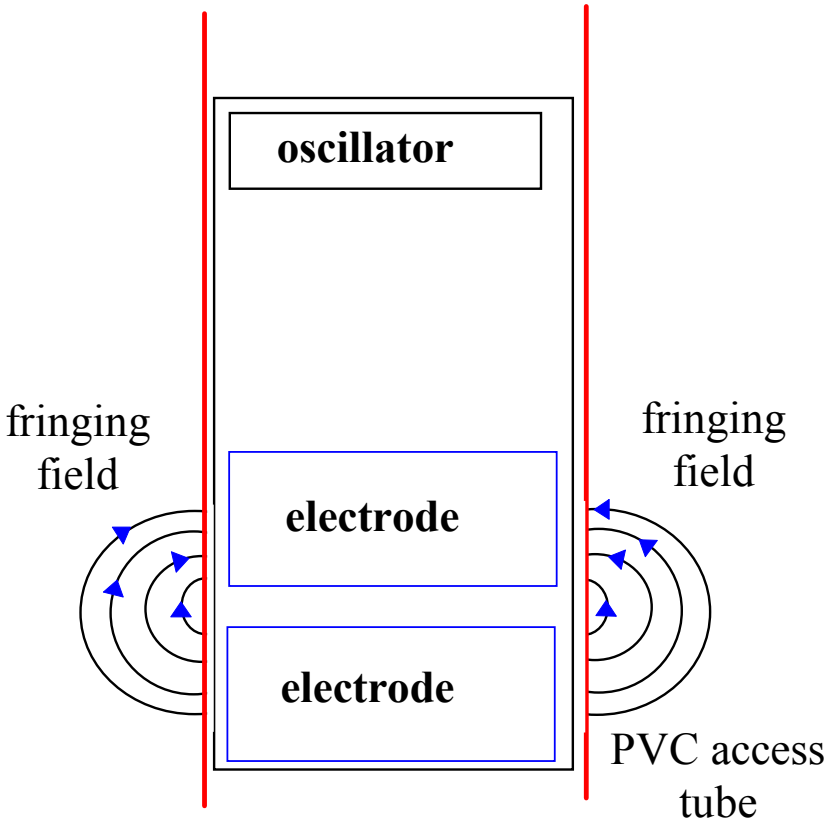

Figure 1-20 Schematic diagram of capacitance probe in a PVC access tube placed vertically in the soil (after Whalley *et al.*, 1992).

1.5.2 FD calibration

Thomas (1966) indicated a two-step process of calibration with a linear relationship at small values ($\theta < 0.10$ m^3 m^{-3}), and a semi-logarithmic relationship for values 4.5 m^3 m^{-3} $< \theta <$ 45 m^3 m^{-3} of the form:

$$\theta = 37.7 \log \Delta C - 20.9 \qquad (1\text{-}45)$$

where ΔC is the measured "fringe" capacitance change to that measured in air. The form of calibration estimation varies with log, exponential and linear calibrations employed. In a sandy soil Mead *et al.* (1994) were satisfied with the latter. Utilizing a different probe system Mead *et al.* (1995) again preferred a linear relationship to a (factory based) exponential based calibration. If higher water contents are not encountered justification of a linear relationship is acceptable (Ould Mohamed *et al.*, 1995). Other authors including Bell *et al.* (1987) and

Paltineanu & Starr (1997) still favour non-linear relationships. Kholsa & Persaud (1997) indicate (their Figure 4) that at larger moisture contents their FD instrument lost sensitivity with a corresponding increase in reported standard error. This is due to the calibration form commonly used with θ exponentially related to the frequency shift. In a field calibration in a loamy sandy soil an upper limit of 0.40 m^3 m^{-3} for reliable results is recommended (Ould Mohamed *et al.*, 1995).

In a laboratory calibration of a FD sensor operating at lower frequency (see Hilhorst & Dirksen (1994) for description) Perdok *et al.* (1996) found the technique sensitive to changes in ρ_b and soil type. Their calibration estimated permittivity with a power relationship dependent on the ρ_b. Calibration, especially with the FD technique is dependent on the sensor configuration and operating frequency.

1.5.3 FD precision

Dean *et al.* (1987) and others claim that the FD technique offers an improved precision in determination of θ compared to other *in situ* techniques, especially NMM. The theory underlying the frequency shift and relationship to θ supports this claim. Field studies have indicated however, that the FD technique is susceptible to noise (i.e. error) in determination of θ. In a fine-loamy mixed thermic Aridic Paleustalf, Evett & Steiner (1995) estimated the root mean square error (RMSE) of θ determination to be three times that of NMM measurement. This lead Evett & Steiner (1995) to question the applicability of the FD technique for soil water content measurement in heterogeneous soil. Ould Mohamed *et al.* (1997), using a FD probe (in a fine loamy, mixed, mesic, Typic Eutrochrept) to account for similar textures, considerably reduced the average 95 % confidence interval to 0.014 - 0.019 m^3 m^{-3}. This was approximately ten times smaller than errors found by Evett & Steiner (1995). Ould Mohamed *et al.* (1997) found the FD technique to be more accurate in determination of θ compared to NMM. Notably, the calibration techniques for the two methods differed, not accounting for the effective NMM measurement area. This issue requires further investigation, especially concerning the different FD systems available.

1.5.4 Influence of air-gaps on measured dielectric

The largest probable source of error in θ determination with the FD technique is related to air-gap occurrence near access tubes that are introduced during installation (Evett & Steiner, 1995; Bell *et al.*, 1987). This could be a particular problem with installation of tubes at drier sites (Evett & Steiner, 1995) or in swelling soils. This corresponds with Tomer & Anderson's (1995) comparison between a FD probe and NMM where the capacitance probe measurement varied near the soil surface. Ould Mohamed *et al.* (1997) conclude in their discussion regarding the error analysis of θ that the difference between FD and NMM θ determination decreases with an increase in soil θ, especially at shallow (< 250 mm) depth. This could be accounted for by the escape of neutrons matched by an increase in air-gaps along installed PVC tubes. Air-gaps present in close proximity to the access tube are accentuated by the weighting function of sphere-of-influence (Bell *et al.*, 1987).

Commercially, there are several FD systems available for moisture determination as shown in Table 1-2. The main advantage of the FD technology is the apparent low cost of the components and the ease of long distance transfer (either through cables or cellular phone) of the measurement signal.

1.5.5 Field application of FD technique

Measurement with the FD technique is undertaken by either lowering a sensor into the access tube (Bell *et al.*, 1987; Tomer & Anderson, 1995); placing an array of sensors into the access tubes and logging the output frequency (Buss, 1994; Paltineanu & Starr, 1997); or by insertion of the instrument directly into the soil (Robinson & Dean, 1993; Hilhorst & Dirksen, 1994). Field studies by Robinson & Dean (1993), Starr & Paltineanu (1997) and Wu (1998) indicate that the FD technique is suitable for *in situ* studies with considerations such as careful tube installation. Tube installation and contact between probe and the soil has been identified as the major constraint in FD implementation in field studies (Malicki, 1983; Bell *et al.*, 1987; Evett & Steiner, 1995 and Tomer & Anderson, 1995).

Table 1-2 Summary of available FD systems (that have been reported in literature) and their relative method of operation.

FD/Impedance Instrument	Operating Principles	Field Operation	Source	Reference Information
Didcot IH1	≈150 MHz	portable down-hole, fringe [(a)]	Didcot Instrument Company, England	Dean *et al.*, 1987; Bell *et al.*, 1987
EnviroSCAN	>100 MHz	stationary multiple sensor down-hole, logging, fringe [(a)]	Sentek, SA, Australia	Paltineanu & Starr, 1997
IMAG	≈20 MHz	point measurement, logging, waveguide configuration [(a)]	AMAG-DLO, Wageningen, Netherlands	Hilhorst & Dirksen, 1994
Sentry 2000	>100 MHz	down-hole, portable or stationary, logging, fringe [(a)]	Troxler, USA	Evett & Steiner, 1995; Tomer & Anderson, 1995
SCIP	≈150 MHz	point measurement, waveguide configuration [(b)]	Institute of Hydrology, Wallingford, England	Robinson & Dean, 1993
SMS (soil moisture sensor)	voltage change (?)	probes in direct contact with media[(b)]	uncertain	Nadler & Lapid, 1996

(a) "fringe" refers to the fact that the sensor is lowered into the soil inside a PVC access tube

(b) stainless steel probes similar in style to TDR, though generally shorter, and are placed in direct contact with the soil.

1.5.6 FD summary

Much discussion, including the operating frequency, indicates that though design is an essential component in the field operation of frequency-domain and impedance devices, currently no two devices are identical in operation and calibration. The measured (angular) frequency is related to the soil moisture content via linear or non-linear calibration. Measurement of absolute (and perhaps relative) moisture content is dependent on soil type and bulk density. With calibration Hilhorst & Dirksen (1994) conclude the FD technique can yield similar moisture content results and (similar) associated error to that of TDR measurements.

The potential for capacitance based soil moisture determination is good (Whalley *et al.*, 1992). However, development is required to determine the actual measurement area of the probe and its spatial sensitivity to change in moisture content. Further, the calibration of the technique *in situ* needs to more fully understood to allow universal use and the effect of electrical conductivity, temperature and acid soil on measured frequency has not been fully studied (pers. comm., T.J. Dean; Institute of Hydrology, England). The most pressing concern regarding the acceptance of FD is the installation process and maintaining contact with the immediate surrounding soil.

1.6. OTHER DIELECTRIC-BASED DEVICES

The recent development of electronics has encouraged researchers to adapt the basic design of frequency-domain techniques in developing sensors such as the "ThetaProbe" (Gaskin & Miller, 1996) and Campbell Scientific Inc. water content reflectometer (CS615-L).

The advances in electronics and study of established techniques such as TDR and FD in the past twenty years has enabled development of devices based on dielectric properties loosely related to time-domain or frequency relationships. Impedance-based probes can be readily designed for continuous logging of θ (Gaskin & Miller, 1996). The relationship between the line impedance and K_a is central to this approach where the known ratio (r_1 radius of inner conductor and r_2 the radius of shield conductor) allows the influence of K_a on impedance (Z) to be measured:

$$Z = \frac{60}{\sqrt{K_a}} \ln\left(\frac{r_2}{r_1}\right) \tag{1-46}$$

The ratio of the measured impedance in soil compared to a standard reference impedance is used to estimate θ:

$$\theta = \frac{\sqrt{K_a} - q}{p} \tag{1-47}$$

where q and p are soil specific constants with typical values 1.6 and 8.1 respectively (Gaskin & Miller, 1996). With a custom calibration, Zhang *et al.* (1997) compared the impedance probe (ThetaProbe; Delta-T Devices, Cambridge, UK) with step-pulse and impulse TDR, and found accurate determination of θ. Further independent testing is required to ascertain the use of this technology, especially in heavy soil situations.

1.7. POTENTIAL

1.7.1 Introduction

The measure of soil water potential is preferred in many hydrological studies as this will indicate likely water flow patterns. There are several techniques utilised to determine the soil tension in the laboratory and *in situ*. Laboratory techniques include the use of pressure vessels (Klute, 1986) where the soil is brought to equilibrium with an applied pressure and the water content change measured. This method readily allows the determination of the "wilting point" (-1500 J kg^{-1} or -1.5 MPa) but requires the destructive sampling of the soil in question. The use of the pressure apparatus for determination of plant water potential is also used extensively in the field and this procedure is outlined by Ritchie & Hinckley (1975), Turner (1988) and others. Direct *in situ* techniques for determining soil potential include tensiometry and psychrometry. Other techniques, e.g. thermal, determine the soil water potential by relating the potential properties to other soil properties (Bristow *et al.*, 1994; Reece, 1996).

1.7.2 Thermal

The proportion of air and water present in the solid matrix influences the thermal properties of soil. Water is a better thermal conductor then air and this difference may be exploited to determine the soil water status. Various attempts at relating the thermal conductivity (or diffusivity or heat capacity) to soil water status have been conducted as described by Fredlund (1992). Indeed, Cummings & Chandler (1940) outlined a field comparison between electrothermal, Bouyoucos (gypsum blocks) and thermocouples, concluding that the electrothermal probes are very sensitive to soil shrinkage away from the sensor and this problem needs to be overcome before the technique can be used with confidence.

One thermal technique identifies the relationship between volumetric specific heat capacity (ρc) and θ as detailed by Campbell *et al.*, (1991), Bristow *et al*, (1993; 1994) and Bristow (1998). This technique utilises a series of in line wires and relies upon a relationship to determine θ:

$$\theta = \frac{\left(\rho c - \rho_b c_s\right)}{\rho_w c_w} \qquad (1\text{-}48)$$

Where ρ_b (Mg m^{-3}) causes the greatest uncertainty in θ determination; ρ_w is the specific heat capacity of water (4.00 ± 0.039 MJ m^{-3} C^{-1}); c_w is the density of water (1 Mg m^{-3}); and c_s is the calculated specific heat capacity of soil (MJ Mg^{-1} C^{-1}) (Campbell *et al.*, 1991). The determination of ρ_w is sensitive to the recorded maximum temperature rise at a distance (r_m) from the line heat source. Using a dual heat-capacity probe, Bristow *et al.* (1993) estimate that a 3.3 % error in r_m can lead to a 12 % error in θ determination.

A second thermal technique relates to heat dissipation sensors as described by Campbell & Gee (1986) and Phene *et al.* (1992). The heat dissipation sensors are embedded in a porous material and strive to measure the soil matric potential (Ψ_m). Sensors are placed in the soil and equilibrate over time. An electric current is passed through the heating wire and a thermocouple (or thermistor; Cornish *et al.*, 1972) measures an increase in temperature. Individual sensors should be calibrated to allow Ψ_m determination (Campbell & Gee, 1986; Fredlund, 1992). Using a modified line heat dissipation sensor Reece (1996) argued for a calibration process based on the thermal conductivity (K):

$$\Psi_m = \exp\left[\frac{\left(K^{-1} - 0.134\right)}{b_1}\right] \tag{1-49}$$

where K is the thermal conductivity (W m^{-1} K^{-1}) and b_1 is a fitted parameter. The calibration was simplified with the measurement of K after oven drying to yield:

$$K_{rel}^{-1} = 0.032 + 0.127\ln\left(-\Psi_m\right) \tag{1-50}$$

Where K_{rel}^{-1} is the relative inverse sensor thermal conductivity derived from the relationship between the inverse thermal conductivity (K^{-1}) and the thermal conductivity measured after the soil was oven dried:

$$K_{rel}^{-1} = \frac{K^{-1}}{K_{dry}^{-1}} \tag{1-51}$$

Equation 1-50 should be considered with some care as the significance was not strong (p = 0.14) and the confidence interval was ± 23 % for ψ_m predictions. Further calibration study is required before this device (and by inference, technique) can be used with confidence.

Two predominant concerns limit the development of the thermal technique for soil moisture measurement. The first concern regards the theoretical basis of relating a change in temperature to moisture content and temperature gradient limitations (Bristow *et al.*, 1993). An absolute determination of moisture content is unlikely due to *in situ* ρ_b variation. The ρ_b

change will also affect the slope and intercept relationship of the change in moisture content as shown by Bristow *et al.* (1993). Further parameterisation such as particle size distribution is complicated by effect of soil mineralogy (Bristow, 1998). The second concern regards several practical problems existing with *in situ* exploitation of thermal probe technology such as: maintaining good contact with the soil; small measurement area; changing ρ_b requiring individual calibration; energy requirements to allow consistent logging; and induced temperature gradient with constant logging changing moisture content.

These problems need to be better understood and overcome before this technology can be used with confidence. The main positive aspect of this technology remains in that it is relatively inexpensive compared to TDR and NMM.

1.7.3 Tensiometry

Energy status of the water may be measured *in situ* with the tensiometry technique as described in detail by Cassel & Klute (1986). Ritchards (1928) first identified the use of ceramic cups attached to monitoring equipment (following the work of Campbell, 1922) for determination of the soil matric potential (Ψ_m). Tensiometers were applied to irrigation scheduling of crops in the late 1950's (Richards & Marsh, 1961). The use of tensiometers is expanding in solute transport studies (beyond the scope of this discussion) as detailed by Vanclooster *et al.* (1993), Yasuda *et al.*, (1994) and Ward *et al.* (1995), amongst others.

Tensiometers fundamentally act in a similar fashion to a plant root, measuring the energy that plants have to exert to obtain moisture from the soil. As the soil dries the water is lost from the tensiometer via a porous ceramic cup. The loss of water creates a vacuum in the tensiometer and is reported as a pressure reading, the drier the soil the higher the pressure reading.

Tensiometers may be placed permanently in the soil giving an analogue or digital output (Cresswell, 1993; Yeh & Guzman-Guzman, 1995). Logging of tensiometers is possible via transducers and a communication cable back to a computer or datalogger (Hoelscher *et al.*, 1993; Lowery *et al.*, 1986), whilst portable tensiometers allow greater freedom of sampling giving relatively quick readings of soil moisture potential (Yeh & Guzman-Guzman, 1995). Tensiometers can take time to equilibrate especially in heavier (clay) soil types and this should be accounted for in determining an irrigation-scheduling regime. The relationship between the ceramic cup size, cup conductance and the response time of the tensiometer to potential change in the soil is important in interpretation of tensiometer data (Hendrickx *et al.*, 1994; Cassel & Klute, 1986). Tensiometers must be installed correctly and well maintained to operate

accurately and the practical limit is around -85 J kg^{-1} (Campbell, 1988) and are temperature dependant (Hoelscher *et al.*, 1993). Thomas (1993) found variation between tensiometer readings that could lead to high standard error in measurement, he goes on to note that care should be taken to carefully zero the gauges and their susceptibility to hysteresis. To test tensiometers Puckett & Dane (1981) developed a method using a vacuum method in controlled conditions.

1.7.4 Electrical resistance blocks

Measurement of the electrical resistance of a block embedded in porous media and in equilibrium with the media was one the first techniques used for determination of soil water status (Colman & Hendrix, 1949; Cummings & Chandler, 1940). Electrodes are embedded in a porous block (including materials such as fiberglass, gypsum and nylon) and placed in the soil. Water in the soil will reach equilibrium with the water in the porous block and the electrical resistance is then determined and related to moisture content as a tension (J kg^{-1}). Measurement of the resistance is dependent on the soil temperature and bulk soil electrical conductivity and considerations for operation of the porous blocks are detailed by Gardner (1986) and Campbell & Gee (1986).

To overcome the problem of changing soil electrical conductivity, gypsum is often used as the medium containing the electrodes. The gypsum dissolves, dominating the immediate soil solution with Ca^{2-} and SO_4^{2-} ions reducing the effect of surrounding soil electrical conductivity (Campbell & Gee, 1986). Gypsum blocks will dissolve over a period of time (with the rate of dissolution increasing in sodic soil) generally lasting for two to three seasons in good conditions (Gardener, 1986). Gypsum blocks are insensitive to moisture content changes at high potentials, 0 to -60 J kg^{-1} (Gardner, 1986). Seyfried (1993) reports the use of a fiberglass electrical resistance sensor with improved sensitivity to change in saturated soil. This concurs with Campbell & Gee (1986) who also show (their Figure 25-1) the improved sensitivity of the fiberglass blocks at lower potentials compared to the gypsum blocks. Seyfried (1993) concluded that an acceptable linear relationship could be obtained for the fiberglass blocks when individually calibrated. Calibration is further complicated by the hysteretic nature of drying soil and ideally calibration for a porous block should include a wetting and drying cycle, (Campbell & Gee, 1986).

Large errors, up to 100 %, can occur due to: slow equilibrium of blocks with the actual soil potential; the dependence of resistance on the block temperature; effect of hysteresis on

calibration of block (if undertaken to improve accuracy) and actual contact with the soil; and blocked pores by fine material (e.g. silt or clay particles) (Gardener 1986, White & Zegelin 1995). Further consideration of soil temperature is required in applications where a large variation (> 20 °K) in soil temperature occurs, or increased sensitivity and accuracy is required (Thomas, 1993).

There are several manufacturers of the blocks and meters and design developments have been reported and evaluated recently indicating moderate success in determination of potential in field conditions (McCann *et al.*, 1992; Spaans & Baker, 1992).

With the accepted limitations, electrical resistance is considered a useful indicator of the soil moisture status in respect to root conditions such as: plentiful water; good growing conditions; approaching water stress; and water stressed plants (Spaans & Baker, 1992).

1.7.5 Psychrometers

In unsaturated soil the pressure potential, (Ψ_p), is zero and the water potential, (Ψ_w), is the sum of the matric potential (Ψ_m) and the osmotic potential (Ψ_o) as shown in Equation 1-2. Thermocouple psychrometers (also termed hygrometers) are used extensively to determine the water potential as described by Rawlins & Campbell (1986), Campbell (1988) and Rasmussen & Rhodes (1995). Measurements are based on the theoretical relationship between the water potential and relative humidity as shown in Equation 1-52. Brown & Oosterhuis (1992) describe some of the considerations required to obtain accurate measurements with psychrometers during *in situ* operation and note the importance of temperature on reported near surface measurements.

$$\Psi_w = \left(\frac{RT}{M_w}\right)\ln\left(\frac{p}{p_0}\right) \qquad (1\text{-}52)$$

where R is the ideal gas constant (8.31 J K^{-1} mol^{-1}); T is the absolute temperature (^oK); M_w is the molecular weight of water (0.018 kg mol^{-1}); p is the water vapour pressure in equilibrium with the liquid phase and p_0 is the saturated water vapour pressure of the liquid phase (Rawlins & Campbell, 1986). An important consideration is the sensitivity required in measuring the relative humidity in soil across a narrow range, 99 % to 100 % (-1500 J kg^{-1} to 0 J kg^{-1}). This sensitivity and instrument fragility often limits the widespread use of psychrometers, especially *in situ* installations. Reece (1996) found in calibrating a thermal probe that psychrometers were unreliable in the range 0 to -400 J kg^{-1} though he did not elaborate on this problem.

Correct procedures and instrument care are essential in obtaining reliable results (Briscoe, 1984).

1.8. NON-INVASIVE TECHNIQUES

1.8.1 Microwave reflectance and attenuation

The microwave reflectance technique has the distinct advantage of being non-invasive, giving great flexibility to sampling procedures. Active microwave reflectance is based on the sensitivity of an incident microwave transmission wave to the K_a of the soil as it passes through different layers (moisture contents) and is reflected. Passive microwave remote sensing systems measure the natural thermal radio emission at a particular wavelength. For wavelengths greater than 50 mm, atmospheric conditions have little impact on EM travel (Jackson *et al.*, 1996). White & Zegelin (1995) detail the measurement principles. The microwave reflectance technique though useful, is not suited for measuring a soil water profile and its use is limited to determination of moisture content in the top few centimetres (Whalley & Bull, 1991). Practical considerations such as surface roughness, vegetation cover, depth of soil measurement and soil type, identified by Schmugge *et al.* (1980) and Jackson (1988) limit the use of this technique with Jackson *et al.* (1996) acknowledging that currently no satellite systems are capable of reliable soil measurement.

A portable dielectric probe developed by Briscoe *et al.* (1992) yielded similar results to Topp *et al.'s* (1980) universal calibration with measurements in the 0.45 GHz (P band) and 1.25 GHz (L band). This instrument measures a layer approximately 10 mm thick. Further field testing is required to gain confidence in potential problems such as surface roughness and contact with the soil.

Incorporating a microwave attenuation sensor into a narrow cultivator tine, Whalley (1991) calibrated for two soil types but the sensor was limited in potential field use by the small sampling area. The use of microwave reflectance and microwave attenuation with respect to incorporation in sensor design is limited due to problems associated with measurement area and contact with soil (Whalley & Stafford, 1992).

1.8.2 Near infrared reflectance

Near-infrared reflectance (NIR) is based on the ratio of reflected infrared light emitted at a strong absorption wavelength (e.g. 1450 nm and 970 nm) and a reference wavelength that is less well absorbed (Bull, 1991). In soil, at 1300 nm a weak absorption band exists for water and at 1450 nm a strong band of NIR absorption occurs (Whalley & Bull, 1991). As water content of the soil increases the sample is considered an optically homogeneous mixture and transmission of the incident wave is increased.

A limiting factor with NIR is the need to carefully consider the clay mineralogy (e.g., reflectance from air-dry kaolinite at 1450 nm was 0.99 compared to 0.47 for bentonite at the same wavelength) (Whalley & Bull, 1991). Viscarra Rossel & McBratney (1998) determined four suitable wavelengths (1600, 1800, 2000 and 2100 nm) for soil moisture determination. However, prediction of θ varied across the field (their Figure 10b), possibly a factor of the sensitivity of the technique at lower θ. They concluded that their system was better suited for clay determination as opposed to estimating θ. One interesting aspect of Whalley's (1991) work is the incorporation of a ceramic material. As the moisture content of the soil changes the ceramic (in equilibrium with the soil) will gain or lose water and this could be measured. Small volume areas and electronic capabilities have so far limited the use of NIR for soil moisture measurement (Whalley & Stafford, 1992).

1.8.3 Gamma ray attenuation

Gardner (1986) reports the use of gamma densiometry over the last forty years. In the field, two access tubes are placed vertically into the soil and a gamma source (e.g. Cesium-137) is lowered into one tube. A detector of gamma radiation is lowered into the other tube and the emitted radiation is recorded. In soil, the electron density of mineral particles is the same (Neiber *et al.*, 1991) and increased attenuation is due to the presence of water. If the combined attenuation is calibrated (via Beer's Law) and considered with the soil bulk density the volumetric moisture content of water can be determined. It is unlikely that this method will become widely used in the field as the operation is more complex than other techniques and due to safety problems handling the radioactive material.

1.8.4 Nuclear magnetic resonance

The nuclear magnetic resonance (NMR) technique determines the soil water status due to the interaction between a static magnetic field and the nuclear magnetic dipole moments (Paetzold *et al.*, 1985). NMR has been successfully incorporated into an implement pulled through the

soil measuring moisture content (Paetzold *et al.*, 1985). Further critical review of the technique has not been undertaken. An important aspect of this technique is the ability to distinguish between bound water and available water (Whalley & Stafford, 1992). The high cost of instrumentation is likely to limit *in situ* technique application (Baker, 1990).

1.8.5 Ground penetrating radar

The GPR technique is similar to TDR in the use of the EM spectrum however, as opposed to TDR the wave is not guided through the soil (Whalley & Stafford, 1992). This technique has good potential because it is non-invasive and can be used in remote sensing systems.

1.9. SUMMARY

In situ soil water status is measured and presented on a gravimetric, volumetric or potential basis. Many techniques are available for *in situ* determination of water status in soil and other porous media, especially dielectric techniques such as time-domain reflectometry and frequency-domain systems. These systems are consistently upgraded and adapted to specific situations.

Field operation is an important consideration in developing robust techniques from new technology. Consideration of installation practices and calibration is continually being studied. However, the application of instrumentation in Australian conditions requires further study, especially concerning emerging technologies. Also, adaptation of existing technologies to measure moisture content in atypical situations enhances the usefulness of these techniques.

The laboratory (Chapter 2 and Chapter 3) and field studies (Chapter 4 and Chapter 5) concentrate on the operation of techniques measuring θ. It is these techniques that are most common in soil water studies, and it is in this area that most development of new techniques is occurring.

The time-domain reflectometry technique is now widely accepted and used in soil water studies. A particular advantage of the technique is the ability to obtain many point measurements across an area via multiple measurements. Probes are connected to the TDR instrument via low-loss extension cable, commonly coaxial cable. The travel of the generated electromagnetic wave along the extension cable is continually impeded as the distance increases. To date most research has concentrated on the frequency domain interpretation of

cable effect on salinity measurements (Heiomovaara, 1994; Reece, 1998). Or the effect of coaxial cable has been ignored (Herkelrath *et al.*, 1991) after qualitative observation. The change in the waveform, due to travel along the coaxial cable, and subsequent end-point determination is investigated in Chapter 2. My hypothesis is that increasing coaxial cable length between the embedded probe and the TDR instrument changes the reported dielectric.

Chapter 3 investigates some of the characteristics of the NMM and FD techniques in reporting the count ratio (NMM) and frequency (FD) readings. This chapter leads to Chapter 4, an investigation of the NMM with TDR and FD systems in measuring θ in Australian conditions.

Time-domain reflectometry is widely used in measuring the moisture content of many porous media materials. Chapter 5 details the calibration and application of TDR in measuring the drainage of an iron ore stockpile during mine operations.

Chapter two

Calibration of TDR and effect of coaxial extension cable on reported apparent dielectric

2.1 ABSTRACT

Time-domain reflectometry (TDR) is used extensively in laboratory and field measurement of soil water content and the technique is well suited to temporal multiple-point measurement. To obtain multiple measurements, extension cables between the buried probes and TDR units are often employed.

The TDR technique relies on reflection of the electromagnetic wave at the end of the embedded probes. Measurement of the travel time from the start of the probe to the end is then calculated. The travel time along the buried probe determines the apparent dielectric (K_a) and eventually the water content (θ, $m^3\ m^{-3}$) of the soil. No study has been conducted to assess the effect of extension cable length on end-point determination of the electromagnetic wave. If there is an effect of extension cable on the reported K_a it needs to be considered in multiple-point measurements with TDR where extension cables are employed.

In three common soils and a standard sand the apparent dielectric was measured with and without increasing lengths of RG-58 and RG-8 extension cable. Measurements were made with two TDR systems, a dedicated unit (TRASE® TDR; Soilmoisture Equipment Corp, Santa Barbara CA, USA) and an adapted cable tester (Tektronics 1502 B/C; Beaverton OR, USA) with purpose designed software for moisture content determination (CSIRO Environmental Mechanics; Canberra ACT, Australia). Measurements were made when the soil was saturated and repeated when the soil was near air-dry.

A calibration of the TRASE® TDR and Pyelab TDR systems in the four soil materials indicated no significant difference between the systems in measuring moisture. The linear relationship between K_a and θ is similar for other published results. The error of calibration (95 % confidence interval) for the Pyelab system ($\pm$ 0.053 $m^3\ m^{-3}$) and the TRASE® system ($\pm$

0.06 $m^3 m^{-3}$) is larger then Topp *et al.*'s (1980) polynomial universal equation (± 0.026 $m^3 m^{-3}$) for mineral soil. The empirical "Topp" model is therefore still preferred.

The reported apparent dielectric by the TRASE® TDR and Pyelab TDR systems is sensitive to extension cable length. In some soil, e.g. a commercial sand, the response to increasing extension length of extension cable is linear. For another soil, a linear response occurs for certain lengths of cable at different moisture contents. A single model accounting for clay content, extension cable length, TDR system, TDR probe and inherent moisture conditions explained 62.2 % of variation from the control (0 m extensions). The extension cable causes a decrease in the returning EM wave energy and this causes the slope used in automatic determination to decline.

This study shows that the slope of the EM wave affects end-point determination (for travel time along the probes) and this should be considered in multiple probe studies. When using the TDR technique for multiple measurement, a uniform extension cable length is recommended. If not, then practitioners should minimise the variation in cable length and be prepared to calibrate for soil type and moisture content effect on the reported K_a.

2.2 INTRODUCTION

Much field study of moisture content with time-domain reflectometry (TDR) has involved adaptation of commercially available cable testers. The most popular instrument is the Tektronix 1502-B or 1502-C metallic cable tester (Tektronix Inc.; Beaverton OR, USA). Cassel *et al.* (1994) elaborate on the field operation and considerations of measuring soil moisture with the Tektronix units. Other instruments are available (Table 1-1) and dedicated TDR instruments are viewed as a positive development in improving soil moisture measurement. One such instrument is the TRASE® TDR developed by Soilmoisture Equipment Corporation (SEC; Santa Barbara CA, USA). Skaling (1992) details the development of the TRASE® TDR. Reported moisture content is dependent on several components within the TDR system from the generation of the EM pulse, to the algorithms used in determining the reflection, and finally to calibration equations utilised in converting apparent dielectric (K_a) to volumetric moisture content (θ). TDR systems therefore behave differently and in certain circumstances one system may be better designed to measure θ than others.

Much use of the TDR technique involves laborious hauling of an instrument through the field or around a laboratory. Most early study was conducted with the instrument plugged via a short extension cable to the probe buried in the soil (Topp *et al.*, 1982a; 1982b). In many situations it is preferred to have a stationary TDR instrument with a series of extension cables (transmission line) connecting the instrument to the probe via a multiplexing unit. Automated multiplexed measurement has been carried out with different techniques including tensiometers (Lowery *et al.*, 1986); frequency-domain sensors (Starr & Paltineanu, 1998) and neutron moisture meters (Moutonnet *et al.*, 1988). The obvious radiation problems with the NMM significantly affect our ability to utilise the technique in unattended situations. However, the ability of dielectric techniques, especially of the TDR technique, to report multiple automated temporal and spatial volumetric moisture content is perceived as a major advantage. Zegelin *et al.* (1989) were the first to report multiple readings in an automated TDR system. Soon after, Baker & Allmaras (1990); Heimovaara & Bouten (1990) and Herkelrath *et al.* (1991) reported different systems for the multiplexing and automating of soil moisture readings with the TDR technique. The use of extension cables in TDR systems in field and laboratory situations has since become widespread (e.g. Topp *et al.*, 1994; Vanclooster *et al.*, 1995; and White & Zegelin, 1995). Most TDR systems allow for connection of different probes via different extension cable lengths to a multiplexing unit automatically.

Casual field observations during my initial trials indicated a bias when using extension cables with a TDR instrument. Discussion with the TDR manufacturer indicated this problem was a factor relating to the loss of signal resolution. Other scientists suggested that the problem could be associated with a particular TDR instrument. Indeed, Herkelrath *et al.* (1991) identified a visual difference in electromagnetic waveforms from 5 m long television cable to the 27 m cable used in a field experiment (Figure 1-14). They concluded however, that there was no significant influence of extension cable on recorded moisture results.

A similar (visual) effect is often found in attenuating soil where electrical conductivity causes a reduction in the returning signal (Zegelin *et al.*, 1992, their Figure 10-8 and Figure 10-9). The signal attenuation can be related to the bulk soil electrical conductivity, σ, (Topp *et al.*, 1988; Zegelin *et al.*, 1989), however this is beyond our interest here. In determining σ, Heimovaara *et al.* (1995) correct for this loss by accounting for the series resistance of the extension cable and connectors. This study indicates that the extension cable length affects the imaginary component (K") of the complex dielectric (equation 1-37). A consideration of the possible effect of extension cable length on reported apparent dielectric (K_a) is therefore worthy of attention. If nothing else, the paucity of information concerning the effect of

extension cables indicates a lack of serious consideration in the development of the TDR technique for moisture measurement.

A laboratory experiment was designed to investigate whether two TDR systems, a CSIRO Pyelab TDR (based on a Tektronix 1502-C cable tester) and a dedicated TDR system (TRASE® TDR, SEC) reported similar measurement of K_a. An independent calibration of the TDR systems comparing them to published results is also defined. A second component of the laboratory study investigated the impact of the length of extension cable between the embedded probe in the soil and the measured K_a and subsequent θ determination. The second component of the experiment is designed to test the TDR systems under standard operational procedures during the set-up for multiple readings.

2.3 MATERIALS AND METHODS

2.3.1 Soil

Soil was collected from 0 - 0.2 m depth (A horizon and upper B horizon) at three field sites; a Chromosol (Isbell, 1996) near Dubbo (NSW), a Ferrosol near Scottsdale (Tasmania) and a Vertosol near Narrabri (NSW) shown in Figure 2-1. TDR is best suited, especially in multiple sensor arrays, to installation in the upper soil profile (0 – 0.4 m) with unbalanced probes placed either horizontally or vertically (e.g. Herkelrath *et al.*, 1991 and McBratney *et al.*, 1997). Also, this area is of greatest interest for soil moisture measurement in shallow-rooted agricultural crops.

The Chromosol (Dubbo) sample is from an irrigated effluent re-use plantation situated on the town outskirts. The mixed species hardwood plantation was established in October 1991 with effluent applied at regular intervals. Soil was collected from the top 0.2 m of the profile in a one hectare block of *Eucalyptus bicostata* spp. *bicostata* further described in chapter 4. The Ferrosol soil (Scottsdale) was collected from an intensively-managed vegetable production farm then planted with potatoes (*Solanum tuberosum* L.).

Collected samples were air-dried (≈ 40 °C) for two weeks and then crushed and sieved to obtain the < 2 mm aggregates. A fourth "standard" soil, a commercial sand, G200 (Commercial Minerals Ltd, Parramatta, NSW) was included with soil physical and chemical characteristics for all soil shown in Table 2-1. The sand is (strictly) described as a Rudosol

(Isbell, 1996), though in this study I will still refer to it as a sand so as not to confuse it with a sample from a particular field site.

The age and nature of (alluvial) formation in Australian soil can lead to a typically heavy texture, containing a considerable portion of clay particles. The soil sampled reflects this. Particle-size analysis (PSA) was determined by hydrometer method of Koppi (1995) adapted from Bouyoucos (1962). Texture was then determined from the USDA texture triangle described by Gee & Bauder (1986). Collected soil texture ranges from a sandy clay loam (Chromosol), to sandy clay (Vertosol) to a clay (Ferrosol).

Soil pH in water and $CaCl_2$ was calculated with a 1:5 (soil:water) dilution. Readings were temperature corrected and obtained with a glass-calomel electrode (PHm83 autocal meter, Radiometer Copenhagen 901-417). Soil pH does not significantly affect the electromagnetic properties utilised by the TDR technique. Measured pH indicates the Vertosol (Narrabri) soil is slightly alkaline, typical of soil in the region; and the Ferrosol soil most acid ($pH_{[CaCl_2]}$ = 4.65).

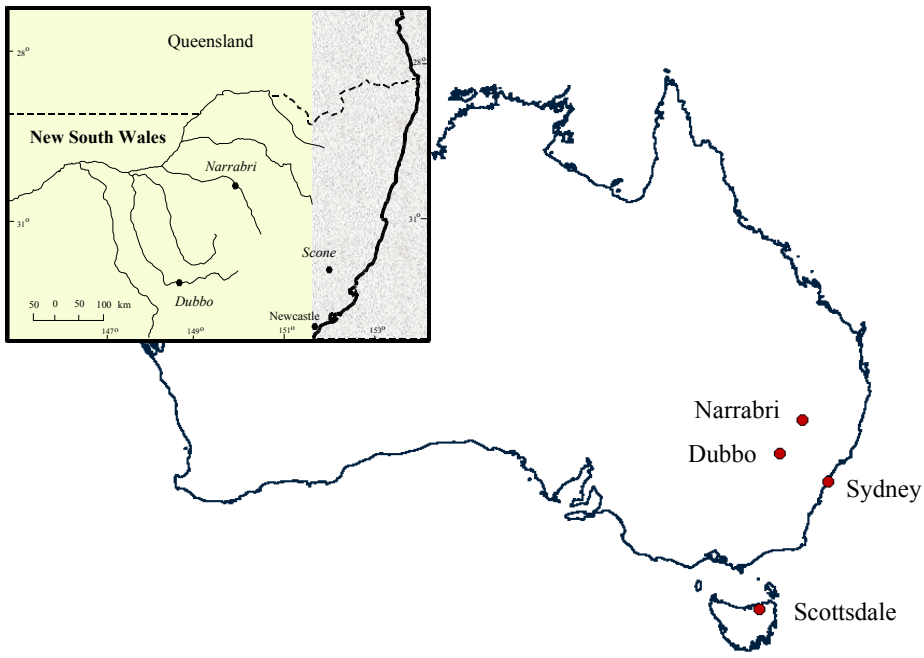

Figure 2-1 Site locations for soil collection used in laboratory study.

The specific surface of the three field soils was determined from water sorption (Newman, 1983). Total iron was determined, after digestion, by atomic adsorption. Samples were washed and prepared (glue added to ensure contact with tile) for x-ray diffraction (Brindley & Brown, 1984). The Chromosol mineralogy is dominated by smectite, kaolin and possibly some

trace mica. A vermiculite chlorite integrade and kaolin dominate the Ferrosol mineralogy. And the Vertosol soil is dominated by smectite and kaolin minerals.

Table 2-1 Soil physical characteristics for Chromosol, Vertosol, Ferrosol and a standard sand soil used in TDR calibration and extension cable experiment.

	Chromosol (Dubbo)		**Vertosol (Narrabri)**		**Ferrosol (Scottsdale)**		**Sand (Parramatta)**	
	Mean	*Std Dev.*	*Mean*	*Std Dev.*	*Mean*	*Std Dev.*	*Mean*	*Std Dev.*
Particle-size analysis								
% clay (< 0.002 mm)	32.88	2.556	37.01	1.640	47.55	0.471		
% silt (0.002 - 0.02 mm)	10.73	1.746	12.53	0.970	18.48	0.299		
% fine sand (0.02 - 0.2 mm)	35.73	1.265	24.54	0.430	19.86	0.777		
% coarse sand (0.2 - 2.0 mm)	20.66	0.691	25.91	1.338	14.11	0.845		
Texture	Sandy clay loam		Sandy clay		Clay		Sand	
Organic Carbon (%)	1.57	0.06	0.91	0.03	2.78	0.62	0.05	0.07
pH $_{[H_2O]}$	6.64		8.14		5.12		6.38	
pH $_{[CaCl_2]}$	5.55		7.35		4.65		4.81	
Electrical conductivity [1:5 H_2O] (dS m^{-1})	1.96	0.017	2.43	0.021	2.47	0.036	0.18	0.022
Specific surface (m^2 g^{-1})	397.4	8.45	375.2	4.24	304.3	5.12		
Total Iron (%)	4.12	0.065	2.81	0.064	15.83	0.126	8.48	
Number of samples	3		3		3		3	3

Organic carbon was determined with an adapted Walkley & Black (1934) method. The organic carbon value is typical for Chromosol soil (Spain *et al.*, 1993) indicating applied effluent has not changed soil organic carbon significantly in the first two years of effluent application. Intuitively, we expect greater organic carbon values due to the application of the nutrient-rich effluent. However, small organic carbon values (1.57 %) are similar to other values in an irrigated plantation in southern NSW (Falkiner & Smith, 1997). This could be due

to the continued wetting and drying cycles created with application of effluent irrigation (Polglase *et al.*,1995). Organic carbon is very small (0.05 %) in the sand and as expected, the largest organic carbon values (2.78 %) obtained for the Ferrosol soil. These values are typical of Ferrosol soil types (Spain *et al.*, 1993).

Electrical conductivity is a major consideration in effectively determining maximum length of TDR probe (Dalton, 1992) and is often a limiting factor in efficient TDR use. To maximise the opportunities to obtain readings, 200 mm probes are utilised. A 1:5 extract of soil in water was utilised to determine the electrical conductivity, with filtered samples analysed with a temperature corrected conductivity meter (Radiometer Copenhagen DMN83).

2.3.2 Equipment

2.3.2.1 Time-domain reflectometers

To assess if the extension cable length was instrument-dependent or problematic of the TDR technique, two instruments were utilised. A TRASE® System I TDR (Soilmoisture Equipment Corporation Inc.; Santa Barbara CA, USA) and a Tektronix 1502B/C metallic cable tester (Tektronix; Beaverton OR, USA) with Pyelab software (CSIRO Environmental Mechanics; Canberra ACT, Australia) were used to measure K_a and determine θ. Technical specifications for the time-domain reflectometry instruments are given in Table 2-2. Both instruments run from internal and external power sources depending on battery status. Extension cables were connected directly to the Bayonet Nelson Connector (BNC) on the measuring instrument. Both TDR systems use automatic algorithms to report K_a to simplify measurement and to minimise error in predicted θ (Timlin & Pachepsky, 1996).

2.3.2.2 Probes and extension cables

Two unbalanced probes from Soilmoisture Equipment Corporation (6000l20) were embedded 50 mm from the bottom of the soil in each of the tension columns. Probes were installed during packing of the columns to ensure thorough contact with the soil and end-effects were minimised by siting the probes at least 20 mm from the side of the tension table as shown in Figure 2-2. The SEC probes are 200 mm in length with wire diameter of 3 mm and nominal wire spacing of 25 mm. The critical spacing between wires should be three times (or more) greater than the diameter of the centre wire (Zegelin *et al.*, 1992). The SEC probes (25 mm /3 mm ≈ 8) therefore should not suffer from a "skin effect" as described by Knight (1992). A 2 m

cable extension on the probes was terminated with a BNC. The extension cable attached to the probe was of type RG-58A/U (Belden YR29183 (9311 type) 1C20 duobond II-braid RG-58A/U type 50 Ω E34972 (UL) CL2 OR AWM 1354---LL7874 CSA CXC FT1 JT..).

Table 2-2 Technical specifications of TRASE® and Pyelab time-domain reflectometry systems used in laboratory studies.

	TRASE® TDR	Pyelab TDR
EM generation	step pulse, step recovery diode	step pulse, tunnel diode circuitry
Digitised sample points	1200 (C9 pulser)	256
software	on-board	remotely controlled (computer)
θ determination	linear interpolation from look-up table of 17 points	polynomial
memory	190 graphs, 5700 readings (std)	computer limited
electrical conductivity determination	no	yes

Probes were also obtained locally from CSIRO Division of Soils in Adelaide SA (C. Hignett). The probe dimensions were similar to the SEC probes with locally sourced components and extension cable (source unknown).

Extension cables were obtained from Soilmoisture Equipment Corporation. Signal loss in extension cables was identified as a problem with the TRASE® system (pers. comm. J. Norris; Soilmoisture Equipment Corporation, USA) and SEC specifically requested low-loss cable from their supplier, Belden. Cable supplied was in two different forms being RG-58A/U (Belden YR40862 MV) and RG-8 (Belden 8214 1C11 braid RG-8 type 50 Ω E34972 (UL) OR AWM 1354...CSA LL7874 CXC FT1 NS..). All cable used in this experiment was from selected production with similar characteristics. The cable is manufactured with nominal impedance of 50 Ω. The extension cable characteristics are given in Table 2-3.).

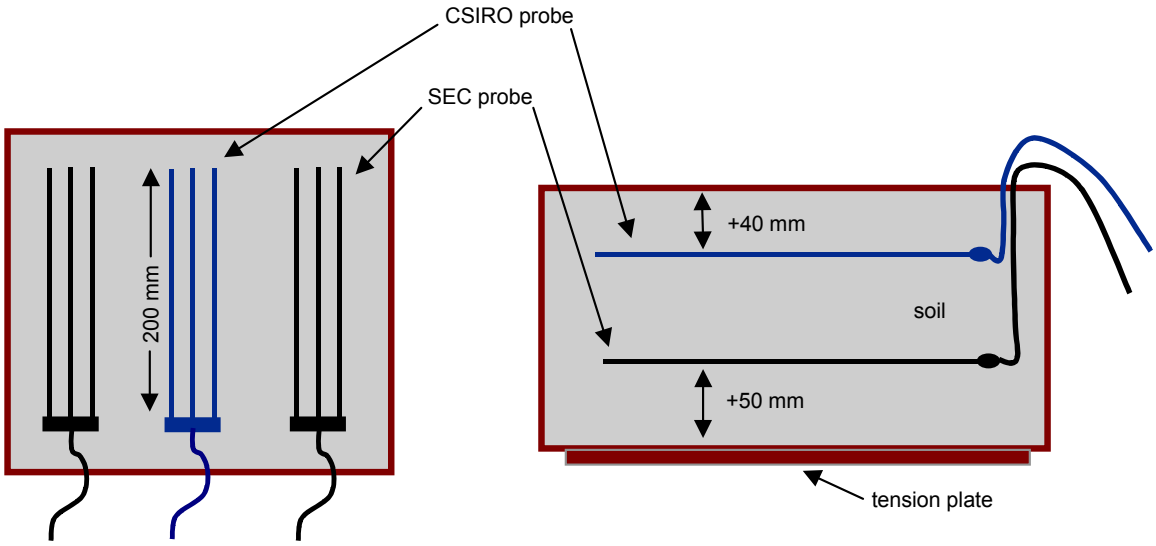

Figure 2-2 Schematic diagram of a tension table with embedded TDR probes. The probes were placed into the table as the soil was packed to ensure good contact.

Though the extension cable is ideally the same (Table 2-3) to minimise differences in EM waves the same cables were utilised. For the RG-58 readings extension cables were connected together for intermediate lengths (e.g. 15 m) and long lengths (> 20 m). A similar situation occurred with RG-8 extension cable for lengths > 25 m. This option minimises the potential for manufactured differences in extension cable causing a change in the generated EM wave. The connection of cables via the BNC connectors causes a small reflection of energy. To minimise this potential problem I did not use increasing lengths of extension cable in simple 5 m extensions. Cables were coiled after attachment to the embedded probe and TDR instrument. This did not significantly affect the EM wave during travel (data not shown).

2.3.2.3 Tension tables

Four tension tables were lined with crystalline silica (Commercial Minerals Ltd, Parramatta NSW, Australia) to ensure good contact between the soil and the tension plate during wetting and drying. The silica (200G) has a nominated silica content (SiO_2) of 99.1 %; Fe_2O_3 0.05 %; pH_{H_20} of 6.7; a specific gravity of 2.62; and a compacted bulk density (ρ_b) of 1.5 Mg m^{-3}. Particle size was < 150 µm with 88 % of sample between 3 µm and 75 µm according to technical information sheet (13th March, 1991 IHH). Care was taken during packing of the tension columns to minimise any mixing between the silica and packing soil. Two SEC TDR probes were horizontally positioned 50 mm from the soil-silica interface during packing. One CSIRO probe was placed 40 mm to 50 mm from the soil surface as the packing of the soil

continued. Packing of the columns varied with the soil type. The sand column was packed dry with thin layers deposited in the column and then slightly compressed (Oliviera *et al.*, 1996). The column containing the Vertosol was wetted during packing to account for potential swelling of the soil, which is a characteristic of Vertosols.

Table 2-3 Measured impedance and nominated loss of extension cable supplied by Soilmoisture Equipment Corporation.

	Measured impedance	Cable loss (db)
RG-58A/U		
5 m	49.5	5.2
10 m	49.8	4.7
20 m	49.6	7.5
RG-8		
15 m	49.9	5.2
20 m	48.9	7.0
25 m	49.2	5.3

The tension tables were connected to a vacuum system to allow for variable moisture control on wetting. The soil column was then slowly filled from the base, allowing for air to escape and achieving fully saturated conditions. Bulk density (ρ_b) was estimated for the column when initially packed and again at the completion of the experiment by the wax-block method (Blake & Hartge, 1986) and calculations and error is shown in Table 2-4. Results indicate small variation in the measured ρ_b. Considering the large clay content of the soil, variation through the soil column during packing is also expected (Yaron *et al.*, 1966). The initial ρ_b measurements were used to calculate θ from wetness (w) when the columns were saturated and the wax-block determination was utilised for later θ caculations. For analysis, error of the known θ is estimated by the combination of w and ρ_b errors outlined by Kendall & Stewart (1977). Where a single measurement of ρ_b is utilised, when the columns were saturated during the first run of TDR measurements, the variance of ρ_b from repeated measurements around SEC probes is employed. For the sand column the largest variance of ρ_b (Ferrosol $\pm$ 0.047; one standard error) was used in calculations.

Table 2-4 **ρ_b measured by total column dimensions prior to TDR measurements and the (post TDR measurements) wax-block method. One standard error in determination is given.**

	Sand	Chromosol	Ferrosol	Vertosol
Dimensions (L×W×H, m)	0.326 × 0.326 × 0.140	0.348 × 0.350 × 0.175	0.349 × 0.351 × 0.167	0.349 × 0.350 × 0.185
Packed volume (m^3)	0.01488	0.02131	0.02045	0.02324
Packed dry mass (kg)	18.5	24.4	23.0	25.6
Estimated ρ_b (Mg m^{-3})	1.42	1.15	1.09	1.10
Wax-block determination				
CSIRO probes	not determined	1.40 (± 0.093)	1.34 (± 0.037)	1.42 (± 0.147)
SEC probes	not determined	1.41 (± 0.026)	1.28 (± 0.022)	1.38 (± 0.063)
Average wax-block ρ_b	not determined	1.40 (± 0.055)	1.29 (± 0.043)	1.40 (± 0.097)

2.3.3 Measurements and determination of K_a

To obtain readings during a "run" the TRASE® TDR and Pyelab TDR were positioned near the tension table and the buried unbalanced probes connected directly to the respective instrument. Prior to each reading, a waveform from step-generation to well past inflection was taken and stored as a check on cable connections and general conditions. For each reported reading three measurements were taken and averaged in a similar fashion to Rothe *et al.* (1997). All measurements with the Pyelab TDR graphs were saved and one of the three readings saved as a graph with the TRASE® TDR. Information was automatically stored on a personal computer with the Pyelab TDR. Collected information on the TRASE® TDR was transferred to the personal computer via Terminal (© Microsoft, 1993) and information inspected with WinTRASE® (V1.11, beta test copy, © SEC and Jibray Inc).

After initial readings, different lengths of extension cable were inserted between the TDR instrument and the unbalanced probe embedded in the column. Again, triplicate readings were taken with each unbalanced probe and extension cable combination. The RG-58 cable readings were taken with cable combinations of: 0 m (connected to probe with 2 m cable), 5 m, 10m, 15 m, 20 m, 25 m, 30 m, and 35 m. The actual length of extension becomes $x + 2$ m as each probe has a 2 m cable from the end of the unbalanced probes to the BNC. Readings were limited to 35 m. The recommended maximum RG-58 extension cable length for the TRASE®

TDR is 30 m. Readings with the RG-8 cable reflected likely current usage. The RG-8 cable, with a heavier shield and supposed lower signal loss characteristics was recommended for longer extensions, especially with the C9 pulser in the TRASE® TDR system. The RG-8 cable was used in combination lengths of: 15 m, 20 m, 25 m, 30 m, 35 m, 40 m, 45 m, and 60 m.

The columns were situated in a temperature-controlled room with readings taken at equilibrium temperature near 20 °C (18 °C – 22 °C). Initial readings measured K_a when the soil in the tension columns was totally saturated. The columns were then air-dried over several weeks and returned to the temperature-controlled room for at least one-week before the measurements were repeated. All readings recorded the travel time (t) of the EM wave along the probes embedded in the soil.

2.4 RESULTS AND DISCUSSION

2.4.1 Comparison of reported θ by TDR instruments to known θ

Reported moisture content (θ) is the soil parameter we are normally interested in measuring with the TDR technique. A comparison of reported θ by the TRASE® TDR and Pyelab TDR systems to known moisture content ($_K\theta$) is shown in Figure 2-3 where the reported TDR θ is regressed against $_K\theta$. There is a significant difference between the $_K\theta$ and measured θ (p = 0.05) for the TRASE® ($p < 0.01$) and Pyelab ($p < 0.05$) TDR systems. Linear regression indicates a good fit of relationship ($r^2 = 0.984$) for the Pyelab TDR system ($_P\theta$) and a similar result ($r^2 = 0.952$) for the TRASE® TDR system ($_T\theta$). However, if the data from the Chromosol (when saturated) is excluded, the results of comparing the measured θ to $_K\theta$ are not significantly different. One explanation for this is the error in estimation of ρ_b when the columns were saturated. Also, the results indicate a sensitivity in the relationship possibly due to the limited data set compared to others (Malicki *et al.*, 1996; Yu *et al.*, 1997).

Error in measured θ and $_K\theta$ was estimated for all probes at smaller and larger moisture contents. The largest standard error of the mean (0.0084 $m^3\ m^{-3}$) was calculated for SEC probe (no. 4) embedded in the Vertosol at the lower $_K\theta$ of 0.153 $m^3\ m^{-3}$. Other values were consistently lower than 0.003 $m^3\ m^{-3}$ indicating little error in the determination of θ from repeated samples. Standard errors reported by the two TDR systems were also very small, generally less than 0.001 $m^3\ m^{-3}$. This is due to the repeatability of the TDR technique and measurements recorded (n = 10) in calibration.

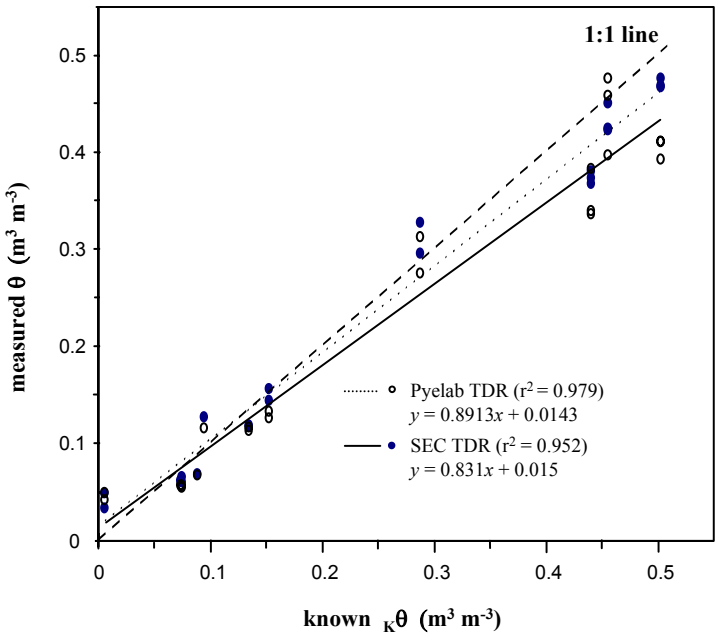

Figure 2-3 **θ measured by TRASE® and Pyelab TDR systems compared to $_K\theta$ (m^3 m^{-3}). When results from the saturated Chromosol are excluded there is no significant difference between the TRASE® TDR and Pyelab TDR systems in reported moisture to known moisture.**

2.4.2 Consideration of bulk density and soil dielectric

In determining the calibration for θ, consideration of the ρ_b is required to determine θ from the measured *w* (equation 1-4). The ρ_b of soil can be included as a parameter in the defining the θ(*K*) relationship shown by Malicki *et al.* (1996) as:

$$_{BD}\theta = \frac{\sqrt{K_a} - 0.819 - 0.168\rho_b - 0.159\rho_b^2}{7.17 + 1.18\rho_b} \qquad (2\text{-}1)$$

Though the ρ_b varied from 1.09 to 1.42 (Mg m^{-3}), analysis of variance of the normalised θ readings (accounting for ρ_b) did not improve the calibration through decreased residual mean square error (RMSE) for the Pyelab TDR. Inclusion of ρ_b in calibration decreased the RMSE for the TRASE® TDR. Equations for the linear fit of data (Figure 2-3) in calibration of the measured θ from $_K\theta$ for the TRASE® TDR and Pyelab TDR systems are shown in Table 2-5. The Pyelab TDR system calibration returned a slightly better fit to the experimental data compared to the TRASE® TDR system for the bulk calibration data set. The inclusion of ρ_b in calibration for θ determination increased the slope of calibration for the Pyelab and TRASE® TDR systems closer to a 1:1 relationship. Though cosmetically appealing, the inclusion of ρ_b did not significantly improve the relationship. At larger known θ the calibrated $_{BD}\theta$ (equation

2-1) for both TDR systems increases with the inclusion of ρ_b, compared to exclusion. The unmeasured error in determination of ρ_b when the soil was saturated could significantly influence the calibration, and the improvement in calibration, if any, needs to be further considered against error in determination of ρ_b.

Table 2-5 Inclusion of bulk density (Malicki *et al.*, 1996) and soil-solid dielectric (K_s) (Whalley, 1993) in calibration of TRASE® TDR and Pyelab TDR systems decreases RMSE for the TRASE® TDR system.

Equation	Coefficient of determination	RMSE ($m^3\ m^{-3}$)
${}_P\theta = 0.0143 + 0.891 \times {}_K\theta$	$r^2 = 0.979$	0.0250
${}_P\theta\ (\rho_b) = 0.0217 + 0.990 \times {}_K\theta$	$r^2 = 0.980$	0.0270
${}_P\theta\ (K_s) = -0.0315 + 1.066 \times {}_K\theta$	$r^2 = 0.981$	0.0289
${}_T\theta = 0.0150 + 0.831 \times {}_K\theta$	$r^2 = 0.952$	0.0357
${}_T\theta\ (\rho_b) = 0.0265 + 0.910 \times {}_K\theta$	$r^2 = 0.970$	0.0308
${}_T\theta\ (K_s) = -0.0297 + 0.981 \times {}_K\theta$	$r^2 = 0.971$	0.0327

Further parameterisation for calibration was considered beneficial by Whalley (1993), where he incorporated the soil-solid dielectric (K_s) in his equation (Equation 1-31). This equation can be re-arranged to give:

$$\theta = \frac{\sqrt{K_a} - \frac{\rho_b}{2.65}(\sqrt{K_s} - 1) - 1}{(\sqrt{K_w} - 1)} \qquad (2\text{-}2)$$

The reported K_s (measured as the oven dry K_a) by the TRASE® and Pyelab TDR systems for each soil is given in Table 2-6. The TRASE® TDR system reports a significantly larger ($p < 0.01$) K_s than the Pyelab system for individual soil. However, the average K_s for soil between the two TDR systems is not significantly different. Individual K_s for the different soils are used in Equation (2-2). The incorporation of the soil-solid dielectric did not significantly improve the $\theta(K)$ relationship (Table 2-5), with the residual error actually increasing for the TRASE® and Pyelab TDR systems compared to exclusion of K_s from the calibration.

Table 2-6 **Measured soil-solid dielectric (K_s) of the oven-dry soil (105 °C for 24 hours) with the TRASE® TDR and Pyelab TDR systems. θ is the reported moisture content from the respective TDR system with associated error.**

Soil	TRASE® TDR		Pyelab TDR	
	K_s (-)	θ ($m^3\ m^{-3}$)	K_s (-)	θ ($m^3\ m^{-3}$)
Sand	2.7 (± 0.0)	0.0188 (± 0.00042)	2.57 (± 0.036)	0.0182 (± 0.0007)
Chromosol	2.59 (± 0.032)	0.0154 (± 0.00052)	2.40 (± 0.019)	0.0141 (± 0.00032)
Vertosol	2.6 (± 0.0)	0.0156 (± 0.00052)	2.47 (± 0.023)	0.0156 (± 0.00084)
Ferrosol	2.82 (± 0.042)	0.0228 (± 0.00063)	2.72 (± 0.036)	0.0226 (± 0.00126)
Average	2.68 (± 0.097)		2.54 (± 0.128)	

2.4.3 Comparison of θ reported by TRASE® TDR and Pyelab TDR systems

The mean reported θ (n = 10) from the Pyelab TDR system for all soil types at saturated and air-dry conditions is plotted against the reported θ for the TRASE® TDR system (Figure 2-4). A paired t-test ($p = 0.05$) indicates no significant difference between the two TDR systems (also not significantly different from the 1:1 line).

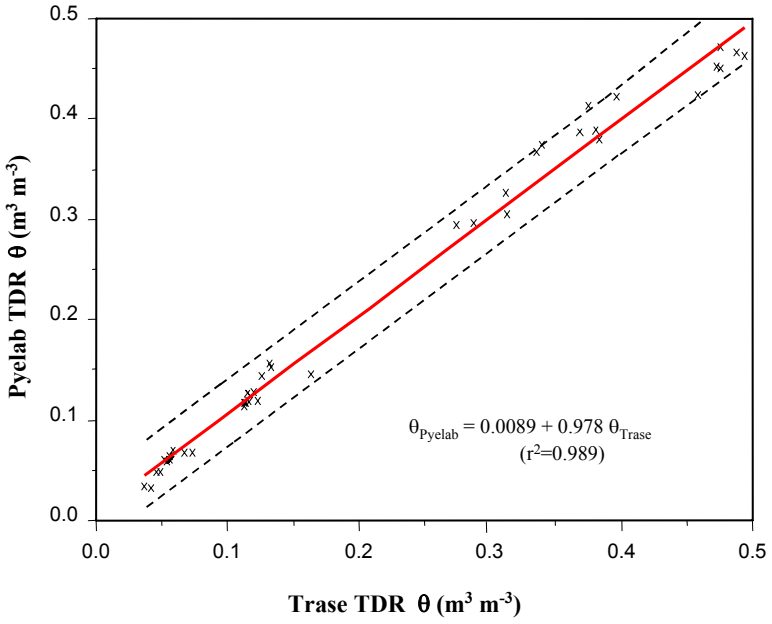

Figure 2-4 **Mean Pyelab TDR moisture content ($_P\theta$) plotted against TRASE® TDR moisture ($_T\theta$) for all probes. There is no significant difference ($p < 0.05$) in the relationship ($\theta_{Pyelab} = 0.0089 + 0.978\ \theta_{TRASE®}$).**

A plot of the residuals is shown in Figure 2-5. The Pyelab TDR system between $0.25 < \theta < 0.40$ m^3 m^{-3} reports a larger θ than the TRASE® TDR system. Also, when $\theta > 0.40$ m^3 m^{-3} the TRASE® TDR system reports lower θ than the Pyelab TDR system. This change in θ could be due to a difference in the measured travel time along the probes (eventually leading to a difference in calculated θ), or due to difference in conversion from measured K_a to reported θ for respective systems. To assess this possible difference in reported θ the determination of reported θ from K_a requires investigation.

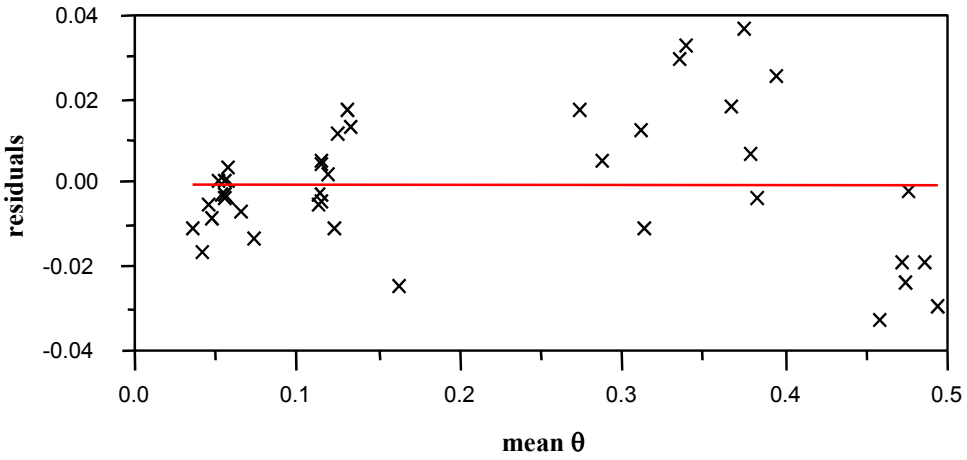

Figure 2-5 **Plot of water content residuals (from Figure 2-4) for all probes in all soil at different θ.**

2.4.4 TDR system conversion from K_a to θ

The Pyelab TDR system employs a third order polynomial relationship (Topp *et al.,* 1980) to determine moisture (θ) content. A "lookup table" using seventeen pairs of points and linear interpolation is utilised to estimate θ by the TRASE® TDR (Figure 9-15; Skaling, 1992). The two relationships are shown in Figure 1-10, noting Topp *et al.* (1980) recommended a limit to their relationship at $\theta_{TOPP} < 0.55$ m^3 m^{-3}. The conversion from measured K_a to θ, for the two TDR systems, is similar at lower moisture contents becoming significantly different when $K_a \geq 31.8$. If Topp *et al.'s* (1980) relationship is extended it is shown in Figure 1-10 to underestimate θ when compared to the TRASE® θ ($_T\theta$).

The increase in the associated residuals reported at larger moisture ($\theta > 0.45$ m^3 m^{-3}) contents is shown in Figure 2-5. This is possibly due to the differing calibration procedures in converting estimated K_a to θ by respective TDR systems. Also both TDR systems underestimate θ at larger moisture contents. Underestimation of θ at larger moisture content, especially in clay textured soil is possibly due to the change in the dielectric properties of the "bound" water (Dobson *et al.*, 1985; Roth *et al.*, 1990; Bohl & Roth, 1994

Underestimation of θ could arise by overestimation of ρ_b in soil columns. This problem of ρ_b determination increasing θ error is also a problem in field studies (Topp & Davis, 1981). Another possible explanation is an error in the derivation of the measured travel time (see equation 1-18.). In heavy (clay) soil, especially when wet, signal attenuation is a major constraint of TDR systems. The technique of end-point determination relies on a portion of the generated EM wave being reflected at the end of the probes. If the reflection is weak the ability of the software to derive the correct tangent fits is hampered (Zegelin *et al.*, 1992).

To nullify any calibration bias (or error) further analysis of the TDR system measurements compares the respective instrument reported K_a.

2.4.5 Comparison of reported K_a by TDR instruments

To evaluate the two TDR systems, comparing the measured K_a (i.e. before calibration is considered) allows estimation of their respective ability to determine K_a from measured travel time of the EM wave along the probes. Measurements were made by directly connecting the TDR instruments to embedded probes. Results shown in Figure 2-6 indicates a close

relationship between K_a measured by the TRASE® TDR compared to the Pyelab TDR system. There is a high correlation (r = 0.996) between readings with the relationship estimated by:

$$ {}_{P}Ka = -0.0828 + 1.037 \times {}_{T}Ka \qquad (2\text{-}3) $$

again with an expected good fit ($r^2 = 0.992$). There is no significant difference between the two slopes or the two intercepts ($p < 0.05$). This indicates that the TDR systems report a similar measured K_a and reported differences are then in determination of θ from K_a (i.e. estimated calibration algorithms).

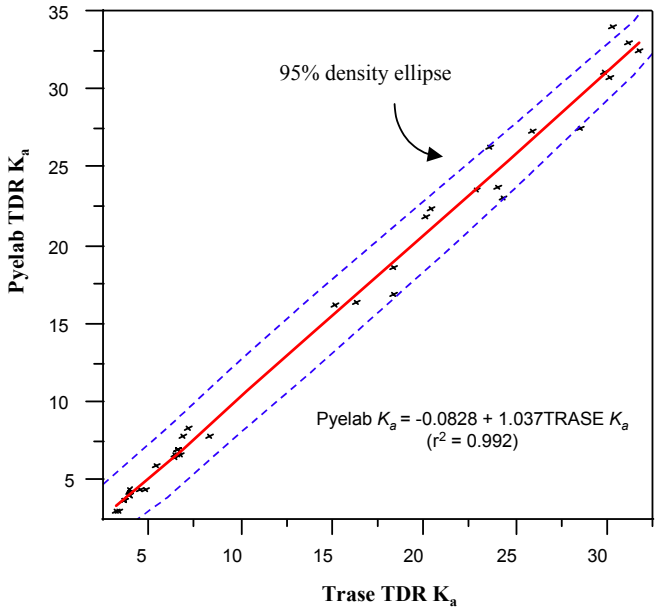

Figure 2-6 Regression of K_a determined by Pyelab TDR and TRASE® TDR systems. The relationship (equation 2-3) shows no significant difference between the reported K_a by the TRASE® and Pyelab TDR systems.

2.4.6 Calibration of Pyelab and TRASE® TDR systems

A preferred calibration involves the physically based relationship between the measured refractive index ($\sqrt{K_a}$) plotted against the ${}_{K}\theta$. The $\sqrt{K_a}$ is the square root of the measured K_a (Section 1.5.6) and several researchers, e.g. Herkelrath *et al.*, (1991); Whalley (1993); and Malicki *et al.*, (1996) have employed the relationship in calibration of the TDR technique in different soil. Figure 2-7 shows the calculated calibration for the TRASE® TDR and Pyelab TDR systems. A significant difference between the TRASE® TDR and Pyelab TDR slopes obtained in calibration exists ($p < 0.01$; t = 7.23, 40 d.f). The determination of $\sqrt{K_a}$ from the

Pyelab and TRASE® TDR systems yield similar relationships to that of Topp *et al.* (1980) when their equation (1-24) is formulated (where $\theta < 0.45$ m^3 m^{-3}).

$$ {}_P\sqrt{K_a} = 1.625 + 7.941\ {}_K\theta \qquad (2\text{-}4) $$

$$ {}_T\sqrt{K_a} = 1.663 + 7.265\ {}_K\theta \qquad (2\text{-}5) $$

$$ {}_{Topp}\sqrt{K_a} = 1.531 + 8.629\ {}_K\theta \qquad (2\text{-}6) $$

Though not incorporating the parameters of the mixing model approach, results are similar to those of Alharti & Lange (1987) and Lediu *et al.* (1986), especially where moisture content is small. The slope of the calibrations is lower than those reported by Lediu *et al.* (1986), possibly due to the limited soil types in calibration with large clay contents. Also, the ρ_b determination was not accounted for following comparison to Malicki *et al.*'s (1996) work considering the potential limitations in ρ_b determination, especially when the soil was saturated.

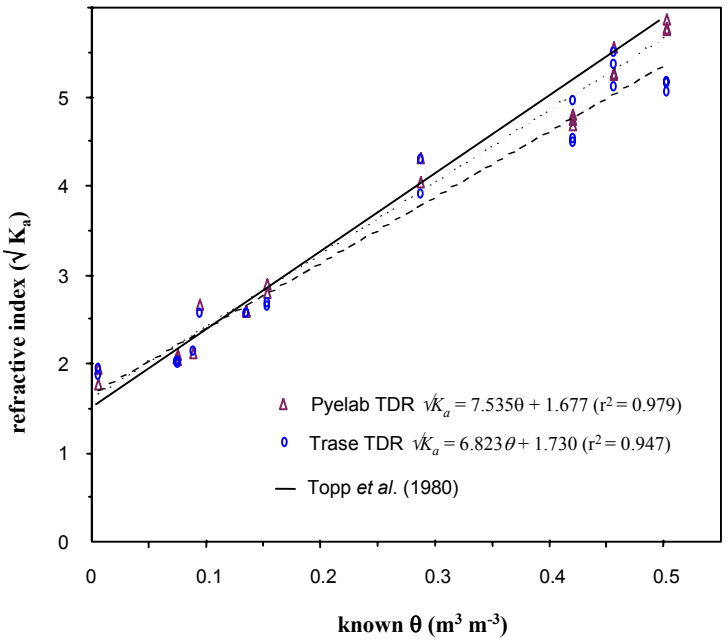

Figure 2-7 Linear relationship for calibration of measured refractive index ($\sqrt{K_a}$) against the known moisture content ($_K\theta$) for the TRASE® and Pyelab TDR systems. At higher moisture contents both TDR systems report a lower $\sqrt{K_a}$ compared to (the re-arranged) Topp *et al.*'s (1980) "universal" calibration.

Figure 2-7 shows the Pyelab TDR system returning larger K_a values compared to the TRASE® TDR system at larger moisture contents. Returning to Figure 2-3 this difference is masked by the system calibration procedures at larger moisture contents where the TRASE® calibration

will yield a larger θ compared to the derivation (via Topp *et al.* (1980) equation) of θ with the Pyelab TDR system at the same measured K_a.

After calibration we are interested in obtaining θ from the calculated K_a. The straight-line calibration curve is the inverse of the initial regression in the form:

$$x = \frac{(y - a)}{b} \tag{2-6}$$

in this case

$$\theta = \frac{(\sqrt{K_a} - a)}{b} \tag{2-7}$$

where *a* is the intercept, *b* the slope and $\sqrt{K_a}$ the refractive index. The error associated with the inverse estimation (prediction) in calibration requires more detailed consideration (Webster, 1997). The variance in determination of ${}_K\theta$ (for determined $\sqrt{K_a}$ against θ) is much less than the sum of the difference between the observed value (x_i) and the centroid ($\bar{x}$) and the confidence limits (*l*) for the calibration can be determined:

$$l = x_o \pm \frac{ts}{b}\sqrt{1 + \frac{1}{n} + \frac{\left(x_o - \bar{x}\right)^2}{\sum\left(x_{i-} \bar{x}\right)^2}} \tag{2-8}$$

where x_o is the predicted variable (θ); *t* is the Students t ($1.725_{0.05,20}$ in this case); *s* is the square root of the variance (of Y,x); *b* is the slope (of Y,x); and *n* is the number of observations in calibration (22 known moisture contents). The two calibration curves for the TRASE® TDR and Pyelab systems including error of prediction is shown in Figure 2-8.

Estimation of θ from measured K_a with the Pyelab TDR system is determined by:

$${}_{est\mathrm{P}}\theta = 0.1259\sqrt{K_a} - 0.2045 \quad (\pm 0.054 \text{ m}^3 \text{ m}^{-3}) \tag{2-9}$$

To estimate the θ from a measured K_a with the TRASE® TDR the equation is:

$${}_{est\mathrm{T}}\theta = 0.1376\sqrt{K_a} - 0.2289 \quad (\pm 0.062 \text{ m}^3 \text{ m}^{-3}) \tag{2-10}$$

The error in determination of θ from measured K_a is larger than that obtained by Topp *et al.* (1980) in an empirical calibration encompassing ρ_b and temperature for mineral soil (two standard errors ± 0.026 m^3 m^{-3}). Also, Skaling (1992) indicates an error of ± 0.02 m^3 m^{-3} for the TRASE® TDR in calibration.

The larger error in calibration for the TRASE® and Pyelab TDR systems could be due to several factors. Schaap *et al.* (1997) suggest the effect of the changing dielectric of water as it is bound to clay particles is considered in establishing a physically based calibration. This differs to the findings of Seyfried & Murdock (1996) where they found organic matter and bound water had an insignificant effect in calibration of a TDR system for measurement in frozen soil. The soil investigated here has large specific surface areas (Table 2-1) leading to a change in the dielectric behavior of the water in the mono-molecular layer (Campbell, 1990).

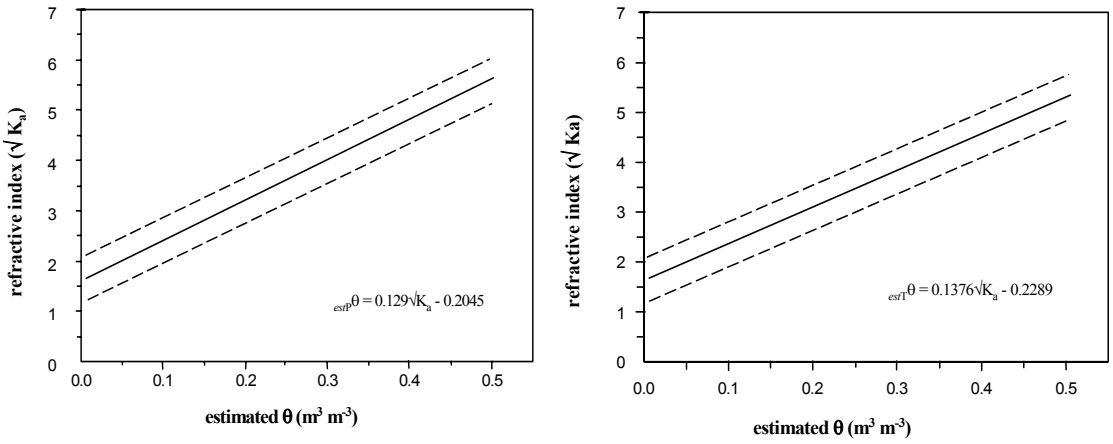

Figure 2-8 (a) Calibration of the Pyelab TDR. The linear θ(*K*) relationship is estimated by $_{est\mathrm{P}}\theta = 0.1259\sqrt{K_a} - 0.2045$. (b) Calibration of the TRASE® TDR. The linear θ(*K*) relationship is estimated by $_{est\mathrm{T}}\theta = 0.1376\sqrt{K_a} - 0.2289$.

Further consideration of determined bulk density (ρ_b) is important in measuring known θ in instrument calibration. Paltineanu & Starr (1997) report an order of magnitude difference in the coefficient of variation between bulk density and instrument reading in calibration of a frequency domain sensor. Error in ρ_b determination could lead to over- or under-estimation of $_K\theta$. Calculation of ρ_b, especially when the soil was saturated was without error estimation and the measurement was a bulk density calculation for the whole soil column. Some shrinkage of the soil during drying was observed and this is partially reflected in the ρ_b determined by the wax-block method. Also, change in the ρ_b of the soil around the actual probe was not considered, though this should be small.

As θ increases, attenuation of the signal occurs. The signal attenuation can lead to increased error in end-point determination as the slope declines. This is particularly problematic in saline soil and often multiple readings are required to obtain an average K_a after filtering of outliers (Herkelrath *et al.*, 1991). Figure 2-9 shows the change in the returning EM wave as soil moisture and extension cable length increases for a 200 mm probe embedded in the

Vertosol measured with the TRASE® TDR system. The decrease in the reflection coefficient with increasing extension cable length is similar to the qualitative findings of Heimovaara (1993). The travel time is measured from t0 to t1 and t2 for the dry and saturated soil respectively. Note the decline in the slope of the EM wave when the soil is wetter. Also, as the length of the extension cable is increased the EM wave is filtered and the slope declines relative to the control (0 m extension cable).

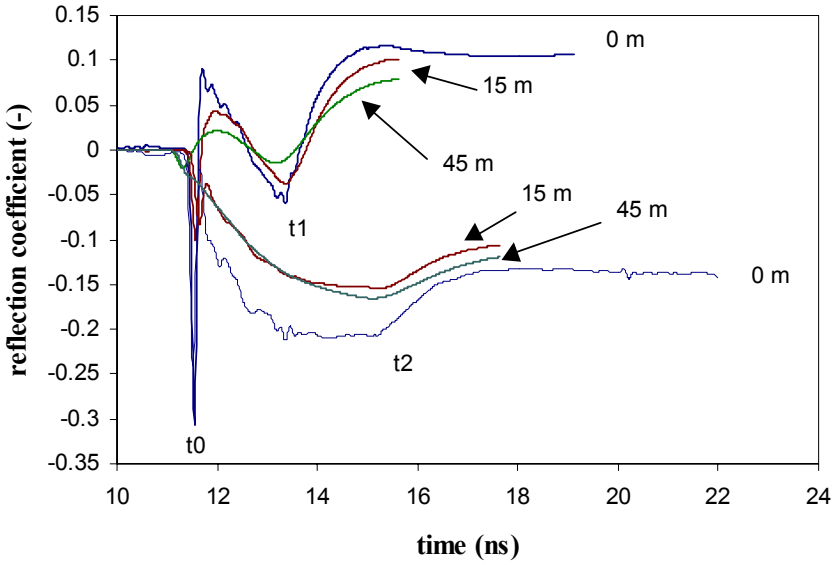

Figure 2-9 EM wave measured by the TRASE® TDR system along 200 mm unbalanced probes embedded in a Vertosol. The travel time is measured from t0 to t1 and t2 when the soil is first dry and then wetted. Note the decrease in the slope as the EM wave is reflected at the end of the probes.

2.4.7 Effect of extension cable on reported K_a

2.4.7.1 Combined data for the RG-58 extension cable

Readings from all measurements were normalised against the readings connected to the respective TDR without extension cable. For example (from Figure 2-11(i)), the normalised reading for the TRASE® TDR with a 10 m extension cable is 5.753/5.624 = 1.023; where 5.735 is the average $\sqrt{K_a}$ (n = 3) for readings with a 10 m extension cable and 5.624 is the average $\sqrt{K_a}$ (n = 3) when the probe is connected directly to the TDR system. A stepwise regression (entry probability 0.05 significance and probability to exit 0.10 significance) was used to determine significant parameters and then the model produced by least squares

estimation (Figure 2-10). To explain 62.2 % of the variation a total of six parameters were used: TDR system; TDR probe; cable length; standard error of measurements; clay content and soil water content (either saturated or air dry). There is no clear relationship between increasing cable extension and change (increase) in measured $\sqrt{K_a}$. To establish if there is a relationship, further differentiation of the data set is considered in more detail.

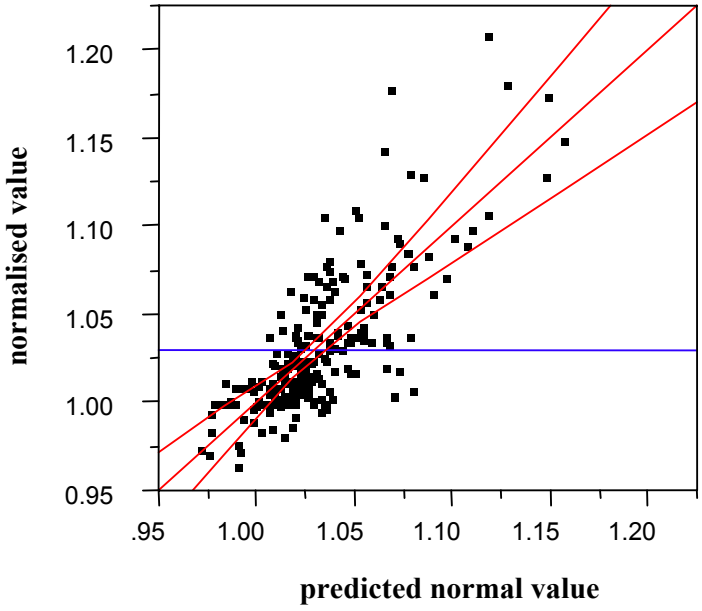

Figure 2-10 Model fit of normalised $\sqrt{K_a}$ for all soil with RG-58 extension cable connections. The model explains 62.2 % of the variation whilst accounting for interactions between soil type (as clay %), cable length, TDR system, TDR probe, moisture conditions of the soil (saturated versus air dry) and standard deviation of measurements. Cable length was not significant as a single parameter.

2.4.7.2 Vertosol as an example

An example of determination of K_a (shown as $\sqrt{K_a}$, the refractive index) in a Vertosol with the RG-58 extension cable attached to Soilmoisture Equipment Corporation (SEC) unbalanced probes and locally produced (CSIRO, Adelaide) probes is shown in Figure 2-11. Further results for individual soil types are shown in Appendix 2-1.

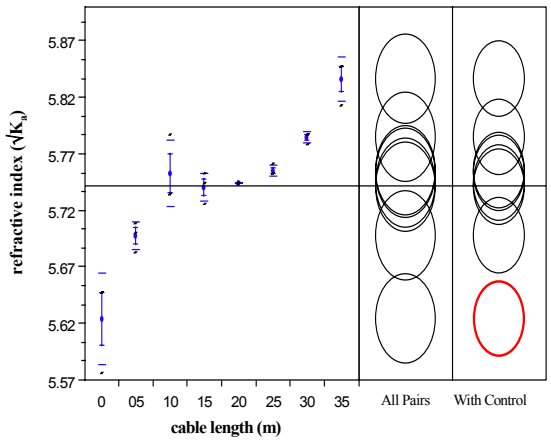

(i)

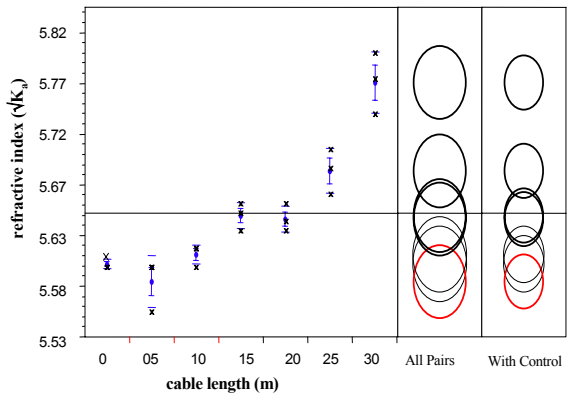

(ii)

Figure 2-11 TRASE® TDR determination of K_a in a saturated Vertosol. (i) is a Soilmoisture Equipment unbalanced probe, (ii) CSIRO unbalanced probe. The TRASE® TDR did not determine the end-point of the reflected EM wave for the 35 m extension cable.

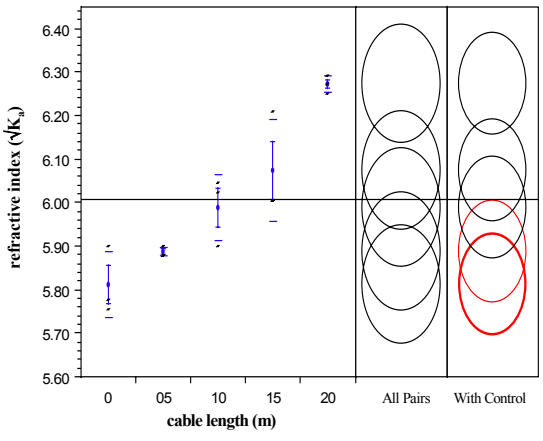

(i)

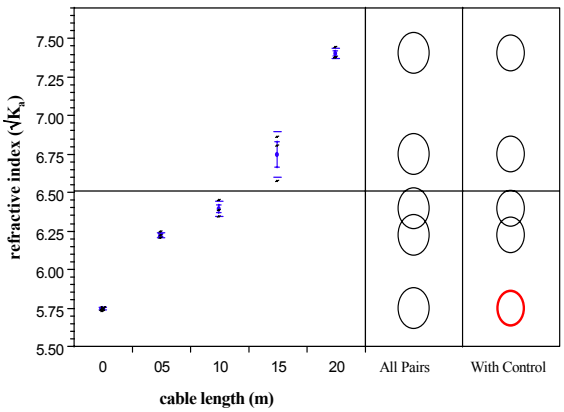

(ii)

Figure 2-12 Pyelab TDR determination of K_a in a saturated Vertosol. (i) is a Soilmoisture Equipment unbalanced probe, (ii) CSIRO unbalanced probe. The Pyelab TDR could not determine the end-point of the reflected EM wave for extension cable lengths greater than 20 m in the saturated Vertosol

A comparison of means test utilising the least significant difference (LSD) from a Tukey-Kramer test indicates differences between triplicate readings. The Tukey-Kramer test is preferred for multiple comparisons to minimise Type I errors (Carmer & Walker, 1982; SAS Institute, 1995). Visually this is interpreted as significant difference in $\sqrt{K_a}$ where the angle of intersection between overlapping circles is < 90°. Also where circles do not overlap at all a significant difference in the measured $\sqrt{K_a}$ is expected. The control is determined as the measured $\sqrt{K_a}$ when the probe is connected directly to the respective TDR system. To estimate

if reported $\sqrt{K_a}$ is significantly different from the control (0) a Dunnett's test (again using the protected LSD at a 5 % significance level) is conducted (SAS Institute, 1995).

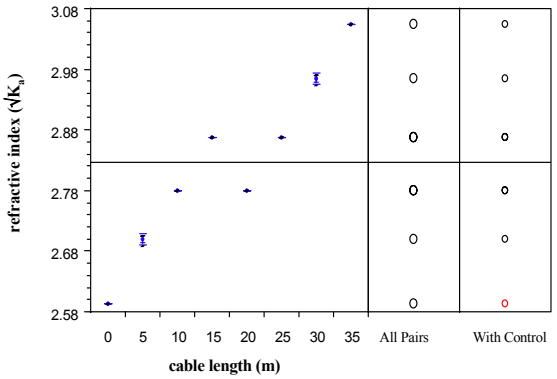

(i)

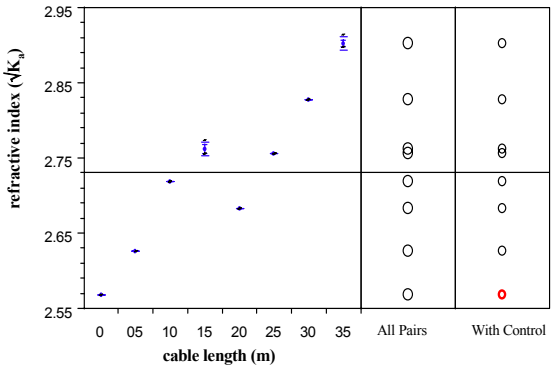

(ii)

Figure 2-13 TRASE® TDR determination of K_a in an air-dry Vertosol. Measurements are taken with 200 mm long probes attached to varying length RG-58 cable. (i) is a SEC unbalanced probe, (ii) CSIRO unbalanced probe. The TRASE® TDR did not determine the end-point of the reflected EM wave for the 35 m extension cable.

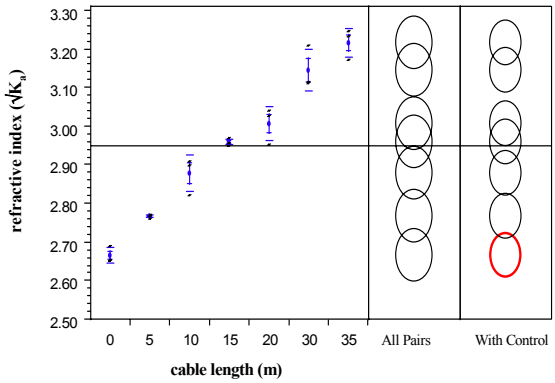

(i)

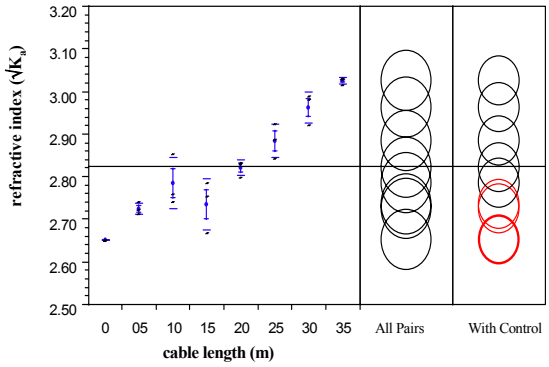

(ii)

Figure 2-14 Pyelab TDR determination of K_a in an air-dry Vertosol. Measurements are taken with 200 mm long probes attached to varying length RG-58 cable. (i) is a SEC unbalanced probe, (ii) CSIRO unbalanced probe. The Pyelab TDR could not determine the end-point of the reflected EM wave for extension cable lengths greater than 20 m in the saturated Vertosol

Significant differences exist between the measured $\sqrt{K_a}$ with the TRASE® TDR and Pyelab TDR systems in saturated and unsaturated soil with both probes. Figures 2-11, 2-12, 2-13 and 2-14 show the differences between reported $\sqrt{K_a}$ due to the addition of RG-58 extension cable. Generally an increase in reported $\sqrt{K_a}$ occurs as the extension cable length increases. When the soil is saturated (Figure 2-11) the TRASE® TDR system obtained readings for all cable lengths from 0 to 35 m extension. Results (Figure 2-12(i)) indicate a saw-tooth pattern with an

increase in reported $\sqrt{K_a}$ from the control (0 m) to 10 m, then no significant increase in reported $\sqrt{K_a}$ until 30 m and 35 m extension cables are employed. The CSIRO probe yielded a different result (Figure 2-12(ii)). There was no significant difference in results with extension cables of 5 m and 10 m length from the control. A difference exists with extension cables greater then 10 m.

The TRASE® TDR and Pyelab TDR systems respond differently to increasing RG-58 extension cable. The SEC probe and CSIRO probes also respond differently to the changing moisture conditions. These changes indicate the response to increasing extension cable length is masked in the model (Figure 2-10) where 62.2 % of the variation is explained. Figure 2-15 and Figure 2-16 shows the modelled response of the increasing extension cable with the different TDR systems, probes and moisture contents. In the saturated Vertosol the Pyelab TDR and TRASE® TDR systems reported increasing refractive index ($\sqrt{K_a}$) with increasing cable length. The linear relationship between the increasing extension cable length and $\sqrt{K_a}$ is shown in Figure 2-15. When the Vertosol was at smaller moisture conditions the Pyelab TDR system still exhibited a linear response to increasing extension cable length. The TRASE® TDR system response is better explained when the extension cable length is split at 15 m to 20 m (Figure 2-16(iii) and Figure 2-16(iv)). This could be due to the timing mechanism used by the TRASE® TDR system and measurement of travel time at different cable lengths that affect the Tektronix TDR systems (Hook & Livingston, 1995). Information on the time-base mechanism used by the TRASE® TDR system is not available.

Analysis of the waveform (data not shown) indicates that the CSIRO probe yields a greater spike (due to larger impedance) in the waveform on entering the soil. This assists in the automatic determination of the start point of the EM wave and by increasing the energy difference could improve the end-point determination in lossy soil, in this case a wet, large specific surface area Vertosol. The increase in the reflection coefficient could also improve the ability of the TDR software to determine the start point (Heimovaara, 1993). However, the increased energy associated with the EM wave entering the soil also leads to greater loss of energy and this reduces the ability of the TDR instrument to obtain a measurement due to increased attenuation.

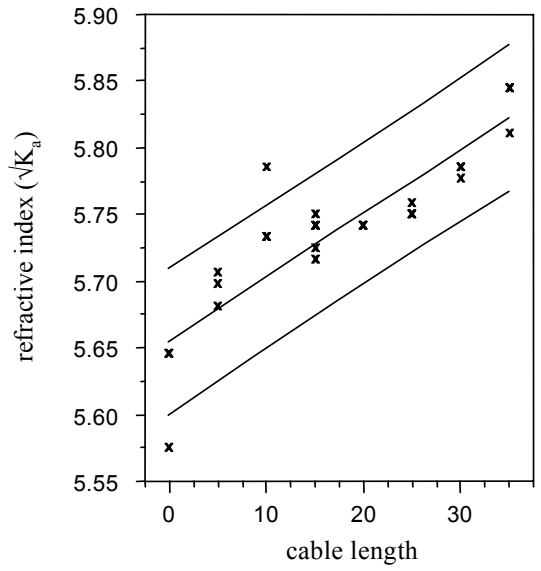

(i)

Figure 2-15 Increase in $\sqrt{K_a}$ measured by a TRASE® TDR connected via RG-58 coaxial cable to a SEC probe in a saturated Vertosol. The relationship is modelled by $\sqrt{K_a}$ = 5.655 + 0.0048 × cable (m) (r^2 = 0.832).

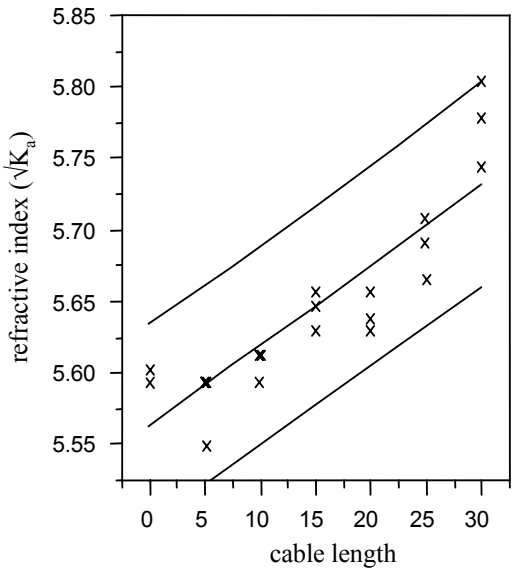

(ii)

Figure 2-15 Increase in $\sqrt{K_a}$ measured by a TRASE® TDR connected via RG-58 coaxial cable to a CSIRO probe in a saturated Vertosol. The relationship is modelled by $\sqrt{K_a}$ = 5.563 + 0.0056 × cable (m) (r^2 = 0.774).

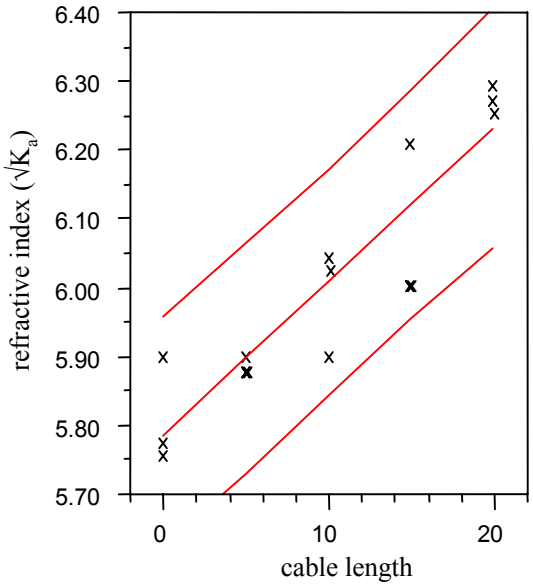

(iii)

Figure 2-15 Increase in $\sqrt{K_a}$ measured by the Pyelab TDR connected via RG-58 coaxial cable to a SEC probe in a saturated Vertosol. The relationship is modelled by $\sqrt{K_a}$ = 5.788 + 0.0223 × cable (m) (r^2 = 0.842).

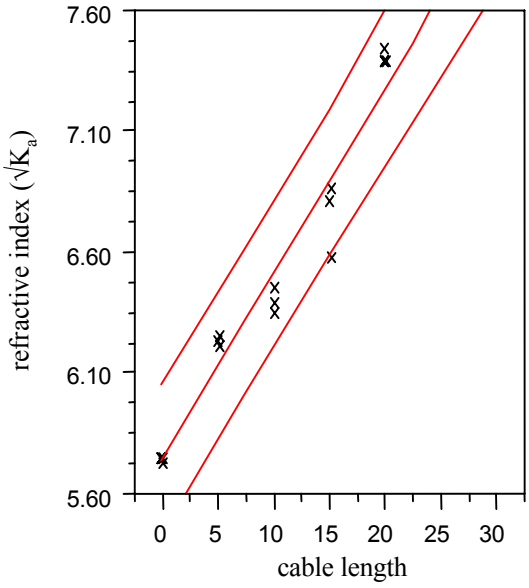

(iv)

Figure 2-15 Increase in $\sqrt{K_a}$ measured by the Pyelab TDR connected via RG-58 coaxial cable to a CSIRO probe in a saturated Vertosol. The relationship is modelled by $\sqrt{K_a}$ = 5.7423 + 0.077 × cable (m) (r^2 = 0.950).

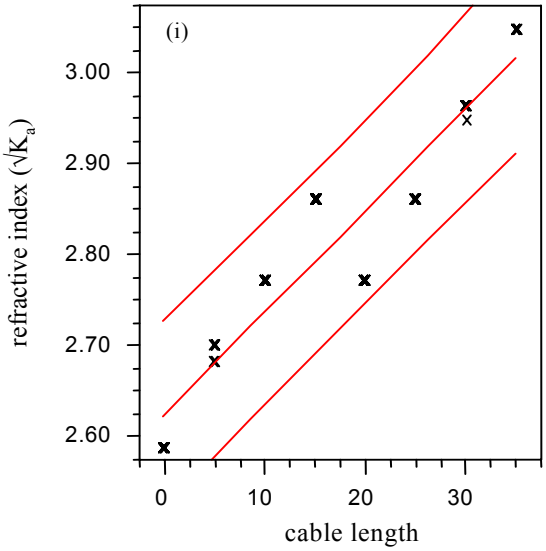

Figure 2-16 Increase in $\sqrt{K_a}$ measured by the TRASE® TDR connected via RG-58 coaxial cable to a SEC probe in an air-dry Vertosol. The relationship is modelled by $\sqrt{K_a}$ = 2.6243 + 0.0113 × cable (m) (r^2 = 0.891).

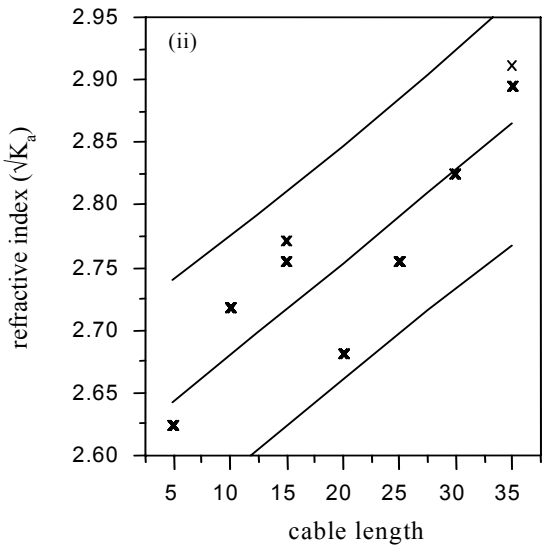

Figure 2-16 Increase in $\sqrt{K_a}$ measured by the TRASE® TDR connected via RG-58 coaxial cable to a CSIRO probe in an air-dry Vertosol. The relationship is modelled by $\sqrt{K_a}$ = 2.6058 + 0.0074 × cable (m) (r^2 = 0.766).

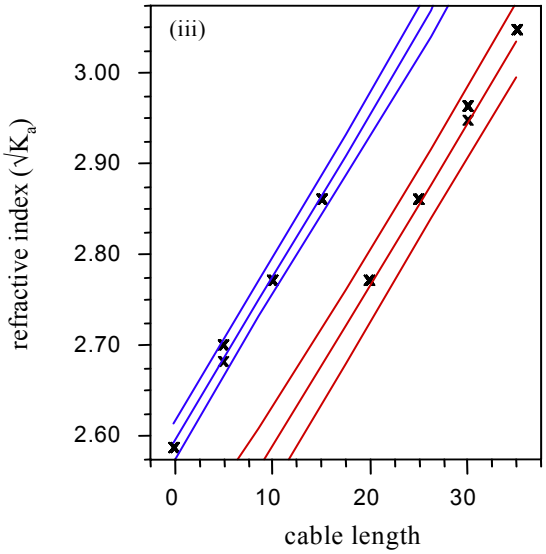

Figure 2-16 Increase in $\sqrt{K_a}$ measured by the TRASE® TDR connected via RG-58 coaxial cable to a SEC probe in an air-dry Vertosol. A straight-line relationship for extension cable ≤ 15 m is $\sqrt{K_a}$ = 2.595 + 0.0181 × cable (m) (r^2 = 0.994) and for RG-58 cable ≥ 20 m the relationship is given by $\sqrt{K_a}$ = 2.4071 + 0.0180 × cable (m) (r^2 = 0.970).

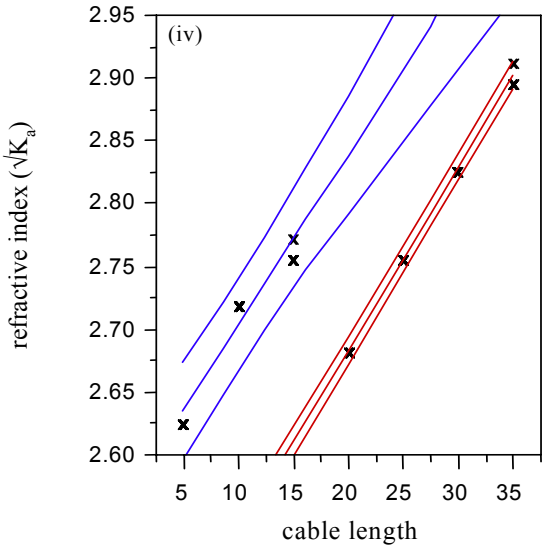

Figure 2-16 Increase in $\sqrt{K_a}$ measured by the TRASE® TDR connected via RG-58 coaxial cable to a CSIRO probe in an air-dry Vertosol. A straight-line relationship for extension cable ≤ 15 m $\sqrt{K_a}$ = 2.5672 + 0.0136 × cable (m) (r^2 = 0.948) and for RG-58 cable ≥ 20 m the relationship is given by $\sqrt{K_a}$ = 2.3895 + 0.0147 × cable (m) (r^2 = 0.997).

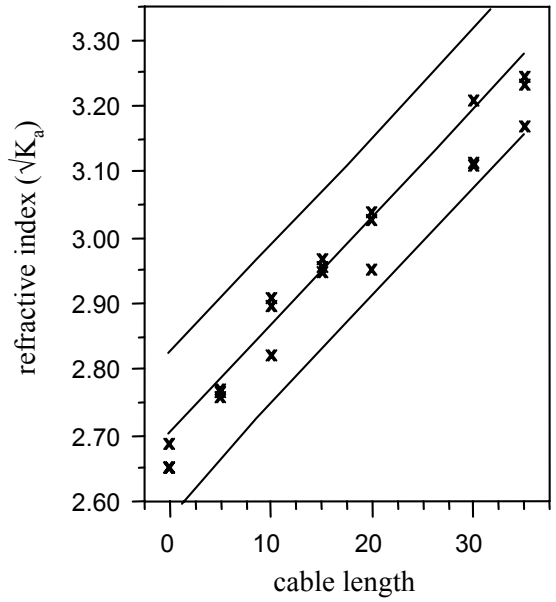

(v)

Figure 2-16 Increase in $\sqrt{K_a}$ measured by the Pyelab TDR connected via RG-58 coaxial cable to a SEC probe in an air-dry Vertosol. A straight-line relationship for RG-58 extension cable is $\sqrt{K_a}$ = 2.7036 + 0.0165 × cable (m) (r^2 = 0.914).

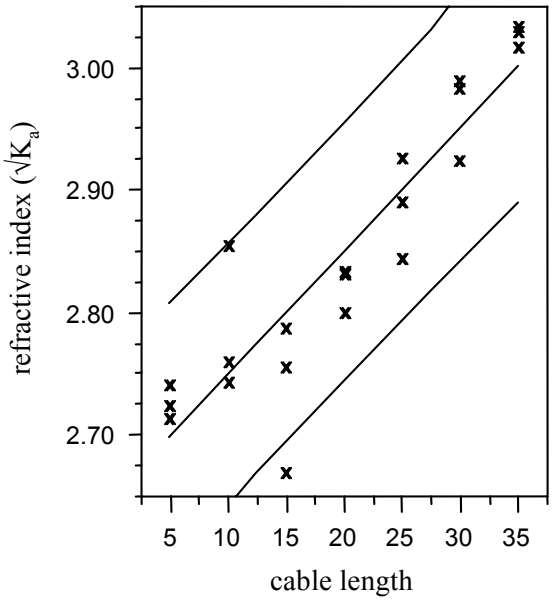

(vi)

Figure 2-16 Increase in $\sqrt{K_a}$ measured by the Pyelab TDR connected via RG-58 coaxial cable to a CSIRO probe in an air-dry Vertosol. A straight-line relationship for RG-58 extension cable is $\sqrt{K_a}$ = 2.6491 + 0.0101 × cable (m) (r^2 = 0.824).

Plotting the normalised waveform for the SEC probe with the CSIRO probe (Figure 2-17) indicates the relative power loss due to increased attenuation with the CSIRO probe when the 25 m extension cable is introduced. The incorporation of a capacitor (in the CSIRO probe) will improve the ability of the TRASE® TDR system in correctly identifying start and end-point in attenuative situations, especially when small extension cable lengths are employed. This benefit could be offset by the increased impedance reducing the ability of the CSIRO probe as the EM signal is filtered (and conducted) with increasing extension cable length.

As the EM wave travels through the lossy medium (in this case soil) guided by the probe, the change in impedance causes many multiple reflections. This is particularly evident when the probe is connected directly (via 2 m cable) to the TDR system. If an extension cable is included the impedance changes are filtered, especially the higher frequencies (pers. comm. H. Fancher; SEC CA, USA). This produces a smoothing of the observed EM waveform as shown in Figure 2-18. The attenuation of the higher frequencies is further complicated by the lower signal to noise ratio as frequency increases (Heimovaara, 1996). The normalised EM

waveforms (Figure 2-18) show a decrease in the proportion of the EM wave returning along the probes buried in the soil.

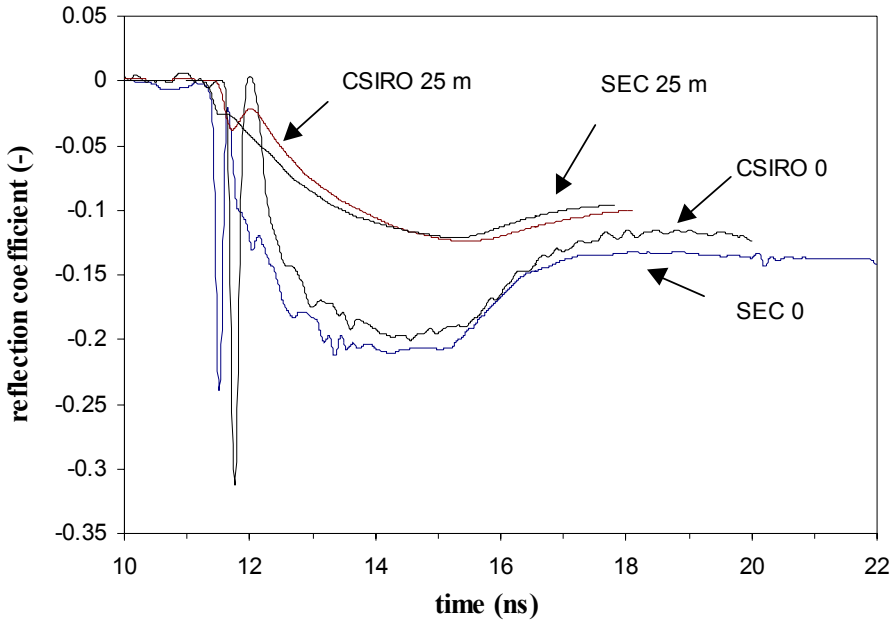

Figure 2-17 Normalised SEC probe and CSIRO probe measured with the TRASE® TDR for control and 25 m extension cable length. The TRASE® TDR did not pick the end-point for the 25 m extension cable measured with the CSIRO probe.

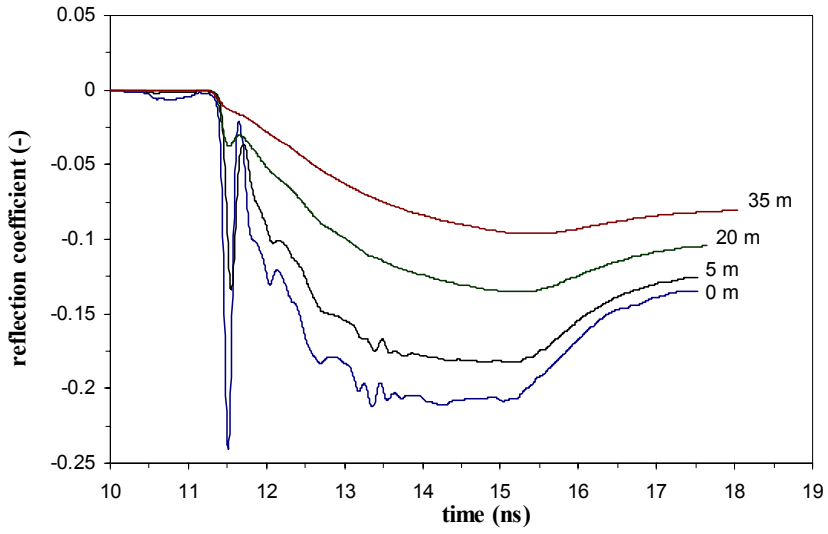

Figure 2-18 Normalised EM waveforms for the SEC probe measured with the TRASE® TDR system in the saturated Vertosol for control, 5 m, 20 m and 35 m RG-58 extension cable. With increasing extension cable there is a decrease in the energy of the returning EM wave and corresponding decline in the slope of the reflected EM wave.

Associated with a decrease in the energy of the returning EM wave is a decline in the measured slope for start and end-point determination. This is readily observed when plotting voltage versus time for different treatments (Figure 2-18). The determination of the slope is important, as the automatic software regimes aim to determine the intersection of the two tangents at the end of the probe (Figure 2-19). To identify a quantitative difference the slopes are measured and compared testing the estimates of slope between regression outlined by Steel & Torrie (1980). The slope is measured from the WinTRASE® output and points manually selected from the accompanying time interval (forced to yield the same slope). As the length of extension cable increases the number of points used in slope estimation decreases from 77 points with the control to a low of 42 points for the 35 m extension measured with the TRASE® TDR. However the pooled variance used in determination of the Student's *t* remains very small due to the existing data relationship of voltage versus time. A significant difference between the control slope and all slopes with the addition of extension cable exists. The difference in slope explains the change in measured $\sqrt{K_a}$ leading to different reported moisture contents. Though slopes may be significantly different the important consideration is the change in reported θ. The change in reported θ is shown in Table 2-6. For the TRASE® TDR system, the maximum difference in θ when the soil is saturated with extension cable is 0.043 $m^3\ m^{-3}$ measured with 35 m length of extension cable. This is a change of + 8.8 % from the control. The greatest change in reported θ with the Pyelab TDR system occurred with the 20 m extension cable (+ 7.4 %). Readings were not obtained with greater extension cable length due to attenuation of the EM waveform and no end-point determination possible. For the TRASE® TDR system, a similar pattern exists when the soil is air-dried. The change in reported θ is greatest when the extension cable is again 35 m. This represents a change of > 40 % from the control. The Pyelab TDR system successfully measured all lengths of extension cable to 35 m. The greatest change from the control (0 m) occurred with the 35 m extension cable, a difference of +0.062 $m^3\ m^{-3}$ (> 40 % increase).

Table 2-6 Difference in reported θ (m^3 m^{-3}) for the TRASE® TDR and Pyelab TDR systems. The maximum difference is bolded for the two TDR systems in saturated and air dry Vertosol measured with increasing lengths of RG-58 extension cable.

	TRASE® TDR system			Pyelab TDR system		
Extension cable length (m)	Reported θ (m^3 m^{-3})	$\theta_0 - \theta_t$ (m^3 m^{-3})	% difference	Reported θ (m^3 m^{-3})	$\theta_0 - \theta_t$ (m^3 m^{-3})	% difference
0	0.491	0.000	0.00	0.472	0.000	0.00
5	0.504	0.013	2.65	0.478	0.006	1.27
10	0.516	0.025	5.09	0.486	0.014	2.97
15	0.513	0.022	4.48	0.492	0.020	4.31
20	0.514	0.023	4.75	**0.507**	**0.035**	**7.42**
25	0.517	0.026	5.30	no reading		
30	0.523	0.032	6.45	no reading		
35	**0.534**	**0.043**	**8.76**	no reading		
0	0.134	0.0	0.0	0.153	0.0	0.0
5	0.139	0.005	3.73	0.161	0.008	5.23
10	0.147	0.013	9.70	0.166	0.013	8.50
15	0.157	0.023	17.16	0.175	0.022	14.38
20	0.147	0.013	9.70	0.183	0.03	19.61
25	0.155	0.021	15.67	0.188	0.035	22.86
30	0.174	0.04	29.85	0.198	0.045	29.41
35	**0.190**	**0.056**	**41.79**	**0.215**	**0.062**	**40.53**

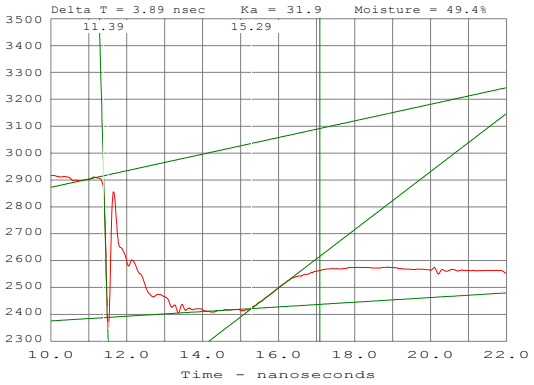

(i) control (0 m extension) with measured travel time of 3.89 ns.

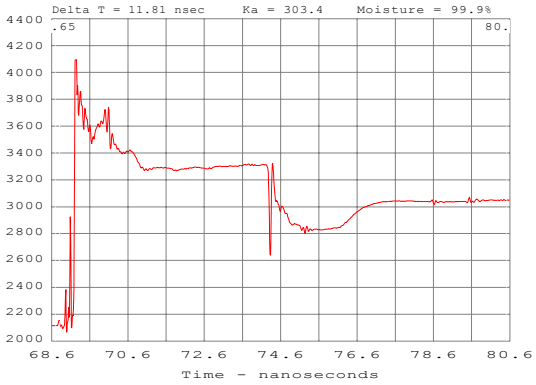

EM wave from generation to travel through the soil (< 74.6 ns to ≈76.4 ns).

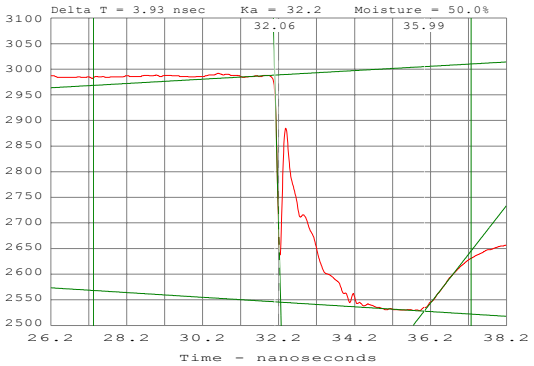

(ii) 5 m extension cable connected to probe with measured travel time of 3.93 ns.

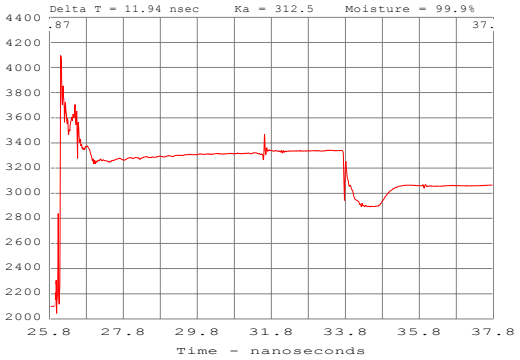

EM wave travel for 5 m extension cable from generation to well past end-point deter-mination.

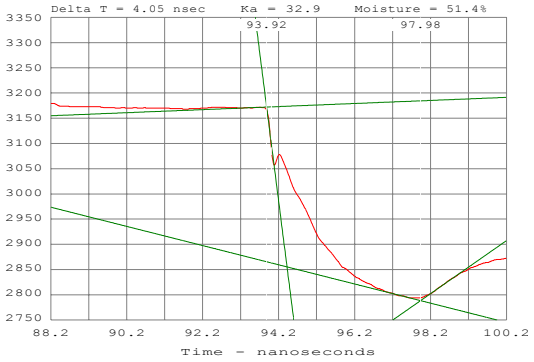

(iii) 20 m extension cable connected to probe with measured travel time of 4.05 ns.

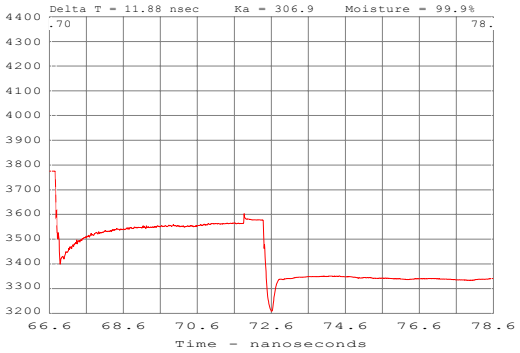

EM wave travel for 20 m extension cable from generation to well past end-point determination.

Figure 2-19 Graphical output from the WinTRASE® program for determination of θ with the TRASE® TDR system. The left-hand column shows the individual waveforms for control, 5 m and 20 m RG-58 extension cable for a SEC probe buried in a saturated Vertosol. The right hand column indicates the travel of the EM wave from generation inside the TDR unit through the extension cable and finally along the embedded probes in the soil. The y-axis is a relative voltage output from the TRASE® TDR system that is autoscaled.

2.4.7.3 Measurement with RG-8 extension cable in a Vertosol

The TRASE® TDR and Pyelab TDR systems report larger K_a as the extension cable length increases. In the saturated and air-dried Vertosol the Pyelab TDR system yields a positive linear response to the increasing extension cable length. Figure 2-20 shows the Pyelab TDR system reports an increase in K_a (shown as $\sqrt{K_a}$) with increasing extension cable at lower moisture contents (determined with Dunnet's test with control). The trend was consistent for all probes.

The TRASE® TDR responds in a similar positive trend when the Vertosol is drier (Figure 2-21(i)). The two SEC probes exhibit a similar increasing trend though with significant differences in $\sqrt{K_a}$ at different extension lengths. Figure 2-21(i) shows a significant ($p < 0.05$) increase in the reported $\sqrt{K_a}$, particularly with the 45 m and 60 m extension cables, when measured with the TRASE® TDR system. This indicates the potential limitation of the RG-8 extension cable at 45 m without calibration. The reported $\sqrt{K_a}$ with the CSIRO probe also increased with increasing length of extension cable.

When the soil is saturated the response is more erratic. However, the TRASE® TDR and Pyelab TDR systems were less affected by the extension cable length on reported $\sqrt{K_a}$. Only the 45 m extension cable reported significantly larger $\sqrt{K_a}$ compared to the control $\sqrt{K_a}$ measured with the SEC probe. The Pyelab TDR system again reported significantly increased $\sqrt{K_a}$ for the 20 m, 25 m and 30 m extension cable. No readings were obtained with the extension length >30 m due to signal attenuation leading to no reflection. Limitations on extension cable length is soil dependent (Herkelrath *et al.*, 1981; Dalton, 1992) and TDR system dependent. Results with the CSIRO probe did not indicate a systematic effect of increase in extension cable length on reported $\sqrt{K_a}$ with the TRASE® TDR system. Initially $\sqrt{K_a}$ declined with increasing cable length and then (>30 m extension) increased with extension cable length.

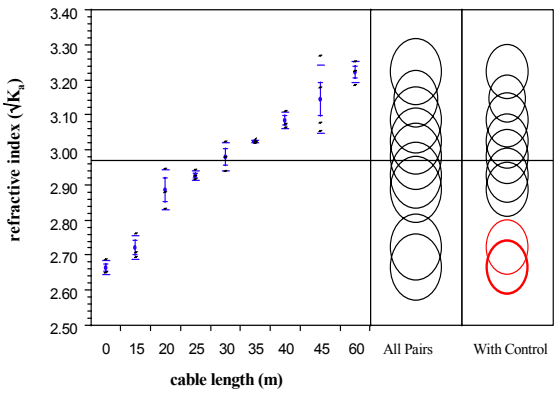

(i)

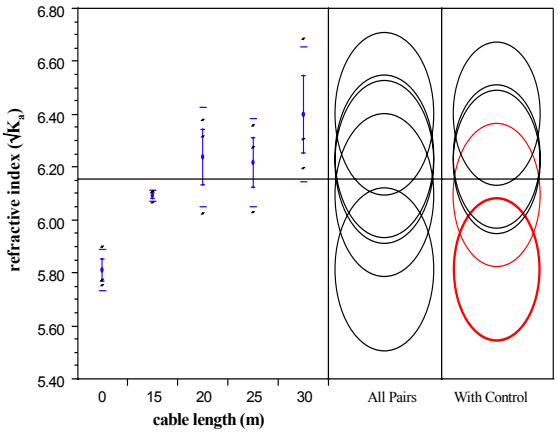

(ii)

Figure 2-20 Pyelab TDR determination of K_a in a Vertosol. (i) increasing $\sqrt{K_a}$ with increasing extension cable in air-dry soil, (ii) increasing $\sqrt{K_a}$ when extension cable was > 20 m before attenuation of the EM wave did not allow end-point determination at 35 m (extension) in wet soil.

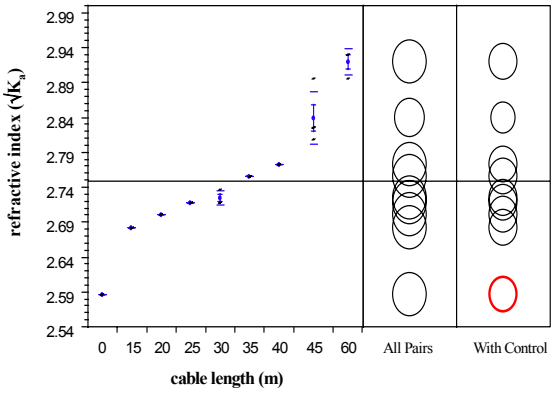

(i)

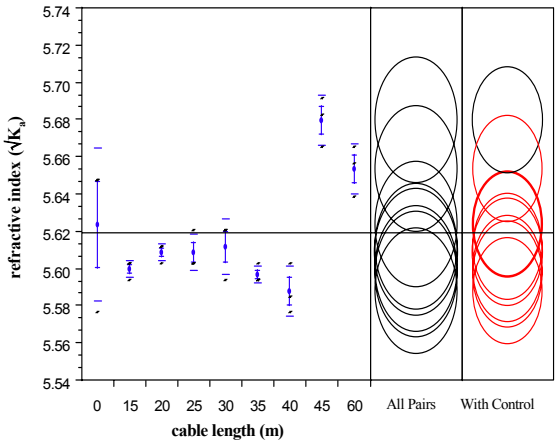

(ii)

Figure 2-21 TRASE® TDR determination of K_a in a Vertosol. (i) increasing $\sqrt{K_a}$ with increasing extension cable in air-dry soil, (ii) large error in control reading masks potential differences by increasing extension cable length. 45 m extension cable is significantly different from the control ($p < 0.05$) in wet soil.

The normalised waveforms for the control plotted with 15 m, 30 m, 45 m and 60 m RG-8 extension cable is shown in Figure 2-22. As with the RG-58 extension cable the EM wave is filtered during travel along the cable resulting in loss of resolution in start and end-point determination procedures. The tangent fitting to the slope becomes increasingly difficult as the extension cable length increases. This often leads to larger standard errors in reading, especially in field situations with heterogeneous dielectric material along the probes. To overcome this problem the number of samples recorded and averaged for each reading is increased (Herkelrath *et al.*, 1991; Heimovaara *et al.*, 1995).

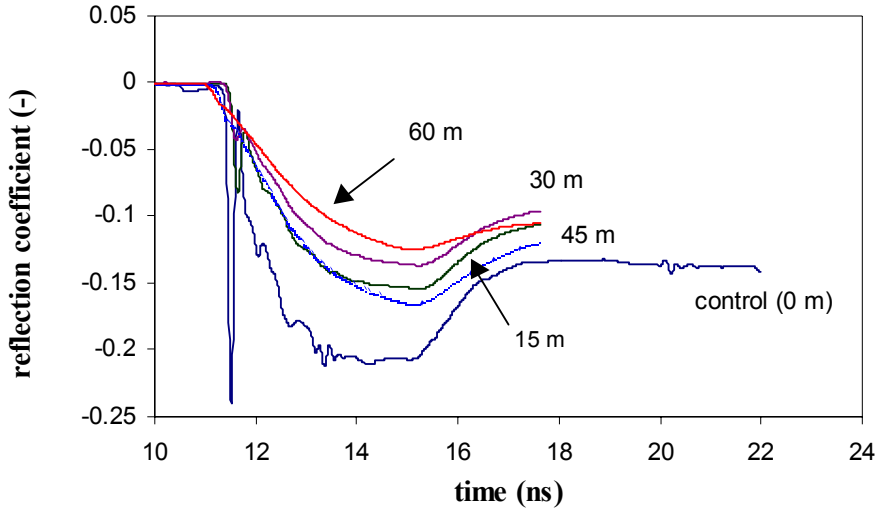

Figure 2-22 Normalised EM waveforms from the TRASE® TDR system with increasing RG-8 extension cable. Measurements are taken in a saturated Vertosol with a 200 mm probe. As the extension cable length increases the proportion of the EM wave reflected decreases. If total attenuation occurs then no end-point determination is possible and the travel time along the probes is not measured.

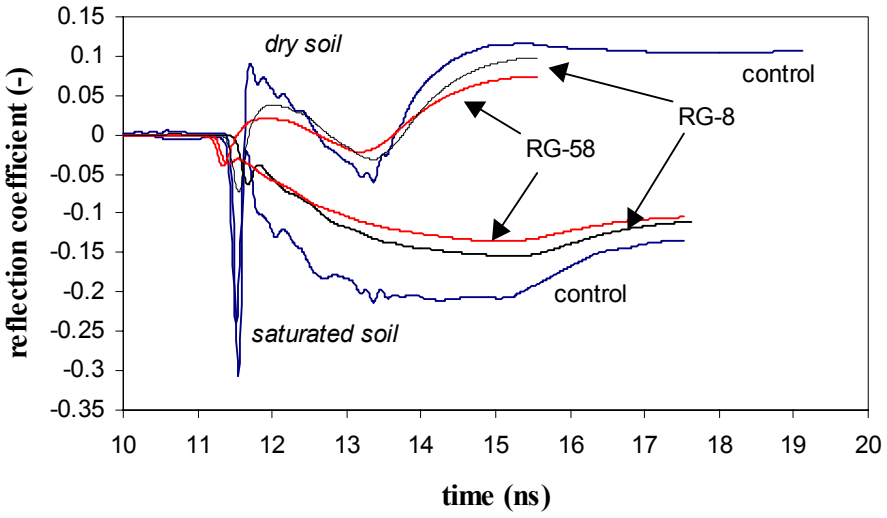

Figure 2-23 Normalised EM waveforms measured with the TRASE® TDR system. The increasing extension cable length filters the signal (seen as less noise) whilst the increase in θ and associated increase in σ reduces the reflection coefficient significantly.

Figure 2-23 shows the normalised waveforms for control and 20 m RG-58 and RG-8 extension cable in a saturated and air-dried Vertosol. The significant filtering of the EM wave is obvious

due to the travel of the EM wave through the extension cables. From the waveforms it is difficult to visually quantify a difference between the RG-58 and RG-8 cable due to signal loss leading to a decline in the slope for end-point estimation.

2.5 CONCLUSIONS

Calibration of the TRASE® TDR and Pyelab TDR systems did not yield a significantly different result to that of the published empirical relationship of Topp *et al.* (1980). Inclusion of bulk density (Malicki *et al.*, 1990) in calibration did not significantly improve the relationship between measured θ and TDR determined $\sqrt{K_a}$. However, the error in prediction is larger compared with the results of Topp *et al.* (1980) and Malicki *et al.* (1996), and larger than the standard calibration for the TRASE® TDR system (Skaling, 1992). Large error could be due to the large clay content and large specific surface of the soil in calibration. Both TRASE® TDR and Pyelab TDR systems underestimated θ at increased moisture contents, as others have found (Rothe *et al.*, 1990; Bohl & Roth, 1994). The calibration results are limited by the uncertainty in determination of ρ_b when the soil columns were saturated.

Extension cable (RG-58 and RG-8) between the buried probe and the TDR instrument significantly affects the reported $\sqrt{K_a}$. However a model accounting for the increasing extension cable length (RG-58), clay content, soil moisture conditions, TDR system and TDR probe accounted for only 62.2 % of the variation. Individual estimation of the affect of extension cable length on reported refractive index shows a linear relationship that is dependent on the soil type, the TDR instrument and inherent moisture conditions. The extension cable filters the high frequency EM waves causing a loss in resolution in the reflected wave by increasing dispersion. I hypothesise that this loss of resolution is shown by a decrease in the slope of the EM wave used for end-point determination by automatic regimes. This in turn leads to a subtle, but significant, change in the reported dielectric. The complex interaction of particle size analysis, specific surface, clay mineralogy and electrical conductivity on travel of the EM wave is difficult to quantify. When using the TDR technique for multiple or spatial soil moisture measurements the present recommendation is to standardise extension cable lengths and calibrate for this extension cable in individual soil types.

The relationship with cable length is partly determined by the probe type with the SEC probe and CSIRO probe reacting differently. The CSIRO probe, with the inclusion of a capacitor assisting generation of the characteristic start point, could be better suited for attenuative

(saline) soil. However, the dissipation of energy (of the reflected EM wave) after travelling through long (> 20 m) extension cables, is a disadvantage of the CSIRO probe.

Chapter three

Instrumental characteristics of neutron moderation and frequency-domain field sensors

3.1. *ABSTRACT*

The chaotic nature of radioactive decay means the optimum count time for a neutron moderation probe influences the error of the instrument in measuring soil water content (θ). For an increasing count time, a CPN Hydroprobe® reported lower variance in a drum of dry sand and a drum filled with water. The increasing count time however leads to increased time for measurement in field operation. In field studies using measurements from single tubes, a 32-second count time is recommended. If tubes are to be averaged, or for farmers planning to schedule irrigation, a 16-second count time is sufficient.

A brief study of the response of the IH1 frequency-domain probe in water and air indicates the sphere of influence of the IH1 down-hole frequency-domain sensor is limited to 203 mm radially and approximately 80 mm axially. These results are in accord with previous studies (Dean *et al.*, 1987) for the IH1 probe and indicate a larger sphere-of-influence than the EnviroSCAN® (Paltineanu & Starr, 1997).

3.2. *NEUTRON MODERATION COUNT RATE AND EFFECT ON ERROR DETERMINATION AND PRECISION*

3.2.1 Introduction

There are many neutron moderation instruments (NMM) commercially available to measure soil moisture and/or density. This discussion concentrates on NMM meters for determination of volumetric soil moisture θ (m^3 m^{-3}). The precision of a NMM meter in measuring θ depends on instrument characteristics and the soil that is being measured (van Bavel, 1962;

Haverkamp *et al.*, 1984). Early measurements were made with the count times measured in minutes (van Bavel *et al.*, 1956) and with varying radiation activities and detector methods for counting the returning thermalised neutrons. More stable electronics and improved count detectors allow for reduced count times, an important consideration for multiple measurements. The radiation source strength also affects the required count time to achieve a nominated precision (Haverkamp *et al.*, 1984; Hodnett & Bell, 1991), however the interaction between the source and the detector needs to be considered (Haverkamp *et al.*, 1984).

A typical source for modern NMM meters used for θ determination in Australian conditions is Am-241/Be with a strength of 1.85 GBq (50 mCi). For improved precision, operators can increase the count time of each measurement (Haverkamp *et al.*, 1984), or take repeated measurements at shorter count rates (Jayawardane *et al.*, 1983). Here I investigate the effect of increasing the count time from 1 seconds to 64 seconds on the precision of a NMM in a drum filled with water and a drum filled with dry sand. This represents the two likely extreme conditions for the NMM in determination of θ.

3.2.2 Methods and Materials

In two sealed drums measurements at each increasing time interval (1-second (s), 4 s, 16 s, 32 s and 64 s) were taken. The NMM was positioned on a single 50 mm diameter aluminium tube located axially in the respective 44-gallon (0.20 m^3) drum. The source was lowered to 450 mm from the top of the drum and fifty readings taken at each time interval. Readings were taken with a CPN 503DR Hydroprobe® containing an Am-241/Be (1.85 GBq, 50 mCi) source. All counts are normalised automatically by the NMM instrument to reflect a 60-second count scale. Readings were taken between 18 °C and 25 °C ambient air temperature.

One drum contained dry sand, the other water, representing the extreme conditions of measurement with the NMM instrument. These sealed drums, in conjunction with three other standards (a drum containing paraffin, one containing a loam soil and one containing concrete), form the basis of the "universal" calibration used extensively for irrigation scheduling in Australia. The drum-based calibration is derived from earlier work in cotton-irrigation scheduling (Cull, 1979).

The water drum, as an infinite source of neutron moderation, is considered as the preferred standard for normalisation of NMM meters (Hodnett & Bell, 1991). The water drum is used to calibrate between different meters and to check for instrument drift. Electronic drift is not a major consideration in modern NMM meters compared to early instruments (Holmes, 1966)

and intermittent checks are considered adequate (Williams & Sinclair, 1980; Hodnett & Bell, 1991).

3.2.3 Results and Discussion

Results of the distribution of readings with increasing count time are shown in Figure 3-1. All count time results are normally distributed (Shapiro & Wilk W test at 5% significance; Steel *et al.* 1997) in the sand and water drums. In the water drum, with a count time of 32 s, the data is normally distributed, however nearly significant (p = 0.061) for non-normal distribution. The distribution for the 32 s count time shows a slight skew towards larger counts. Testing between time indicates no difference in the reported mean values (Figure 3-1). Testing homogeneity of variances indicates a significant difference (corrected χ^2 = 1402.28, 196 d.f.; p < 0.001) using Bartlett's test (Steel *et al.*, 1997). There is a significant difference between the count variances with respect to increasing time of count interval. The normal quantile plot, from readings in the sand drum, is also shown in Figure 3-1 where the shallower the slope indicates a smaller variance.

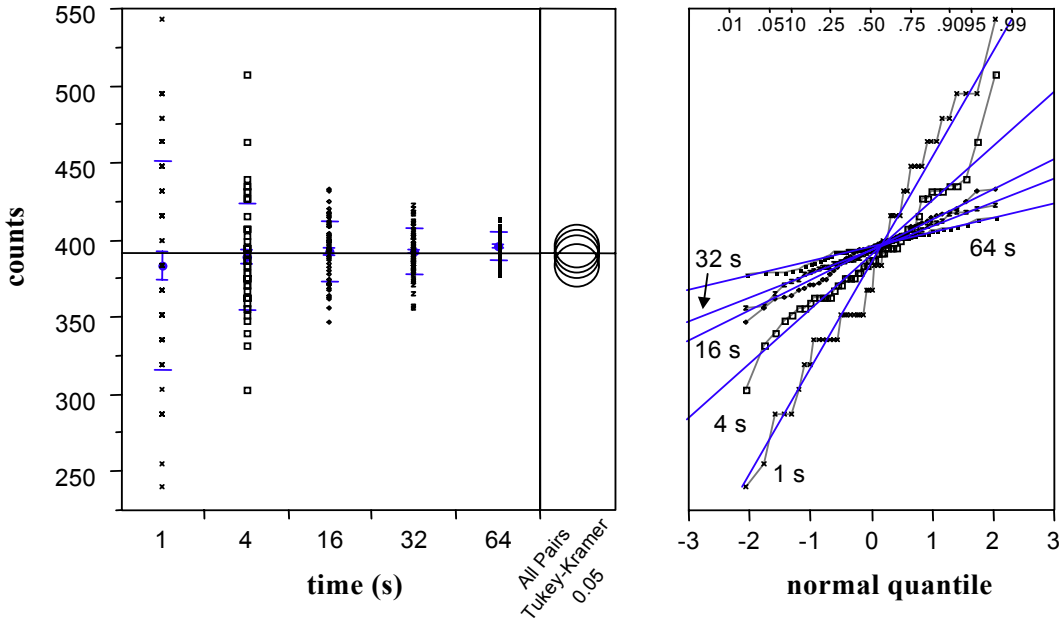

Figure 3-1 Plot of data in sand drum with increasing count time (seconds) showing (a) spread of data (variance) decreasing with increasing time count; (b) the Tukey-Kramer test indicating no significant difference (p = 0.05) between reported means and; (c) the normal quantile plot (right hand side) showing a decreasing slope with increasing count time indicating a lower standard deviation.

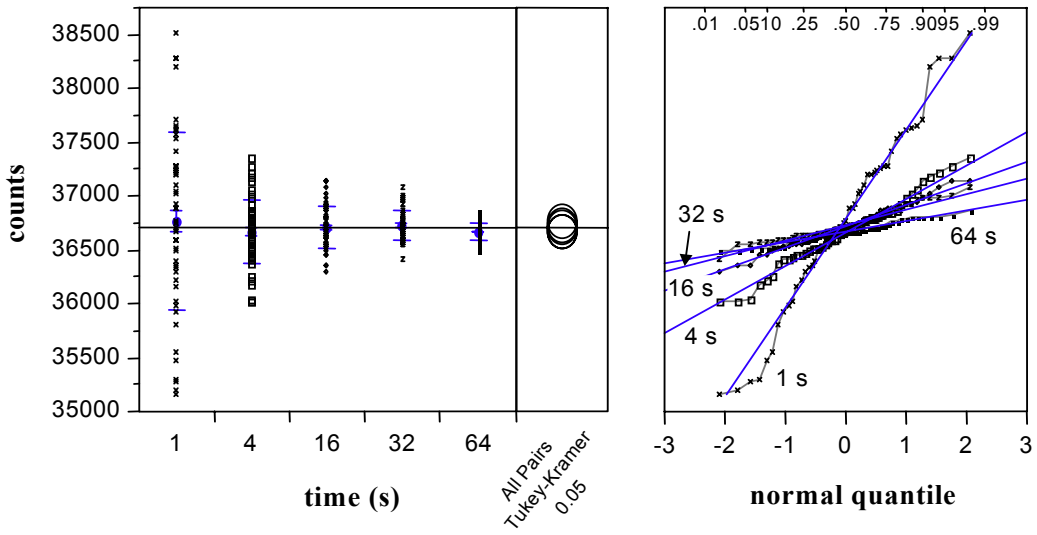

Figure 3-2 Plot of data in water drum with increasing count time (seconds) showing (a) spread of data (variance) decreasing with increasing time count; (b) the Tukey-Kramer test indicating no significant difference (p = 0.05) between reported means and; (c) the normal quantile plot (right hand side) showing a decreasing slope with increasing count time indicating a lower standard deviation. The rate of decrease in slope is inversely proportional to time.

Results for increasing count time measurements in the water drum are similar to sand (Figure 3-2). Testing homogeneity of variances indicates significant difference between the time count intervals and their variances (corrected χ^2 = 324.48, 196 d.f.; $p < 0.001$). The normal quantile plot in the water shows the most dramatic improvement in slope between 1 s and 4 s count time. As the count time further increases the slope of the normal quantile plot (right-hand side of Figure 3-2) decreases at a smaller rate.

The count variance shown as standard deviation and standard error of the mean in Table 3-1 decreases as the count time increases. This is expected as the increase in count time part counters the chaotic (and random) nature of the decay of the Am-241/Be source and Poisson distribution of the emitted high-energy neutrons. However the increase in measurement time, whilst reducing variation, obviously increases the total time for measurements with the NMM in field operations.

The precision also improves as the count time increases (Table 3-1). Precision for the CPN 503 DR Hydroprobe® with respect to time is calculated:

$$\% \text{ error} = 100 \times \frac{1}{\sqrt{\frac{x \times t}{60}}} \tag{3-1}$$

Where the reading value (x) is multiplied by the count time (t) and then normalised to account for the standard 60 s display value (Boart Longyear CPN, 1995). The value (as a percentage) represents the precision with respect to one standard deviation. This value is then multiplied by the slope of the calibration curve to yield a precision in terms of $\pm \theta$ ($m^3 m^{-3}$).

For the sand drum changing count time from 1 s to 64 s improves precision by nearly an order of magnitude (> 8 times). In the water drum the precision is also improved by a similar magnitude. The absolute change in precision is however much lower from 4.04 % (1 s count) to 0.51 % (64 s count). This smaller change is due to the increased presence of H^+ (in water compared to sand) thermalising the emitted high-energy neutrons. This increase in H^+ is reflected by the mean count being nearly one hundred times greater in water compared to the sand drum. Associated with a higher count are an increase in the range of measurements, and a decrease (by nearly an order of magnitude) in the reported standard deviation (Table 3-1). The coefficient of variation, however, improves in the H^+ rich water compared to the sand. In field conditions, especially in clay soil with greater inherent H^+, the count is likely to be greater than that reported in dry sand. The precision (0.71 %) with a 32 s count is optimal for research application with this 503DR Hydroprobe®. Some NMM probes are "hotter" than others and yield larger average counts due to greater radioactivity, or increased count detection sensitivity. A greater count will improve the precision, given a similar count time (Haverkamp *et al.*, 1984). For irrigation scheduling purposes a ≈16 s count is preferred to reduce time for readings whilst maintaining acceptable precision (Jayawardane *et al.*, 1983; pers. comm., P. Cull; ICT International, Australia).

Table 3-1 Influence of NMM count time on the reported raw counts by a CPN Hydroprobe® in a drum filled with water and a drum filled with dry sand. The increasing count time significantly improves the precision of the instrument.

Count Time (seconds)	Mean Count	Standard Deviation	Standard Error of the Mean	Range	Coefficient of Variation (%)	Precision (% error)
Sand						
1	384.64	68.645	9.708	304	17.8	39.50
4	390.32	35.476	5.017	204	9.1	19.60
16	393.8	19.878	2.811	87	5.0	9.76
32	393.48	15.471	2.188	67	3.9	6.90
64	396.5	9.384	1.327	37	2.4	4.86
Water						
1	36784.0	825.73	116.78	3360	2.2	4.04
4	36673.4	311.542	44.06	1341	0.8	2.02
16	36722.7	198.415	28.06	841	0.5	1.01
32	36737.6	141.995	20.08	672	0.4	0.71
64	36677.0	96.969	13.71	383	0.3	0.51

3.3. *MEASUREMENT CHARACTERISTICS OF A DOWN-HOLE FREQUENCY-DOMAIN SENSOR*

3.3.1 Introduction

The use of frequency-domain (FD) based instruments for measurement of biological substances began in the late 1920s (Wyman, 1930) with initial application to soil in the 1930s (Smith-Rose, 1933). However the need to attain accurate high frequency control limited the development of FD sensors until the 1960s (Thomas, 1966). Indeed the application of the FD technology for measurement of down-hole (profile) soil moisture was only popularised in the

late 1980s (Dean *et al.*, 1987; Bell *et al.*, 1987). Since then many changes to the circuit technology and application requirements such as continual measurement systems and portable sensors, have lead to varied studies of the FD technique (Whalley *et al.*, 1993; Tomer & Anderson, 1995; Paltineau & Starr, 1997; Wu, 1998).

One question concerning the use of FD technology is the field of influence, or zone of measurement. The determination of the sphere of influence is in part determined by the sensor design. This experiment concentrates on the use of down-hole FD probes. The IH1 probe has a vertical axial sensitivity of 340 mm to 350 mm with 90 % of the influence limited to ± 85 mm from the FD probe centre of sensitivity. Radial sensitivity indicates 90 % of measurement influence lies within a 130 mm diameter (Dean *et al.*, 1987). The sensitivity of FD probes in field measurement when compared to neutron moderation method (NMM) is smaller. This is viewed as an advantage in uniform soil (Ould Mohamed *et al.*, 1997) and a disadvantage in heterogeneous soil (Evett & Steiner, 1995). This experiment tests the FD probe sensitivity. Also, I test if there is any effect of rotating the IH1 probe within the access tube during measurement.

3.3.2 Materials and Methods

In the first experiment readings were taken with a Didcot capacitance soil moisture probe (Type IH1) inside a 50-mm polyvinyl chloride (PVC) pipe. The readings were taken by lowering the IH1 probe into the access tube immersed in water. A series of concentric PVC cylinders of increasing internal diameter (Table 3-2, n = 6) were machined and water was placed between the IH1 probe and the surrounding PVC at increasing diameters (Figure 3-3). The IH1 probe has a nominal centre of sensitivity of 114 mm from the bottom of the probe (Figure 3-4). The frequency was measured in 10 mm increments when the centre of sensitivity was 20 mm from the water surface to 160 mm from the surface. Six measurements were recorded at each depth and increasing diameter of the outer tube containing the water. The readings were taken with the air temperature between 23 °C and 28 °C.

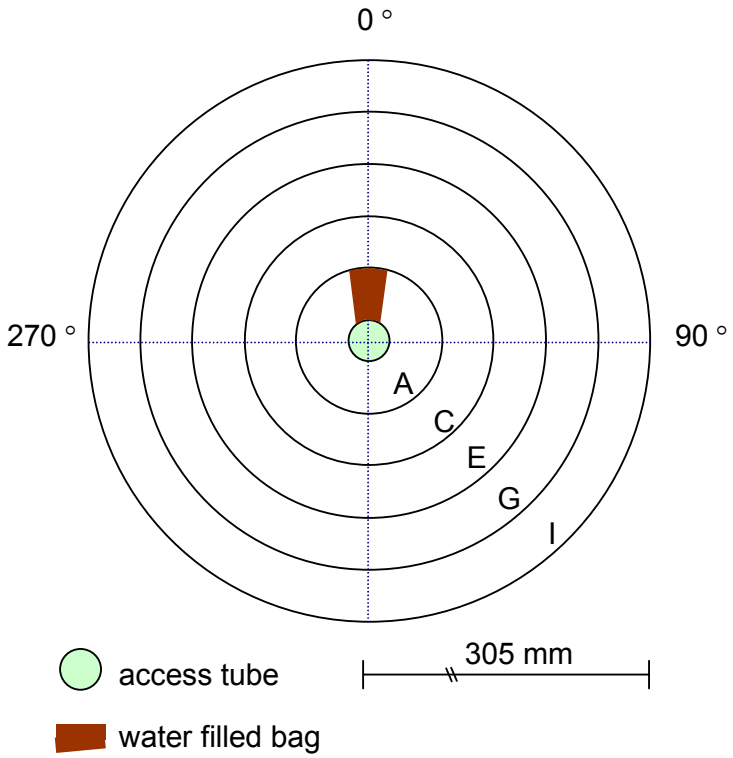

Figure 3-3 **Concentric PVC pipes for measurement of the sphere of influence around the Didcot IH1 FD probe. The PVC access used to lower the FD sensor is centered. The water-filled bag used in the experiment detecting the sensitivity of the sensor to rotation is shown with the degrees for rotation from 0° to 345°. To test the volume of influence the outer PVC tubes were filled with water starting from A (102 mm diameter) and increasing to I (305 mm diameter).**

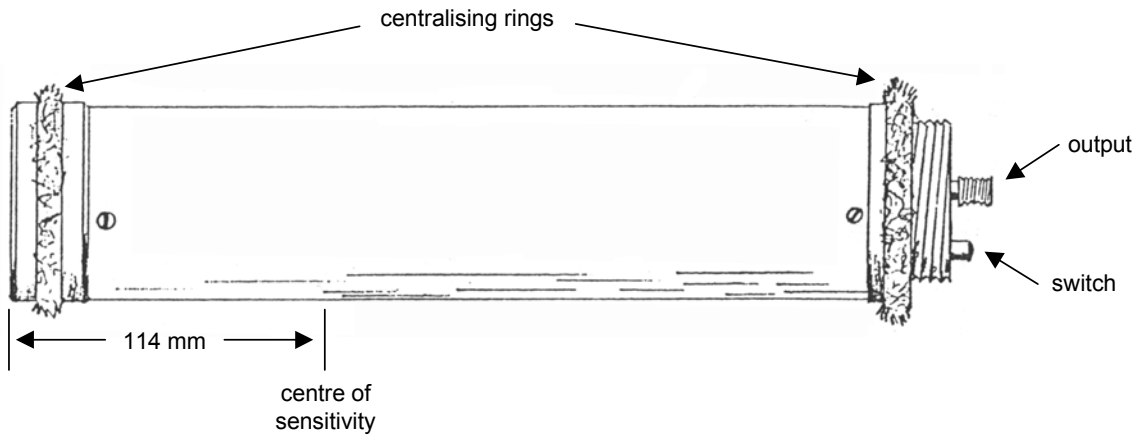

Figure 3-4 **Dimensions and external components of the Didcot IH1 capacitance probe (Provisional Manual for the Type IH1 probe, 1992).**

In the second experiment a portion of the area between the access tube and the 101.6 mm diameter PVC pipe was blocked off (approximate cross-sectional area of 2500 mm^2) and filled

with water (Figure 3-3). The FD technique is more responsive to change in dry soil (Dean *et al.*, 1987; Kholsa & Persaud, 1997) and the water filled compartment enabled testing of the probe positioning in the most sensitive frequency range.

The IH1 probe was lowered to 200 mm depth (centre of probe measurement) and a reading taken. This was performed three times and then the probe rotated 15°. Again the probe was lowered three times to a depth of 200 mm centre of sensitivity and frequency recorded. The IH1 probe output is the frequency (Hz) divided by eighty (80). All readings reported here are the scalar output frequency (true frequency/80).

Table 3-2 PVC pipe dimensions for IH1 FD down-hole probe experiments estimating volume of influence.

PVC Pipe Internal Diameter (mm)	Average Wall Thickness (mm)	Experimental "run" Number (Figure 3-5)
102	6.4	A
152	7.9	C
203	8.5	E
254	11.0	G
305	11.4	I

3.3.3 Results and Discussion

The reported frequency (*f*/80 Hz) as the IH1 probe was lowered into the access tube and the volume of water increased (Table 3-4), is shown in Figure 3-5. Frequency declined as the probe was lowered into the access tube. An interesting change occurred as the frequency first stabilised (around 70 mm from the water surface) and then decreased again to a minimum at 140 - 160 mm. The results indicate the majority of the sensitivity (to the water surface) is within 80 mm of the probe reference point. This is in accord with earlier findings of Dean *et al.* (1987) and indicates a larger axial influence than the EnviroSCAN® system studied by Paltineanu & Starr (1997). The rapid decline between 80 mm and 120 mm below the water surface, experienced at all diameter increases, is possibly due to the probe design.

Frequency also declined for increasing outer PVC diameters stabilising at 203 mm. Increasing the diameter of the water filled PVC pipe beyond 203 mm did not significantly (p = 0.05)

lower the frequency. An approximate volume of measurement can be calculated for the probe sensitivity in a water medium. Assuming an 80 mm radial effect, the volume of the medium influencing the IH1 FD probe is 0.002145 m^3 (2145 cm^3). This estimation of the measurement volume does not however, account for the decreasing sensitivity with increasing distance from the installed access tubes (*Bell et al.*, 1987; White & Zegelin, 1995).

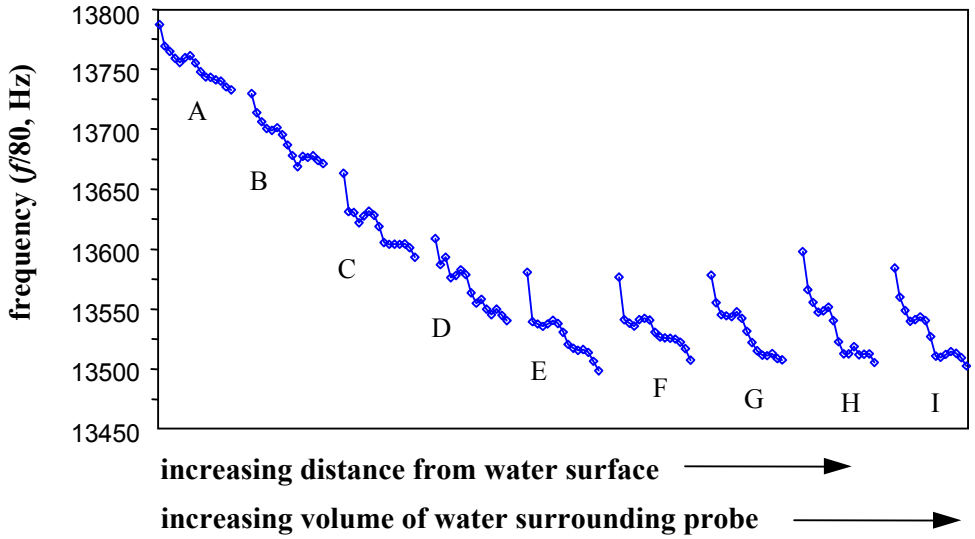

Figure 3-5 Change in frequency as the IH1 probe is lowered into the increasing (volume) water column. A, C, E, G, and I diameter are shown. B relates to 102 mm and 152 mm diameter PVC pipes in position and filled with water. D is the 152 mm and 203 mm PVC pipes filled, etc. The majority of sensitivity is constrained within the 203 mm diameter PVC tube.

Results of the IH1 probe when rotated in 15° increments is shown in Figure 3-6. There are three peaks in the reported frequency around 45°, 180°-195° and 315°. The maximum frequency value (16798.3 Hz/80) at 195° is an increase of 0.36 % from the minimum "true" frequency reported at 0° (16737.7 Hz/80). Using the standard calibration curve (Provisional Manual for the Type IH1 probe, 1992) a change of ± 80 counts in reported frequency (/80 Hz) at 0.10 m^3 m^{-3}, changes reported θ by 0.011 m^3 m^{-3} when added, and 0.012 m^3 m^{-3} when subtracted from the "true" frequency. The change, though small, needs to be considered in the field operation of the IH1 probe.

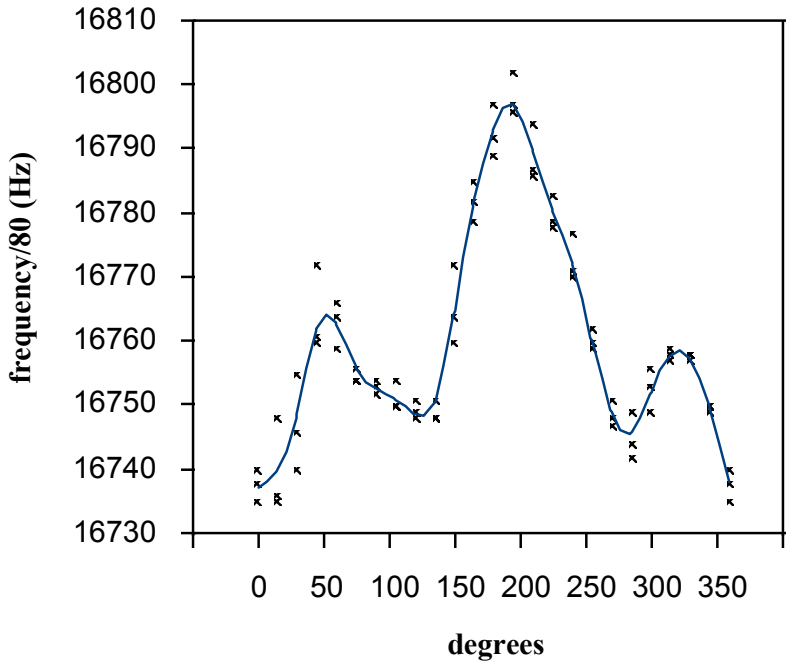

Figure 3-6 Change in reported frequency by the IH1 probe when rotated from 0 to 360 in 15 increments. The maximum change in reported frequency corresponds to a change of approximately ± 0.01 $m^3 m^{-3}$ using the standard calibration.

3.4. *CONCLUSIONS*

For field measurements, a 32-second time count is recommended for the neutron moderation method. This can be reduced to 16 seconds, minimising the time for reading each soil profile, if multiple access tubes are employed at each monitoring site.

The sphere of influence of the IH1 down-hole FD meter when tested in water indicates the sphere of influence is + 80 mm from the water surface. The FD probe was insensitive to changing conditions outside a 203 mm diameter of water filled PVC. From the extreme conditions, the estimated maximum sphere of influence for the FD sensor is 0.002145 m^3 for a surrounding water medium. However, the influence of the medium closer to the sensor will be far greater than that at the outer boundary limits. The FD sensor responded to the axial orientation of the sensor in a uniform media. In this experiment, the maximum change in reported θ using the standard calibration is ≈ 0.01 $m^3 m^{-3}$. This change occurred at 180° - 195° rotation. Care should be taken to standardise the operation of the FD sensor in field applications.

Chapter four

Field measurement of θ with neutron moderation and dielectric techniques

4.1. ABSTRACT

In situ determination of soil water content (θ) is an important consideration in many soil studies. For many years the neutron moderation method (NMM) for θ determination down the soil profile has been carried out. Recently, development in dielectric based techniques for *in situ* θ (m^3 m^{-3}) measurement has expanded their application and adaptability. However, little information on how the systems operate in Australian soil conditions is available.

To determine the operational characteristics of the dielectric and NMM techniques, an experiment in an effluent irrigated Eucalypt plantation was designed. An *in situ* calibration for the NMM technique is more sensitive to changing θ than the factory supplied "universal" calibration. Comparison of the EnviroSCAN® frequency-domain (FD) system and the NMM count ratio indicates the FD technique is more sensitive to change in θ conditions. The EnviroSCAN® FD system is well suited to continuous profile-based measurement of θ. Results with the TDR technique were disappointing, indicating the limited applicability of TDR in profile based θ measurement in heavy-textured soil, or soil with a large electrical conductivity. The method of auguring to a known depth and placement of the TDR probe into undisturbed soil is not recommended.

4.2. INTRODUCTION

Measurement of *in situ* soil water content (θ) is an important parameter in many soil studies. The neutron moderation (NMM) technique is widely used and reported for *in situ* studies (e.g. Williams *et al.*, 1981; Kamgar *et al.*, 1993). However, little information is available concerning the use of down-hole frequency-domain (FD) sensors for measurement of θ,

especially in Australian conditions. Most field studies of the down-hole FD technique are in light-textured soil (Tomer & Anderson, 1995; Kholsa & Persaud, 1997; Starr & Paltineanu, 1998). Reports concerning operation of FD sensors in heavy-textured soil are scarce, and poor precision of a portable down-hole FD system in a fine sandy loam overlaying a sandy clay loam B horizon soil lead Evett & Steiner (1995) to still favour the NMM technique. However, the benefits of the FD technology, including the ability to continually measure θ (Paltineanu & Starr, 1997), being a non-radioactive technology, sensor adaptability (Whalley *et al.*, 1992), and the improved resolution compared to NMM measurement (Dean *et al.*, 1987), indicate the potential for the FD technology development. Limiting the FD technology is the need for site calibration in different soil types (Bell *et al.*, 1987).

The field experiment was designed to investigate the operation of a down-hole FD sensor (Didcot IH1 probe), a logging FD system (EnviroSCAN®) and a dedicated TDR (TRASE® TDR). These systems could then be compared with the "standard" NMM (503-DR Hydroprobe®) technology in an irrigated Eucalypt plantation established in a Brown Chromosol.

4.3. MATERIALS AND METHODS

4.3.1 The site

The field site is located in the Bunglegumbie Road effluent irrigated plantation on the outskirts of Dubbo, in NSW (Figure 2-1). The site was developed by the Dubbo City Council for application of effluent generated in the city. Approximately 20 ha of trees were planted in 1 ha blocks (Figure 4-1) in 1992. Sensors were located in a block on the northern side of the plantation in a block of *Eucalyptus bicostata spp. bicostata* (Victorian Bluegum) shown in Figure 4-1.

The soil is a Brown Chromosol (Isbell, 1996) typical of the region. The profile description is detailed in Table 4-1. The applied effluent has not significantly changed the soil chemical or physical conditions at the site (see Section 3.1 for discussion).

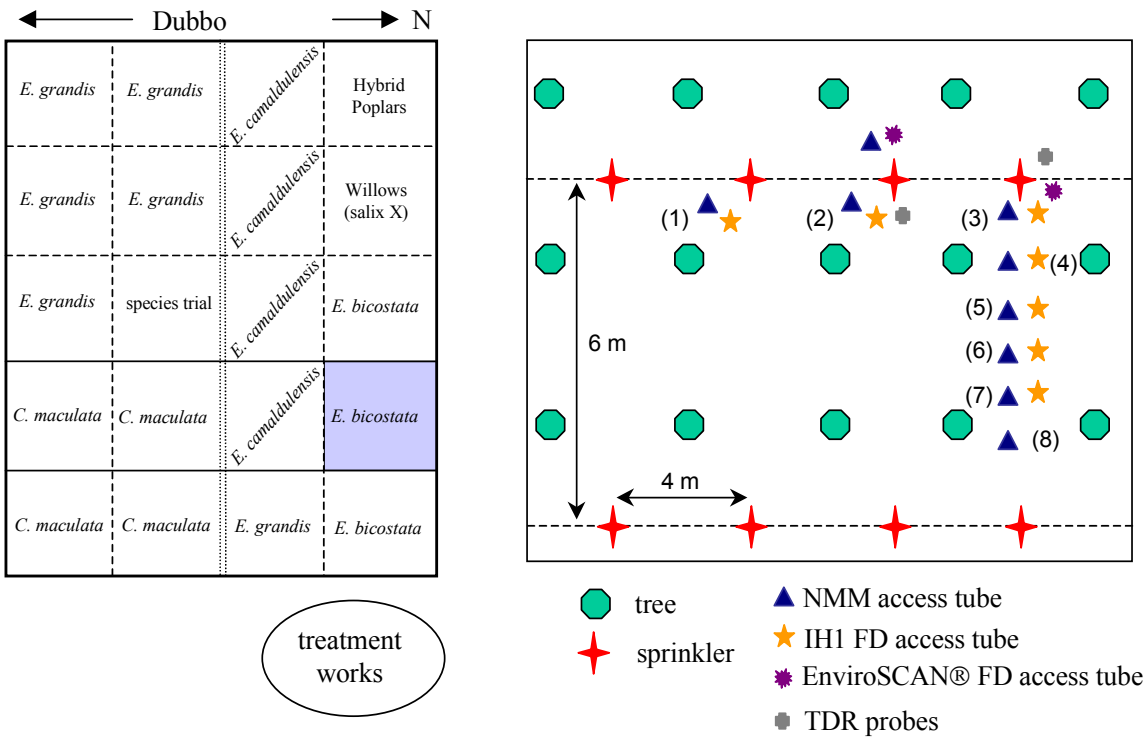

Figure 4-1 Effluent irrigated plantation located on the outskirts of Dubbo. The field site is located in a 1 ha block of *E. bicostata* trees. The right hand side shows the position of the access tubes and sensors relative to the *E. bicostata* trees and sprinklers for irrigation.

4.3.2 Equipment and installation

Neutron moderation (NMM) access tubes were installed in two short transects (Figure 4-1). Along the first transect, the aluminium access tubes (1.7 m long with a 50 mm outside diameter) were installed within a 0.5 m radius of three sprinklers. A second transect of NMM access tubes were installed between the sprinklers (Figure 4-1) approximately 0.7 m apart normal to the first transect. All NMM readings were taken with a CPN 503DR Hydroprobe® containing an Am-241/Be (1.85 GBq, 50 mCi) source. Following consideration of the count time and effect on variance (Section 3.1.3) a 32 second count was used. Readings are normalised against a water drum count, considered an infinite H^+ source (Greacen *et al.*, 1981; Hodnet & Bell, 1991). Water drum counts were taken approximately weekly during the field trials with no drift in readings observed.

Table 4-1 Profile description at the effluent irrigated plantation.

Horizon	Depth (m)	Description
A	0 – 0.16	Black to dark reddish brown (5YR 2.5/1 moist, 5YR 3/3 dry); light sandy clay loam; smooth faced peds; weakly sub-angular blocky (20 – 50 mm); crumbly; pH = 5.5; even and clear to -
B_{21}	0.16 – 0.50	Very dark brown to dark brown (7.5YR 2.5/3 moist, 7.5YR 3/2); light medium clay; smooth faced peds; strongly angular blocky (50 – 100 mm); crumbly, pH = 7.0; irregular and gradual to -
B_{22}	0.5 -	Dark reddish brown (5YR 3/3 moist, 5YR 3/2 dry); light clay; smooth faced peds; strongly angular blocky (50 – 100 mm); brittle, pH = 6.5

Polyvinyl chloride (PVC) access tubes (1.7 m long with a 50 mm outside diameter) for a Didcot IH1 FD probe were installed approximately 0.25 m from the NMM access tubes in all positions (Figure 4-1) following the procedure outlined by Bell *et al.*, 1987. Reported readings are the average of three (occasionally six) successive readings. During each measurement the IH1 probe orientation was consistent (setting 0° from East) to reduce bias due to changing response of the IH1 FD probe to rotation (Figure 3-6). Before and after soil readings the frequency in air was measured. This is then used with the measured frequency in water to calculate the universal frequency. For the IH1 down-hole FD probe the universal frequency (*UF*) is given by (Didcot Instrument Company, 1992):

$$UF = \frac{(F_{air}^{7.692} - F_{soil}^{7.692})}{(F_{air}^{7.692} - F_{water}^{7.692})} \qquad (4\text{-}1)$$

At site (2) and site (3) PVC access tubes were installed for positioning of an EnviroSCAN® FD system. Though a prototype, the EnviroSCAN® system used was essentially the same in operation as the system described by Paltineanu & Starr (1997). Fixed sensors were located at differing depths (Table 4-2) and logged at 20 minute intervals. The software (version 1.1a) does not allow access to the universal frequency (or *scaled frequency*) as described by Paltineanu & Starr (1997). However, a reasonable assumption is that the process to measure and calculate the *UF* is the same for prototype EnviroSCAN® used in this experiment. The *UF* calibration coefficients for the EnviroSCAN® probe are given in Appendix 4-1.

To install the access tubes, an undersized (the diameter of the access tube minus 2 mm) hole was hand augured. Each access tube was then pushed into the soil to a depth of approximately 1.4 m. Some water was used during installation to assist with the maneuvering of the access tubes into the soil. Due to the sensitivity of the FD technique to air-gaps located in close proximity to the access tube (Bell *et al.*, 1987), special care was taken in the auguring and placement procedure. After installation, at least one application (irrigation) of effluent was applied before readings commenced. Readings were taken regularly during three wetting and drying cycles in January and March 1993, and January 1994.

Unbalanced TDR probes (0.2 m long SEC probes as described in Chapter 2) were buried vertically at increasing depths from the soil surface to 0.8 m. A hole was augured to the respective depth (0.20 m, 0.4 m and 0.6 m) and then a probe pushed into the undisturbed soil. During this process it is likely that the three rods did not remain evenly spaced. This could affect the electromagnetic (EM) wave (Zegelin *et al.*, 1992) and this installation process is not recommended due to this uncertainty. Probes for a thermal based moisture system were also buried within 0.2 m (at depths 0.20 m, 0.3 m, 0.4m and 0.5 m) of two NMM and IH1 access tubes. However, the system power requirements could not be consistently maintained and insufficient information was obtained from the thermal system for comparison.

4.3.3 In situ *calibration of the NMM probe*

At the completion of the experiment a calibration of the NMM and IH1 FD sensors was undertaken. Readings were obtained from two access tubes and then gravimetric soil samples taken at increasing soil depth. At each depth, between four and eight cores of known volume were used to determine the dry bulk density (Mg m^{-3}) and calculate θ (m^3 m^{-3}) from wetness (w, g g^{-1}) described by Equation 1-4. Wetness was also determined from 2 to 6 samples at each depth. Samples were collected following the process of Greacen *et al.* (1981) for calibration of the NMM with the cores located immediately around the access tube. Detailed description of the core method for bulk density determination is given by Blake & Hartge (1986). There was no significant swelling of the soil (qualitative assessment) negating the need, during calibration, for consideration of the field $\rho_b(w)$ relationships developed by Jayawardane *et al.* (1983). The sampling process was repeated at two other paired access tubes after saturation with water for two days. Though no irrigation or significant rainfall had occurred in the five weeks prior to the calibration, the range of soil water values obtained was limited. This indicates the soil was saturated before the irrigation ceased. Trees immediately surrounding the site were dead, most likely from insect attack observed during the

measurement period. This significantly limited the transpiration of water from the soil, leading to wetter than expected conditions.

Calibration of the IH1 FD probe was carried out, however, instrument instability lead to questioning of the validity of the data and therefore it is not presented here. Others have experienced similar difficulty in operation of the IH1 FD sensor (pers. comm., P. Lane; Centre for Forest Tree Technology, Vic). The IH1 FD probe needs to be used with care in field situations as damage to components is common. In particular, the fibre optic cable is fragile and prone to catch on branches during measurement. The fibre optic cable links the sensor output (Figure 3-4) to the readout meter via the inside of the connecting PVC tube. When operating in the field this cable becomes entangled with leaves or branches and is easily broken. Also, batteries required by the probe are expensive (≈ $20 each) and last about six hours. The probe is not designed for continued (rugged) field use.

Table 4-2 Installation depth of sensors in the soil profile.

Depth (m)	NMM	IH1	EnviroSCAN®	TDR
0.10	√	√	√	0 – 20
0.20	√	√	√	×
0.30	√	√	√	0.20 – 0.40
0.40	√	√	√	×
0.50	√	√	√	0.40 – 0.60
0.60	√	√	×	×
0.70	×	×	√	0.60 – 0.80
0.80	√	√	×	×
0.90	×	×	√	×
1.00	√	√	×	×
1.20	√	√	√	×

4.4. RESULTS AND DISCUSSION

4.4.1 Calibration of the NMM probe

The NMM probe is supplied with a factory based calibration. In Australia, this is based on calibrations developed by Cull (1979) for a Vertosol in northern NSW. It is accepted that calibration is required for determination of θ in different soil types (see Section 1.3.3 for detailed discussion of calibration). The need for calibration in different soil also relates to the change in bulk density (ρ_b) down the soil profile (Greacen *et al.*, 1981; Wilson & Ritchie, 1986). The change in ρ_b and the 95 % confidence interval at the Dubbo site is shown in Figure 4-2. Within sites the ρ_b is uniform through the soil profile. There is a considerable difference in the ρ_b at sites (5) and (6) compared to the larger measured ρ_b at sites (3) and (7). During site preparation, for planting of the trees, the soil was ripped to 0.4 m to reduce ρ_b and improve root penetration. However, site (3), located near the tree planting line where ripping occurs, has a significantly larger average ρ_b than sites (5) and (6). The change in ρ_b at the four sites is not readily explained and will affect the calibration process (Fleming *et al.*, 1993). To account for the change in ρ_b the count ratio is corrected (with respect to soil dry density) by the equation of Greacen & Schrale (1976):

$$n' = \sqrt{\frac{\overline{\rho}_b}{\rho_i}} \times n \qquad (4\text{-}2)$$

Where n is the count ratio (raw NMM count divided by mean of count in a water drum), $\overline{\rho}_b$ is the mean bulk density for the site, and ρ_i an individual determination of bulk density at a particular depth. The factory calibration (Irricrop Technologies Pty. Ltd., NSW Australia) is based on the work of Cull (1979). This calibration was developed from field studies in a Vertosol where the ρ_b down the soil profile remained uniform. The calibration does not account for different ρ_b encountered in different soil and within a soil profile. The methodology for ρ_b determination used by Cull (1979), with a small surface area and wall sampling could have influenced his determination of ρ_b leading to erroneous determination (Jayawardane *et al.*, 1983).

The combination of information from all horizons will improve the precision of the calibration (shown by a larger reported r^2). However, this procedure introduces an unknown bias into the

calibration (Williams & Sinclair, 1981). The introduced experimental bias is minimised by using a standard technique for tube installation and calibration sampling (Williams and Sinclair, 1981) and by close location of access tubes relative to each other (Greacen & Hignett, 1979). Instrument bias is more difficult to quantify but should be negligible. A composite measure of the bias and variance of reported measurement is given by the root mean square error (RMSE) in the form (Kempthorne & Allmaras, 1986):

$$\text{RMSE} = \sqrt{\text{bias}^2 + \text{variance}} \tag{4-3}$$

This experiment does not specifically address the issue of bias in reported measurement; however, minimisation of the RMSE indicates a smaller combined bias and experimental error (Williams & Sinclair, 1981).

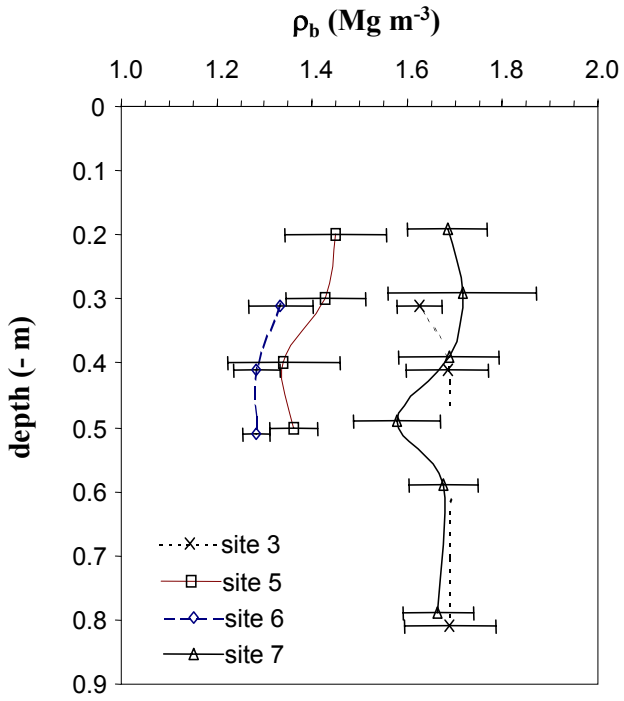

Figure 4-2 Estimation of ρ_b down the soil profile at four sites during calibration. The 95 % confidence interval is given. Measurements for ρ_b were taken at the nominated depth ± 0.03 m.

The estimation of the relationship between the known θ and count ratio (*n*) for the NMM across all depths is shown in Figure 4-3a. The estimation is limited by the lack of data at smaller θ. If several points are removed the fit is significantly improved (Figure 4-3b). Though corrected for ρ_b (Equation 4-2) the shaded points represent the smallest ρ_b at the site. To reduce the error in establishing the relationship these points are excluded from the prediction curve (Figure 4-4) with a decreased RMSE (0.029 from Figure 4-3b). Even so, the error in prediction is still large, and the calibration should be considered with care. Clearly,

more data, especially at smaller θ, is required before confidence in this calibration is reasonable (< 0.03 m^3 m^{-3} 95 % confidence).

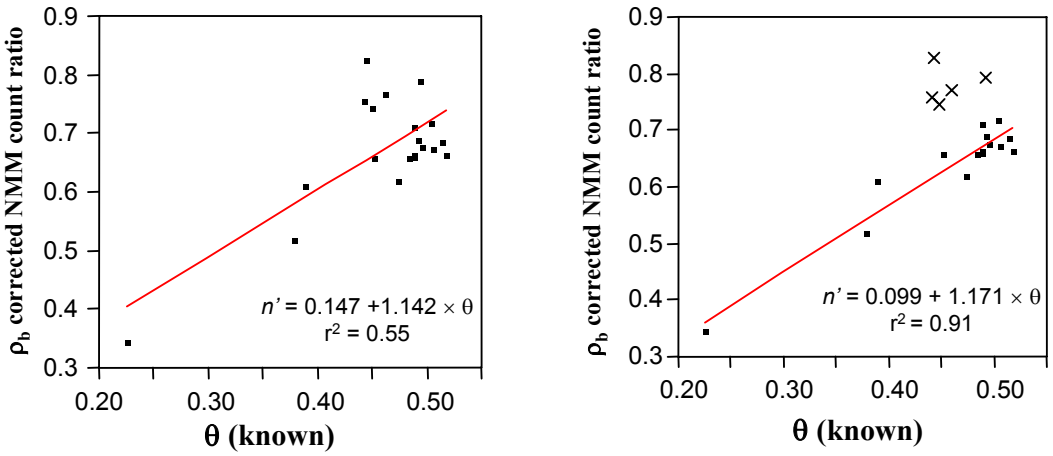

Figure 4-3 **(a) Estimation of the relationship between the corrected count ratio (*n'*), accounting for ρ_b, and known θ (RMSE = 0.071). (b) Estimation of the relationship between the corrected count ratio (*n'*) and known θ, with points excluded (shown) where ρ_b correction did not improve the relationship (RMSE = 0.029).**

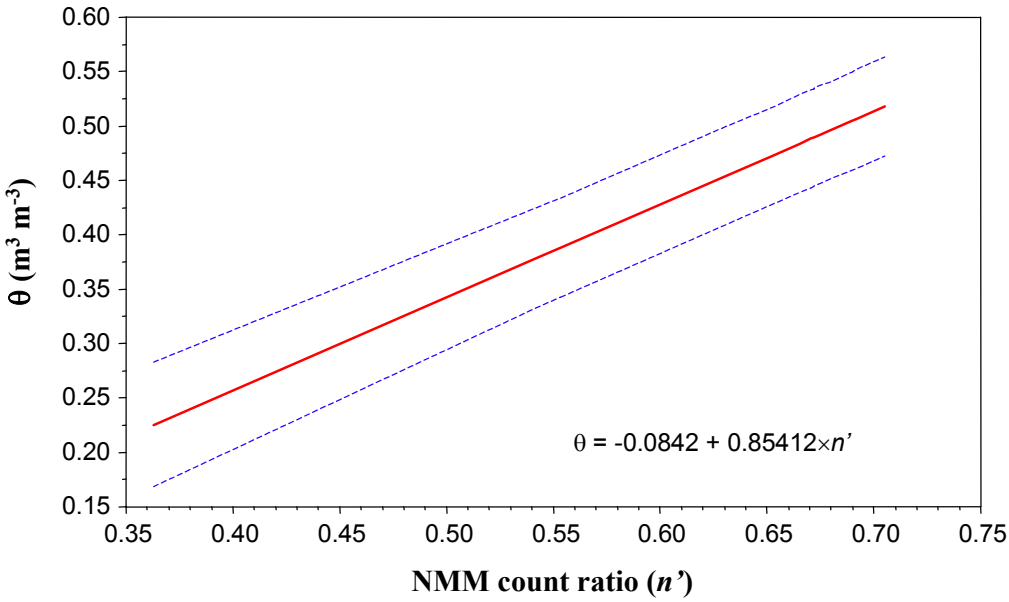

Figure 4-4 **Calibration for the NMM probe at the Dubbo site. To predict θ from the adjusted *n* (for ρ_b) the relationship is given by: θ = -0.0842 + 0.85412 × *n'*. The 95 % confidence interval (CI) is shown indicating large error (≈ 0.05 m^3 m^{-3}) associated with this calibration.**

Calibration of the NMM for prediction of θ is shown in Figure 4-4. The error estimate in prediction, the 95 % confidence interval, is based on Equation 2-8 (Webster, 1997). There is

significant error in determination of the known θ for calibration. To improve this calibration, further sampling at smaller moisture contents is required.

4.4.2 Comparison with the factory supplied "universal" calibration

The relationship between the calibration for the NMM in the Brown Chromosol to the factory supplied "universal" calibration is shown in Figure 4-5a. The effect of ρ_b is encompassed in the "universal" calibration and different depths are readily identified. The modeled effect of ρ_b on the "universal" calibration is then compared to the site calibration (Figure 4-5b). There is still an identified difference when $\rho_b < 1.5$ Mg m^{-3}. This is possibly due to the prediction of the "universal calibration" not accurately estimating the effect of ρ_b, or the inability of the ρ_b normalisation of Greacen & Shrale (1976) to account for changing ρ_b at the Dubbo site.

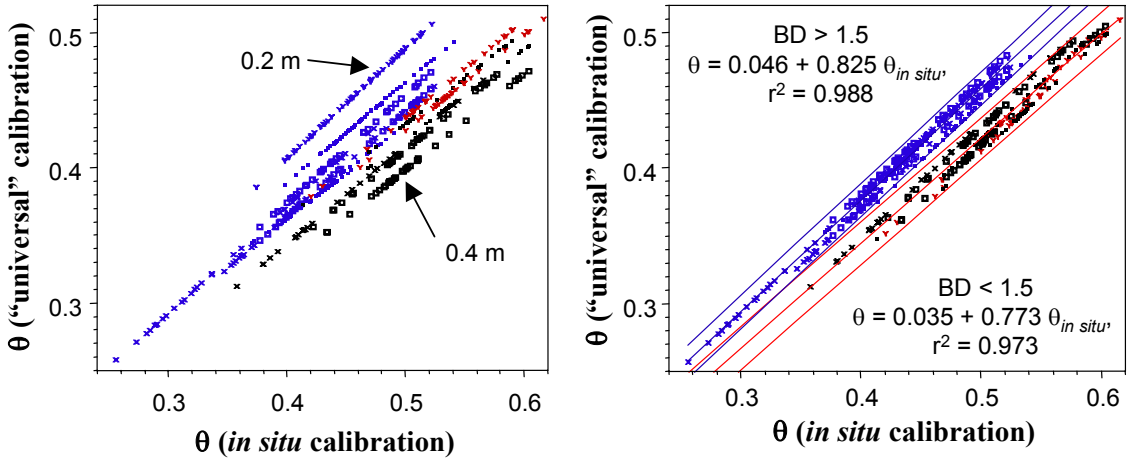

Figure 4-5 (a) Plot of θ reported by the factory supplied "universal calibration" and the *in situ* site calibration. The different calibrations (from Appendix 4-2) are readily identified. (b) Relationship between the modeled "universal calibration" and the site based calibration accounting for the site ρ_b at different depths in the four measured profiles.

The site calibration reports a greater θ compared to the "universal" calibration, particularly when the soil is wet. Given the large error in the site calibration (≈ 0.05 m^3 m^{-3}, 95 % CI), there is no significant difference between the reported θ from the site calibration and the "universal" equation at depths < 0.6 m when the soil profile dries (Figure 4-6).

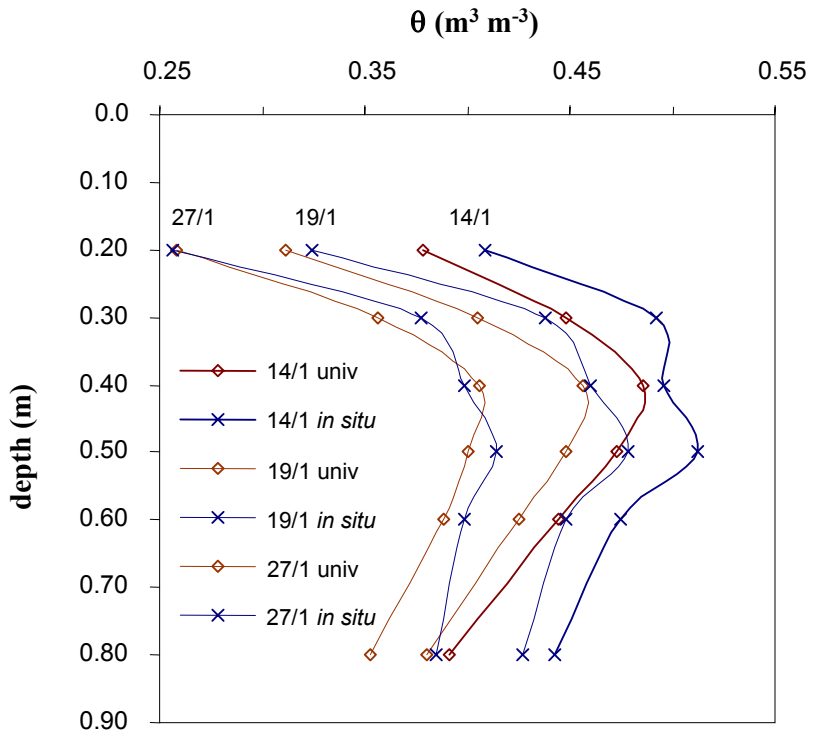

Figure 4-6 Estimation of θ down a soil profile at three stages during a drying cycle (site (7)) using an *in situ* calibration and the factory supplied "universal calibration" (univ). As the soil dries there is no significant difference between the reported θ < 0.6 m from the soil surface.

Consideration of the respective technique response to change in soil water content will be based on comparison of respective output (count ratio for the NMM and *UF* for the FD sensors) where possible. In comparing the EnviroSCAN® to the NMM, the factory-based θ output are used as the software (version 1.1a) supplied with the EnviroSCAN® system does not readily allow output of the *UF*. The relationship used in determination from *UF* to θ for the EnviroSCAN® system is given in Appendix 4-1; with the *in situ* site calibration and the factory "universal" calibration for the NMM used for comparison.

4.4.3 Measurement of θ during a drying cycle

Several drying cycles, from field capacity to re-fill point, were measured during the field experiment. Deliberate over-irrigation and significant fortuitous rainfall saturated the soil profile during measurement on three occasions. The irrigation was then shut down and measurements made regularly through the drying cycle. Figure 4-7 shows a typical drying cycle measured by the NMM and IH1 FD sensors. The reported θ is derived from the respective "universal" calibrations supplied by the manufacturers. The IH1 FD probe is more sensitive to the temporally changing θ conditions (also shown in Figure 4-7 and Figure 4-8).

For all field measurements two times the standard deviation (for 95 % of this time) of the measured frequency was < 6 counts (Hz/80) giving a confidence interval of 0.01 – 0.03 m^3 m^{-3} depending on θ. This repeatability is typical of the FD technique (Bell *et al*., 1987).

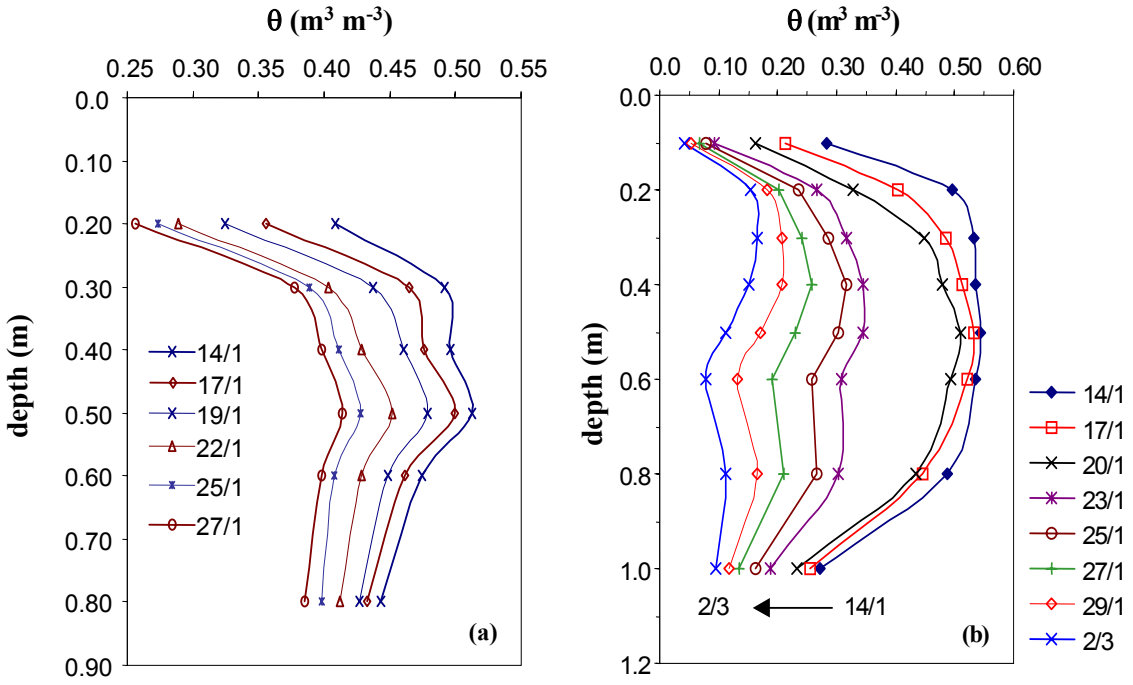

Figure 4-7 Drying cycle measured with the NMM at site (7) using the in situ calibration (a) and by the IH1 FD probe (b).

The IH1 FD probe is more sensitive to change in the θ when the factory "universal" calibration is used. The relationship between reported θ by the NMM ("universal" and *in situ* calibration) and IH1 FD probe ("universal" calibration) is shown in Figure 4-8. The increased range (between the two respective readings) indicates the FD probe is more sensitive to the change in θ compared to the NMM. The IH1 FD probe reports smaller θ than the NMM instrument as the profile dries. This could be due to the sensitivity of the technique (Dean *et al*., 1987) or an effect of the calibration procedure.

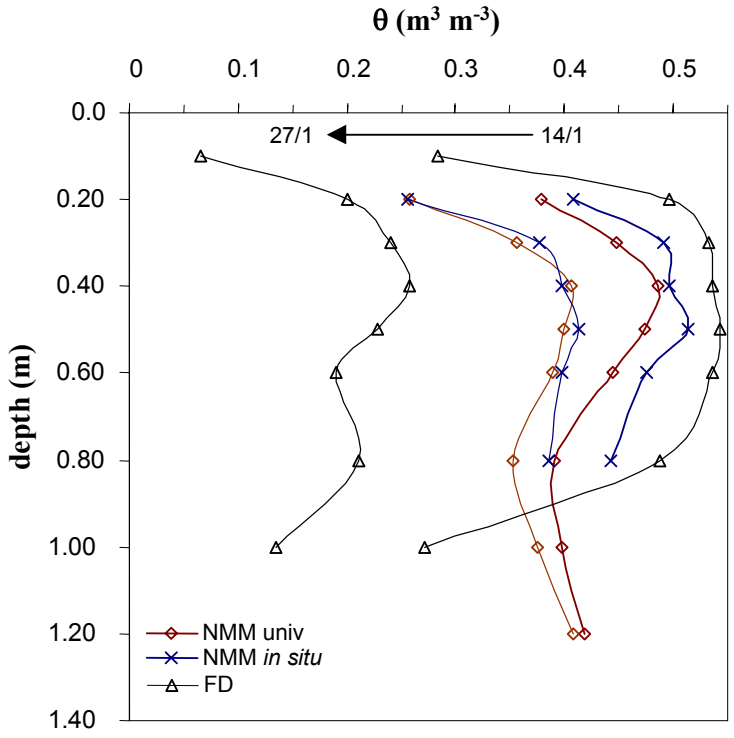

Figure 4-8 Determination of θ by the FD and NMM instruments with factory "universal" calibration and *in situ* calibration for the NMM instrument. The IH1 FD sensor is more sensitive to the change in θ conditions compared to the NMM technique shown by the large range of reported θ during the drying cycle.

4.4.4 Calibration and operational considerations of the IH1 probe

The NMM calibration almost exclusively indicates a linear response to increasing θ in soil conditions (e.g. Holmes, 1966; Cull, 1979; Greacen & Hignett, 1979; Jayawardane *et al.*, 1983; O'Leary & Incerti, 1993). The response of the IH1 FD probe to θ is soil dependent (Bell *et al.*, 1987). Initial field calibration indicated a linear relationship for small variations in θ, and, when considering the measured frequency, this could be incorporated into a general calibration (Bell *et al.*, 1987). The IH1 FD probe is supplied with a factory calibration based on a power function shown in Equation 4-4. The equation (4-4) is sensitive to change in θ condition especially when the soil is wet.

$$\theta_{IH1} = 50.21 \times \left(UF^{(12.73 \times UF)}\right) \tag{4-4}$$

As the measured frequency in soil approaches the water based frequency the determination of θ increases dramatically. Smaller frequency readings leading to a $UF > 1$ (from Equation 4-1) are not reported in the literature. However, soil with significant electrical conductivity can

cause a decline in the measured frequency, leading to overestimation of the *UF* and therefore overestimation of θ. A response to increasing salinity can be estimated by Equation 4-5 modeling the complex impedance of a capacitor (*C*) in parallel with a conductance (*G*).

For the IH1 down-hole FD probe, *C* is the capacitance of the soil-electrode (assembly) in a non-conductive soil. In a conductive soil let C_{eff} be the effective capacitance. Noting the angular frequency of oscillation (ϖ) is constant for the IH1 probe (7×10^8 s^{-1}). When the electrodes are placed in the soil, the *G*/*C* ratio is equal to specific conductance of the soil. For small values of *G*, *C* is not changed significantly (the multiplier in the bracket ≈ 1). However, as the conductance increases, the effective *C* increases leading to a smaller measured frequency. This can lead to a *UF* > 1 and overestimation of θ (pers. comm., J.D. Cooper; Institute of Hydrology, UK).

$$C_{eff} = C\left(1 + \frac{G^2}{\varpi^2 C^2}\right)^4 \tag{4-5}$$

In determining the *UF*, the water used in calculation of F_{water} should be indicative of the likely soil electrical conductivity conditions. During this experiment calculation of the *UF* was undertaken with available tap water and this introduced a small but unmeasured error into the *UF* determination.

Another non-linear relationship (for the FD technique) developed from measurement in a silt loam soil (Paltineanu & Starr, 1997) uses a power function:

$$\theta_{P\&S} = 0.490 \times UF^{2.1674} \tag{4-6}$$

This equation is more sensitive at small soil water contents (θ), becoming less sensitive as the θ increases and is related to Equation 4-4 by:

$$\theta_{P\&S} = 0.54707 + 0.0829 \times \log \theta_{IH1} \tag{4-7}$$

Where $\theta_{P\&S}$ is the θ from Equation 4-6, and θ_{IH1} is the θ in Equation 4-4. If we assume the NMM responds linearly to increasing θ we can plot the *UF* against the count ratio (*n*) to see how the IH1 FD sensor responds to increasing θ (shown by increasing *n*). Figure 4-9 shows all data of the IH1 down-hole FD probe plotted against the corresponding NMM count ratio. There is no readily identified relationship and an investigation of specific depths (Figure 4-10) shows little relationship between the measured *UF* and the measured *n*. The linear fit, at each depth, is shown for reference. Transformation of data (including log and reciprocal of both axis) and different fit techniques (including spline and polynomial fit) did not significantly

reduce the RMSE in fit. The IH1 FD probe is sensitive to change in θ conditions, however this change cannot be readily related to the NMM technique. Also, heterogeneity in θ condition immediately surrounding the IH1 FD probe could lead to reporting of different θ conditions. Clearly further study is required to gain confidence in the field use of the IH1 probe for reporting θ.

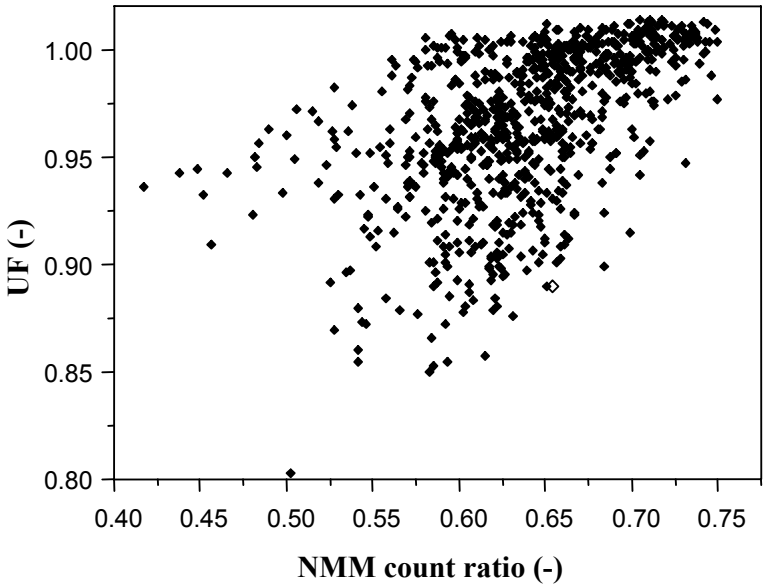

Figure 4-9 Plot of all *UF* data (combined sites and depths) against the NMM count ratio (*n*) at the Dubbo site. There is no readily identified relationship between the data indicating a different response to θ conditions.

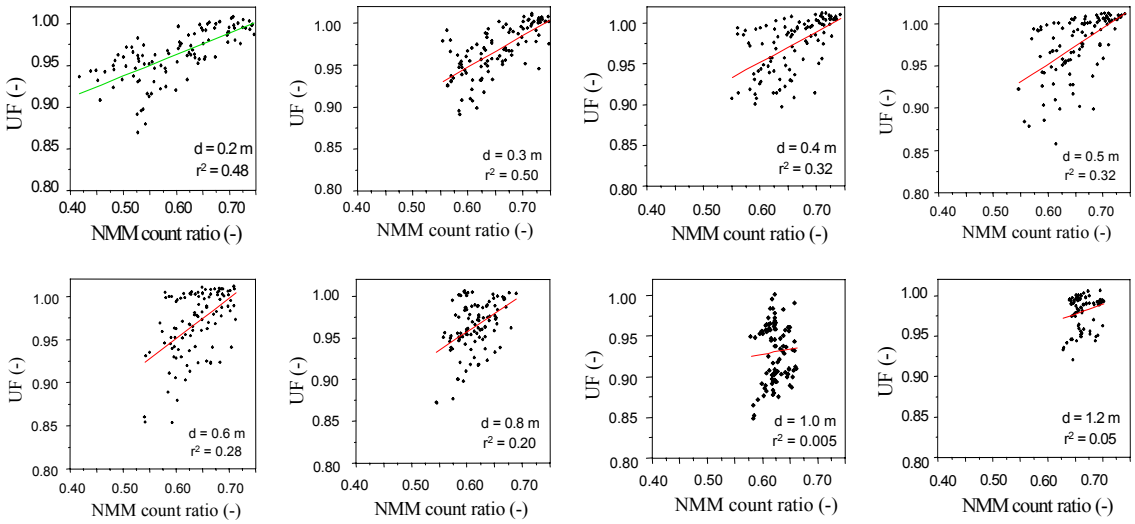

Figure 4-10 Depth plots of *UF* measured by the IH1 FD probe and the NMM count ratio (*n*). The linear fit is shown.

4.4.5 *Continual θ measurement*

The reported soil water stored (mm) from 0.0 to 0.7 m during a drying cycle (Figure 4-7), as measured by the EnviroSCAN® system, is shown in Figure 4-11. The EnviroSCAN® successfully measured the initial irrigation (≈ 10 mm), subsequent rainfall (≈ 75 mm) and following drying cycle as the *E. bicostata* trees used the available soil water. The reported EnviroSCAN® θ at different depths (0.2, 0.3, 0.4, 0.5 and 1.2 m) during the measured drying cycle (January 1994) is plotted against the NMM count ratio (*n*) in Figure 4-12. There is a reasonable agreement ($r^2 = 0.836$) between the reported θ from the EnviroSCAN® system and the NMM probe. The EnviroSCAN® system is more sensitive to change in θ conditions near the soil surface and this will contribute towards the error in comparing against the NMM *n*.

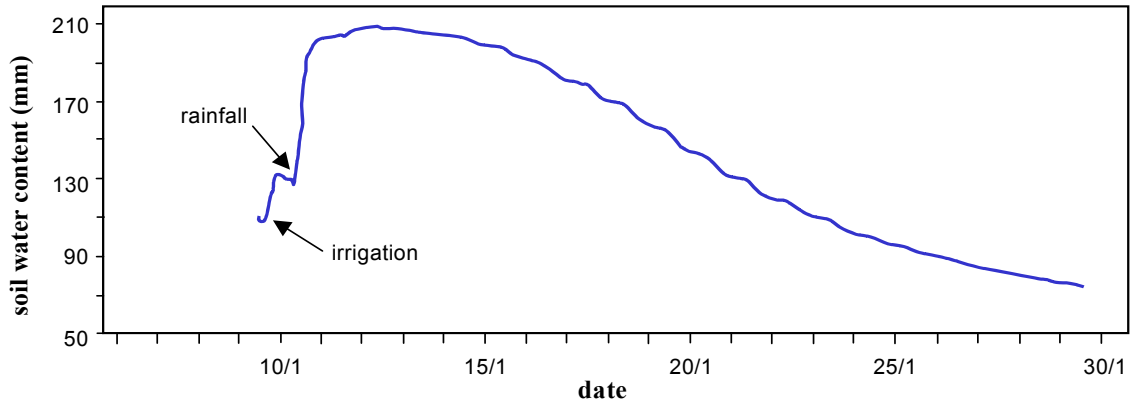

Figure 4-11 **Soil water content (mm) from 0.0 to 0.7 m depth measured by the EnviroSCAN® FD system during a drying cycle. Irrigation and rainfall events are shown.**

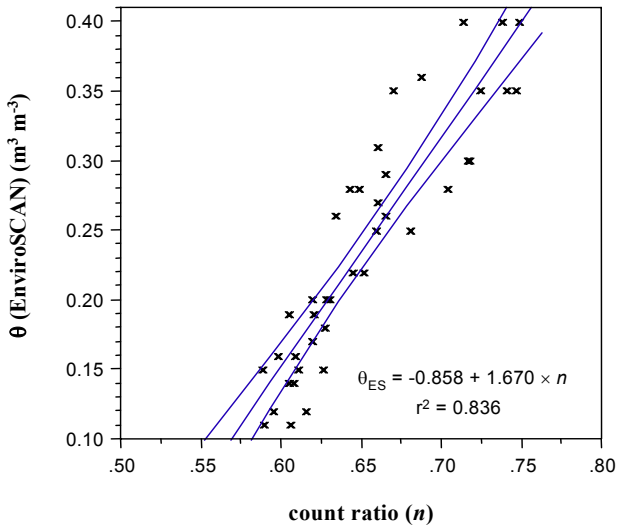

Figure 4-12 ***In situ*** **relationship between the EnviroSCAN® reported θ and the NMM count ratio (*n*) at site (2) during a drying cycle for depths 0.2, 0.3, 0.4, 0.5 and 1.2 m.**

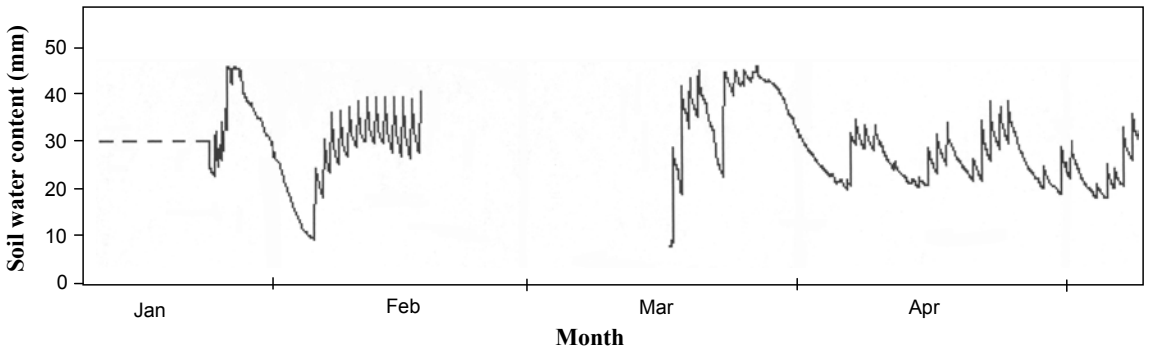

Figure 4-13 Continual measurement of θ at 0.1 m depth with the EnviroSCAN® system in 1993. The continual monitoring shows the effect of the short irrigation system used for effluent application in February.

A major advantage of the EnviroSCAN® system is the ability to continually obtain data. Figure 4-14 shows the changing soil water conditions with continued irrigation during late summer and autumn in 1993. Concentrating on the period between March 17 and April 10, θ at 0.10 m varies with the small irrigation amounts applied (nominally 5 mm daily). In this system the small increase in reported θ at 1.20 m depth around March 25 indicates the soil profile at that time was saturated with water moving beyond the sensor depth.

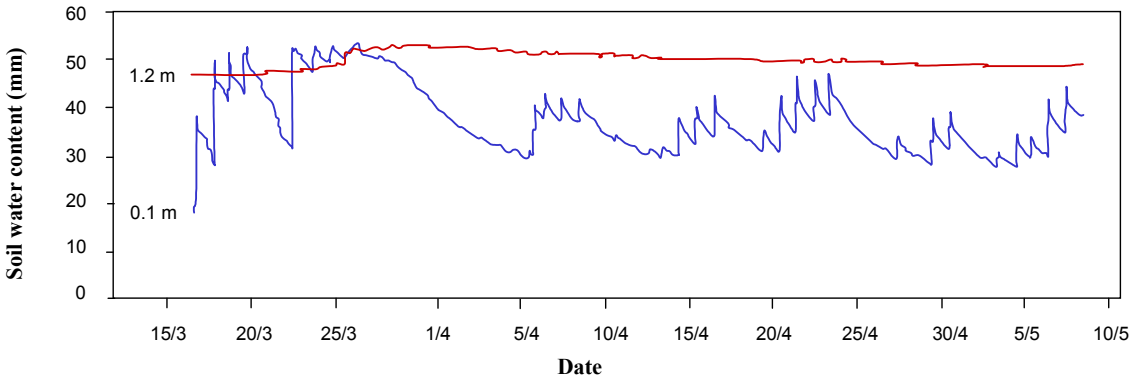

Figure 4-14 Continual measurement of θ at 0.1 m and 1.2 m depth with the EnviroSCAN® system in 1993.

4.4.6 Measurement with time-domain reflectometry (TDR)

Temporal measurement of θ down the TDR profile (Table 4-2) was not successful at site (2) or site (3) where TDR probes were installed (Figure 4-1). Probes continually failed, especially at large θ. Associated with the large reported θ was an increasing error (Figure 4-15), notably

deeper in the soil profile. Attenuation of the generated electromagnetic (EM) waveform caused most failure. Figure 4-16 shows the attenuation of the EM wave during measurement. The inability to obtain the end-point reflection was consistent at both sites and all depths, except 0 – 0.2 m, at varying times. One possible reason for the ability to continually monitor θ in the 0 – 0.2 m depth is the lighter textured soil due to the A horizon. As the clay content increases with depth it is possible that the electrical conductivity also increases leading to attenuation of the EM wave, especially in wet conditions. The electrical conductivity hindered the use of TDR probes > 0.2 m in a Vertosol because of the EM attenuation (Bridge *et al.*, 1996). Also, at the Dubbo field site, the installation of the TDR probes was sub-optimal. Some converging (unmeasured) of the three prong unbalanced probes could potentially have lead to changing the properties of the EM wave travelling through the soil. The ability of the TDR instrument to obtain and interpret a significant reflection is dependent on the power of the generated EM wave (pers. comm., H. Fancher; Soilmoisture Equipment Corp., CA USA), the interaction of the probe spacing (Zegelin *et al.*, 1989), and soil properties such as bulk electrical conductivity (Dalton, 1992).

Attenuation of the EM waveform is a significant problem in Australian soil where increased clay contents and inherent salt leads to increasing electrical conductivity. This is a particular problem when the soil is wet. There are several options to improve the ability of the TDR technique in saline environments including: an increase in the power generation of the EM wave; reduction of the length of the probes embedded in the soil (the EM wave then has less opportunity for attenuation); or coating the probes with a small dielectric material (Knight *et al.*, 1997). During calibration measurements with a 0.15 m unbalanced probe, at depths greater than 0.15 m, could not be obtained (graph not shown) indicating that the problem is significant in Brown Chromosols and probably other soil with a large clay content. Attenuation in saturated Vertosols can limit the (TRASE®) TDR to 0.15 m probes in the top soil (data not shown). If the bulk soil electrical conductivity is measured the maximum probe length can be estimated using the procedure outlined by Dalton (1992). By reducing the maximum operating length of the probes the reported TDR results become more susceptible to local variation in θ and the interpretation of the EM waveforms by automated analysis more difficult (Young *et al.*, 1997).

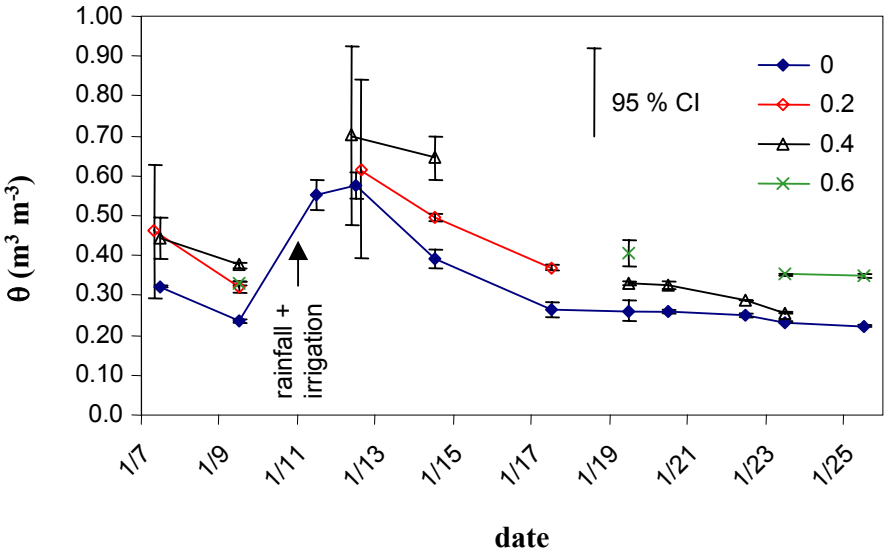

Figure 4-15 **Measuring θ during a drying cycle with TDR probes buried at 0 – 0.2 m, 0.2 - 0.4 m, 0.4 – 0.6 m and 0.6 – 0.8 m own a soil profile. Error shown is the 95 % confidence interval for measured θ. Readings on 1-Jan and 13-Jan are slightly offset for interpretation of associated error.**

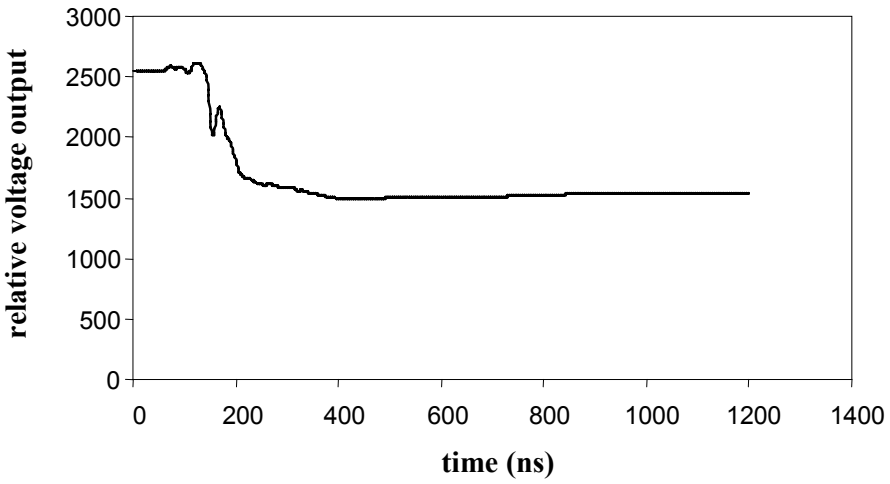

Figure 4-16 **Attenuation of the EM waveform due to increased electrical conductivity leading to an inability to detect the EM reflection from the end of the probes in the soil.**

4.5. CONCLUSIONS

An *in situ* calibration of an NMM probe in a Brown Chromosol suggests the "universal calibration" underestimates θ at large water contents. The calibration was carried out in a limited θ range and the associated error limits the application of the *in situ* calibration. Error was reduced by the application of a bulk density correction function (Greacen & Shrale, 1976). However, at smaller bulk density ($\rho_b < 1.4$), the correction function was not as effective.

The determination of the frequency of FD probes in water (F_{water}) as part of the *UF* should be considered in more detail. Results here indicate that the determination of *UF* in available tap water may lead to an overestimation of the *UF* in saline soil conditions. The FD technology is more sensitive to change in θ, especially when compared to the NMM technique. This improved resolution allows detection of small changes in θ but could be a disadvantage in heterogeneous soil.

A good relationship between the EnviroSCAN® system and the measured NMM count ratio (*n*) indicates the two systems both respond to changing θ conditions. The ability of the EnviroSCAN® system to continually monitor θ is a considerable advantage over other labour intensive systems.

The TDR technique was unable to measure θ when the soil was wet, especially at depths > 0.2 m. This was due to the attenuation of the EM wave along the 0.2 m unbalanced probes and this is likely to limit the application of the TDR technique for profile based measurement.

Chapter five

Measuring moisture content of stockpiled iron ore with the Time-Domain Reflectometry technique

5.1. ABSTRACT

Moisture content is important in determining the handling characteristics of processed iron ore. When moisture content is too high (> 0.1 g g^{-1}) handling is difficult and causes excess wear on machinery. If the stockpiled ore moisture can be measured, transport at optimum moisture contents may be undertaken. Time-domain reflectometry is a technique suited to *in situ* measurement of moisture in porous media. However, iron (Fe) present in soil is known to affect the dielectric properties. Recent studies suggest that large concentrations of Fe are likely to limit the ability of TDR in moisture determination (Robinson *et al.*, 1994). The electromagnetic waveforms require careful analysis to ensure accurate measurement of the actual travel time along the embedded probes in the iron ore. Calibration of TDR for determination of moisture content is recommended.

I calibrated the TDR method to measure moisture in a processed iron ore. The polynomial relationship between the refractive index ($\sqrt{K_a}$) measured by the TDR technique and known moisture (m^3 m^{-3}), $\theta = -0.776 + 0.410 \times \sqrt{K_a} - 0.034 \times K_a$, is particularly sensitive at higher moisture contents.

I then conducted a field trial to measure the change in moisture over time of iron ore layered in a stockpile. In the field study, a linear relationship between refractive index and moisture exists. This relationship, $\theta = \sqrt{(Ka_m - 0.197)} \times 0.0725 - 0.077$ (± 0.053) (m^3 m^{-3}), is not significantly different from the laboratory polynomial fit when constrained to similar moisture contents.

The 28 m extension cable used to connect the probes to the TDR affected the end-point determination of the TDR system. To account for this, 0.197 should be subtracted from reported K_a before calculation of volumetric moisture content. Protection of the extension

cable from the buried probe to the measurement node is necessary to stop the shear force of the ore stretching and snapping the cable. This is overcome by placing the extension cable inside a common garden hose and looping the hose near the probe insertion place in the stockpile.

5.2. INTRODUCTION

Time-domain reflectometry (TDR) is widely utilised in the study of saturated and unsaturated water determination and movement in soil. The technique, being based on the media dielectric surrounding the probes, can be influenced by the magnetic properties. However, in determination of volumetric moisture content (θ, $m^3\ m^{-3}$) in porous media, the effect of inherent magnetic properties (H, tesla; see Mullins, 1977 for discussion of appropriate units) is neglected as the electromagnetic (EM) wave travels in transverse mode (see Equation 1-12 and Equation 1-21). One element that has magnetic properties is iron (Fe). Iron is generally found in some soil in the form of goethite, haematite, ferrihydrite, maghemite and to a lesser extent (the primary mineral) magnetite. Robinson *et al.* (1994) found that very high concentrations of Fe present in the soil significantly affected the θ reported by the TDR technique. However, in most soil-based situations, this effect is unlikely to be a major influence on reported θ. The changing response of the TDR technique in determining the apparent dielectric (K_a) is an opportunity to exploit the TDR technique if a reasonable calibration is developed.

The mining and processing of iron ore is a major enterprise in the Australian economy. Ranked fourth in the world, Australia is a major producer and exporter of iron ore (http://www.minerals.org.au/facts/iron.htm). The ore is mined and then processed for bulk transfer, generally by train and/or ship, for further processing. The moisture content of iron ore (during processing and in stockpiles) is an important consideration of post-processing handling characteristics (Harbert *et al.*, 1974). During the refining process water is added. If the moisture content of the ore is too large then handling is difficult (Guerra, 1974). The main concern is freighting the iron ore to the port facility by train, and the "dumping" process where the ore is removed from train to conveyors for loading onto ore carriers (ships). Further problems can arise in maintaining processed ore within contract specifications for total moisture content (pers. comm. W. Thomas; Advanced Technical Development, Technical Resources Pty. Ltd., Australia).

On-line measurement of iron ore is not routinely carried out though Yip & Cutmore (1993) have successfully investigated continued measurement of free and bound water in iron ore during process transport. Bound water in this context relates to water retained by the iron ore

after drying at 378 °K (Yip & Cutmore, 1993). There are different techniques available for moisture content determination including infra-red reflectance (Harbert *et al.*, 1974) and neutron moderation and attenuation (Cutmore *et al.*, 1996). Non-invasive on-line measurement is carried out by microwave attenuation at high frequencies between 2 to 4 GHz. However attenuation of the generated EM wave restricts the penetration of the wave into the ore sample. Cutmore *et al.* (1996) suggest a maximum penetration of 150 mm at 10 % moisture by weight (w = 0.1 g g^{-1}). The TDR technique can partially overcome this uncertainty by utilisation of probes to guide the travel of the EM wave through the iron ore. Also the ability to connect probes to extension cable allows for measurement of θ within formed stockpiles. Our aim is to measure θ in stockpiles. To achieve this we first need to establish the relationship between the refractive index ($\sqrt{K_a}$) of the ore material and θ in controlled conditions. From this understanding we can then adapt the TDR technique for field based measurement of iron ore.

5.3. LABORATORY CALIBRATION

5.3.1 Materials and Methods

Processed iron ore from the Mt Tom Price mine (22° 40' 00", 117° 46' 00"; Western Australia), shown in Figure 5-1, was sieved to remove the > 5 mm diameter fraction. The cumulative ore characteristics are shown in Table 5-1. Haematite is the dominant form of iron present in the high-grade processed ore. The ore was dried (378 °K for 24 hours) and packed into a 0.25 m × 0.25 m × 0.20 m plastic container. 11.701 kg of ore was placed into the container filling a volume of 4.05 l. Thus the ore was packed to a (natural) density of 2.89 Mg m^{-3}. An unbalanced three-wire TDR probe (200 mm long) was placed into the middle of the container after half the ore was poured in. The rest of the ore was poured over the probe ensuring good contact with the stainless steel rods. Possible end effects were minimised by ensuring at least 20 mm between the end of the probe and the side of the container.

All readings were taken with the ore temperature between 18 °C – 19 °C (291 °K – 293 °K). Six readings of the K_a were recorded with a TRASE® TDR system (Soilmoisture Equipment Corporation, Santa Barbara, CA, USA) with one reading stored as a graph. The container was then emptied and repacked twice more to obtain further readings. This process was then repeated with a different TDR probe. For each known moisture content the associated TDR reading consisted of triplicate packing of the container and six measurements made each time

for both probes, giving a total of 36 readings per moisture increment. When the last replicate set of readings for each probe at the different moisture contents was taken a 28 m extension cable (RG50 MIL 17D 50 Ω Avico coaxial cable) was attached between the buried probe and the TDR instrument. Again six readings were taken with at least one saved as a graph for further interpretation. The ore was initially oven dry, that is a wetness (w, g g^{-1}) of 0.0 free water (Yip & Cutmore, 1993). After the initial TDR readings, deionised water was added to increase the w by 0.015 g g^{-1}. Water was added by spraying the sample and mixing thoroughly before re-packing. The ore sample was allowed to equilibrate for at least two hours before further TDR measurements were taken and more water added in similar increments (0, 0.015, 0.03, 0.045,…, 0.15 g g^{-1}). Triplicate samples were taken at 0.03, 0.06, 0.09, 0.12 & 0.15 g g^{-1} increments to check the actual moisture content and ensure even wetting. The wetness (w) was adjusted to account for the removal of ore during the calibration procedure.

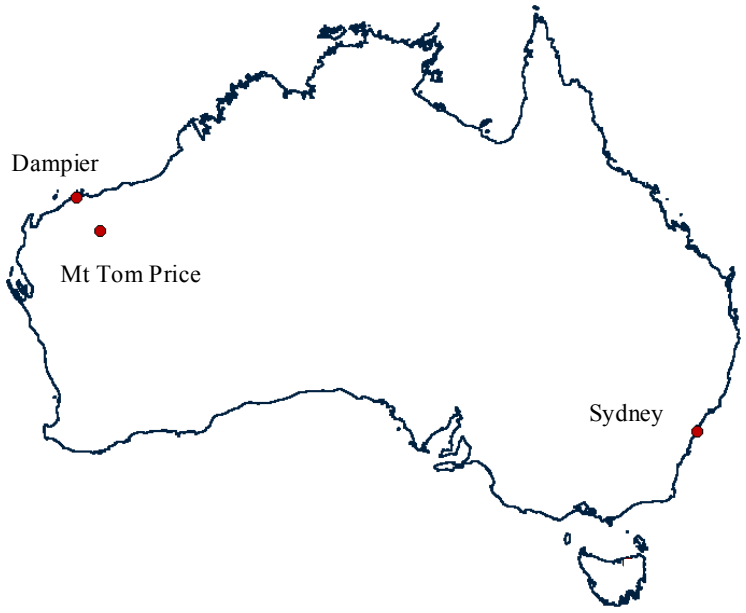

Figure 5-1 Location of Mt Tom Price iron ore mine and port facilities at Dampier, WA.

Table 5-1 **Physical and chemical analysis of ore production in feeder plant (before stockpiling) during field trial.**

Day	Total ore production (tonnes)	'Cyclone' feeder [+0.5mm] (tonnes)	'WHIMS' feeder [<0.5mm] (tonnes)	Total Fe (%)	Total Al_2O_3 (%)	Total SiO_2 (%)	Total P (%)	Bulk density (Mgm^{-3})	Total wetness ($MgMg^{-1}$)	Wetness 'WHIMS'	Total size [>0.5mm] (%)	Total size [>0.063] (%)	Total size [<0.063] (%)
one	3961	2660	1301	64.49	2.17	3.33	0.059	2.45	8.32	14.13	76.89	18.63	4.48
two	5282	3317	1965	64.83	1.61	3.62	0.081	2.81	8.25	14.82	85.22	12.08	2.71
three	8771	5485	3286	65.73	1.73	2.57	0.067	2.61	8.16	14.08	83.89	12.29	4.44
four	7614	5313	2301	65.75	1.88	2.51	0.051	2.56	7.63	14.13	84.55	13.08	2.37
five	9524	6360	3164	65.9	1.78	2.43	0.05	2.74	7.88	14.24	83.63	13.73	2.64
six	7607	4798	2809	65.41	2.1	2.86	0.05	2.84	7.56	13.36	82.2	13.73	4.08
total (average)				**65.49**	**1.86**	**2.78**	**0.06**	**2.68**	**7.92**	**14.09**	**83.16**	**13.57**	**3.40**
cumulative total	**42759**	**27933**	**14826**										

5.3.2 Results and Discussion

5.3.2.1 Calibration of TDR for estimation of iron ore moisture content

The spray wetting procedure produced an even wetting in the iron ore sample used in calibration with a low reported standard error in the sampled ore at five increasing *w* values (Table 5-2). The removal of ore to estimate *w* required a small change in the calculation of actual *w*. This corrected *w* value is used in all further calculations.

The first check of *w* (0.03 g g^{-1}) reported close to the correct wetness. As moisture content increased a maximum difference of 0.0131 g g^{-1} between actual (average) *w* and measured *w* occurred at a target moisture content of 0.15 g g^{-1}. During the wetting up process segregation of finer material into clumps was observed and this could account for the differences in total average *w* and measured *w* from three samples. The deviation of measured *w* (n = 3) did not increase at higher moisture contents.

Table 5-2 Actual *w* for calibration with TRASE® TDR and associated check values.

Target *w* (g g^{-1})	Actual *w* (g g^{-1})	Measured *w* (g g^{-1})	Standard Deviation (± g g^{-1})	Actual – Measured
0.00	0.00	--	--	--
0.015	0.0150	--	--	--
0.030	0.0299	0.0295	0.00036	0.0005
0.045	0.0454	--	--	--
0.060	0.0609	0.0569	0.0013	-0.0040
0.070	0.0768	--	--	--
0.090	0.0928	0.0879	0.0012	0.0049
0.105	0.1091	--	--	--
0.120	0.1255	0.1158	0.00096	0.0097
0.135	0.1423	--	--	--
0.150	0.1593	0.1462	0.00089	0.0131

The TDR technique successfully measured the change in K_a with the increase in *w*. The change in the TDR waveform with increasing moisture content is shown in Figure 5-2. The waveforms are normalised according to Equation 1-23 (White & Zegelin, 1995). The increase in *w* is associated with EM wave attenuation due to increasing bulk soil electrical conductivity (σ). This is shown by a decline in the returning EM wave reflection. However the signal was not totally attenuated during the calibration process even at 0.159 g g^{-1} (θ = 0.46 m^3 m^{-3}) with readings successfully obtained. The form of iron present in the ore will affect the travel of the EM wave. Robinson *et al.* (1994) found an increase in the presence of magnetite significantly increased the travel time along the probes though there was no increase in actual moisture content. In this calibration procedure there is no change in the composition of the iron present, only moisture, thus simplifying the interpretation. Robinson *et al.* (1994) indicated that increasing iron present in the form of haematite or goethite will not significantly change the travel time along the embedded probes.

Table 5-3 Determination of refractive index for all readings (used in calibration to moisture), readings with and without RG-58 extension cable (Figure 5-7). Error is shown as ± the standard error of the mean.

w (g g^{-1})	θ (m^3 m^{-3})	$\sqrt{K_a}$ (-) all readings	$\sqrt{K_a}$ (-) no extension	$\sqrt{K_a}$ (-) 28 m extension
0.00	0.00	2.493 (± 0.0280)	2.582 (± 0.0021)	2.761 (± 0.0020)
0.0150	0.0433	2.701 (± 0.0063)	2.676 (± 0.0019)	2.925 (± 0.0023)
0.0299	0.0864	2.757 (± 0.0107)	2.833 (± 0.0031)	3.110 (± 0.0021)
0.0454	0.1312	2.851 (± 0.0058)	2.875 (± 0.0019)	3.169 (± 0.0023)
0.0609	0.1760	3.101 (± 0.0151)	3.124 (± 0.0022)	3.375 (± 0.0158)
0.0768	0.2220	3.243 (± 0.0085)	3.260 (± 0.0017)	3.474 (± 0.0017)
0.0928	0.2682	3.682 (± 0.0141)	3.762 (± 0.0013)	3.963 (± 0.0012)
0.1091	0.3153	4.307 (± 0.0096)	4.335 (± 0.0038)	4.620 (± 0.0018)
0.1255	0.3627	4.821 (± 0.0417)	4.742 (± 0.0020)	5.367 (± 0.0025)
0.1423	0.4112	6.375 (± 0.0307)	6.207 (± 0.0061)	6.388 (± 0.0033)
0.1593	0.4604	6.536 (± 0.0119)	6.577 (± 0.0230)	6.922 (± 0.0038)

The TRASE® TDR reported sensible[1] K_a values for measurements from dry to wet conditions with the standard error of the mean shown in Table 5-3. Robinson *et al.* (1994) found the TRASE® TDR interpretation inconsistent at low moisture contents with a mixture of magnetite and sand. This is possibly due to the short travel time along the unbalanced probes with high impedance yielding confusing multiple reflections (from their figure 2). During the calibration of the TDR system in iron ore this problem was not encountered at smaller moisture contents.

Error is greater in the combined readings. This is due to the process of re-packing the ore around the probes (six times at each nominated moisture) producing a small change in the measured moisture. Further error is derived from the TDR determination of the end-point (travel time of the EM wave along the probes). The greatest error (± 0.0417) occurred with a known θ value of 0.363 m^3 m^{-3}.

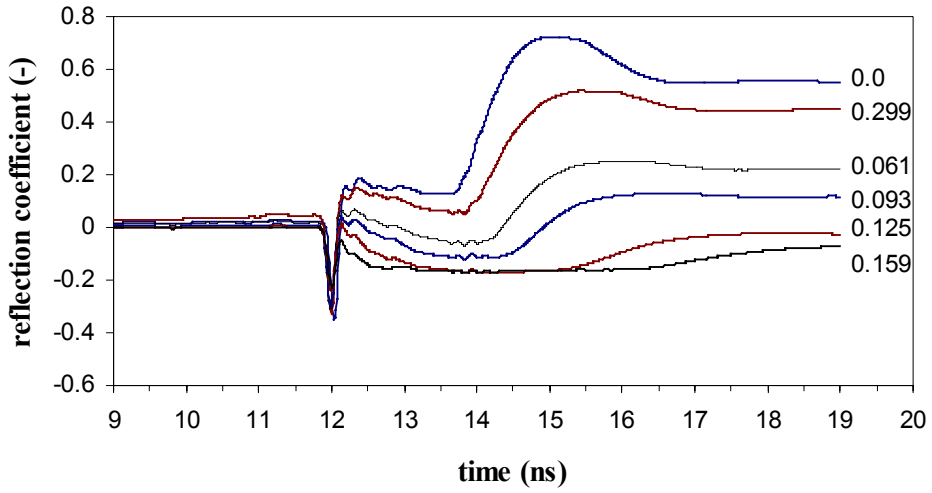

Figure 5-2 Normalised waveforms for increasing moisture content (*w*, g g^{-1}) of iron ore during calibration.

The relationship between the mean measured refractive index (n = 17) and θ is best estimated by a second-order polynomial equation shown in Figure 5-3. Using stepwise regression, the Mallows Cp (at 5% significance level) indicates significant improvement in the model fit with incorporation of added parameters. In this case the parameters are the higher order polynomials. Table 5-4 shows the results of parameter inclusion with the linear and quadratic polynomial improving model fit significantly. The Cp does not decline with further parameter

[1] "sensible" dielectric in this context refers to the absence of obvious outliers (e.g. K_a = +1000) found by Robinson *et al.*, 1994.

inclusion indicating that the cubic fit is not necessary. This is also seen with the small increase in model fit (r^2).

Straight-line estimation is poor ($r^2 = 0.856$) compared to the polynomial equation ($r^2 = 0.972$):

$$\sqrt{K_a} = 2.659 - 2.752 \times \theta + 25.239 \times \theta^2 \quad (5\text{-}1)$$

This differs from soil calibration where the $\sqrt{K_a}$ versus θ plot normally yields a linear relationship (Whalley, 1993; Topp *et al.*, 1994). However, Zegelin & White (1994), in calibrating TDR for different ores, found different polynomial relationships of the third and fourth orders offering a better estimation compared to the linear model. If restrained to $\theta < 0.3$ $m^3\ m^{-3}$ the linear relationship can be compared to those reported by Robinson *et al.* (1994) for iron present in different forms (their Figure 4). In this calibration the TDR technique exhibits a lower sensitivity to moisture content change (that is, the slope of the calibration is smaller).

Table 5-4 Stepwise regression for determination of significant model fit in calibration.

Step	Significance	Model SS	r^2	Cp
1	0.0000	18.3434	0.872	57.50
2	**0.0003**	**2.2080**	**0.977**	**6.48**
3	0.6943	0.0112	0.978	8.21
4	0.1213	0.1642	0.986	6.27
5	0.1922	0.0946	0.990	6.00

As $\theta \rightarrow 0$ the polynomial relationship indicates an increase in estimated Ka. The $\sqrt{K_a}$ of the oven-dry material (2.46 ± 0.15) is the lowest $\sqrt{K_a}$ measured by the TDR during this experiment. The estimation below 0.05 $m^3\ m^{-3}$ should be considered with care. It is unlikely that moisture content determination will occur in this range and is not considered significant in calculation.

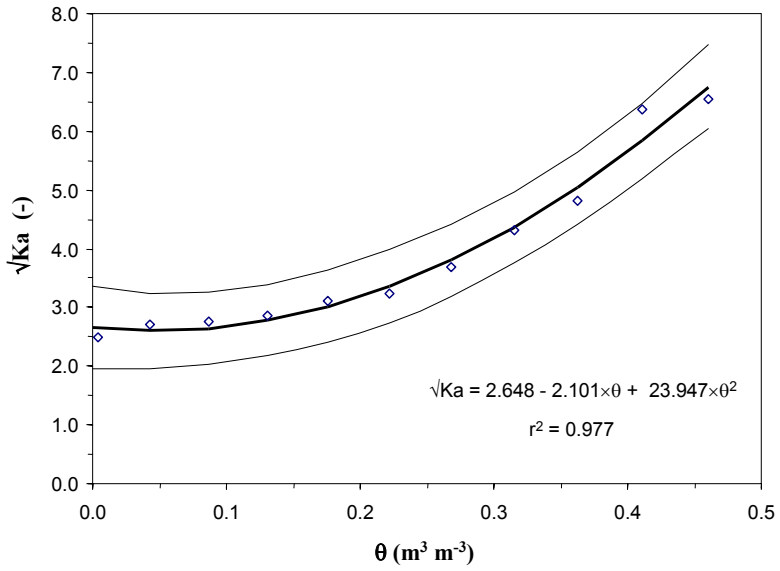

Figure 5-3 Polynomial relationship between the $\sqrt{K_a}$ (-) and the known volumetric moisture content, θ ($m^3\ m^{-3}$), for processed iron ore from Mt. Tom Price mine. The highest standard error of the mean (±0.05) occurred when known θ was 0.39 $m^3\ m^{-3}$. The 95% confidence interval for the equation fit is shown.

In order to exploit a relationship between the measured $\sqrt{K_a}$ and θ the inverse estimation technique (Webster, 1997) is employed. Thus, inverting equation 5-1 the estimation of θ from measured $\sqrt{K_a}$ for the iron ore is given by the equation:

$$\theta = -0.776 + 0.410 \times \sqrt{K_a} - 0.034 \times K_a \qquad (5\text{-}2)$$

and shown in Figure 5-4 with associated error in prediction.

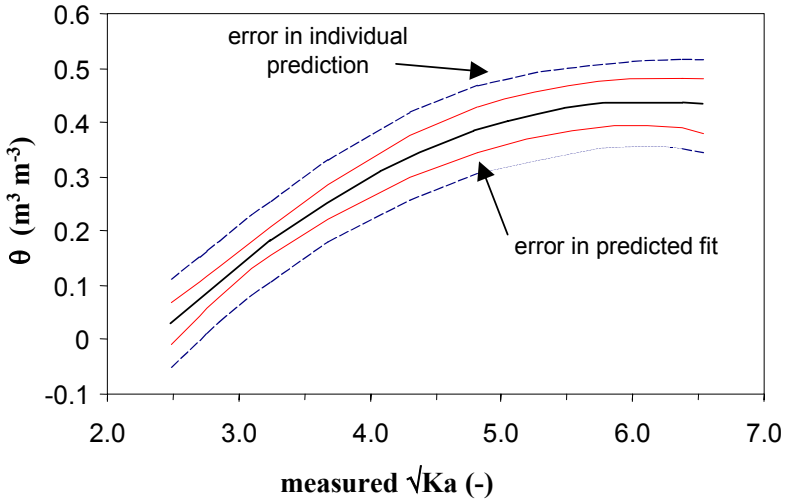

Figure 5-4 Calibration of TDR for determination of θ in iron ore from measured $\sqrt{K_a}$. Confidence limits are 95% for prediction of line and individual points respectively (SAS, 1995).

5.3.2.2 Effect of transmission cable on reported $\sqrt{K_a}$

In field based measurements an RG-58 transmission cable (28 m length) was utilised to connect the buried probe to the measuring TDR instrument. The extension cable influences the travel of the EM wave (Chapter 2). Normalised waveforms (Equation 1-23) at 0.0, 0.061 and 0.126 g g^{-1} are shown in Figure 5-5. The EM waveform is filtered, as it travels through the cable, and then into the lossy media (iron ore). Qualitatively this is observed with a loss of resolution in resulting waveform. For all moisture contents the transmission cable caused a loss of signal. The information loss can also lead to a small change in the start and end-point determination of the EM wave. Most TDR systems employ an automatic end-point determination analysis. These systems will preferably err in a systematic form with the change in end-point determination then quantified.

The relationship of measured $\sqrt{K_a}$ and the influence of the extension cable is shown in Figure 5-6. The linear fit ($r^2 = 0.991$) of the plotted mean (n = 5 - 10) measurements shows that the addition of extension cable between the TDR instrument and the probe increases the reported $\sqrt{K_a}$. The modeled increase:

$$\sqrt{K_a}\ (\text{extension}) = 0.1966 + 1.0211 \times \sqrt{K_a}\ (\text{no extension}) \tag{5-3}$$

requires further consideration in field based estimation of iron ore θ by the TDR technique. Though statistically significant (p = 0.05, paired t-test output for slope, data not shown) indicating a difference from a slope equal to one, the relationship between K_a with extension cable and without extension cable is essentially 1:1.

The statistical difference is due to the low error associated between reading with, and without, extension cable. Therefore in order to account for the effect of the extension cable on the EM wave in determining true $\sqrt{K_a}$, 0.197 should be subtracted from the measured $\sqrt{K_a}$ before predicting θ when this RG-58 cable is used.

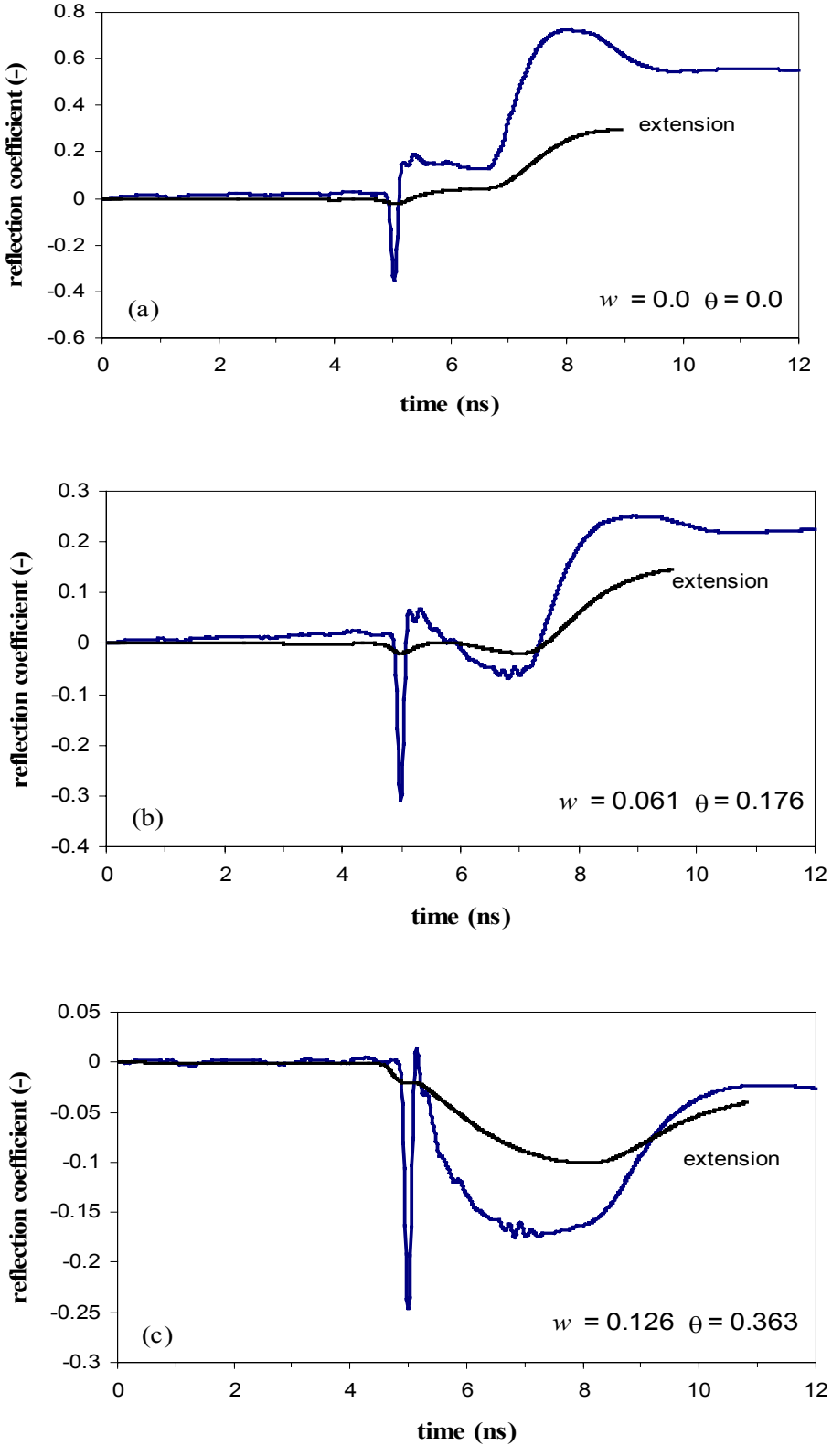

Figure 5-5 **Effect of a 28 m RG-58 transmission cable on reflection coefficient for increasing moisture content in iron ore: (*a*) 0.0 g g^{-1}; (*b*) 0.061 g g^{-1}; (*c*) 0.126 g g^{-1}.**

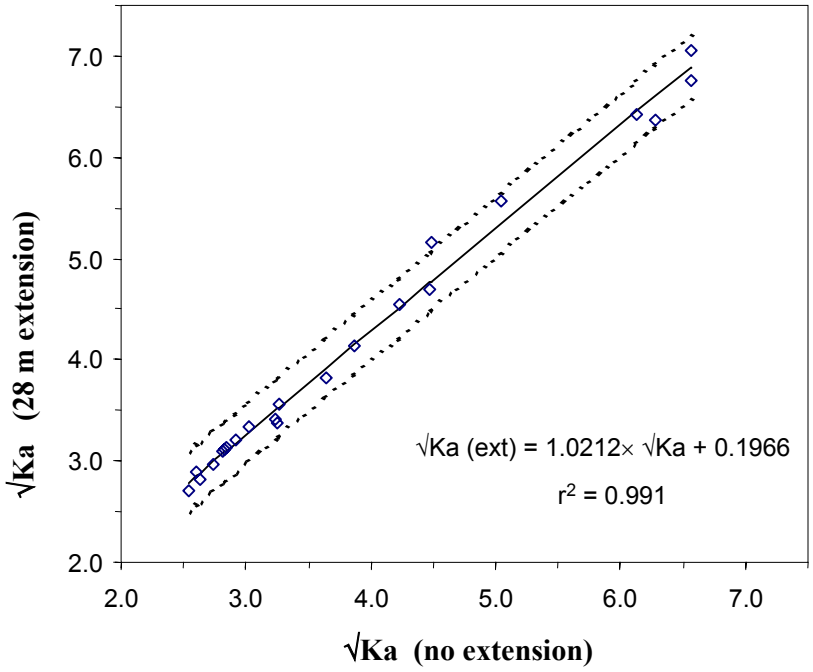

Figure 5-6 Effect of a 28 m RG-58 extension cable on reported K_a by TRASE® TDR at increasing moisture contents for iron ore. The 95% confidence interval for estimation is derived from a combination of estimate variability and the variability of observation (SAS, 1995).

5.4. FIELD MEASUREMENT AND CALIBRATION

5.4.1 Materials and Methods

5.4.1.1 The site

The field trial was conducted at Mt Tom Price, owned and operated by Hamersley Iron Pty Ltd a company in the Rio Tinto mining group. The site is situated in the Pilbara region containing the Hamersley Range as shown in Figure 5-1. The Hamersley Group ore body was formed during the Early Proteozoic age mostly by chemical sedimentation following a phase of basic volcanism and clastic sedimentation in the Fortesque group. The banded iron formation in the Hamersley Group typically contains about 30% iron (Fe) by weight. The high-grade ore is predominantly haematite interleaved with shale bands of varying thickness (RTZ-internet address: http://www.mining-technology.com/projects/hamersley/mounttp_index.html). The ore formation could reflect local pedologic formation with haematite dominating in the well-drained conditions (Singer *et al.*, 1998). Three main groups of iron ore deposits are found in

the local region. At the Mt Tom price mine the most common ore is from the Brockman Iron Formation. This ore, further defined by composition of elements, is considered a "premium lump" with low phosphate (< 0.05 %) and high Fe (> 64 %) contents (http://www.mining-technology.com/projects/hamersley/ mounttp_index.html).

The mining operation commenced in 1966 and extends 7.5 km over six principal locations in the ore body. The mining procedures aim to separate the high grade from the lower grade ore. The lower grade ore is fed to the concentrator plant where ore is physically treated to produce three fractions:

- oversize (> 30mm)
- lump product (6 mm < lump < 30 mm)
- fines product (< 6 mm)

The oversize fraction is returned through the processing plant to produce either lump product or fines. The fines fraction is then stockpiled for blending with other quality product in shipments to the port facility (based at Dampier, WA). The fines generally end processing with a (gravimetric) moisture content between 10 – 14 % (w = 0.10 – 0.14 g g^{-1}). Due to the high moisture content the fines are termed "wet fines". For handling and shipping purposes an optimum w of 0.08 g g^{-1} is preferred (pers. comm. N. Poetschka; Hamersley Iron Pty Ltd., Australia). To achieve this the wet fines ore is stockpiled for several days before transportation to the port facilities. The WHIMS plant is the final processing stage where the wet fines are produced before stockpiling.

The stockpiles are created by a 'stacker' that normally produces a stockpile of dimensions 18.5 m high, 53 m wide, approximately 375 m long with an internal wall angle of 35^{o} (pers. comm. W. Thomas, Advanced Technical Development, Australia). This process requires approximately 160 passes of the stacker, normally taking about five days, with the ore layered in a chevron pattern. After a period of draining the wet fines are reclaimed and loaded into train cars for shipment to the port facility.

5.4.1.2 Experimental design

The original design placed thirty horizontally buried TDR probes (supplied by CSIRO; Glen Osmond, SA) in the stockpile in three locations, points (A), (B) and (C) in Figure 5-7. The probes were to be stratified to assist in determining the intra-stockpile variability. Production problems in the WHIMS section of the ore processing forced a change in the stockpile design and location of TDR probes. The final dimensions of the stockpile are shown in Figure 5-7.

At cross section A, the final height of the stockpile was 9.35 m. For cross sections B and C the heights were 11.11 m and 14.75 m respectively.

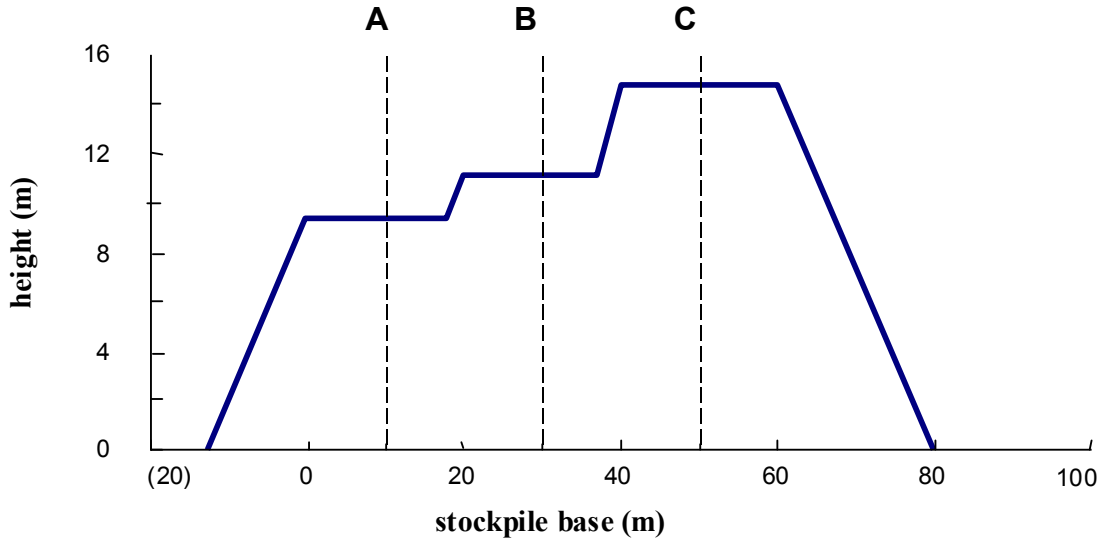

Figure 5-7. Schematic side view of actual stockpile of wet fines ore with cross sections where TDR probes were positioned. At the completion of the experiment density and calibration samples were taken from these cross-sections.

The stockpile was built over a period of six days by the stacker moving along the length of the stockpile dropping the ore from varying height (typically 1.5 ± 0.5 m) above the pile. As the stacker passed a position in the pile the probes were buried in the recently layed ore. The probes were covered with ore (using a hand shovel) and once the stacker had returned to cover the position again a measurement was taken with the probe connected directly to the TRASE® TDR (Soilmoisture Equipment Corporation, Santa Barbara, CA, USA). A 28 m extension cable (RG-58 coaxial cable) was connected to the probe and buried at 300 mm depth along the side of the stockpile leading to a common point for the cross section (A, B and C respectively). Initial readings with the TDR instrument were satisfactory. Some probes (e.g. C01) failed when further ore stacked on top of the building stockpile cause mass movement down the edge of the stockpile shearing the extension cable. This problem was overcome by threading the extension cable through common garden hose before burying the probe and extension cable in the stockpile. The extension cable, now housed in the garden hose, was collected in two loops (approximately 2m of cable) at the base of the buried probe. This technique was utilised to account for shift of the TDR probe as the layered ore above was stacked. Probe locations are shown in Figure 5-8. Five probes failed at some stage during the ore stacking processes. Notably none of the probes protected with the common garden hose failed.

The calibration of the TRASE® TDR required determination of bulk density (ρ_b). Two techniques were tested in ρ_b determination. The core method (Blake & Hartge, 1986) is commonly used in calibration for TDR measurements in porous material. To obtain measurements steel cylinders (51.2 mm internal diameter, 200 mm length) were hammered in around the buried probe. The wet and dry ρ_b was then determined after weighing and drying. A second technique, the sand replacement method (Blake & Hartge, 1986), was also used. This is the more common method for mining engineers in this situation. A small hole (approximately 300 mm deep and a radius of 200 mm) is dug in the iron ore and a known mass of sand then replaces the iron ore. The mass and volume are then used to calculate the ρ_b as described by Blake & Hartge (1986).

Permeability was determined at all cross-sections during reclamation (unpublished data, P.Lam, MPA Williams & Associates, Australia). Values for cross section C are included in Appendix 5-1. Personal observations indicated lower permeability occurred where finer material congregated on falling from the stacker. This was not quantitatively assessed. Generally the ore is considered free draining.

5.4.2 Results and Discussion

After insertion and connection to an extension cable, triplicate readings on all probes were taken at approximately six-hour intervals. A field calibration was established accounting for changes in ρ_b. The field calibration also tested the laboratory calibration *in situ*. Further, probes were measured with a TRASE® TDR immediately after installation before extension cable was attached and then immediately after the extension cable was connected. This accounted for the influence of cable extension on the reported K_a and is discussed in further detail. The determination of ρ_b was attempted with two techniques and a consideration of the limitation in measurement with the standard core method (Section 1.2.4.1) in comparison to the more robust sand-replacement technique is discussed.

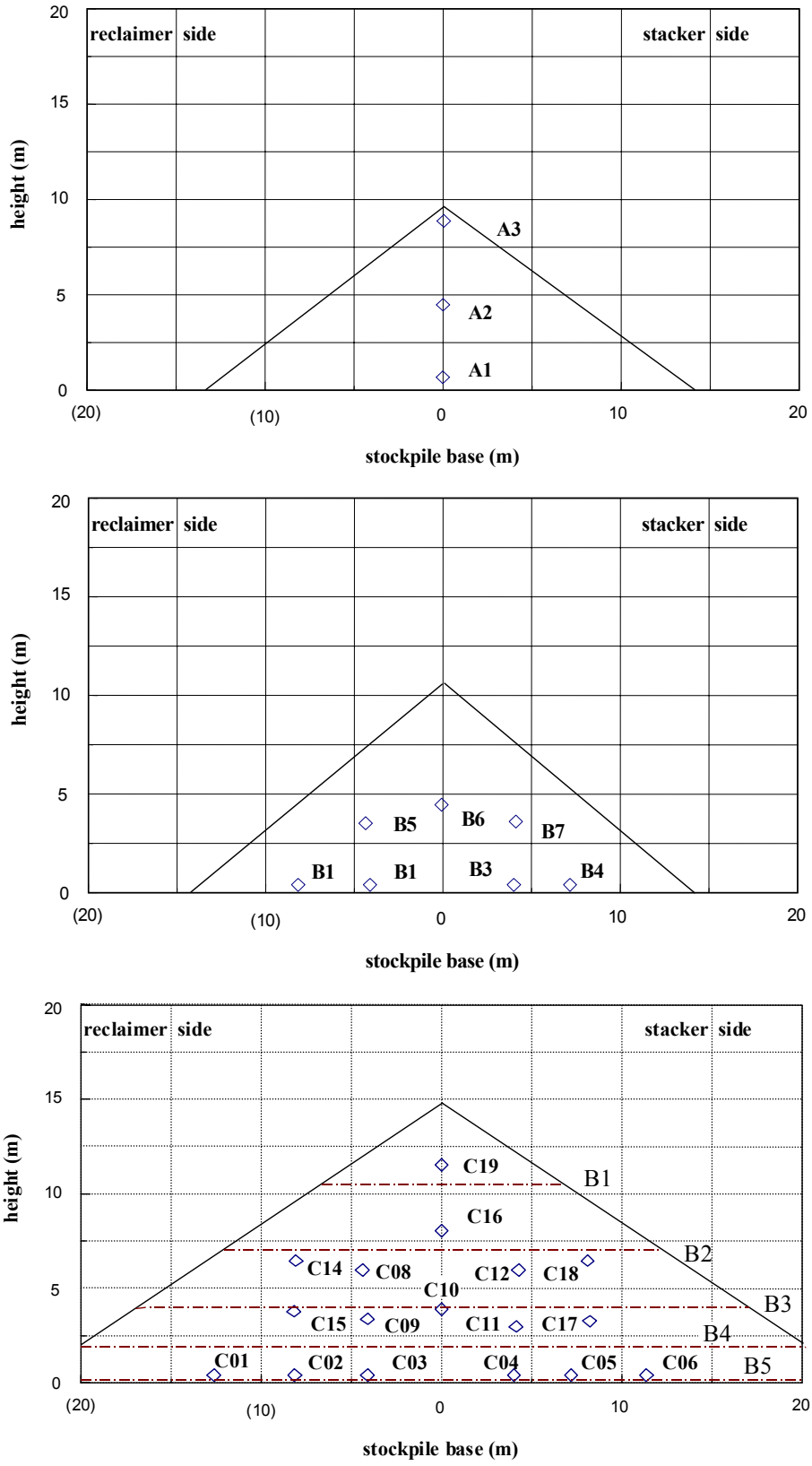

Figure 5-8 **TDR probe locations at three cross-sections of stockpile. Due to production problems ore was directed over cross-section C to achieve regular stockpile height and formation.**

5.4.2.1 Calibration to θ

To obtain an estimation of the ore θ, a field calibration of the TDR technique is required. Calibration of the TDR measured K_a against the calculated θ is shown in Figure 5-9 with the refractive index ($\sqrt{K_a}$) plotted against the calculated moisture content of the ore. Testing the linear relationships (Mead *et al.*, 1993) indicates no significant difference between field and laboratory calibrations ($p = 0.05$) with $F_{2,22}$ degrees of freedom. Similar results were obtained with a t-test procedure for determination of slope difference outlined by Steel & Torrie (1980). In comparison, data from the laboratory calibration below 0.15 m^3 m^{-3} were excluded and a linear model fitted. The two linear calibrations are shown in Figure 5-9. The slopes are almost identical with the significant difference in the intercept. For a measured θ the predicted $\sqrt{K_a}$ is higher (+0.634) in the field calibration. This calibration is used for conversion to θ for the field trial results.

One possible explanation for the increase in intercept for field calibration is the changing ρ_b conditions. ρ_b was estimated around the probe locations during the reclamation of the ore stockpile (for transport). Across the stockpile mean dry ρ_b was 2.66 (± 0.18) Mg m^{-3} from 41 sand replacement measurements. The mean was used where ρ_b determination was not made within 2 m of the TDR probe. The determination of ρ_b is discussed further in Section *5.4.2.3*.

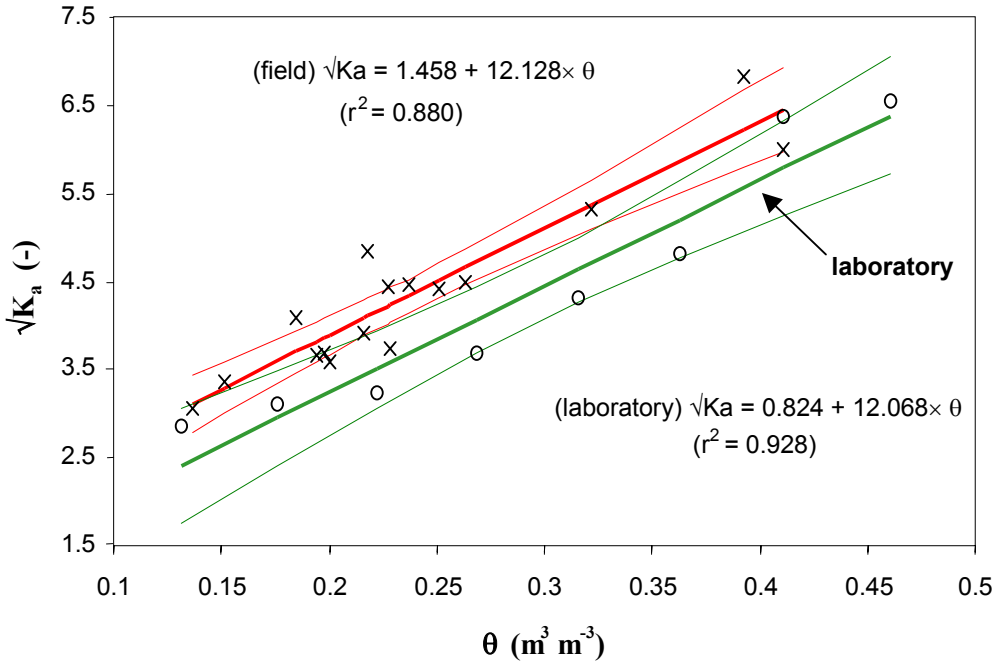

Figure 5-9 Calibration of *in situ* iron ore moisture content from refractive index measured by TDR.

For moisture $0.1 < \theta < 0.45$ the relationship is estimated:

$$\sqrt{K_a} = 12.128 \times \theta + 1.458 \quad (5\text{-}4)$$

Zegelin & White (1994) calibrating coal and nickel ore media, found similar relationships especially for a Bayswater meta-anthracite coal. I am unaware of other published results of iron ore calibrations. Zegelin & White (1994) reported several different calibrations for coal with different physical make-up and it is expected that iron ore from different sources could require unique calibration. For prediction of θ the inverse estimation (Webster, 1997) is used, producing the relationship:

$$\theta = 0.0725 \times \sqrt{K_a} - 0.077 \quad (5\text{-}5)$$

shown in Figure 5-10 with the error associated in prediction.

5.4.2.2 Calibration for extension cable length

The 200 mm long unbalanced probes were connected to RG-58 coaxial cable and measurements taken from set nodes around the stockpile. The extension cable influences the reported K_a and this needs to be accounted for in the calibration. The relationship of reported K_a measured with the 28 m extension against measured K_a with no extension is shown in Figure 5-11 with the laboratory calibration. Comparison of the two regression slopes indicates no significant difference ($p = 0.05$).

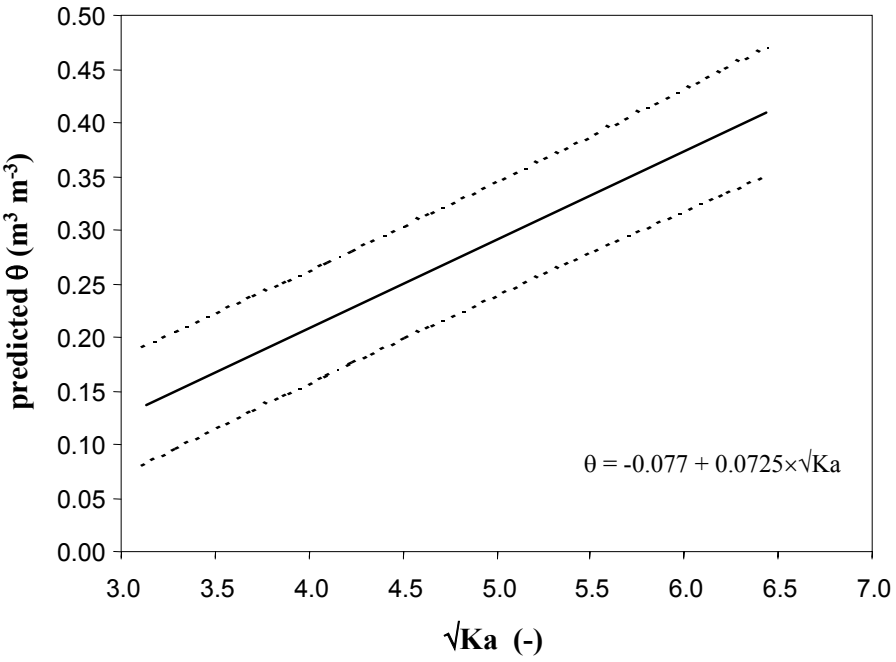

Figure 5-10 Field calibration of TDR for prediction of moisture content (θ) in field experiment.

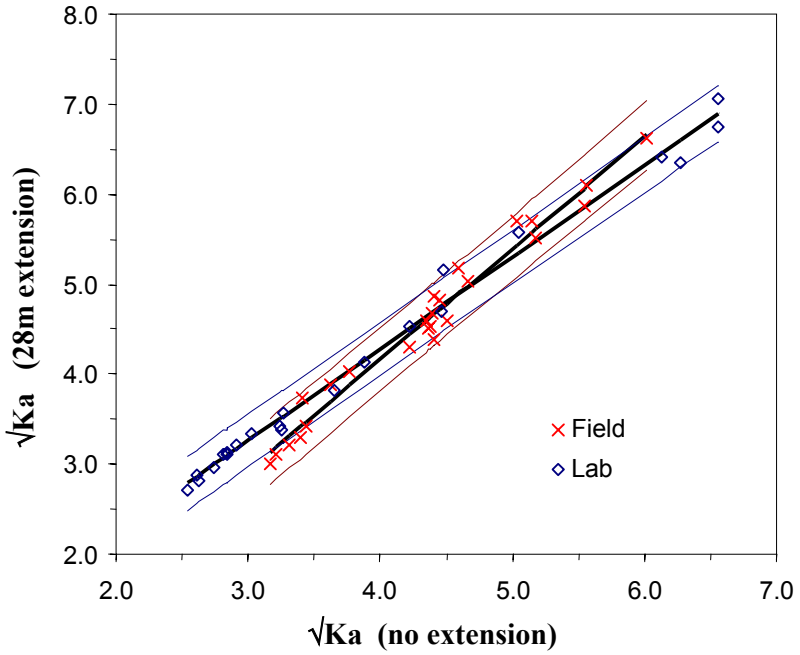

Figure 5-11 The effect of 28 m RG-58 extension cable on reported refractive index with the TRASE® TDR in field and laboratory conditions. 95 % Confidence intervals are shown for respective data sets.

5.4.2.3 Determination of *in situ* bulk density (ρ_b)

ρ_b (Mg m^{-3}) is required to calculate wetness (w, g g^{-1}) from the measured θ from equation (1-4). ρ_b was determined by two methods as described by Blake & Hartge (1986). The core method is widely used for *in situ* calibration of the TDR technique. A sample of known volume is extracted and w determined by weight difference after drying (378 ºK for 24 hours). In mining operations the sand replacement method is preferred. The sand replacement method avoids the compaction that can easily occur with the structure-less iron ore. Thirteen paired ρ_b samples (from duplicate or triplicate measurements) were obtained with the core and sand replacement methods during stockpile reclamation. The core method reported a significantly higher ρ_b (3.33±0.21 Mg m^{-3}) compared to the sand replacement technique (2.66 ± 0.18 Mg m^{-3}) across the stockpile ($p < 0.01$). The measurements were poorly correlated (r = 0.178). This can be shown graphically (Figure 5-12) where no relationship is identified in the scatter plot. The core method is prone to overestimation of ρ_b in weakly structured material (McIntrye & Barrow, 1972). Observation during the sampling process indicated ore movement leading to

potential compaction, however a rigorous assessment of the two density determination techniques was not undertaken in the field trial. With poor correlation and concerns regarding the sampling procedure the core method was not employed for conversion and analysis of moisture contents. Estimated ρ_b from the sand replacement measurement is used in calibration calculations.

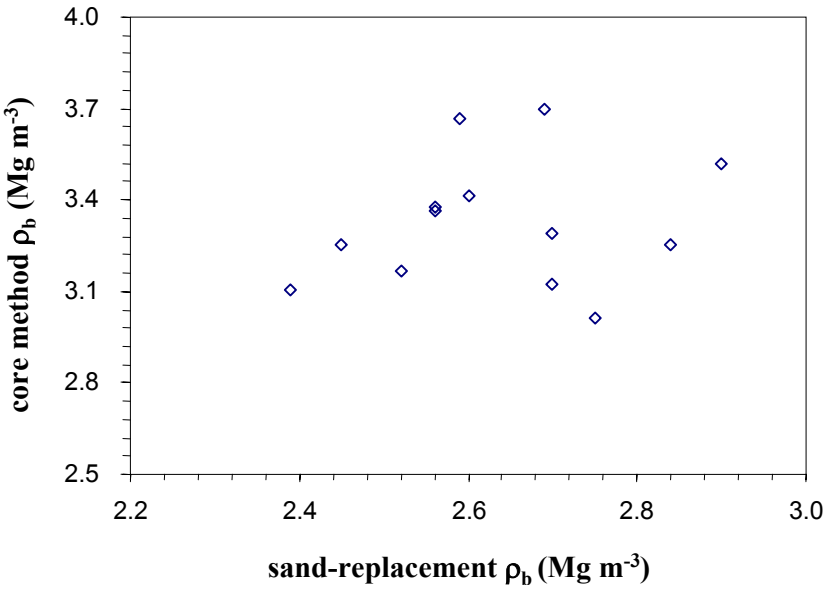

Figure 5-12 Plot of BD determined by the core method and sand-replacement method in the iron ore stockpile.

The wet and dry ρ_b was determined across the stockpile. The correlation between the $\rho_b w$ and $\rho_b d$ calculation for the sand replacement method is strong (r = 0.962). The stockpiled iron ore does not exhibit any shrink-swell properties and a high correlation between the $\rho_b w$ and $\rho_b d$ is expected. The relationship between wet and dry ρ_b is shown in Figure 5-13.

5.4.2.4 Moisture measurement across stockpile

After checking the field calibration for determination of θ against the laboratory determined relationship, and accounting for the effect of extension cable on measured Ka, moisture content in the stockpile can be estimated with the TDR.

For a measured K_a (Ka_m) the procedure to determine θ for iron ore in the stockpile is:

$$\theta = \sqrt{(Ka_m - 0.197)} \times 0.0725 - 0.077 \cdot (\pm 0.053)\ \mathrm{m^3\ m^{-3}} \qquad (5\text{-}6)$$

All reported data is calculated with Equation 5-6 from averaged Ka_m (normally n = 3 TDR readings). Moisture content varied across the profile depending on probe position. Normal

stockpile formation takes two to three days. Due to production problems this period was extended to six days. Ore supplied to the stockpile was not as uniform as normal production (pers. comm. N. Poetscha; Hamersley Iron, Australia). This resulted in segregation of fine material in the chevron stacking process during stockpile formation. The segregation of fines was predominantly down the stacker side of the stockpile (see Figure 5-8).

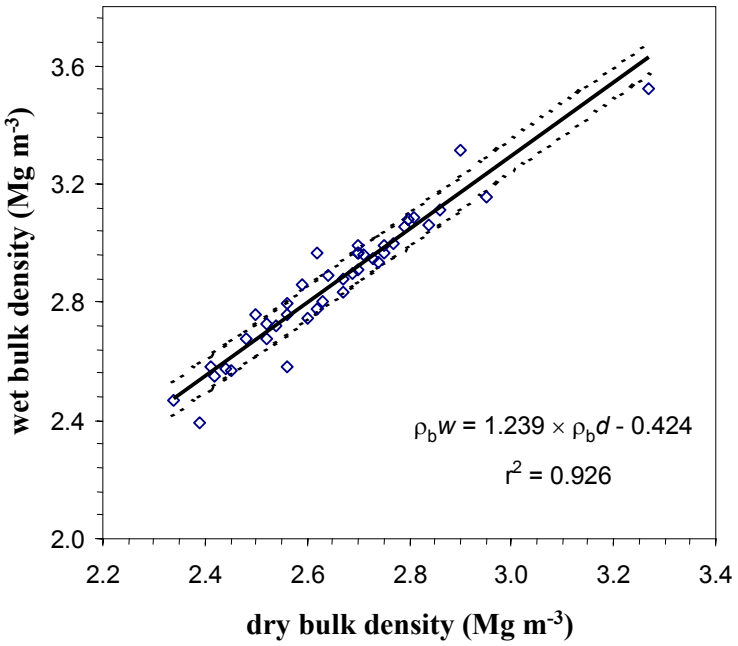

Figure 5-13 Relationship of wet and dry ρ_b across iron ore stockpile with 95% confidence interval for the linear fit. All measurements were taken during the reclamation process from different "benches" identified in Figure 5-8c.

Probe C18 shown in Figure 5-14 is typical of the probes used in the stockpile during stacking and drainage. An increase in the measured θ is due to ore placed above the probe and a likely increase in ρ_b. θ peaks around hour 140 with a decline in θ to hour 200. The polynomial fit then predicts a small increase in θ. This is unlikely and the spline fit (SAS, 1995) better predicts the likely θ relationship with time. However, the spline fitting process has a higher unexplained error (RSS = 0.007) in fitting the model compared to the polynomial fit (RSS = 0.005).

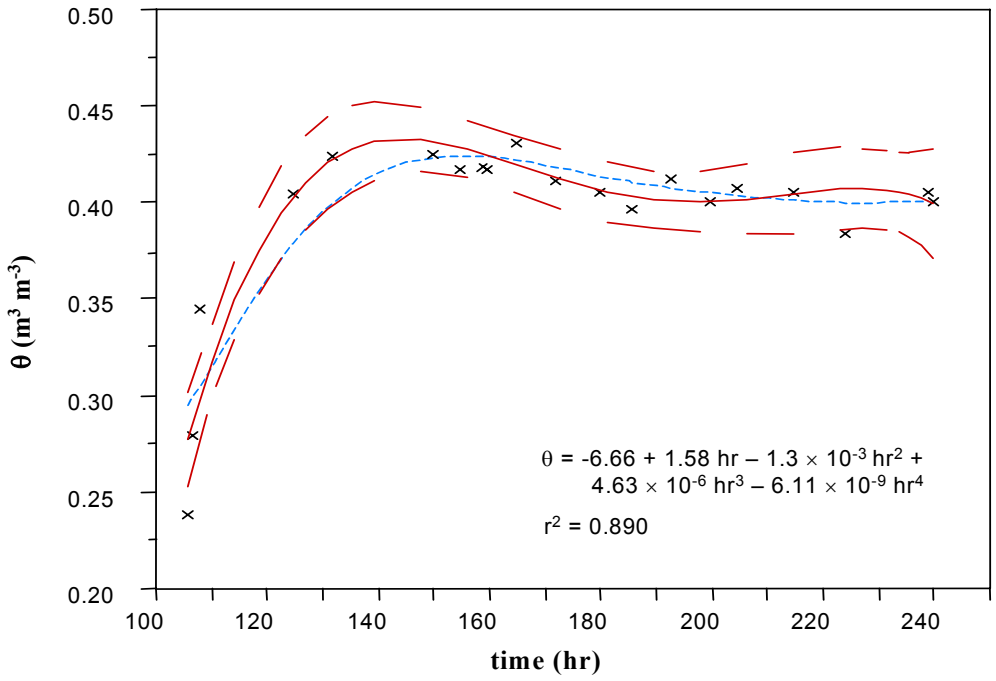

Figure 5-14 Moisture content measured with probe C18 in iron ore stockpile from hour 100 to hour 240 during laying of stockpile and subsequent drainage. The large dashed lines indicate 95% confidence interval for polynomial fit. A spline fit (λ = 10000) is also shown (dashed line). Time is standardised where t_0 (0 hour) is when the stockpile formation commenced.

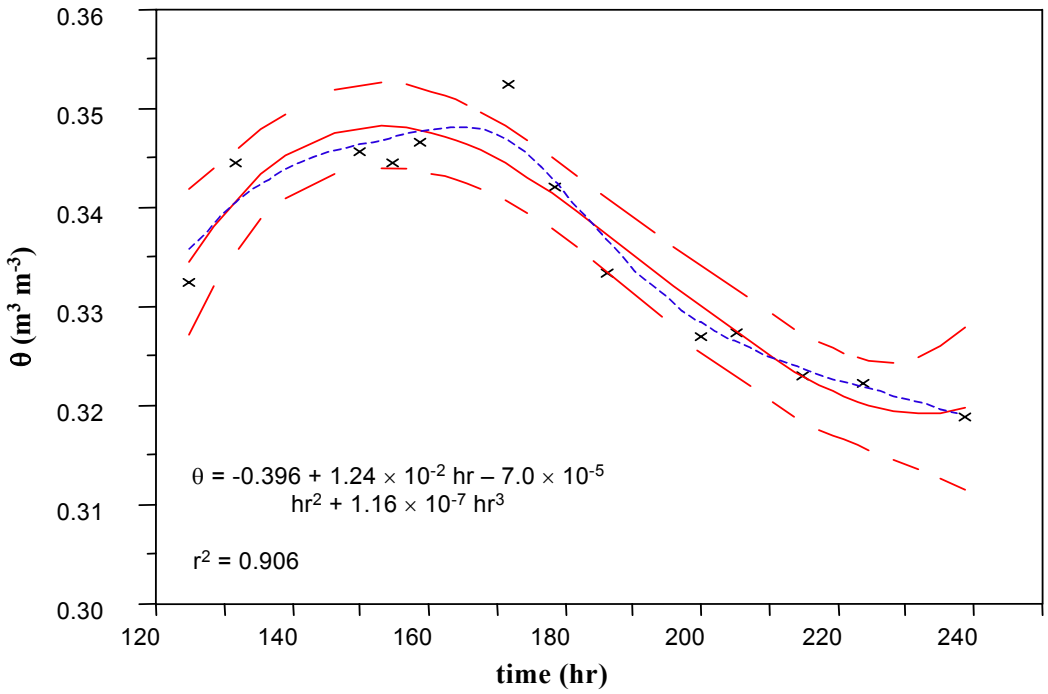

Figure 5-15 θ measured with probe C12 from placement (125 hours) to stockpile reclamation at hour 240.

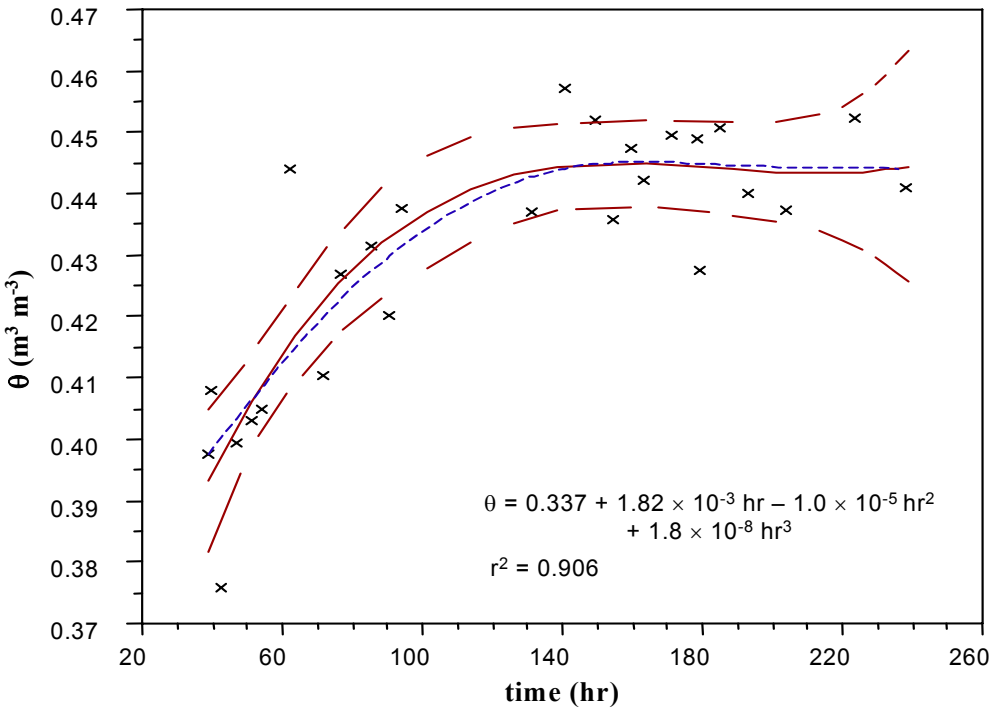

Figure 5-16 θ measured with probe C11 from placement (40 hours) to stockpile reclamation at hour 240. Maximum θ is obtained near hour 140 and maintained till reclamation indicating little drainage with time.

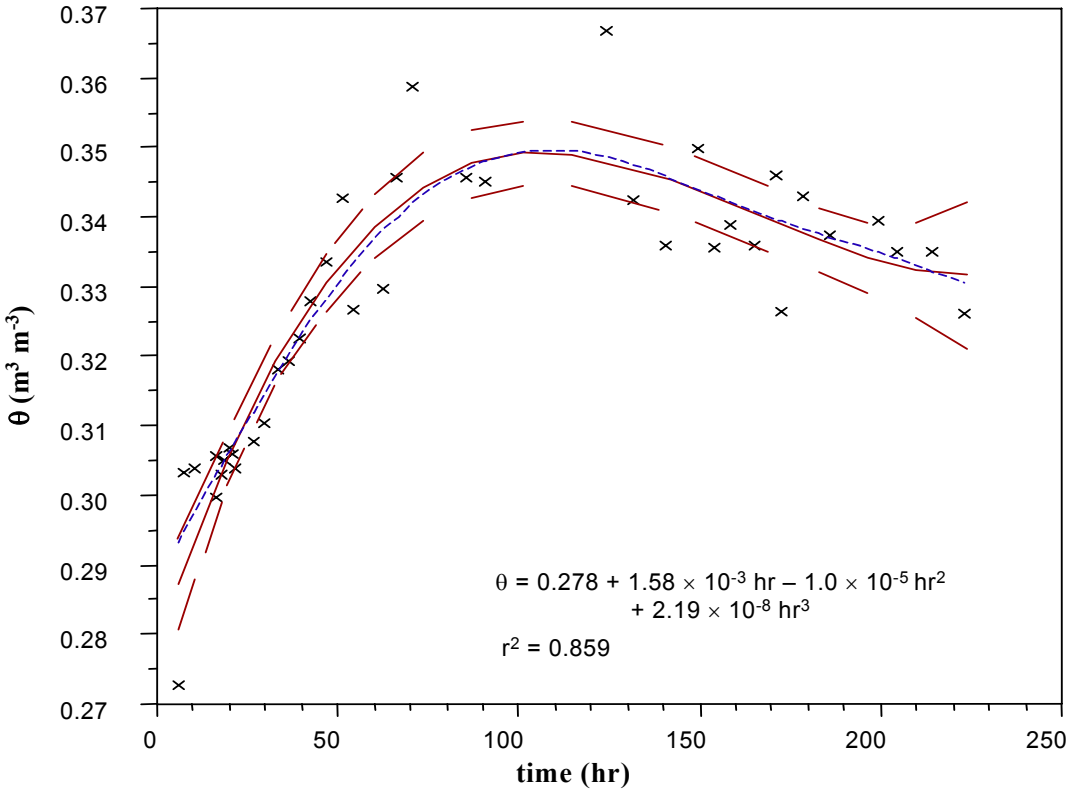

Figure 5-17 θ measured with probe C04 from placement (5 hours) to stockpile reclamation at hour 240. θ peaks around hour 100 with continues decline in reported θ till reclamation.

Drainage characteristics of the stockpile for three probes in the C-cross section are shown in Figures 5-14 to 5-17. The probes are located at different heights approximately four meters, stacker side, from the centre of the stockpile shown in Figure 5-8. Polynomial fits are shown for all probes with appropriate spline fits carried out in JMP® (SAS Institute).

Results from probe C12 indicate an initial increase in θ followed by a constant decline. This is to be expected as the water movement is dictated by gravity through the stockpile after the ore is deposited. High measured hydraulic conductivity (Appendix 5-1) allows quick drainage through the stockpile. Processed ore was dumped till hour 150 just prior to the peak in measured θ.

Probes C11 and C04 exhibited a similar increase in θ with peak values at 140 h and 100 h respectively. Calculated θ at probe C11 was noticeably higher than C12 (located directly above C11 in the stockpile) and probe C04 (located below C11). This is most likely due to the probe location, surrounded by "fines" (< 0.5 mm) ore material. θ remained constant (≈ 0.44 m^3m^{-3}) at C11. However, the probes above and below C11 declined with time. Again this indicates congregation of fine material around the probe. Smaller material will retain water due to smaller pore size distribution slowing drainage capability.

The TDR technique has a small ill-defined measurement area. Knight (1992) mathematically derived the volume of measurement for unbalanced probes and the relative influence is shown in Figure 1.9 (after Zegelin *et al.*, 1989). Empirical derivation (by Baker and Lascano, 1989) suggests a measurement cross-section area of 3500 to 4000 mm^2 with the majority of influence within 1000 mm^2.

The material located closest to the TDR probe centre wire will have the greatest influence on the EM wave with the measurement volume (m^3) calculated (Zegelin *et al.*, 1992):

$$V = \pi L\left(R - \frac{d}{2}\right)^2 \tag{5-7}$$

Where L is the length of the probe (200 mm); d the centre wire diameter (3 mm) and; using the assumption of Zegelin *et al.* (1992), R maximum radius of influence (0.05 m). The volume of measurement with a 0.2 m long unbalanced probe is 0.00093 m^3. The probe dimensions for a radial influence of 0.05 m was considerably different with Zegelin *et al.*'s original study (1989). If a maximum radius of measurement for this probe is actually 0.025 m then the volume of measurement is even smaller by a three-fold factor (0.00035 m^3; 350 ml).

The small measurement volume is important in determination of θ for large (many thousands of tonnes) stockpiles and is a limitation of the TDR technique for continued monitoring. Three options exist for improving the measurement volume. Probes may have a different geometry (larger probe diameter and spacing, Zegelin *et al.*, 1989); probes may be longer in length (L in equation 5-7); or more probes can be utilised in stockpile measurement.

5.5. CONCLUSIONS

Moisture content of iron ore can be determined by the TDR technique after calibration is established. The influence of the iron content was found to not significantly affect the ability of the TDR technique in determining moisture content. The ability to obtain the end-point analysis contradicts the findings of Robinson *et al.* (1994) for an anthroposol soil with a high (15 %) magnetite content. A good relationship was found between the laboratory and *in situ* calibration for similar moisture contents, though the field calibration returned a significantly higher intercept. This could be due to the change in *in situ* bulk density. The laboratory calibration is a polynomial relationship with the TDR technique becoming more sensitive to change in θ at higher moisture contents. Though the average stockpile ρ_b is higher (2.66 Mg m^{-3}) than found in most soil situations the calibration is robust to change experienced in field conditions. Still, it is recommended that a calibration be conducted for each material.

For *in situ* θ determination extension cables are used to connect probes to the TDR instrument. For measurement in stockpiles protection of the cable (RG-58) was necessary. A simple process utilising common garden hose was found to successful. The extension cable affects the EM travel and subsequent determination of the apparent dielectric by the automatic software. A small but significant subtraction (-0.197) from the measured dielectric (Ka_m) accounts for the effect of a 28 m extension cable. To ensure sustained measurement of embedded probes some protection of the RG-58 coaxial extension is required. This can be readily achieved in field situation by threading the coaxial cable through commonly available garden hose.

The TDR technique can be successfully employed in determination of moisture content change during stockpile formation and subsequent drainage period till reclamation is undertaken. However, the small measurement volume of the TDR probes employed was susceptible to immediate ore characteristics. In the stockpile creation, congregation of finer material was observed and probes placed in this material measured comparatively higher moisture contents.

This sensitivity to local conditions may be overcome by increasing the probe dimensions particularly length.

TDR is a potential alternative to other techniques currently used in continuous moisture determination (Yip & Cutmore, 1993; Cutmore *et al.*, 1996). However the invasive nature of the probes limits the techniques' capability for on-line measurement of the abrasive processed iron ore during conveyor transport. An advantage of the TDR technique is the ability to determined θ relationships inside stockpiles.

6.1. GENERAL DISCUSSION

Technology for the measurement of soil water content (θ) continues to develop rapidly. This development, particularly during the last 15 years, has predominantly concentrated on exploiting the difference between the dielectric of water (≈ 80) and the dielectric of the soil matrix (≈ 3 - 5). Measurement of the combined components, the apparent dielectric (K_a), is undertaken in the time-domain or the frequency-domain. There are, however, existing limitations to measurement of soil water with the time-domain and frequency-domain techniques. The understanding of the time-domain technique is better developed than frequency-domain, as shown in the available literature (Chapter 1). The time-domain technique is particularly well suited to near-surface, continued spatial measurements (e.g. McBratney *et al.*, 1997), though development of profile-based measurement (following the initial work of Topp & Davis, 1985), has recently extended the application of time-domain reflectometry (Hook & Livingstone, 1992; Ferre *et al.*, 1997). Reducing the effectiveness of the down-hole (profile) measurement, is the sensitivity of dielectric techniques to the effect of air-gaps around the sensors (Dean *et al.*, 1987; Knight *et al.*, 1997). Though more sensitive to the change in soil water content compared to the neutron moderation method, as shown in Figure 4-8, the need for careful field installation cannot be over-emphasised. The sensitivity to air-gaps around the sensors may continue to limit the application of dielectric techniques to non-swelling soil.

Soil water content, reported with the time-domain reflectometry (TDR) technique, is still widely based on use of Topp and his co-workers' seminal research (Topp *et al.*, 1980). Different studies, especially in Europe (e.g. Roth *et al.*, 1990; Roth *et al.*, 1992), have concentrated on developing a physical relationship based on the refractive index (Whalley, 1993). To develop a physically-based relationship between the K_a and θ, further paramaterisation is required. Often this can be difficult to achieve in field conditions (Jacobsen & Schjonning, 1993b). This difficulty in minimising the error associated with field calibration, was experienced with bulk density measurement in a field calibration of the NMM probe, shown in Chapter 4. Though not conclusive, results in Chapter 2 indicate a difference in the equation of Topp *et al.* (1980) and measurement of θ in some typical Australian soil. This is probably due to the effect of bound water on the measured apparent dielectric. The potential effect of bound water, though recognised, is poorly understood, especially when considered with other physical parameters. For example, the effect of particle size analysis

(PSA) is considered by different researchers to have minimal or no significant impact on the calibration of the TDR technique (Roth *et al.*, 1990; Jacobsen & Schjonning, 1993a; and Malicki *et al.*, 1996). In their early work developing a "universal" calibration, Topp *et al.* (1980) reported a difference in the response of a clay soil but still encompassed these results in their calibration. The complex interaction between the PSA, specific surface area and the clay mineralogy are difficult to define. Various models accounting for these parameters, or the effect of bound water (as a surrogate of specific surface area or mineralogy) have yet to be exploited in calibration of the TDR in some typical Australian soil. Bridge *et al.* (1996) found measurement of θ based on the empirical calibration of Topp *et al.* (1980) to underestimate the known θ in a Vertosol. I obtained similar results (Figure 2-3) in measurement of θ in a saturated Vertosol where the (factory) supplied calibrations underestimated the gravimetrically calculated θ. In explaining the underestimation of θ by determination with the "universal" equation, three likely contributing reasons are: (i) the change in the imaginary component of the dielectric as the electrical conductivity increases (White and Zegelin, 1995); (ii) a large change in the bulk density due to the swell-shrink properties of the soil (Bridge *et al.*, 1996) and; (iii) the change in the bound-water component, especially the mono-molecular layer.

Bohl & Roth (1994) following the study of Dobson *et al*. (1985) consider the influence of bound-water in some detail. Assuming a single molecular layer of water with a thickness of 3 $\times 10^{-10}$ m, Bohl & Roth (1994) found an optimal value (for their model) of bound water of 0.03 $m^3\ m^{-3}$ (θ_{bw}) for mineral soil. Whether this value can be applied to different Australian soils is yet to be seen and understood.

This returns us to the original problem where the interaction of the PSA, specific surface area and mineralogy clouds development of a physical K(θ) relationship. The continued parameterisation often leads to a small improvement in the attained calibration (Zegelin & White, 1994). This desire to achieve a physical relationship by backward parameterisation for different soil, persists (Yu *et al.*, 1997). However, further calibration of the TDR technique, particularly in heavy textured soil and specifically, soil that exhibits shrink-swell characteristics, is certainly warranted.

With the TDR technique now widely used for θ measurement the use of extension cables connecting the TDR unit to the buried probes is common. Most extension cables are coaxial cables designed to minimise electromagnetic signal loss and often used in arrays of various lengths. The determination of the K_a is shown in Section 2.4.7 to vary in different soil water conditions and also vary with increasing length of extension cable. The relationship between

the change in reported K_a and the extension cable is not simply defined and the results presented here (Figure 2-10) show the significance of the problem without fully explaining the link between increasing extension cable length and K_a. The change in the reported K_a could be linked to the decrease in the slope of the returning electromagnetic wave (Section 2.4.7.2). Others have qualitatively observed the difference in the generated EM traces (Herkelrath *et al.*, 1991), deciding the measurement process was robust and there was no significant effect on the reported K_a. As the use of the TDR technique increases, accounting for the effect of different extension cable lengths connecting probes to the respective instrument will be important in maintaining confidence in the measured K_a.

The application of dielectric techniques in measurement of soil water content and water content in other porous media continues. Chapter 5 results show the ability of the TDR technique to measure the water content of processed iron ore. The calibration is similar (in form) to those developed by Zegelin & White (1994) for other ore-based products, and encompasses the increasing imaginary component of the dielectric (K") due to the ferromagnetic properties of the iron ore. As opposed to Robinson *et al.* (1994), who experienced difficulties in automatic determination of the EM wave end-point in a soil with increased iron content, the TDR technique measured the changing moisture conditions successfully (Figure 5-2) in the iron ore. The TDR technique is better adapted for water content determination within the stockpile than other non-invasive techniques reported so far (Yip & Cutmore, 1993), and has the potential for further development in process-based industries.

During the field experiment (Chapter 4) the neutron moderation method performed well again indicating that the technique is well suited for profile based measurements. The need for site, or at least soil specific calibrations was again shown (Section 4.4.1) and this result is in accordance with the findings of others (Hodgson & Chan, 1979; Greacen *et al.*, 1981; Ruprecht & Schoefield, 1990). The *in situ* calibration was more sensitive to the change in soil water content compared to the "universal" calibration supplied by the manufacturer and this could be due to the calibration process accounting for the *in situ* bulk density. The calibration results need to be considered with some care as the range of soil water content, during calibration, was limited and Cull (1979) showed that a large range of soil water content for calibration is necessary for optimum calibration. For application of the calibration in the Chromosol, further calibration should be carried out.

The NMM method, though less precise, due to the chaotic nature of radioactive decay (Table 3-1), and measuring a larger volume of soil, is a more robust technique for determination of θ,

compared to TDR in attenuative soil. For TDR to be used in irrigation scheduling the technique needs to consistently report the soil water content and not be limited in saturated conditions if the EM wave attenuates and no end-point is derived. The FD sensors, the IH1 and the EnviroSCAN®, both reported measurement of θ in all soil water conditions experienced. The operation of the IH1 probe will be limited due to the fragile nature of the instrument (particularly the fibre optic cable), and the cost of batteries for operation. The EnviroSCAN® system in these experiments operated well, reporting θ from saturated conditions to small water contents (below refill point). Results from the field experiment (Figure 4-12), indicate a good relationship between the increasing neutron count, with the NMM, and the reported θ by the EnviroSCAN® FD system. However, the need for calibration requires further research.

6.2. CONCLUSIONS

From the observations during the laboratory and field experiments with dielectric and neutron moderation techniques I conclude:

- When using extension cables with the TDR technique for soil water content measurement, a calibration for the effect of the extension cable is necessary. The calibration should account for the type of cable, the different cable length and changing soil water content conditions.
- The "universal" calibration developed by Topp *et al.* (1980) for the TDR technique can underestimate the soil water content in heavy-textured soil. However, the increased electrical conductivity often associated with clay soil in Australia, can lead to attenuation of the electromagnetic wave causing difficulty in automatic end-point determination. This difficulty can lead to large erroneous θ values and increased standard error of measurement. Further, the increasing electrical conductivity can limit the application of the TDR technique if there is no end-point reflection obtained.
- The TDR technique is capable, after calibration, of θ measurement in iron ore; and the technique is well suited to measurement of water content in iron ore stockpiles.
- The IH1 down-hole frequency-domain probe is sensitive to the axial orientation of the sensor in the access tube and rotation can lead to an error (bias) of 0.01 m^3 m^{-3} (using the factory supplied "universal" calibration).

- The frequency-domain technique is more sensitive to the change in soil water conditions than the neutron moderation technique.
- An *in situ* calibration improves the sensitivity of the neutron moderation technique in a Brown Chromosol compared to the factory supplied "universal" calibration. However, the calibration procedure is limited by a large error in prediction (≈ 0.05 m^3 m^{-3}) and limited water content range for determination.

6.3. FUTURE DIRECTIONS

Following the study undertaken in the different chapters, this component of my work is probably the easiest to formulate. During the course of individual experiments the paths of study more often diverge rather than converge. The study of the available dielectric techniques is most interesting. Significant work during the late 1980s and early 1990s by Ian White, Steve Zegelin and John Knight at CSIRO developed a good understanding of the TDR technique and some applications. However, little research (apart from Bridge *et al.*, 1996) has been undertaken to develop a better understanding of the limitations of the TDR technique in heavy textured Australian soil, particularly soil with high electrical conductivity and specific surface area that actively shrinks and swells during drying and wetting cycles.

From my study (Chapter 2), of particular concern is the effect of extension cable on the reported dielectric. Future research needs to explore the effect of the extension cable and ideally develop a model for this effect on reported dielectric when using TDR instruments.

The ability of the TDR technique to measure different porous materials (Zegelin *et al.*, 1994) by sensor development and adaptation offers many opportunities for future study with the technique. Of particular interest is the on-line measurement of ore material from mining operations and other process-based industries. The key to development obviously remains the ability to measure a change in dielectric and relate that to a relevant parameter. For θ determination in iron ore one particular challenge is the ability to measure θ in a large sample volume. To achieve this, development of TDR probe technology is required.

A rigorous *in situ* assessment of the frequency-domain technique is certainly warranted. Initial results (Chapter 4) show a good relationship with the increase in θ measured by the NMM. However there is little reported information on field operation of FD sensors in Australian soil conditions. The measured frequency in water and air is important for the measurement of the universal frequency. Concerns of increasing salinity and high temperature on the methodology

of using the universal frequency approach need investigation. The field methodology for FD technique should also consider the small measurement volume of FD sensors and the sensor placement and susceptibility to change in the reported θ due to air gaps and sensor orientation.

Ahuja, L.R. & Nielsen, D.R., 1990. Field soil-water relations. In: (eds. B.A.Stewart & D.R.Nielsen) *Irrigation of Agricultural Crops*. Agronomy Monograph No. 30., pp144-190.

Alharthi, A. & Lange, J., 1987. Soil water saturation: dielectric determination. *Water Resources Research*, 23:591-595.

Allyn, R.B. & Work, R.A., 1941. The availameter and its use in soil moisture control: I. the instrument and its use. *Soil Science*, 51:307-321.

Anonymous, 1991. Soil moisture measurement with time-domain reflectometry. *The Campbell Update*, Campbell Scientific Newsletter, Utah, USA. 2(1):1-2.

Anonymous, 1994. Moisture point: A new way to measure soil moisture content - quickly, easily and accurately. *Environmental Sensors Technical Specification Sheet for MP917*, British Columbia, Canada, pp2.

Anonymous, 1995. Berriquin Land and Water Management Plan. Deniliquin, NSW, Australia. Murray Irrigation pp120

ASTM, 1991. D-1556 Test method for density of soil in place by the sand-cone method. In: *ASTM Annual Book of Standards*. American Society of Testing and Materials, 4.08:359-365.

Baker, J.M.,1990. Measurement of soil water content. *Remote Sensing Reviews*, 5:263-279.

Baker, J.M. & Allmaras, R.R., 1990. System for automating and multiplexing soil moisture measurement by time-domain reflectometry. *Soil Science Society of America Journal*, 54:1-6.

Baker, J.M. & Lascano, R.J., 1989. The spatial sensitivity of time-domain reflectometry. *Soil Science*, 147:378-384.

Baran, E., 1994. Use of time domain reflectometry for monitoring moisture changes in crushed rock pavements. *Symposium and Workshop on Time-domain Reflectometry in Environmental, Infrastructure, and Mining Applications*. United States Bureau of Mines, SP 19-94, pp349-356.

Baumgartner, N., Parkin, G.W. & Elrick, D.E., 1994. Soil water content and potential measured by hollow time-domain reflectometry probe. *Soil Science Society of America Journal*, 58:315-318.

Bavel, C.H.M. van, 1962. Accuracy and source strength in soil moisture neutron probes. *Proceeding of the Soil Science Society of America*, pp405.

Bavel, C.H.M. van, Nielsen, D.R. & Davidson, J.M., 1961. Calibration and characteristics of two neutron moisture probes. *Soil Science Society of America Proceedings*, 25:329-334.

Bavel, C.H.M. van, Underwood, N. & Swanson, R.W., 1956. Soil moisture measurement by neutron moderation. *Soil Science*, 82:29-41.

Bell, J.P., Dean, T.J. & Hodnett, M.G., 1987. Soil Moisture Measurement by an Improved Capacitance Technique, Part II. Field Techniques, Evaluation and Calibration. *Journal of Hydrology*, 93:79-90.

Birchak, R.J., Gardner, C.G., Hipp, J.E. & Victor, J.M., 1974. High dielectric constant microwave probes for sensing soil moisture. *Proceedings IEEE*, 62:93-98.

Blake, G.R. & Hartge, K.H., 1986. Bulk density. In: (ed. A. Klute) *Methods of Soil Analysis, Part 1. Physical and Mineralogical Methods*. Agronomy Monongraph No.9 (2nd edn). pp363-375.

Boart Longyear CPN, 1995. CPN 503 DR Hydroprobe Neutron Moisture Gauge, Operating Manual. Boart Longyear CPN; Martinez CA USA. pp50.

Bohl, H. & Roth, K., 1994. Evaluation of dielectric mixing models to describe the θ(ε)-relation. *Symposium and Workshop on Time-domain Reflectometry in Environmental, Infrastructure, and Mining Applications*. United States Bureau of Mines, SP 19-94, pp309-319.

Bouyoucos, G.J., 1962. Hydrometer method improved for making particle size analysis of soils. *Agronomy Journal*. 54:464-465.

Boyer, J.S., 1982. Plant productivity and the environment. *Science*, 218:443-448.

Brindley, G.W. & Brown, G., 1984. *Crystal Structures of Clay Minerals and their X-ray Identification*. Mineralogical Society, London UK. pp495.

Brown, R.W. & Oosterhuis, D.M., 1992. Measuring plant and soil water potentials with thermocouple psychrometers: some concerns. *Agronomy Journal*, 84:78-86.

Bridge, B.J., Sabburg, J., Habash, K.O., Ball, J.A.R. & Hancock, N.H., 1996. The dielectric behaviour of clay soils and its application to time-domain reflectometry. *Australian Journal of Soil Research*, 23:825-835.

Brisco, B., Pultz, T.J., Brown, R.J., Topp, G.C., Hares, M.A. & Zebchuk, W.D., 1992. Soil moisture measurement using portable dielectric probes and time-domain reflectometry. *Water Resources Research*, 28:1339-1346.

Briscoe, R.D., 1984. Thermocouple psychrometers for potential measurements. *Proceedings NATO Advanced Study Institute on "Advanced Agricultural Instrumentation"* Il Ciocco, Italy, May 27 - June 9, 1984.

Bristow, K.L., 1998. Measurement of thermal properties and water content of unsaturated sandy soil using dual-probe heat-pulse probes. *Agricultural and Forest Meterology*, 89:75-84.

Bristow, K.L., Campbell, G.S. & Calissendorff, K., 1993. Test of heat-pulse probe for measuring changes in soil water content. *Soil Science Society of America Journal*, 57:930-934.

Bristow, K.L, Kluitenberg, G.J. & Horton, R.,1994. Measurement of soil thermal properties with a dual-probe heat-pulse technique. *Soil Science Society of America Journal*, 58:1288-1294.

Brown, R.W. & Oosterhuis, D.M., 1992. Measuring plant and soil water potentials with thermocouple psychrometers: some concerns. *Agronomy Journal*, 84:78-86.

Bull, C.R., 1991. Wavelength selection for near-infrared reflectance moisture meters. *Journal of Agricultural Engineering Research*, 49:113-125.

Burrows, W.C. & Kirkham, D., 1958. Measurement of field capacity with a neutron meter. *Soil Science Society Proceedings*, (United States of America) pp103-105.

Buss, P., 1994. Continuous monitoring of moisture in hardwood plantations irrigated with secondary treated effluent. *AWWA Recycled Water Seminar*, *Newcastle Australia*. pp180-189.

Campbell, G.S., 1988. Soil water potential measurement: an overview. *Irrigation Science*, 9:265-273.

Campbell, G.S., Calissendorff, C. & Williams, J.H., 1991. Probe for measuring soil specific heat using a heat-pulse method. *Soil Science Society of America Journal*, 55:291-293.

Campbell, G.S. & Gee, G.W., 1986. Water potential: miscellaneous methods. In: (ed. A. Klute) *Methods of Soil Analysis, Part 1. Physical and Mineralogical Methods*. Agronomy Monongraph No.9 (2nd edn). pp619-633.

Campbell, J.E., 1990. Dielectric properties and influence of conductivity in soils at one to fifty

megahertz. *Soil Science Society of America Journal*, 54:332-341.

Carmer, S.G. & Walker, W.M., 1982. Baby Bear's dilema: A statistical tale., *Agronomy Journal*, 74:122-124.

Carneiro, C. & De Jong, E., 1985. In situ determination of the slope of the calibration curve of a neutron probe using a volumetric technique. *Soil Science*, 139:250-254.

Carrow, R.N., Shearman, R.C. & Watson, J.R., 1990. Turfgrass. In: (eds. B.A. Stewart & D.R. Nielsen) *Irrigation of Agricultural Crops*. SSSA Monograph No. 30. pp889-919.

Cassel, D.K., Kachanoski, R.G. & Topp, G.C., 1994. Practical considerations for using a TDR cable tester. *Soil Technology*, 7:113-126.

Chanasyk, D.S. & McKenzie, R.H., 1986. Field calibration of a neutron probe. *Canadian Journal of Soil Science*, 66:173-176.

Childs, E.C., (1940). The use of soil moisture characteristics in soil studies. *Soil Science*, 50:239-252.

Colman, E.A. & Hendrix, T.M., 1949. The fibreglass electrical soil-moisture instrument. *Soil Science*, 67:425-438.

Corey, A.T. & Klute, A., 1985. Application of the potential concept to soil water equilibrium and transport. *Soil Science Society of America Journal*, 49:3-11.

Cornish, P.M., Laryea, K. & Bridge, B.J., 1972. A nondestructive method of following moisture content and temperature changes in soils using thermistsors. *Soil Science*, 115:309-314.

Cresswell, H.P.,1993. Evaluation of the portable pressure transducer technique for measuring field tensiometers. *Australian Journal of Soil Research*, 31:397-406.

Cull, P.O., 1979. Unpublished PhD thesis. University of Armidale, NSW Australia. pp241.

Cull, P.O., 1992. Irrigation scheduling - techniques and profitability. *National Irrigation Convention Proceedings*. Melbourne, Australia. pp131-170.

Cullen, S.J. & Everett, L.G., 1995. Estimating the storage capacity of the vadose zone. In: (eds. L.G. Wilson, L.G. Everett & S.J. Cullen) *Handbook of Vadose Zone Characterization and Monitoring*. CRC Press, Baco Raton, Fl USA. pp159-176.

Cummings, R.W. & Chandler, R.F., 1940. A field comparison of the electrothermal and gypsum block electrical resistance methods with the tensiometer method for estimating soil moisture in situ. *Soil Science Society of America Proceedings*, 5:80-85.

Cutmore, N.G., Eberhardt, J.E., Sowerby, B.D. & Watt, J.S., 1996. On-line measurement of composition for the Australian mineral and energy industries. *IEEE Instrumentation and Measurement Technology Conference*, Brussels, Belgium; June 4-6 1996. pp330-334.

Dalton, F.N., 1992. Development of time-domain reflectometry for measuring soil water content and bulk soil electrical conductivity. In: (eds. G.C. Topp, W.D. Reynolds & R.E. Green) *Advances in Measurement of Soil Physical Properties: Bringing Theory into Practice*. pp143-168.

Dasberg, S., Alksnis, H., Daniel, P., Kalma, J.D. and Zegelin, S.J., 1995. Calibration of the "moisture point" TDR system. *Cooperative research Centre for Catchment Hydrology Report 95/4* (Australia) pp1-15.

Dean, T.J., Bell, J.P. & Baty, A.J.B., 1987. Soil Moisture Measurement by an Improved Capacitance Technique. Part I. Sensor Design

and Performance. *Journal of Hydrology*, 93:67-78.

Dickey, G.L., Allen, R.G., Wright, J.L., Murray, N.R., Stone, J.F. & Hunsaker, D.J., 1993. Soil bulk density sampling for neutron gauge calibration. Proceedings of the ASCE National Conference on Irrigation and Drainage Engineering, Park City, UT, USA.

Didcot , 1992. Capacitance Soil Moisture Probe Type IH1 - Provisional Manual. Didcot Instrument Company, Oxford, UK. pp 15.

Dirksen, C. & Dasberg, S., 1993. Improved calibration of time-domain reflectometry soil water content measurements. *Soil Science Society of America Journal*, 57:660-667.

Dobson, M.C., Ulaby, F.T., Hallikainen, M.T. & El-Rayes, M.A., 1985. Microwave dielectric behaviour of wet soil - Part II: Dielectric mixing models. *Institution of Electrical and Electronic Engineers Transactions on Geoscience and Remote Sensing*, GE-23, 35-46.

Drake, F.H., Pierce, G.W. & Dow, M.T., 1930. Measurement of the Dielectric Constsant and Index of Refractions of Water and Aqueous Solutions of KCL at High Frequencies. *Physical Reviews*, 35:613-622.

Evett, S.R., 1994. TDR-temperature arrays for analysis of field soil thermal properties. *Symposium and Workshop on Time-domain Reflectometry in Environmental, Infrastructure, and Mining Applications*. United States Bureau of Mines, SP 19-94, pp320-327.

Evett, S.R. & Steiner, J.L., 1995. Precision of neutron scattering and capacitance type soil water content gauges from field calibration. *Soil Science Society of America Journal*, 59:961-968.

Falkiner, R.A. & Smith, C.J., 1997. Changes in soil chemistry in effluent-irrigated *Pinus radiata* and *Eucalyptus grandis* plantations. *Australian Journal of Soil Research*. 35:131-147.

Fellner-Feldegg, H., 1969. The measurement of dielectrics in the time-domain. *Journal of Physical Chemistry*, 73:616-623.

Ferre, P.A., Rudolph, D.L. & Kachanoski, R.G., 1996. Spatial averaging of water content by time-domain reflectometry: implications for twin rod probes with and without dielectric coatings. *Water Resources Research*, 32(2):271-279.

Fleming, R.L., Black, T.A. & Eldridge, N.R., 1993. Water content, bulk density, and coarse fragment content measurement in forest soils. *Soil Science Society of America Journal*, 57:261-270.

Fredlund, D.G., 1992. Background, theory, and research related to the use of thermal conductivity sensors for matric suction measurement. In: (eds. G.C. Topp, W.D. Reynolds & R.E. Green) *Advances in Measurement of Soil Physical Properties: Bringing Theory into Practice*. SSSA Special Publication No 30. pp249-261.

Frueh, W.T. & Hopmans, J.W., 1997. Soil moisture calibration of a TDR multilevel probe in gravely soil. *Soil Science*, 162(8):554-565.

Fundinger, R., Kohler, K. & Stacheder, M., 1995. Measurement of material and soil moisture with the TRIME-method. *TRIME Product Guide*, IMKO GMbH, Ettlingen, Germany.

Gardner, W. & Kirkham, D., 1952. Determination of soil moisture by neutron scattering. *Soil Science*, 73:391-401.

Gardner, W., Israelsen, O.W., Edlefsen, N.E. & Clyde, D., 1922. The capillary potential function and its relation to irrigation practice. *Physical Revue*, 20:196-204.

Gardner, W.H., 1986. Water content. In: (ed. A. Klute) *Methods of Soil Analysis, Part 1.*

Physical and Mineralogical Methods. Agronomy Monograph No.9 (2nd edn). pp493-544.

Gaskin, G.J. & Miller, J.D., 1996. Measurement of soil water content using a simplified impedance measuring technique. *Journal of Agricultural Engineering Research*, 63:153-160.

Gee, G.W. & Bauder, J.W., 1986. Particle-size analysis. In: (ed: A.Klute) *Methods of Soil Analysis, Part 1. Physical and Mineralogical Methods*. Agronomy Monongraph no.9 (2nd edn). pp383-411.

Gee, G.W., Silver, J.F. & Borchert, H.R., 1976. Radiation hazard from Americium-Beryllium neutron moisture probes. *Soil Science Society of America Journal*, 40:492-494.

Greacen, E.L., Correll, R.L., Cunningham, R.B., Johns, G.G. & Nicolls, K.D., 1981. Calibration. In: (ed. E.L. Greacen) *Soil Water Assessment by the Neutron Method*. CSIRO, Melbourne, pp 50-72.

Greacen, E.L. & Hignett, C.T., 1979. Sources of bias in the field calibration of a neutron meter. *Australian Journal of Soil Research*, 17:405-415.

Greacen, E.L. & Schrale, G., 1976. The effect of bulk density on neutron meter calibration. *Australian Journal of Soil Research*, 17:159-169.

Green, R.E. & Topp, G.C., 1992. Survey of use of field methods for measuring soil hydraulic properties. In: (eds. G.C. Topp, W.D. Reynolds & R.E. Green) *Advances in Measurement of Soil Physical Properties: Bringing Theory into Practice*. SSSA Special Publication No 30, pp281-288.

Guerra, F., 1974. Handling of wet, sticky ores. *Proceedings from International Symposium on Transport and Handling of Minerals*. Miller Freeman Publishing Inc., San Francisco, CA, USA. pp175-200.

Halbertsma, J., van den Elsen, E., Bohl, H., & Skierucha, W., 1995. Temperature effects on TDR determined soil water content.. In: (eds. L.W. Petersen & O.H. Jacobsen), *Proceedings from the Symposium on Time-domain reflectometry applications in soil science*. Research Centre Foulum, Denmark, September 16, 1994. SP Report Danish Institute of Plant and Soil Science, 11(3):35-37.

Hanks, R.J., 1992. Water Potentials. In: *Applied soil physics. Soil water and temperature applications*. Springer-Verlag, New York. pp176.

Hanson, B.R. & Dickey, G.L., 1993. Field practices affect neutron moisture meter accuracy. *California Agriculture*, November-December 1993, pp29-31.

Haverkamp, R., Vauclin, M. & Vachaud, G., 1984. Error analysis in estimating soil water content from neutron probe measurements: 1. local standpoint. *Soil Science*, 137:78-90.

Heimovaara, T.J., 1993. Design of triple-wire time-domain reflectometry probes in practice and theory. *Soil Science Society of America Journal*, 57:1410-1417.

Heimovaara, T.J., 1994a. Frequency domain analysis of time domain reflectometry waveforms. 1. Measurement of the complex dielectric permittivity of soils. *Water Resources Research*, 30:189-199.

Heimovaara, T.J., 1994b. Frequency domain analysis of time domain reflectometry wave-forms. 2. A four-component complex dielectric mixing model for soils. *Water Resources Research*, 30:200-209.

Heimovaara, T.J. & Bouten, W., 1990. A computer controlled 36-channel time-domain reflect-

ometry system for monitoring soil water contents. *Water Resources Research*, 26:2311-2316.

Heimovaara, T.J, Focke, A.G., Bouten, W. & Verstraten, J.M., 1995. Assessing temporal variations in soil water composition with time domain reflectometry. *Soil Science Society of America Journal*, 59:689-698.

Heimovaara, T.J. & de Water, E., 1993. A computer controlled TDR system for measuring water content and bulk electrical conductivity of soils. *Report No. 41*, Laboratory of Physical Geography and Soil Science, Universtiy of Amsterdam, pp27.

Hendrickx, J.M.H., Nieber, J.L. & Siccama, P.D., 1994. Effect of tensiometer cup size on field soil water tension variability. *Soil Science Society of America Journal*, 58:309-315.

Herkelrath, W.N., Hamburg, S.P. & Murphy, F., 1991. Automatic, real-time monitoring of soil moisture in a remote field area with time-domain reflectometry. *Water Resources Research*, 27:857-864.

Hilhorst, M,A. & Dirksen, C., 1994. Dielectric water content sensors: time-domain versus frequency domain. *Symposium and Workshop on Time-domain Reflectometry in Environmental, Infrastructure, and Mining Applications*. United States Bureau of Mines Special Publication SP 19-94, pp23-33.

Hillel, D.K., 1991. *Out of the Earth*. The Free Press. New York, USA.

Hipp, J.E., 1974. Soil Electromagnetic Parameters as Functions of Frequency, Soil Density, and Soil Moisture. *Proceedings IEEE*, 62:98-103.

Von Hippel, A.T. (ed.), 1954. *Dielectric Materials and Applications*. MIT Press, Cambridge, USA.

Hodgson, A.S. & Chan, K.Y., 1979. Field calibration of a neutron moisture meter in a cracking grey clay. *Irrigation Science*, 8:233-244.

Hodnett, M.G. & Bell, J.P., 1991. Neutron Probe Standards: Transport Shields or a Large Drum of Water? *Soil Science*, 51:113-120.

Hoelscher, J.R., Nuttle, W.K. & Harvey, J.W.,1993. The calibration and use of pressure transducers in tensiometer systems. *Hydrological Processes*, 7:205-211.

Holmes, J.W., 1956. Calibration and the field use of the neutron scattering method of measuring soil water content. *Australian Journal of Applied Science*, 7:45-58.

Holmes, J.W., 1966. Influence of bulk density of the soil on neutron moisture meter calibration. *Soil Science*.

Hook, W.R. & Livingston, N.J., 1995. Propagation velocity errors in time-domain refletometry measurements of soil water. *Soil Science Society of America Journal*, 59:92-96.

Hook, W.R. & Livingston, N.J., 1996. Errors in converting time domain reflectometry measurements of propagation velocity to estimates of soil water content. *Soil Science Society of America Journal*, 59:35-41.

Hook, W.R., Livingston, N.J., Sun, Z.J. & Hook, P.B., 1992. Remote diode shorting improves measurement of soil water by time-domain reflectometry. *Soil Science Society of America Journal*, 56:1384-1391.

Isbell, R.F., 1996. *The Australian Soil Classification*. CSIRO Publishing, Collingwood, Australia. pp 143.

Jackson, T.J., 1988. Research toward an operational passive microwave remote sensing system for

soil moisture. *Journal of Hydrology*, 102:95-112.

Jackson, T.J., Schmugge, J. & Engman, E.T., 1996. Remote sensing applications to hydrology: soil moisture. *Hydrological Sciences*, 41(4):517-530.

Jacobsen O.H, & Schjonning P., 1993a. A laboratory calibration of time-domain reflectometry for soil water measurement including effects of bulk density and texture. *Journal of Hydrology*, 151:147-157.

Jacobsen, O.H. & Schjonning, P., 1993b. Field evaluation of time-domain reflectometry for soil water measurements. *Journal of Hydrology*, 151:159-172.

Janoo, V., Berg, R.L., Simonsen, E. & Harrison, A., 1994. Seasonal changes in moisture content in airport and highway pavements. *Symposium and Workshop on Time-domain Reflectometry in Environmental, Infra-structure, and Mining Applications*. United States Bureau of Mines, SP 19-94, pp357-363.

Jayawardane, N.S., Meyer, W.S. & Barrs, H.D., 1983. Moisture measurement in a swelling clay soil using neutron moisture meters. *Australian Journal of Soil Research*. 22:109-117.

Johnson, R. & Borough, C., 1992. Irrigating trees with pulpmill effluent - a living tribute to the late Wilf Crane. *ANM Special Liftout No. 21*, Winter 1992, 15(2).

Kabat, P. & Beekma, J., 1994. Water in the unsaturated zone. In: (eds. H.P. Ritzema) *Drainage Principles and Applications*. IRLI Publication 16, pp383-434.

Kachanoski, R.G., Pringle, E. & Ward, A., 1992. Field Measurements of Solute Travel Times Using Time Domain Reflectometry. *Soil Science Society of America Journal*, 56:47-52.

Kachanoski, R.G., Thony, J.L., Vauclin, M., Vauchaud, G. & Laty, R., 1994. Measurement of solute transport during constant infiltration from a point source. *Soil Science Society of America Journal*, 58:304-309.

Kamgar, A., Hopmans, J.W., Wallender, W.W. & Wendroth, O., 1993. Plotsize and sample number for neutron probe measurements in small field trials. *Soil Science*, 156:213-224.

Kempthorne, O. & Allmaras, R.R., 1986. Errors and variability of observations. In: (ed: A.Klute) *Methods of Soil Analysis, Part 1. Physical and Mineralogical Methods*. Agronomy Monograph No.9 (2nd edn). pp1-31.

Kendall, M. & Stewart, A., 1977. *The Advanced Theory Of Statistics - Distribution Theory*. Charles Griffin & Company, Vol 4., pp261.

Khosla, R. & Persaud, N., 1997. Performance of a non-nuclear resonant frequency capacitance probe. I. calibration and field testing. *Communications in Soil Science & Plant Analysis*. 28:(15&16)1333-1345.

Kim, D.J., Vanclooster, M., Feyen, J., & Vereecken, H., 1998. Simple linear model for calibration of time domain reflectometry measurements on solute concentration. *Soil Science Society of America Journal*, 62:83-89.

Klute, A., 1986. Water retentiaon: laboratory methods. In: (ed. A. Klute) *Methods of Soil Analysis, Part 1. Physical and Mineralogical Methods*. Agronomy Monongraph No.9 (2nd edn). pp635-662.

Knight, J.H., 1991. Discussion of "The spatial sensitivity of time-domain reflectometry" by J.M.Baker & R.J.Lascano. *Soil Science*, 151:254-255.

Knight, J.H., 1992. Sensitivity of time-domain reflectometry measurements to lateral variations

in soil water content. *Water Resources Research*, 28:2345-2352.

Knight, J.H., Ferre, P.A., Rudolph, D.L. & Kachanoski, R.G., 1997. A numerical analysis of the effects of coatings and gaps upon relative dielectric permittivity measurement with time domain reflectometry. *Water Resources Research*, 33(6):1455-1460.

Koppi, T. (ed), 1995. *Soil Properties & Processes*. Soil Science 2 course notes, University of Sydney, NSW Australia.

Kraus, J.D., 1984. Waveguides and resonators. In: *Electromagnetics*. McGraw-Hill Book Co, Singapore. pp 534-611.

Lal, R., 1974. The effect of soil texture and density on the neutron probe calibration for some tropical soils. *Soil Science*, 117:183-190.

Ledieu, J., de Ridder, P., de Clarck, P. & Dautrebande, S., 1986. A method of measuring soil moisture by time-domain reflectometry. *Journal of Hydrology*, 88:319-328.

Look, B.G., Reeves, I.N. & Williams, D.J., 1994. Field experiments using time domain reflectometry for monitoring moisture changes in road embankments and pavements. *Symposium and Workshop on Time-domain Reflectometry in Environmental, Infrastructure, and Mining Applications*. United States Bureau of Mines, SP 19-94, pp374-385.

Loon, W.K.P. van, Perfect, E., Groenevelt, P.H. & Kay, B.D., 1991. Application of dispersion theory to time-domain reflectometry in soils. *Transport in Porous Media*, 6:391-406.

Lowery, B., Datiri, B.C. & Andraski, B.J., 1986. An electrical readout system for tensiometers. *Soil Science Society of America Journal*, 50:494-496.

Malicki, M., 1983. A capacity meter for the investigation of soil moisture dynamics. *Zesty Problemowe Postepow Nauk Rolniczych*, pp 201-214.

Malicki, M., 1990. A reflectometric (TDR) meter of moisture content in soils and other capillary-porous materials. *Zeszyty Problemowe Postepow Nauk Rolniczych*, 388:107-114.

Malicki, M.A., Plagge, R., Renger, M. & Walczak, R.T., 1992. Application of time-domain reflectometry (TDR) soil moisture miniprobe for the determination of unsaturated soil water characteristics from undisturbed soil cores. *Irrigation Science*, 13:65-72.

Malicki, M.A., Plagge, R. & Roth, C.H., 1996. Improving the calibration of dielectric TDR soil moisture determination taking into account the solid soil. *European Journal of Soil Science*, 47:357-366.

Malicki, M.A. & Skierucha, W.M., 1989. A manually controlled TDR soil moisture meter operating with 300 ps rise-time needle pulse. *Irrigation Science*, 10:153-163.

Malicki, M.A., Walczak, R.T., Koch, S. & Fluher, H., 1994. Determining Soil Salinity from Simultaneous Readings of its Electrical Conductivity and Permittivity using TDR. *Symposium and Workshop on Time-domain Reflectometry in Environmental, Infra-structure, and Mining Applications.* United States Bureau of Mines, SP 19-94, pp328-336.

McBratney, A.B., Whelan, B.W. & Shatar, T.M., 1997. Variability and uncertainty in spatial, temporal and spatiotemporal crop-yield and related data. *Precision Agriculture: Spatial and Temporal Variability of Environmental Quality*. Wiley Chichester, Ciba Foundation Symposium 210; pp141-160.

McCann, I.R., Stark, J.C. & King, B.A., 1992. Evaluation and interpretation of the crop water stress index for well watered potatoes. *American Potato Journal*, 69:831-841.

McKenzie, D.C., Hucker, K.W., Morthorpe, L.J. & Baker, P.J., 1990. Field calibration of a neutron-gamma probe in three agriculturally important soils of the lower Macquarie valley. *Australian Journal of Experimental Agriculture*, 30:115-122.

McIntyre, D.S. & Barrow, K.J., 1972. An improved sampling method for small undisturbed cores. *Soil Science*, 114:239-141.

Mead, R., Curnow, R.N. & Hasted, A.M., 1993. *Statistical Methods in Agriculture and Experimental Biology*. 2nd edition. Chapman & Hall, London, UK. pp415.

Mead, R.M., Ayars, J.E. & Liu, J., 1995. Evaluating the influence of soil texture, bulk density and soil water salinity on a capacitance probe calibration. *ASAE Summer Meeting, Chicago Il, USA. June 18-23, 1995*. ASAE paper 95-3264.

Mead, R.M., Paltineanu, I.C., Ayars, J.E. & Liu, J., 1994. Capacitance probe use in soil water measurements. *ASAE Summer Meeting, Kansas City MO, USA. June 20-22, 1994*. ASAE paper 942122.

Monteith, J.L. & Owen, P.C., 1958. *Journal of Scientific Instruments*. 35:443-

Moutonnet, P., Pluyette, E., El Mourabit, N. & Couchat, P., 1988. Measuring the spatial variability of soil hydraulic conductivity using an autometic neutron moisture gauge. *Soil Science Society of America Journal,* 52:1521-1526.

Mullins, C.E., 1977. Magnetic suseptibility of the soil and its significance in soil science – a review. *Journal of Soil Science*, 28:223-246.

Nadler, A. & Lapid, Y., 1996. An improved capacitance sensor for in situ monitoring of soil moisture. *Australian Journal of Soil Research*, 34:361-368.

Newman, A.C.D., 1983. The specific surface of soils determined by water sorption. *Journal of Soil Science*, 34:23-32.

Nieber, J.L., Baker, J.M. & Spaans, J.A., 1991. Evaluation of soil water sensors in frozen soils. *Road & Airport Pavement Response Monitoring Systems Conference Proceedings*. TCCRE/ ASCE West Lebanon NH/Sept 12-16 1991. pp168-181.

Nissan, H.H., Moldrup, P. & Henriksen, K., 1998. High-resolution time domain reflectometry coil probe for measuring soil water content. *Soil Science Society of America Journal*, 62:1203–1211.

Nutting, P.G., 1943. Some standard thermal dehydration curves of minerals. *U.S. Geological Survey Professional Paper197-E*.

O'Leary, G.J. & Incerti, M., 1993. A field comparison of three neutron moisture meters. *Australian Journal of Experimental Agriculture*, 33:59-69.

Olgaard, P.L. & Haahr, V., 1967. Comparative experimental and theoretical investigations of the DM neutron moisture probe. *Nuclear Engineering Design*, 5:311-324.

Olgaard, P.L. & Haahr, V., 1968. On the sensitivity of subsurface neutron moisture gauges to variations in bulk density. *Soil Science*, 105:62-64.

Oliviera, I.B., Demond, A.H. & Salehzadeh, A., 1996. Packing sands for the production of homogeneous porous media. *Soil Science Society of America Journal*, 60:49-53.

Oostrum, M., Hofstee, C., Dane, H. & Lenhard, R.J., 1998. Single-source gamma radiation procedures for improved calibration and measurements in porous media. *Soil Science*, 163(8)646-656.

Ould Mohamed, S., Bertuzzi, P., Bruand, A., Raison, L. & Bruckler, L., 1997. Field evaluation and error analysis of soil water content measurement using the capacitance probe method. *Soil Science Society of Amercia Journal*, 61:399-408.

Paetzold, R.F., Matzkanin, G.A. & De Los Santos, A., 1985. Surface soil water content measurement using pulsed nuclear magnetic resonance techniques. *Soil Science Society of America Journal*, 49:537-540.

Paltineanu, I.C. & Starr, J.L., 1997. Real-time soil water dynamics using multisensor capacitance probes: laboratory calibration. *Soil Science Society of America Journal*, 61:1576-1585.

Payne, D., 1988. *The behaviour of water in soil*. In: (ed. A. Wild) Russel's Soil Conditions and Plant Growth. pp991.

Pepin, S., Livingston, N.J. & Hook, W.R., 1995. Temperature-dependent measurement errors in time-domain reflectometry determinations of soil water. *Soil Science Society of America Journal*, 59:38-43.

Perdok, U.D., Kroesbergen, B. and Hilhorst, M.A., 1996. Influence of gravimetric water content and bulk density on the dielectric properties of soil. *European Journal of Soil Science*, 47:367-371.

Persson, M. & Berndtsson R., 1998. Texture and electrical conductivity effects on temperature dependency in time domain reflectometry. *Soil Science Society of America Journal*, 62:887-893.

Phene, C.J., Clark, D.A., Cardon, G.E. & Mead, R.M., 1992. Soil matric potential sensor research and applications. In: (eds. G.C. Topp, W.D. Reynolds & R.E. Green) *Advances in Measurement of Soil Physical Properties: Bringing Theory into Practice*. SSSA Special Publication No 30. pp263-280.

Polglase, P.J., Tomkins, D., Stewart, L.G. & Falkiner, R.A., 1995. Mineralization and leaching of nitrogen in an effluent-irrigated pine plantation. *Journal of Environmental Quality*, 24:911-920.

Prebble et al. 1981

Puckett, W.E. & Dane J.H., 1981. Testing tensiometers by a vacuum method. *Soil Science*, 132:48-50.

Rasmussen, T.C. & Rhodes, S.C., 1995. Energy-related methods:psychrometers. In: (eds. L.G. Wilson, L.G. Everett & S.J. Cullen) *Handbook of vadose zone characterization and monitoring*. CRC Press, Boca Raton, Fl USA. pp329-341.

Rawlins, S.L. & Campbell, G.S., 1986. Water potential: thermocouple psychrometry. In: (ed. A. Klute) *Methods of soil analysis. Part 1 - Physical and mineralogical methods*. Agronomy Monograph No. 9 part 1. pp597-618.

Reece, C.F., 1996. Evaluation of a line heat dissipation sensor for measuring soil matric potential. *Soil Science Society of America Journal*, 60:1022-1028.

Reynolds, S.G., 1970a. The gravimetric method of soil moisture determination, part I. A study of equipment, and methodological problems. *Journal of Hydrology*, 11:258-273.

Reynolds, S.G., 1970b. The gravimetric method of soil moisture determination, part II. Typical required sample sizes and methods of reducing variability. *Journal of Hydrology*, 11:274-287.

Reynolds, S.G., 1970c. The gravimetric method of soil moisture determination, part III. An

examination of factors influencing soil moisture variabilty. *Journal of Hydrology*, 11:288-300.

Richards, S.K. & Marsh, A.W., 1961. Irrigation based on soil suction measurements. *Soil Science Society Proceedings*, pp65-69.

Ritchards, L.A., 1928. The usefulness of capillary potential to soil moisture and plant investigators. *Journal of Agricultural Research*, 37:719-742.

Ritchie, G.A. & Hinckley, T.M., 1975. The pressure chamber as an instrument for ecological research. *Advances in Ecological Research*, 9:165-178.

Robinson, D.S., Bell, J.P. & Batchelor, C.H., 1994. Influence of iron minerals on the determination of soil water content using dielectric techniques. *Journal of Hydrology*, 161:169-180.

Robinson, M. & Dean, T.J., 1993. Measurement of near surface soil water content using a capacitance probe. *Hydrological Processes*, 7:77-86.

Rose, C.W., 1968. Water transport in soil with a daily temperature wave I. theory and experiment. *Australian Journal of Soil Research*, 6:31-44.

Ross, P.J., 1985. Using bulk density to calculate soil water changes in soils with shrinkage cracks. *Australian Journal of Soil Research*, 23:109-113.

Roth, C.H., Malicki, M.A. & Plagge, R., 1992. Empirical evaluation of the relationship between soil dielectric constant and volumetric water content as the basis for calibrating soil moisture measurements by TDR. *Soil Science*, 43:1-13.

Roth, K., Schulin, R., Fluhler, H. & Attinger, W., 1990. Calibration of time-domain reflectometry for water content measurement using a composite dielectric approach. *Water Resources Research*, 26:2267-2273.

Rothe, A., Weis, W., Kreutzer, K., Matthies, D., Hess, U. & Ansorge, B., 1997. Changes in soil structure caused by the installation of time domain reflectometry probes and their influence on the measurement of soil moisture. *Water Resources Research*, 33(7):1585-1593.

SAS Institute, 1995. One-way layout: fit y by x. In: *JMP® Statistics and Graphics Guide, Version 3.1*. pp66-97. SAS Institute Inc, Cary, NC, USA.

Schaap, M.G., Delange, L. & Heimovaara, T.J., 1997. TDR calibration of organic forest floor media. *Soil Technology*. 11(2):205-217.

Schmugge, T.J., Jackson, T.J. & Mckim, H.L., 1980. Survey of methods for soil moisture determination. *Water Resources Research*, 16:961-979.

Selker, J.S., Graff, L. & Steenhuis, T., 1993. Noninvasive time-domain reflectometry moisture measurement probe. *Soil Science Society of America Journal*, 57:934-936.

Seyfried, M.S., 1992. Field calibration and monitoring of soil-water content with fiberglass electrical resistance sensors. *Soil Science Society of America Journal*, 57:1432-1436.

Seyfried, M.S. and Murdock, M.D., 1996. Calibration of time domain reflectometry for measurement of liquid water in frozen soils. *Soil Science*, 161(2):87-98.

Schrale, G., 1976. Studies of underground water storage and recharge by means of nuclear well logging techniques. Unpublished PhD thesis. Flinders University, SA, Australia.

Singer, A., Schwertmann, U. & Freidl, J., 1998. Iron oxide mineralogy of Terre Rosse and Rendzinas in relation to their moisture and temperature regimes. *European Journal of Soil Science*, 49:385-395.

Skaling, W., 1992. Trase: a product history. In: (eds. G.C. Topp, W.D. Reynolds & R.E. Green) *Advances in Measurement of Soil Physical Properties: Bringing Theory into Practice*. SSSA Special Publication No 30, pp169-185.

Smith-Rose, R.L., 1933. The electrical properties of soils for alternating currents at radio frequencies. *Proceedings of Royal. Society London*. 140:359-377.

Soane, B.D & Calissendorff, C., 1961. The rapid determination of soil water content using the carbide method. *Rhodesian Agricultural Journal*, 58:386-392.

Soilmoisture Equipment Corporation, 1993. *Trase system I - operating instructions*. Soilmoisture Equipment Corporation Incorporated, Santa Barbara CA, USA.

Spaans, E.J.A. & Baker, J.M., 1992. Calibration of Watermark soil moisture sensors for soil matric potential and temperature. *Plant and Soil*, 143:213-217.

Spain, A.V., Isbell, R.F. & Probert, M.E., 1993. Soil organic matter. In: *Soils: an Australian Viewpoint*. Division of Soils, CSIRO. CSIRO, Melbourne. pp551-564.

Stacheder, M., Fundinger, R. & Koehler, K., 1994. A new time-domain reflectometry system (Trime) to measure soil moisture and electrical conductivity. *Symposium and Workshop on Time-domain Reflectometry in Environmental, Infrastructure, and Mining Applications.* United states Bureau of Mines, SP 19-94, pp56-65.

Starr, J.L. & Paltineanu, I.C., 1998. Soil water dynamics using multisensor capacitance probes in nontraffic interrows of corn. *Soil Science Society of America Journal*, 62:114-122.

Starr, J.L., Parkin, T.B. & Meisinger, J.J., 1995. Influence of sample size on chemical and physical soil measurements. *Soil Science Society of America Journal*, 59:713-719.

Steel, R.G. & Torrie, J.H., 1980. Linear Regression (pp173). In: *Principles and Procedures of Statistics. A Biometrical Approach*. McGraw-Hill Companies Inc., NY USA.

Steel, R.G., Torrie, J.H. & Dickey, 1997. *Principles and Procedures of Statistics*. A Biometrical Approach. McGraw-Hill Companies Inc., NY USA. pp666.

Stewart, B.A. & Nielsen, D.R., 1990. Scope and objective of monograph. In: (eds. B.A. Stewart & D.R. Nielsen) *Irrigation of agricultural crops*. Agronomy Monograph No. 30: pp1-4.

Thomas, A.M., 1966. *In situ* measurement of moisture in soil and similar substances by 'fringe' capacitance. *Journal of Scientific Instrumentation*, 43:21-27.

Timlin, D.J. and Pachepsky, Y.A., 1996. Comparison of three methods to obtain the apparent dielectric constant from time domain reflectometry wave traces. *Soil Science Society of America Journal*, 60:970-977.

Tinga, W.R., Voss, W.A.G. & Blossey, D.F., 1973. Generalised approach to multiphase dielectric mixture theory. *Journal of Applied Physics*, 44(9):3897-3902.

Check date on tisdal – 55 or 51

Tisdall, A.L., 1951. Comparison of methods of determining apparent density of soils. *Australian Journal of Agricultural Research*. 2:349-354.

Tomer, M.D. & Anderson, J.L., 1995. Field evaluation of a soil water-capacitance probe in a find sand. *Soil Science*, 159(2):90-98.

Topp, G.C. & Davis, J.L., 1981. Detecting infiltration of water through soil cracks by time-domain reflectometry. *Geoderma*, 26:13-23.

Topp, G.C. & Davis, J.L., 1985. Measurement of soil water content using time-domain reflectometry (TDR): A field evaluation. *Soil Science Society of America Journal*, 49:19-24.

Topp, G.C., Davis, J.L. & Annan, A.P., 1980. Electromagnetic determination of soil water content: measurements in coaxial transmission lines. *Water Resources Research*, 16:574-582.

Topp, G.C., Davis, J.L. & Annan, A.P., 1982a. Electromagnetic determination of soil water content using TDR: I. Applications to wetting fronts and steep gradients. *Soil Science Society of America Journal*, 46:672-678.

Topp, G.C., Davis, J.L. & Annan, A.P., 1982b. Electromagnetic determination of soil water content using TDR: II. evaluation of installation and configuration of parallel transmission lines. *Soil Science Society of America Journal*, 46:678-684.

Topp, G.C., Yanuka, M., Zebchuk, W.D. & Zegelin, S., 1988. Determination of electrical conductivity using time-domain reflectometry soil and water experiments in coaxial lines. *Water Resources Research*, 24:945-952.

Topp, G.C., Zegelin, S.J. & White, I., 1994. Monitoring soil water content using TDR: an overview of progress. *Symposium and Workshop on Time-domain Reflectometry in Environmental, Infrastructure, and Mining Applications. Bureau of Mines*, SP 19-94, pp56-65.

Turner, N.C., 1988. Measurement of the plant water status by the pressure chamber technique. *Irrigation Science*, 9:289-308.

Vachaud, G., Royer, J.M. & Cooper, J.D., 1977. Comparison of methods of calibration of a neutron probe by gravimetry or neutron-capture model. *Journal of Hydrology*, 34:343-356.

Vanclooster, M., Mallants, D., Diels, J. & Feyen, J., 1993. Determining local-scale solute transport parameters using time-domain reflectometry (TDR). *Journal of Hydrology*, 148:93-107.

Vanclooster, M., Mallants, D., Vanderborght, J., Diels, J., Van Orshoven, J. & Feyen, J., 1995. Monitoring solute transport in a multi-layered sandy lysimeter using time domain reflectometry. *Soil Science Society of America Journal*, 59:337-344.

Vauclin, M., Haverkamp, R. & Vachaud, G., 1984. Error analysis in estimating soil water content from neutron probe measurements: 2 spatial standpoint. *Soil Science*, 137:141-148.

Viscarra Rossel, R.A. & McBratney, A.B., 1998. Laboratory evaluation of a proximal sensing technique for simultaneous measurement of soil clay and water content. *Geoderma*, 85:19-39.

Vomocil, J.A., 1954. *In situ* measurement of soil bulk density. *Agricultural Engineering*. 35:651-654.

Walkley, A., & Black, C.I., 1934. An examination of the Degtjareff method for determining soil organic matter and a proposed modification of the chromic acid titration method. *Soil Science*, 37:29-38.

Ward, A.L., Kachanoski, R.G., von Bertoldi, A.P. & Elrick, D.E., 1995. Field and undisturbed-column measurements for predicting transport in unsaturated layered soil. *Soil Science Society of America Journal*, 59:52-59.

Ward, A.L., Kachanoski, R.G. & Elrick, D.E., 1994. Laboratory measurements of solute transport using time domain reflectometry. *Soil Science Society of America Journal*, 58:1031-1039.

Weast, R.C. (ed.), 1975. General physical constants. *Handbook of Chemistry and Physics*, CRC Press, Cleveland, USA. ppE-61.

Webster, R., 1997. Regression and functional relations. *European Journal of Soil Science*, 48:557-566.

Whalley, W.R., 1991. Development and evaluation of a microwave soil moisture sensor for incorporation in a narrow cultivator tine. *Journal of Agricultural Engineering Research*, 50:25-33.

Whalley, W.R., 1993. Considerations on the use of time-domain reflectometry (TDR) for measuring soil water content. *Soil Science*, 44:1-9.

Whalley, W.R., 1994. Response to: Comments on 'Considerations on the use of time-domain reflectometry (TDR) for measuring soil water content' by W.R.Whalley, by I. White, J.H. Knight, S.J. Zegelin, & G.C. Topp. *European Journal of Soil Science*, 45:509-510.

Whalley, W.R. & Bull, C.R., 1991. An assessment of microwave reflectance as a technique for estimating the volumetric water content of soil. *Journal of Agricultural Engineering Research*, 50:315-326.

Whalley, W.R., Dean, T.J. & Izzard, P., 1992. Evaluation of the capacitance technique as a method for dynamically measuring soil water content. *Journal of Agricultural Engineering Research*, 52:147-155.

Whalley, W.R. & Stafford, J.V., 1992. Real-time sensing of soil water content from mobile machinery: options for sensor design. *Computers and Electronics in Agriculture*, 7:269-284.

White, I., Knight, J.H., Zegelin, S.J. & Topp, G.C., 1994. Comments on 'Considerations on the use of time-domain reflectometry (TDR) for measuring soil water content' by W.R.Whalley. *European Journal of Soil Science*, 45:503-508.

White, I. & Zegelin, S.J., 1995. Electric and dielectric methods for monitoring soil-water content. In: (eds. L.G. Wilson, L.G. Everett & S.J. Cullen) *Handbook of Vadose Zone Characterization and Monitoring*. CRC Press, Boca Raton, pp343-385.

Williams, J., Holmes, J.W., Williams, B.G. & Winkworth, R.E., 1981. Application in agriculture, forestry and environmental science. In: (ed. E.L. Greacen) *Soil Water Assessment by the Neutron Method*. pp3-15. CSIRO, East Melbourne.

Williams, J. & Sinclair, D.F., 1981. Accuracy, bias and precision. In: (ed. E.L. Greacen) *Soil Water Assessment by the Neutron Method*. CSIRO, Melbourne, pp35-49.

Wilson, D.J., 1988. Neutron moisture meters: the minimum error in the derived water density. *Australian Journal of Soil Research*, 26:97-104.

Wilson, D.J. & Ritchie, A.I.M, 1986. Neutron moisture meters: the dependence of their response on soil parameters. *Australian Journal of Soil Research*, 24:11-23.

Wu, K., 1998. Measurement of soil moisture change in spatially heterogenous weathered soils using a capacitance probe. *Hydrological Processes*, 12:135-146.

Wyman, J., 1930. Measurements of the Dielectric Constants of Conducting Media. *Physical Review*, 35:623-634.

Wyseure, G.C.L, Mojid, M.A. & Malik, M.A., 1997. Measurement of volumetric water content by TDR in saline soils. *Journal of Soil Science*, 48:347-354.

Yanuka, M., Topp, G.C., Zegelin, S. & Zebchuk, W.D., 1988. Multiple reflection and attenuation of time-domain reflectometry pulses: theoretical considerations for applications to soil and water. *Water Resources Research*, 24:939-944.

Yaron, B., Bresler, E. & Shalhevet, J., 1966. A method for uniform packing of soil columns. *Soil Science*, 101(3):205-209.

Yasuda, H., Berndtsson, R., Bahri, A. & Jinno, K., 1994. Plot-scale solute transport in a semiarid agricultural soil. *Soil Science Society of America Journal*, 58:1052-1060.

Yeh, J.T.-C. & Guzman-Guzman, A., 1995. Tensiometry. In: (eds. L.G. Wilson, L.G. Everett & S.J. Cullen) *Handbook of vadose zone characterization and monitoring*. CRC Press, Baco Raton, Fl USA. pp319-328.

Yip, V. & Cutmore, N.G., 1993. On-line determination of freee and bound moisture in iron ore. *Proceedings from the 18th International Mineral Processing Congress*, Sydney, 23-28 May 1993. pp 457-460.

Yu, C., Warrick, A.W., Conklin, M.H., Young, M.H. and Zreda, M., 1997. Two- and three-parameter calibrations of time domain reflectometry for soil moisture measurement. Water Resources Research, 33(10):2417-2421.

Zegelin, S.J., 1992. Pyelab TDR system (users guide). CSIRO Centre for Environmental Mechanics, Canberra , Australia. pp128.

Zegelin, S.J. & White, I., 1994. Calibration of TDR for applications in mining, grains, and fruit storage and handling. *Time-domain Reflectometry in Environmental, Infrastructure, & Mining Applications, US Department of Interior Bureau of Mines*, SP 19-94:115-129.

Zegelin, S.J., White, I. & Jenkins, D.R., 1989. Improved Field Probes for Soil Water Content and Electrical Conductivity Measurement Using Time-domain Reflectometry. *Water Resources Research*, 25:2367-2376.

Zegelin, S.J., White, I. & Russell, G.F., 1992. A critique of the time-domain reflectometry technique for determining field soil-water content. In: (eds G.C.Topp, W.D.Reynolds & R.E.Green) *Advances in Measurement of Soil Physical Properties: Bringing Theory into Practice*. SSSA Special Publication No 30. pp187-208.

Zhang, B., Gao, G., Zhang, T. & Sun, Y., 1997. Determination of water content in clayey red soil using techniques based on measurement of dielectric constant. *Pedosphere*, 7(2):149-154.

Appendix 2-1

Comparison of respective TDR readings for the Ferrosol, Chromosol and sand in determining the effect of extension cable on measured dielectric.

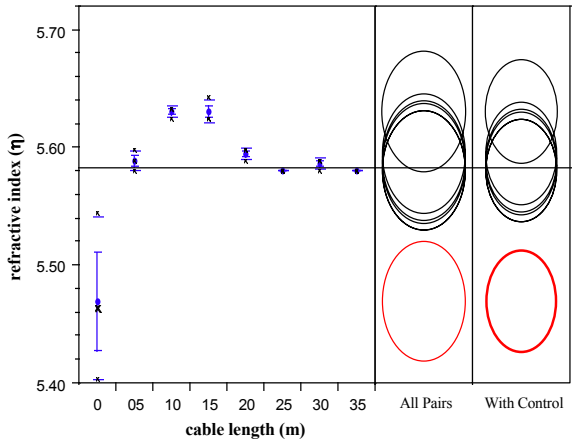

TRASE® TDR measuring probe S1 in a saturated Ferrosol with RG-58 extension cable

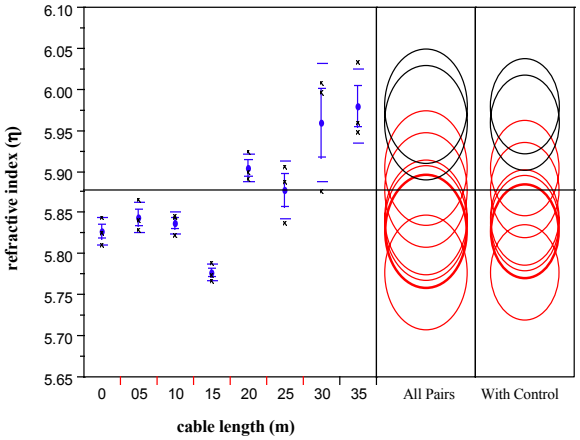

Pyelab TDR measuring probe S1 in a saturated Ferrosol with RG-58 extension cable

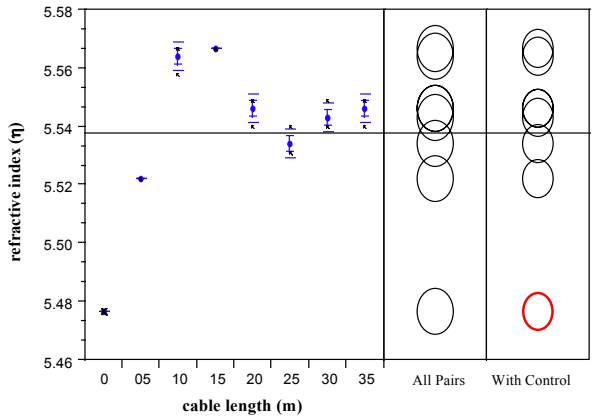

TRASE® TDR measuring probe S2 in a saturated Ferrosol with RG-58 extension cable

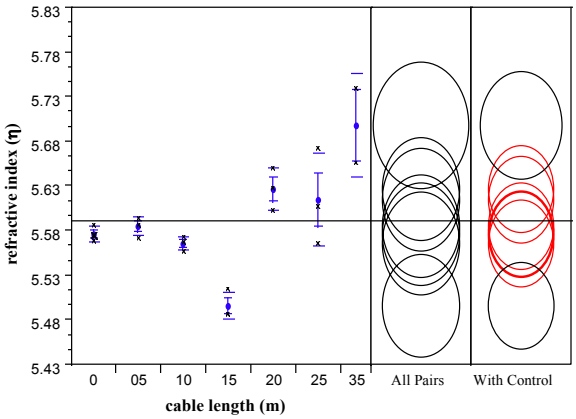

Pyelab TDR measuring probe S2 in a saturated Ferrosol with RG-58 extension cable

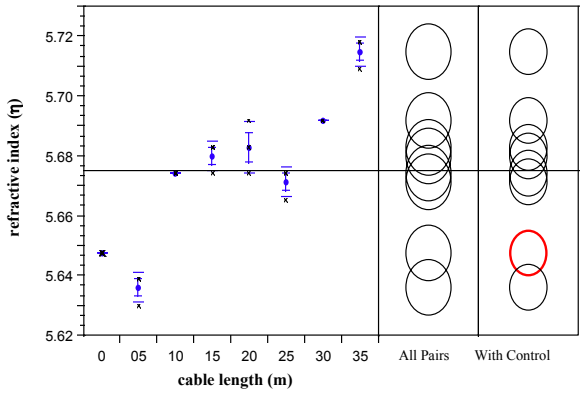

TRASE® TDR measuring probe C3 in a saturated Ferrosol with RG-58 extension cable

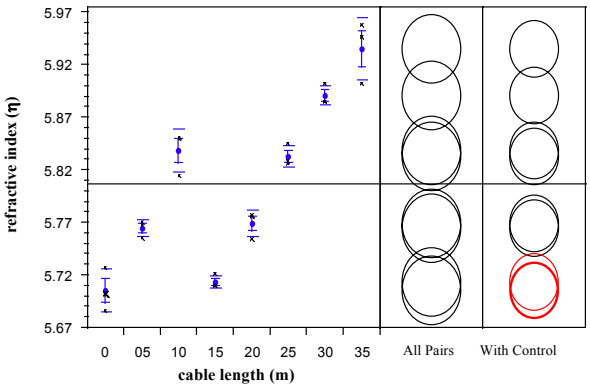

Pyelab TDR measuring probe C3 in a saturated Ferrosol with RG-58 extension cable

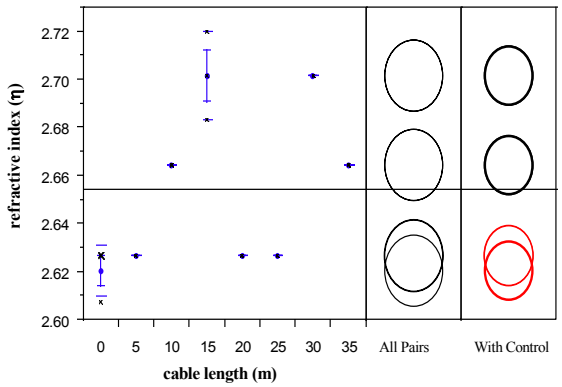

TRASE® TDR measuring probe S1 in an air-dry Ferrosol with RG-58 extension cable

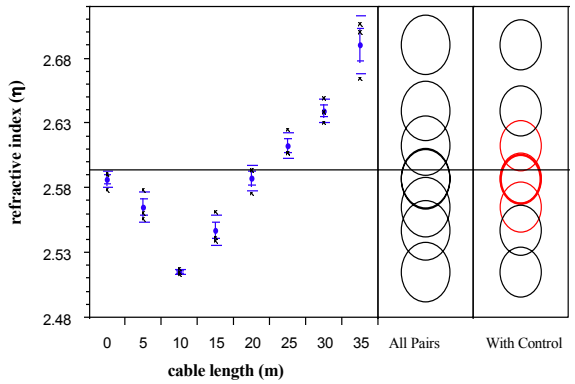

Pyelab TDR measuring probe S1 in an air-dry Ferrosol with RG-58 extension cable

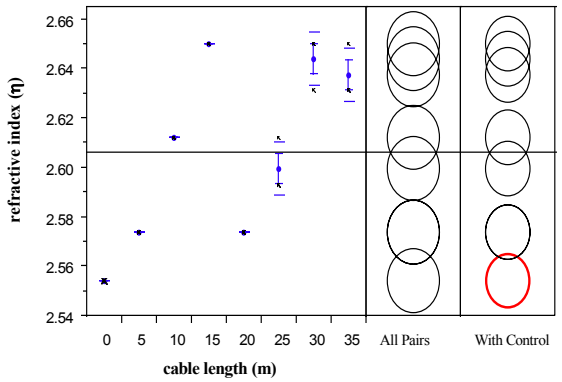

TRASE® TDR measuring probe S2 in an air-dry Ferrosol with RG-58 extension cable

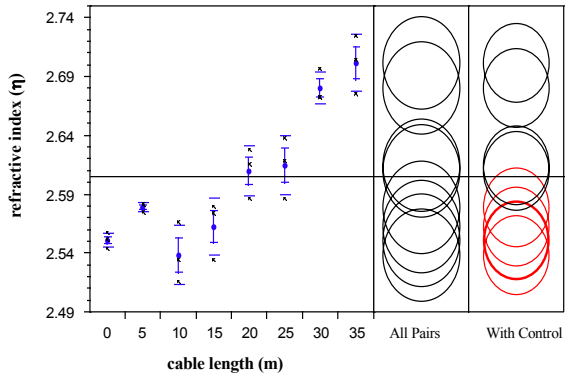

Pyelab TDR measuring probe S2 in an air-dry Ferrosol with RG-58 extension cable

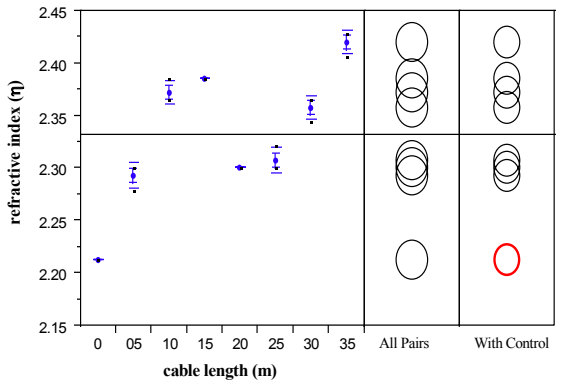

TRASE® TDR measuring probe C3 in an air-dry Ferrosol with RG-58 extension cable

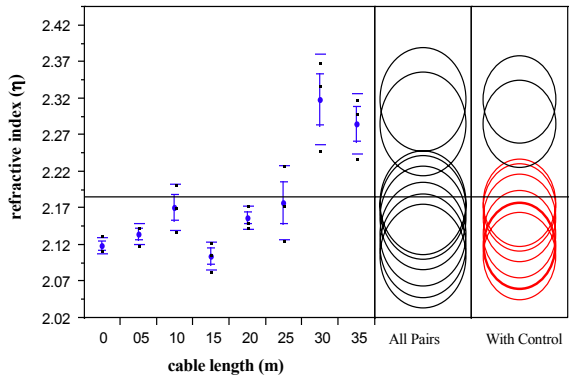

Pyelab TDR measuring probe C3 in an air-dry Ferrosol with RG-58 extension cable

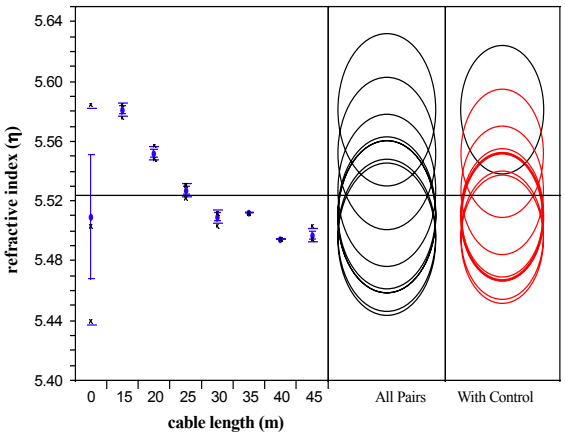

TRASE® TDR measuring probe S1 in a saturated Ferrosol with RG-8 extension cable

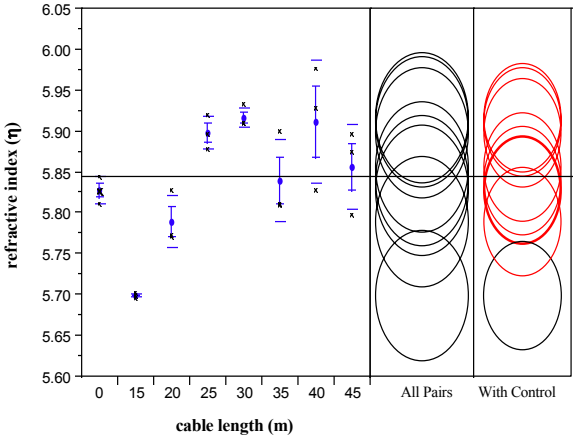

Pyelab TDR measuring probe S1 in a saturated Ferrosol with RG-8 extension cable CSIRO S1R2 RG8

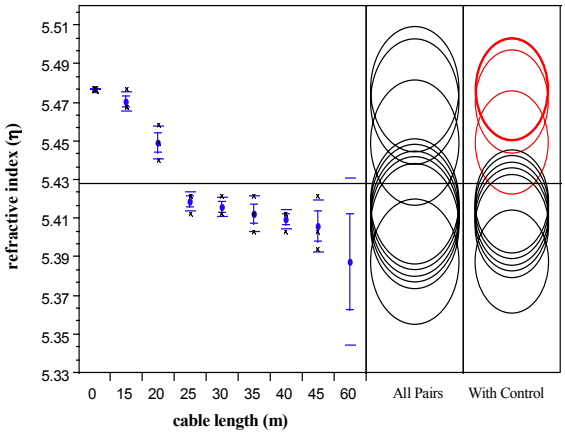

TRASE® TDR measuring probe S2 in a saturated Ferrosol with RG-8 extension cable

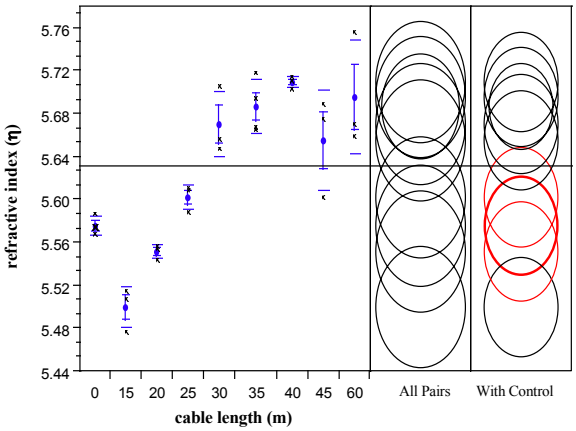

Pyelab TDR measuring probe S2 in a saturated Ferrosol with RG-8 extension cable

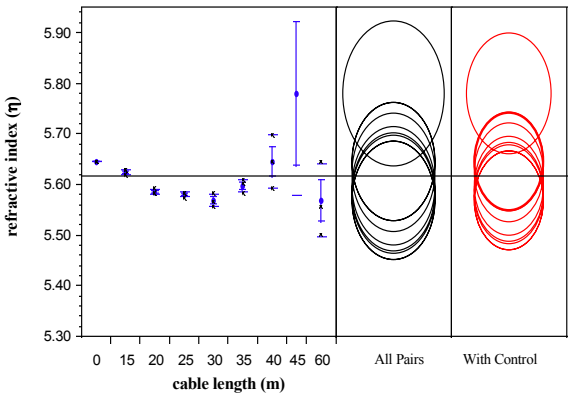

TRASE® TDR measuring probe C3 in a saturated Ferrosol with RG-8 extension cable

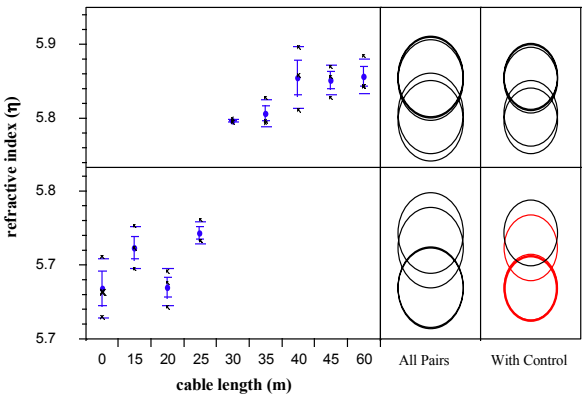

Pyelab TDR measuring probe C3 in a saturated Ferrosol with RG-8 extension cable

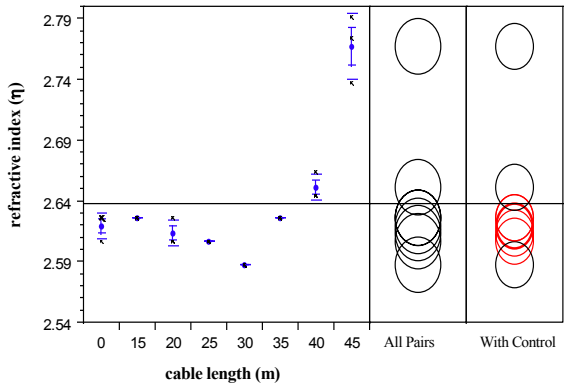

TRASE® TDR measuring probe S1 in an air-dry Ferrosol with RG-8 extension cable

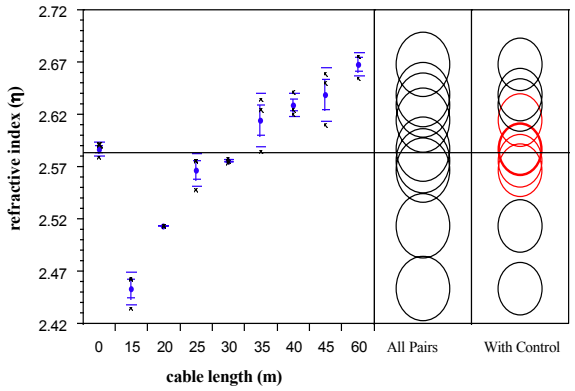

Pyelab TDR measuring probe S1 in an air-dry Ferrosol with RG-8 extension cable

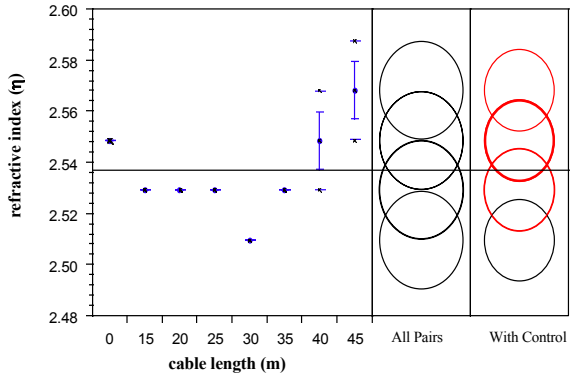

TRASE® TDR measuring probe S2 in an air-dry Ferrosol with RG-8 extension cable

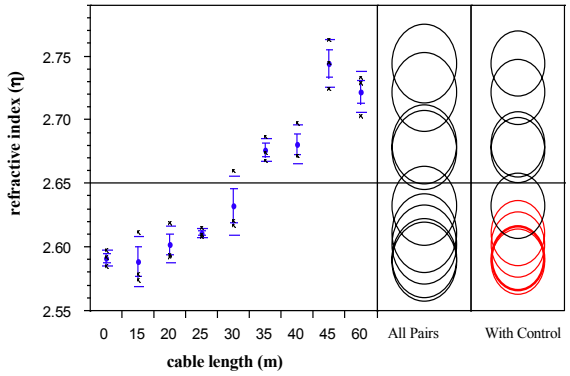

Pyelab TDR measuring probe S2 in an air-dry Ferrosol with RG-8 extension cable

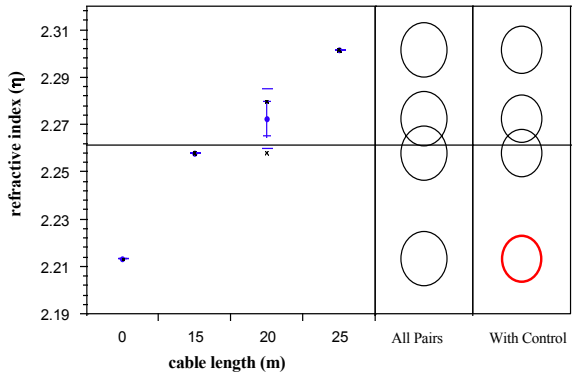

TRASE® TDR measuring probe C3 in an air-dry Ferrosol with RG-8 extension cable

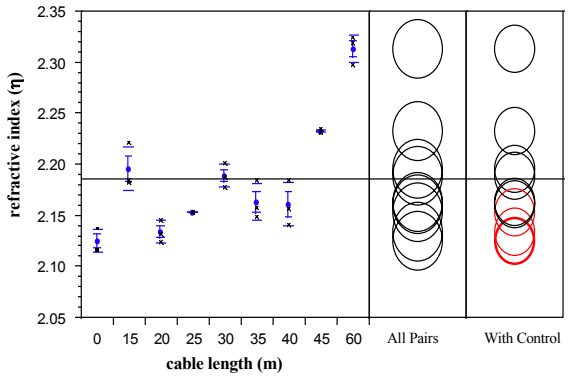

Pyelab TDR measuring probe C3 in an air-dry Ferrosol with RG-8 extension cable

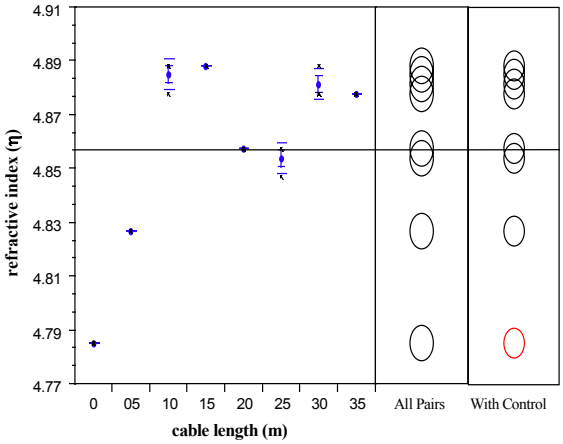

TRASE® TDR measuring probe S7 in a saturated Chromosol with RG-58 extension cable

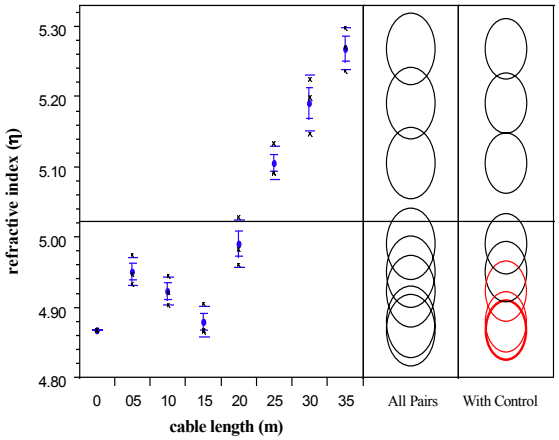

Pyelab TDR measuring probe S7 in a saturated Chromosol with RG-58 extension cable

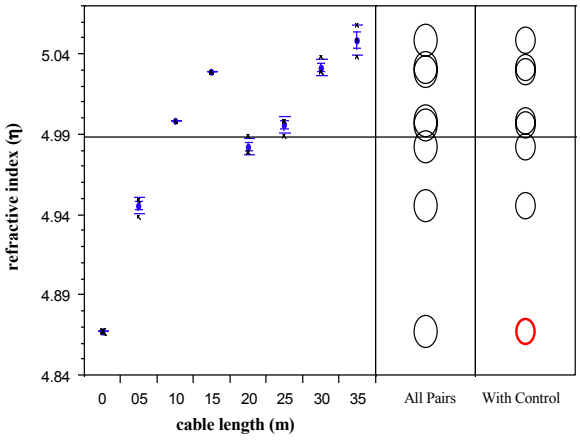

TRASE® TDR measuring probe S8 in a saturated Chromosol with RG-58 extension cable

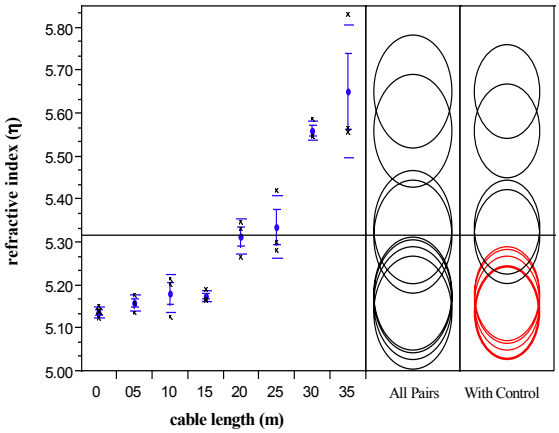

Pyelab TDR measuring probe S8 in a saturated Chromosol with RG-58 extension cable

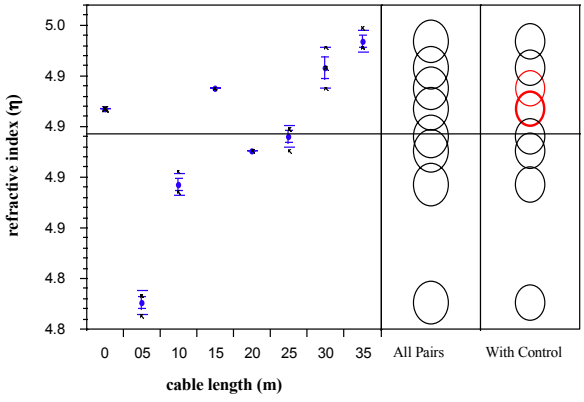

TRASE® TDR measuring probe C9 in a saturated Chromosol with RG-58 extension cable

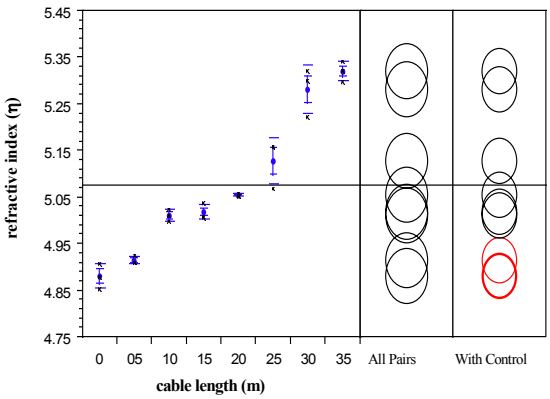

Pyelab TDR measuring probe C9 in a saturated Chromosol with RG-58 extension cable

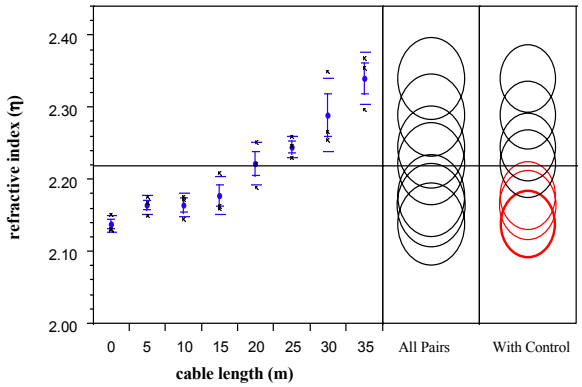

Pyelab TDR measuring probe S7 in an air-dry Chromosol with RG-58 extension

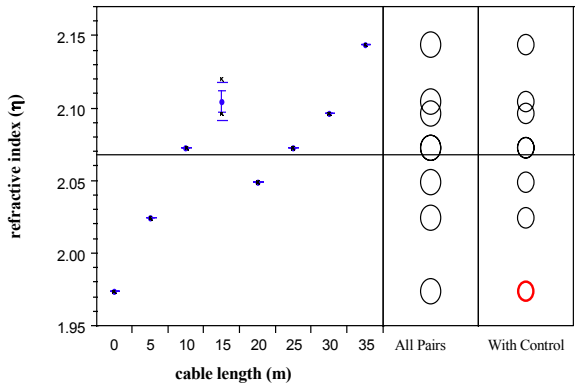

TRASE® TDR measuring probe S8 in an air-dry Chromosol with RG-58 extension cable

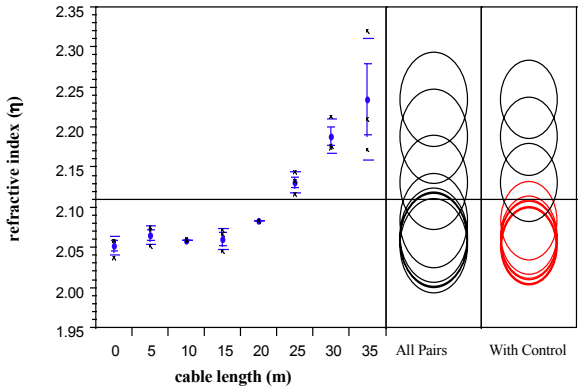

Pyelab TDR measuring probe S8 in an air-dry Chromosol with RG-58 extension cable

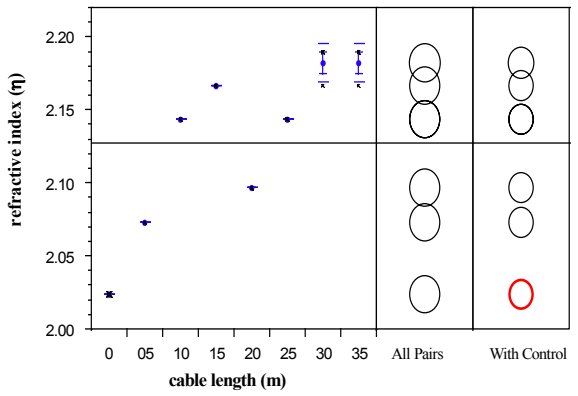

TRASE® TDR measuring probe C9 in an air-dry Chromosol with RG-58 extension cable

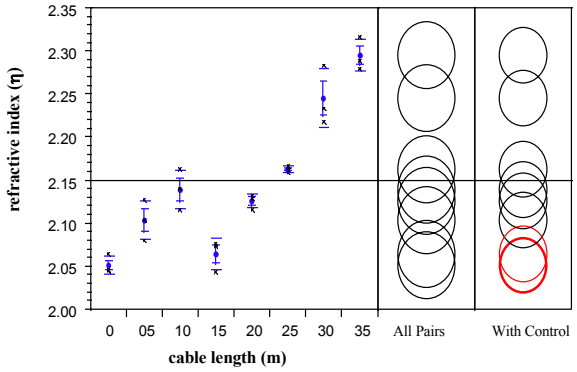

Pyelab TDR measuring probe C9 in an air-dry Chromosol with RG-58 extension cable

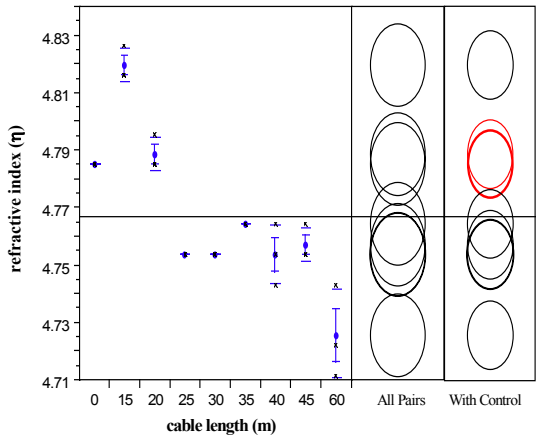

TRASE® TDR measuring probe S7 in a saturated Chromosol with RG-8 extension cable

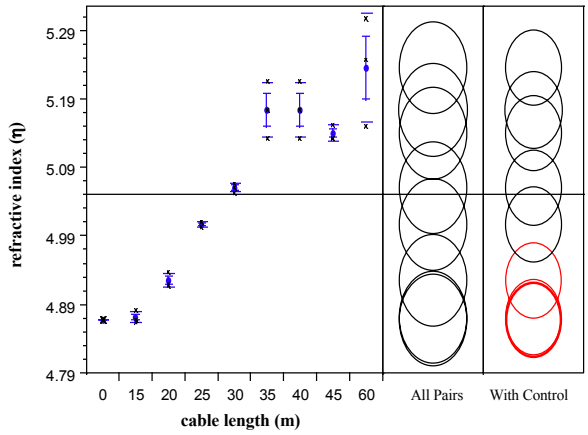

Pyelab TDR measuring probe S7 in a saturated Chromosol with RG-8 extension cable

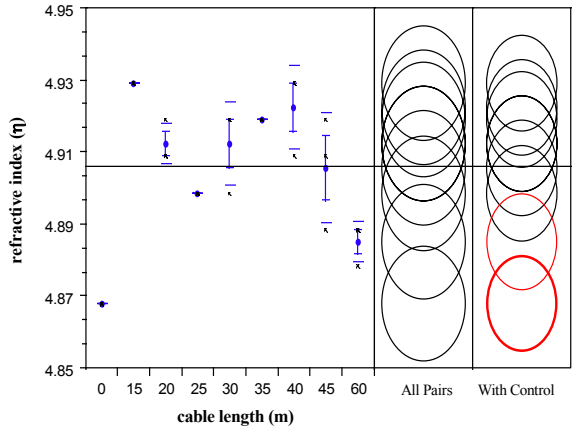

TRASE® TDR measuring probe S8 in a saturated Chromosol with RG-8 extension cable

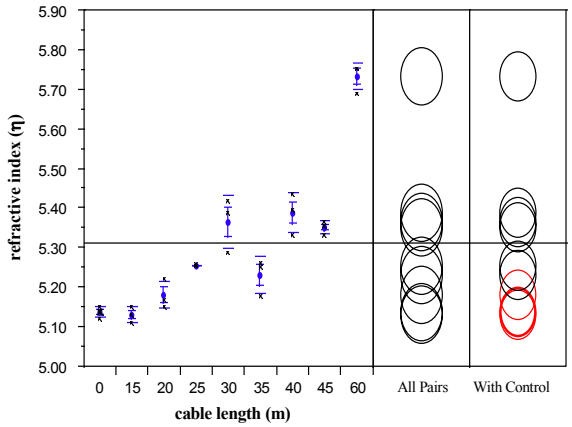

Pyelab TDR measuring probe S8 in a saturated Chromosol with RG-8 extension cable

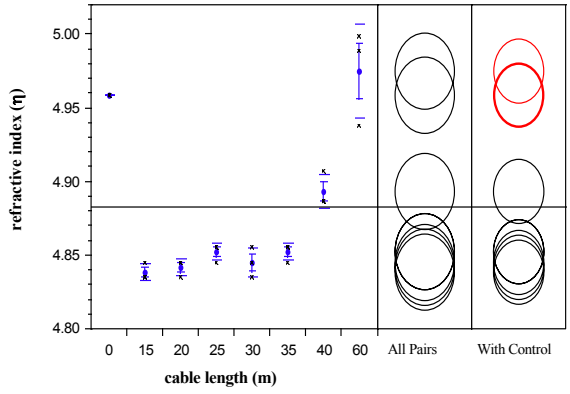

TRASE® TDR measuring probe C9 in a saturated Chromosol with RG-8 extension cable

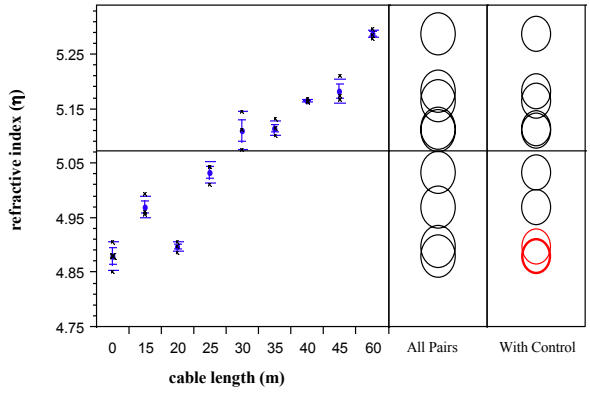

Pyelab TDR measuring probe C9 in a saturated Chromosol with RG-8 extension cable

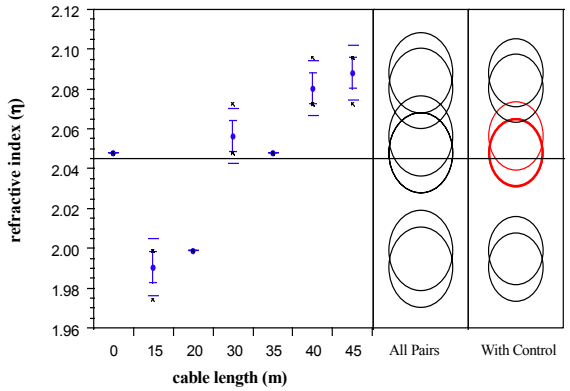

TRASE® TDR measuring probe C7 in an air-dry Chromosol with RG-8 extension

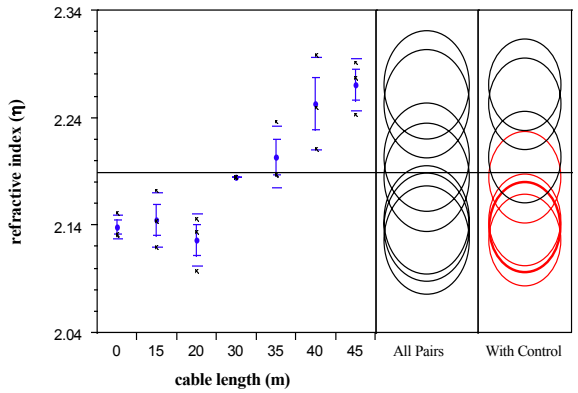

Pyelab TDR measuring probe C7 in an air-dry Chromosol with RG-8 extension cable

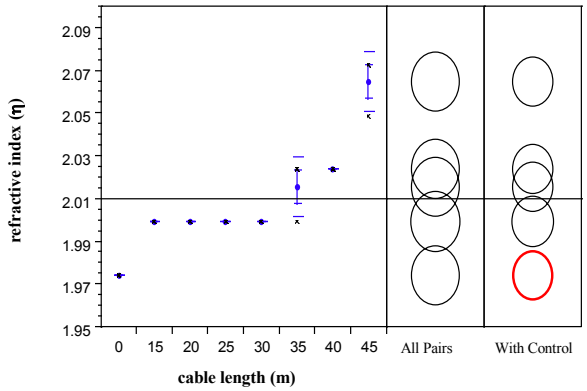

TRASE® TDR measuring probe C8 in an air-dry Chromosol with RG-8 extension cable

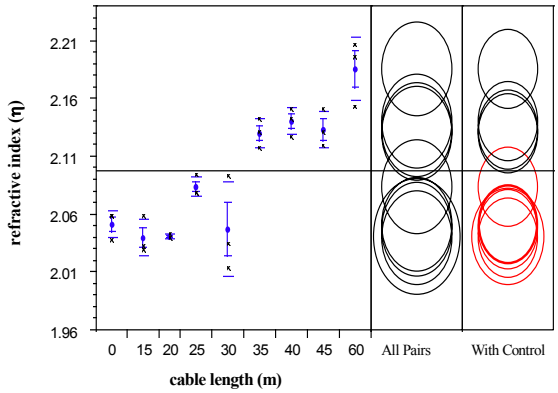

Pyelab TDR measuring probe S8 in an air-dry Chromosol with RG-8 extension cable

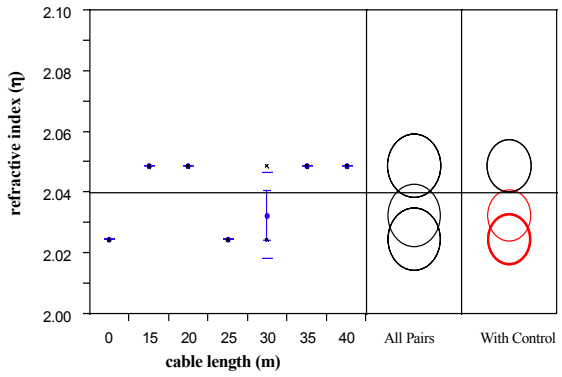

TRASE® TDR measuring probe C9 in an air-dry Chromosol with RG-8 extension cable

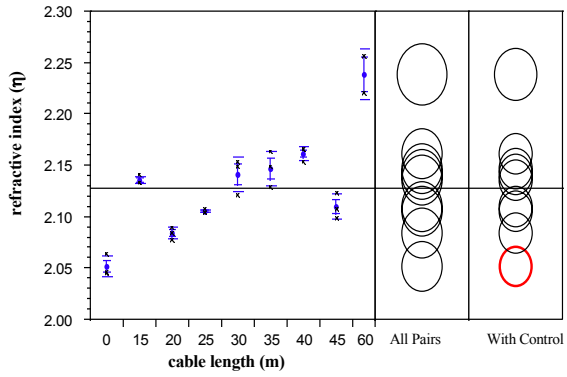

Pyelab TDR measuring probe C9 in an air-dry Chromosol with RG-8 extension cable

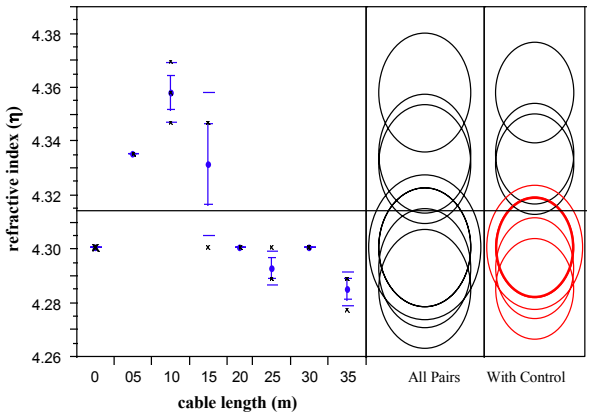

TRASE® TDR measuring probe S10 in a saturated sand with RG-8 extension cable

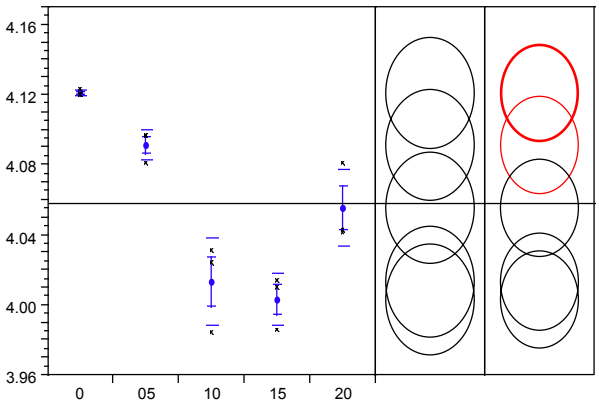

Pyelab TDR measuring probe S10 in a saturated sand with RG-58 extension cable

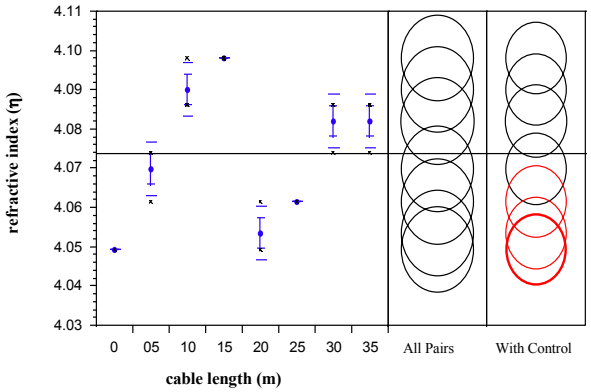

TRASE® TDR measuring probe C11 in a saturated sand with RG-58 extension cable

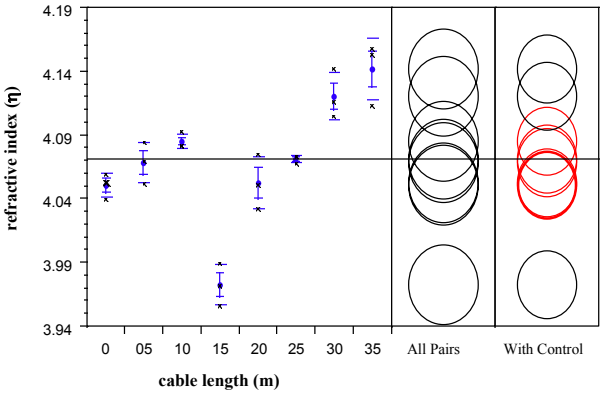

Pyelab TDR measuring probe C11 in a saturated sand with RG-58 extension cable

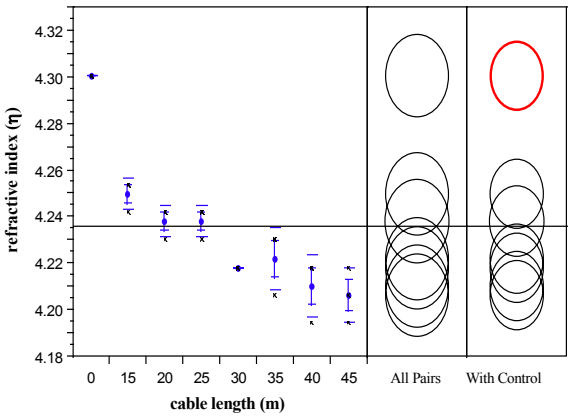

TRASE® TDR measuring probe S10 in a saturated sand with RG-8 extension cable

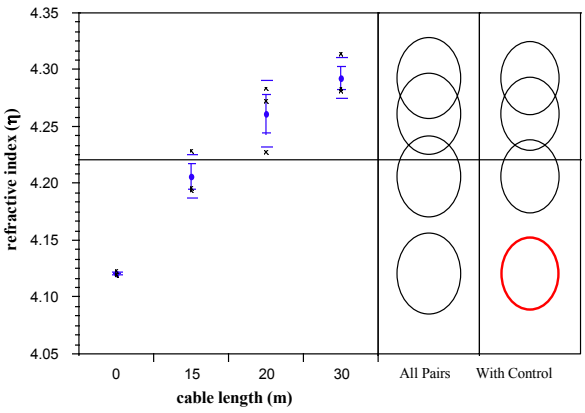

Pyelab TDR measuring probe S10 in a saturated sand with RG-8 extension cable

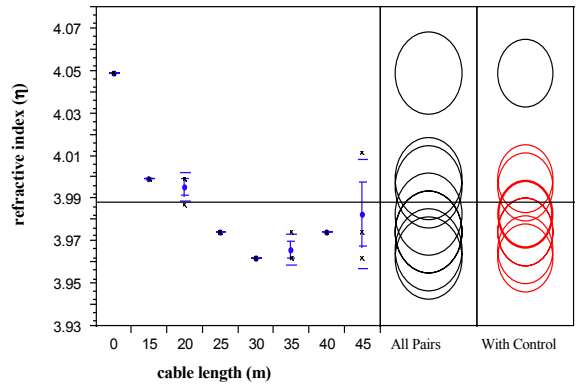

TRASE® TDR measuring probe C11 in a saturated sand with RG-8 extension cable

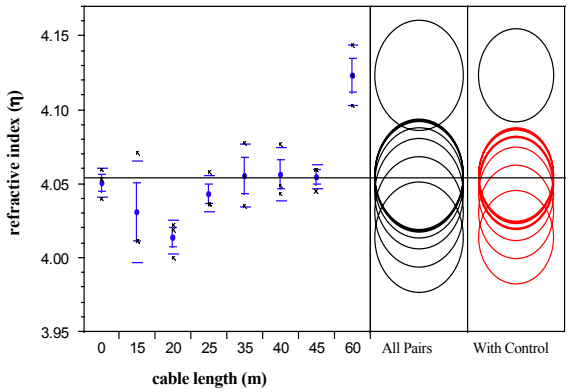

Pyelab TDR measuring probe C11 in a saturated sand with RG-8 extension cable

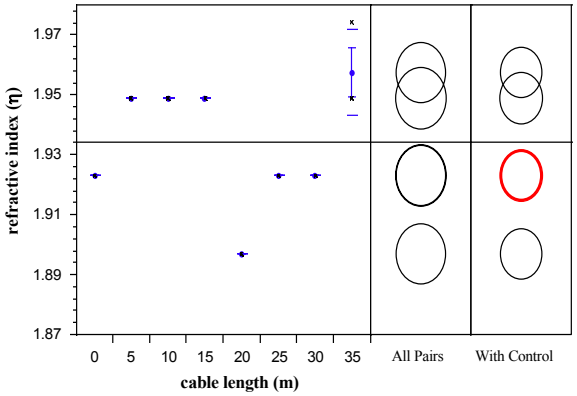

TRASE® TDR measuring probe S10 in an unsaturated sand with RG-8 extension cable

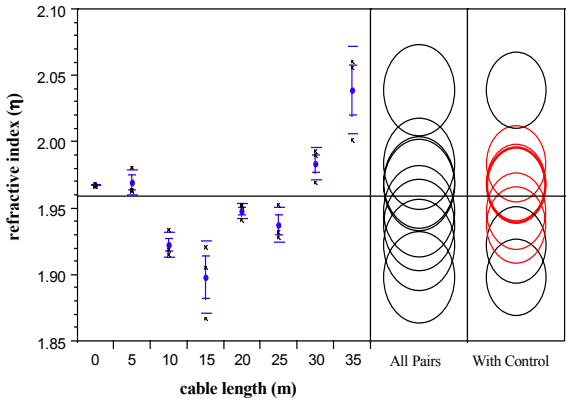

Pyelab TDR measuring probe S10 in an unsaturated sand with RG-8 extension cable

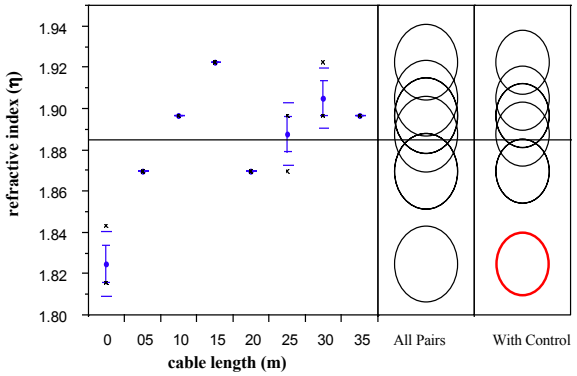

TRASE® TDR measuring probe C11 in an unsaturated sand with RG-58 extension cable

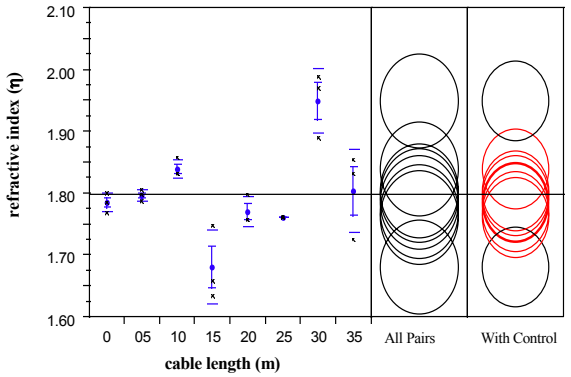

Pyelab TDR measuring probe C11 in an unsaturated sand with RG-58 extension cable

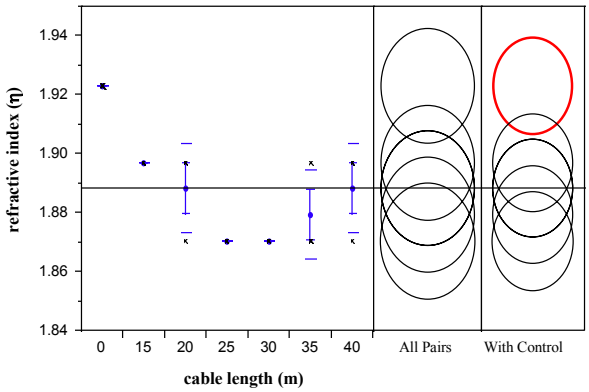

TRASE® TDR measuring probe S10 in an air-dry sand with RG-8 extension cable

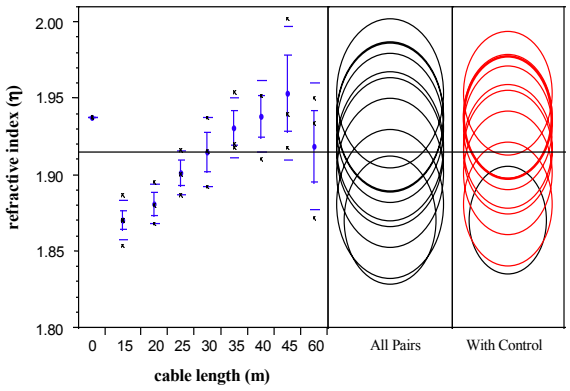

Pyelab TDR measuring probe S10 in an air-dry sand with RG-8 extension

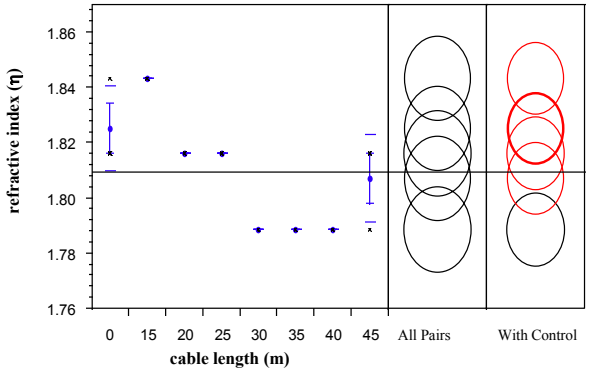

TRASE® TDR measuring probe C11 in an sir-dry sand with RG-8 extension cable

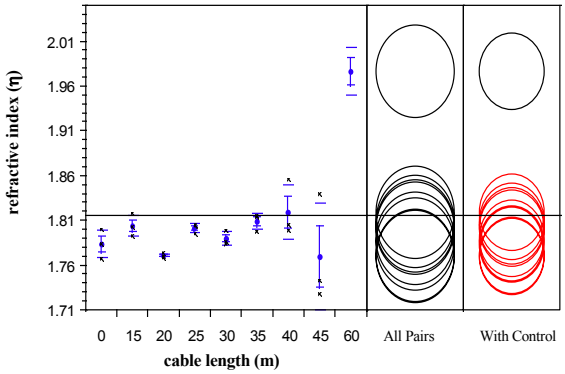

Pyelab TDR measuring probe C11 in an air-dry sand with RG-8 extension

Appendix 3-1

Distribution of the NMM counts in a sand drum and water drum representing the likely extreme conditions of measurement with the NMM technology.

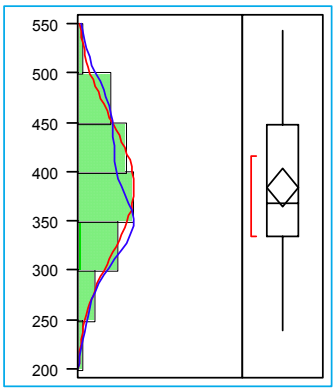

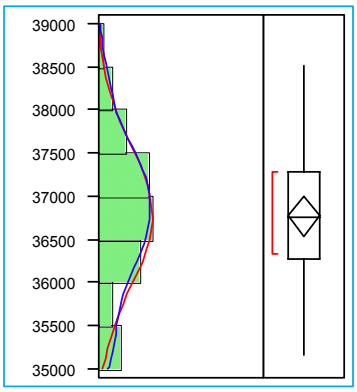

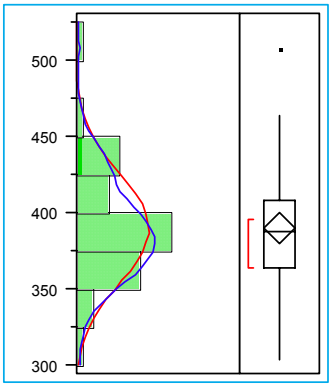

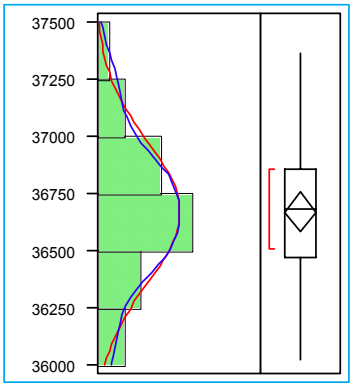

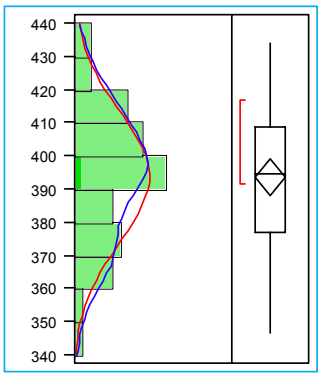

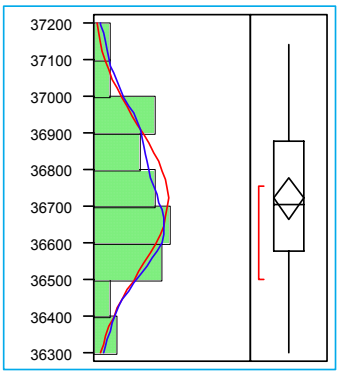

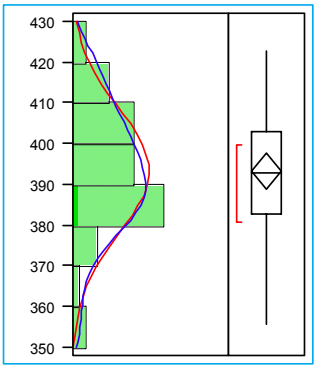

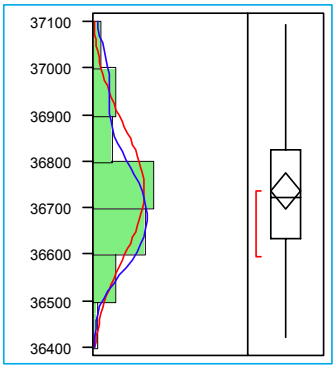

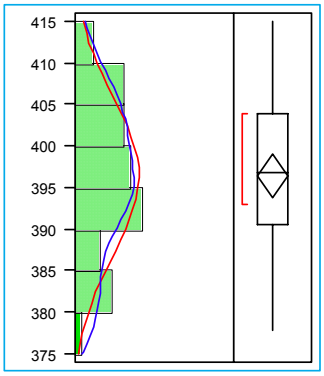

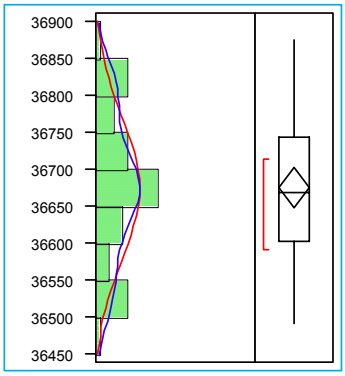

Spread of NMM counts in a sand drum at 1-second (over page top), 4-seconds, 16-seconds, 32-seconds (this page top) and 64-seconds count time.

Spread of NMM counts in a water drum at 1-second (over page top), 4-seconds, 16-seconds, 32-seconds (this page top) and 64-seconds count time.

Appendix 4-1

Calibration coefficients for the EnviroSCAN® FD system S0077 supplied with the instrument.

Sensor depth (m)	Sensor 1 (air)	Sensor 1 (water)	Sensor 2 (air)	Sensor 2 (water)
0.1	48493	33123	49241	32734
0.2	49445	32867	48659	32246
0.3	48832	33259	49867	32930
0.4	50079	33657	49905	33873
0.5	49544	33317	49200	33424
0.7	48785	33371	49858	32802
0.9	48745	32927	49573	32847
1.2	50261	32809	49362	33085

The relationship used for the conversion of universal frequency (UF) to volumetric soil water content (θ) for the EnviroSCAN® FD system is based on unpublished results of J.C. Dighton & P.J. Dillon (CSIRO, Adelaide) from two soil types (unknown) where the $UF = 0.3316 (\pm 0.0337) + \theta \times 1.520665 (\pm 0.0611)$.

Appendix 4-2

Calibration for the NMM probe (serial number 2966) used during the experiment at Dubbo, NSW. θ is calculated from the raw neutron count, not the count ratio. This calibration is supplied by Irricrop Technologies Pty. Ltd. as a "universal" calibration for the particular instrument.

Calibration number	Slope	Intercept	Depth (m)
1	0.001759	-1.086	0.20
2	0.001759	-1.086	0.30
3	0.00181	1.343	0.40
4	0.0017	3.255	0.50
5	0.001645	3.3	0.60
6	0.00149	4.113	0.80
7	0.001538	3.317	1.00
8	0.001634	-0.274	1.20

Appendix 5-1

Permeability in the iron ore stockpile at cross-section C.

	Hydraulic conductivity (m s^{-1})						
Location [(1)]	- 8.4	- 5.6	- 2.8	0.0	2.8	5.6	8.4
Bench 1			5.3×10^{-5}	5.6×10^{-5}	3.4×10^{-5}		
Bench 2		2.7×10^{-5}	4.2×10^{-6}	5.2×10^{-6}	8.0×10^{-5}	2.7×10^{-4}	
Bench 3	6.1×10^{-5}	2.6×10^{-5}	1.2×10^{-4}	$> 5 \times 10^{-2}$	$> 5 \times 10^{-2}$	$> 5 \times 10^{-2}$	$> 5 \times 10^{-2}$
Bench 4	$> 5 \times 10^{-2}$	5.4×10^{-5}	$> 5 \times 10^{-2}$	$> 5 \times 10^{-2}$	$> 5 \times 10^{-2}$	$> 5 \times 10^{-2}$	$> 5 \times 10^{-2}$

[(1)] distance (m) from the centreline of the stockpile.